Putative virulence factors and novel antimicrobial targets of the *Burkholderia cepacia* complex.

Sara Josefin Bartholdson

PhD Thesis

The University of Edinburgh 2009

Supported by

CYSTIC FIBROSIS TRUST

UK CYSTIC FIBROSIS MICROBIOLOGY CONSORTIUM

BIG LOTTERY FUND

Acknowledgements

First of all, I would like to thank Dominic Campopiano and John Govan for their supervision, support and guidance, both before and during my PhD, with a special thanks to John for supplying summer jobs and cheering me up while waiting for funding. I am very grateful and have thoroughly enjoyed my experience in both labs.

A big thank you to Cathy Doherty, Vicky Barcus, Dervla Kenna and Ross Langley in the CF lab; and thanks to everyone from Chemistry lab 229, especially Gareth Morrison, Dave Clarke, Paul Bilton, Montse Pérez-Navarro, Beverley Yard, Scott Baxter and Marine Raman. Thanks also to the many randomly helpful people in the Chemistry Department and the CID.

I would like to thank Miguel Valvano, Slade Loutet, Gail Ferguson and David Allcock for their help with the LPS project; and I thank Ben Mewburn, Stephen Fry, Janice Miller, and Alan Brown for their help on the EPS project.

Many thanks to the UK CF Microbiology Consortium and the CF trust and Big lottery fund for funding this PhD.

Finally, I would like to thank my family for their love and support, and especially Bruce for always being there - I couldn't have done it without you.

Abbreviations

AMP antimicrobial peptide
APS ammonium persulfate
ArnT L-Ara4N transferase
Bcc *Burkholderia cepacia* complex
BCA bicinchoninic acid
BCESM *Burkholderia cepacia* epidemic strain marker
cblA cable pilus
CF cystic fibrosis
CFTR cystic fibrosis transmembrane conductance regulator
cfu colony forming units
CGD chronic granulomatous disease
Da Dalton
DDM n-Dodecyl-ß-maltoside
DOC deoxycholate
ECFML Edinburgh CF microbiology laboratory
EDTA ethylenediaminetetraacetic acid
EPS exopolysaccharide
FA fatty acyl
FPLC fast protein liquid chromatography
GDP guanosine diphosphate
HBD-3 human β-defensin – 3
HMW high molecular weight
HPAE-PAD high-performance anion-exchange chromatography with pulsed amperometric detection
IL interleukin
IMAC immobilized metal affinity chromatography
IPTG isopyl-β, D-thiogalactopyranoside
IRAK IL-1 receptor associated kinase
ISA isosensitest agar
ISB isosensitest broth
Kdo 3-deoxy-D-*manno*-oct-2-ulosonic acid
Ko D-*glycero*-α-D-*talo*-oct-2-ulosonic acid
L-Ara4N 4-amino-4-deoxy-*β*-L-arbinose
LB Luria Broth
LC-ESI-MS liquid chromatography - electrospray ionization mass spectrometry
LMW low molecular weight
LPB LPS binding protein
LPS lipopolysaccharide
MIC minimum inhibitory concentration
MLST multi locus sequence typing
MRSA methicillin-resistant *Staphylococcus aureus*
MyD88 myeloid differentiation factor
NA nutrient agar
NAD^+/NADH nicotinamide adenine dinucleotide
NB nutrient broth
NEB New England Biolabs
NHS *N*-hydroxysuccinimide
ORF open-reading frame
PBS phosphate buffered saline
PCR polymerase chain reaction
PET phosphoethanolamine
PFGE pulsed-field gel electrophoresis
PIA *Pseudomonas* isolation agar
PMB polymyxin B
QS quorum sensing
RFLP restriction fragment length polymorphism
RT reverse transcriptase
SAM S-adenosyl methionine
SCFM synthetic CF sputum medium
SDS sodium dodecyl sulfate
smp sodium-m-periodate
SOB super optimal broth
SOC super optimal broth with catabolite repression
SOD superoxide dismutase
Sulfo-NHS-biotin *N* – hydroxysulfosuccinimide
TAE tris-acetate-EDTA
TCS two-component system
TEMED *N,N,N*,N-tetramethyl-ethane-1,2-diamine
TFA trifluoroacetic acid
TMHMM Tied Mixture Hidden Markov Model
TLR toll-like receptor
TNF tumor necrosis factor
UDP uridine diphosphate glucose
Ugd UDP-glucose dehydrogenase
Upp undecaprenyl phosphate
VRE vancomycin-resistant *Enterococcus faecium*
YE yeast extract
$ZnIm_2$ zinc imidizolate

Abstract

Cystic fibrosis (CF) is the most common life-threatening monogenic autosomal recessive disease in Caucasians, and results from mutations in the *cftr* gene. These mutations lead to an immuno-compromised lung, pancreatic insufficiency, bilary disorders, infertility and diabetes. The inability to clear respiratory pathogens and chronic lung damaging inflammation are the major causes of mortality in CF patients. From the relative narrow spectrum of opportunistic bacteria able to infect the CF lung, members of the *Burkholderia cepacia* complex (Bcc) are arguably the greatest cause of anxiety for CF patients and their carers. Originally described as onion pathogens the Bcc have emerged as major pulmonary pathogens of CF patients over the past three decades. The worst-case scenario is the onset of a fatal necrotizing pneumonia with bacteraemia, known as "cepacia syndrome", that occurs in 20% of all infected CF patients. In addition, Bcc are inherently resistant to all classes of antibiotics and antimicrobial peptides (AMPs) with the result that successful treatment of cepacia syndrome is rare.

The Bcc genomes display a number of putative virulence factors, none of which has been unequivocally and solely associated with CF lung infection. However, as the main problem of Bcc infections is without question the virtually untreatable chronic inflammatory airway infection which leads to the fatal deterioration of the lung, a number of Bcc-specific virulence factors are thought to be involved in bacterial pathogenesis. Here we investigated two Bcc putative virulence factors; exopolysaccharides (EPS) which play roles in enhanced pulmonary persistence, and lipopolysaccharides (LPS) which causes pulmonary inflammation and have been linked to extremely high cationic AMP resistance. The aims of this thesis were: first, to investigate induction of EPS biosynthesis of the Bcc in response to the original onion host; second, to investigate the structure of *B. cenocepacia* LPS, and to characterise enzymes involved in LPS modification.

Members of the Bcc, previously described as non-mucoid, produced copious amounts of EPS when onion extract was provided as a sole nutrient. When

investigating the onion extract content, it was found that fructose, sucrose and alcohol sugars were able to induce this change in phenotype. Interestingly, none of the virulent *B. cenocepacia* ET-12 isolates was able to produce EPS on any medium tested. This loss of EPS phenotype correlated with an 11 bp deletion in *bceB*, which is part of the *bce* gene cluster associated with the biosynthesis of cepacian, a previously characterised *Burkholderia* EPS. It has been proposed that instead of a non-mucoid to mucoid conversion, which is strikingly characteristic of *P. aeruginosa* infections in CF patients, members of the Bcc revert from a mucoid to a non-mucoid phenotype, suggesting a role for EPS in initial persistence, and that a loss of mucoidy may lead to increased virulence.

Bcc LPS has previously been shown to be constitutively modified with 4-amino-4-deoxy-β-L-arbinose (L-Ara4N). The enzymes involved in L-Ara4N biosynthesis were recently shown to be essential for *B. cenocepacia* viability. In this study, UDP-glucose dehydrogenase (Ugd) and 4-amino-4-deoxy-β-L-arbinose transferase (ArnT), the first and last enzymes of the biosynthetic pathway, were investigated. Of the three putative *ugd* genes detected in the *B. cenocepacia* J2315 genome, only two encoded enzymes with Ugd activity. $ugd_{BCAL2946}$ is required for full polymyxin B (PMB) resistance and is found in a gene cluster with LPS core modifying enzymes; and $ugd_{BCAM0855}$ is found in the *bce* cluster involved in EPS biosynthesis. Together, these two Ugds are essential for the viability of *B. cenocepacia*. $Ugd_{BCAM0855}$ is also able to compensate for the loss of $Ugd_{BCAL2946}$ *in vivo*. Only one *arnT* candidate gene was found in the *B. cenocepacia* J2315 genome, which was associated with the *arn* gene cluster. A conditional mutant of this *arnT* was previously shown to be essential for viability. In this present study, the protein expressed by the *B. cenocepacia* J2315 *arnT* appeared to restore growth of the *B. cenocepacia* conditional *ΔarnT* mutant XOA11 under repressive conditions, and was also able to restore resistance of a PMB sensitive *E. coli ΔarnT* mutant. Thus, the L-Ara4N biosynthetic enzymes may be an Achilles' heel of *B. cenocepacia*. Inhibitors to any of the enzymes in the L-Ara4N biosynthetic pathway could potentially be used alone, or in combination with other antimicrobial agents that would, under normal conditions, not be able to penetrate the outer membrane.

Table of Contents

Attached publications:

Bartholdson SJ, Brown AR, Mewburn BR, Clarke DJ, Fry SC, Campopiano DJ, John R. W. Govan. *Plant host and sugar alcohol induced exopolysaccharide biosynthesis in the Burkholderia cepacia complex*. Microbiology, 2008, 154: 2513 - 2521.

Loutet SA, **Bartholdson SJ**, Govan JRW, Campopiano DJ & Valvano MA. *Contributions of two UDP-glucose dehydrogenases to viability and polymyxin B resistance of Burkholderia cenocepacia.* Microbiology, 2009, 155: 2029-2039

Chapter 1: Introduction

1.1. Cystic Fibrosis

1.1.1 Molecular basis of cystic fibrosis

Cystic fibrosis (CF) is the most common severe monogenic autosomal recessive disease in Caucasians. With an incidence rate of 1 in 2500, there are presently around 8000 people in the UK with CF (www.cftrust.org.uk). CF results from mutations in the *cftr* gene which encodes the ABC transporter protein the cystic fibrosis transmembrane conductance regulator (CFTR). In healthy epithelial membranes, CFTR is essential to maintain ion and fluid homeostasis. CFTR is expressed in various organs, for example in the gastrointestinal, hepatobilary, reproductive and respiratory tracts. Its main function is to regulate liquid volume on epithelial surfaces through chloride secretion and inhibition of sodium absorption. CFTR has also been proposed to be involved in regulating other ion channels, HCO_3^- concentration, pH, endosome fusion and intravesicular trafficking, apoptosis and protection from cell transformation (Riordan, 2008). Mutations in the *cftr* gene can lead to different pathophysiological outcomes, affecting synthesis, processing or regulation of the CFTR, or producing a partly defective CFTR (Ratjen & Doring, 2003). Disease outcome can vary depending on the inherited mutation. To date there are 1604 different types of *cftr* mutations (www.genet.sickkids.on.ca/cftr/). The most common mutation is ΔF508, which is found in 70% of patients on at least one allele (www.ornl.gov/sci/techresources/Human_Genome/posters/chromosome/cftr.shtlm).
This malfunctional CFTR leads to impaired chloride secretions and enhanced sodium absorption, dehydration and plugging of mucous secretions in ducts of exocrine glands. This can lead to pancreatic insufficiency, bilary disorders, infertility and diabetes and provide an immuno-compromised lung environment suitable for chronic airway infection by opportunistic infections. Inability to clear respiratory pathogens and chronic lung damaging inflammation are the major causes of mortality in CF patients.

1.1.2 Diagnosis, pathophysiology and prognosis for CF patients

In the UK, and increasingly elsewhere, all newborn babies are screened for CF with a Guthrie blood spot test, which screens for raised levels of immunoreactive trypsinogen; that is followed by a sweat test if positive (Davies *et al.*, 2007), and identification of a CF mutation via buccal cells (de Vries *et al.*, 2006). Today, early diagnosis, aggressive nutritional rehabilitation and high dose antimicrobial chemotherapy have improved prognosis significantly and a person with CF can now live until the age of 50 years, although the average life expectancy is 31 years (Davies *et al.*, 2007).

CF affects the upper and lower airways, pancreas, bowel and reproductive tracts, but it is lung infections that are the most problematic and potentially fatal. With a non-functional CFTR, the lung environment is prone to opportunistic infections, and there are several hypotheses as to why that is: for example, some believe that CFTR-induced inflammation precedes infection; or that pH changes result in altered epithelial receptors enabling bacteria to bind and colonise (Ratjen & Doring, 2003). A recent study by Teichgraber and colleagues showed that, in a mouse model, a dysfunctional CFTR leads to more alkaline pH which was associated with increased levels of ceramide in the lung, which correlated with constitutive inflammation in an uninfected lung and also increased the susceptibility of *Pseudomonas aeruginosa* infection (Teichgraber *et al.*, 2008). Additionally, Hamai *et al.* showed that decreased CFTR expression or expression of a defective CFTR results in increased sphingolipid synthesis and affects ceramide composition, perhaps to increase membrane stability (Hamai *et al.*, 2009). Other hypotheses are the inactivation of salt-sensitive cationic antimicrobial peptides (AMPs), such as defensins, and the isotonic fluid depletion hypothesis (Ratjen & Doring, 2003). In the first case, it is believed that increased sodium levels in the airway surface fluid impair the activity of charged peptides of the host immune system, thus limiting a major antimicrobial lung defence. However, there is growing consensus that the most important defect is the impaired mucociliary clearance due to depleted periciliary liquid and increased mucus viscosity, enabling bacteria to attach and colonise in the mucus.

In healthy individuals, inhaled bacteria encounter the mucus blanket lining the major airways, and are either destroyed by epithelial defences or efficiently removed by mucociliary clearance, then swallowed and destroyed by stomach acids. In the CF lung the mucus blanket is dehydrated and mucociliary clearance is impaired enabling opportunistic bacteria to colonise. In addition, these CF pathogens have evolved ways of resisting the other innate immune defences of the lung.

Several studies have implicated direct roles for the wild type CFTR protein in the innate immune response. For example, it has been shown that CFTR acts as an epithelial receptor for binding, internalising and clearing of *P. aeruginosa* infection, and that the *cftr* mutations lead to impaired endocytosis and increased bacterial burden in the CF lung (Pier *et al.*, 1997)). In addition, an intact CFTR is involved in regulating phagosome acidification in macrophages aiding effective killing of bacteria (Di *et al.*, 2006).

The major pathophysiological outcome of CF lung infection is the repeating cycle of inflammation due to bacterial aggravation, imbalance between proteases and protease inhibitors, pro- and anti-inflammatory cytokines and probably oxidants and antioxidants (Tummler & Kiewitz, 1999). The fact that bacteria cannot be cleared leads to expression of tissue damaging neutrophil elastase and increased number of neutrophils which eventually leads to frustrated phagocytosis and neutrophil breakdown and release of high molecular weight DNA that increase viscosity of the secretions which contribute to the reduced mucociliary clearance (Gibson *et al.*, 2003). This vicious circle of inflammation leads to lung tissue damage and eventually loss of lung function.

A last resort for many patients is lung transplantation. However, depending on infection status, all patients are not offered this option. For example, patients infected with species from the *Burkholderia cepacia* complex (Bcc) are excluded from the transplant list. Unfortunately, Bcc infected individuals are also excluded from all ongoing clinical trials.

Treatment of many CF pathogens is difficult and requires combinations of aerosolised and intravenous antibiotics, anti-inflammatory agents and osmolytes to improve mucociliary clearance. These treatments are time-consuming, unpleasant and involve repeated hospital visits. In general, current treatments at best slow the decline of lung function.

Antimicrobial peptides, such as aerosolised colistin (polymyxin E), in combination with ciprofloxacin are being used strategically against early *P. aeruginosa* infection (Hoiby *et al.*, 2005); macrolides are also used to reduce inflammation (Taccetti *et al.*, 2008). Hypertonic saline is widely used to improve mucociliary clearance, but hexitols are currently in clinical trials as a more pleasant tasting alternative (Daviskas *et al.*, 2005; Wills, 2007; www.pharmaxis.com.au). Ongoing research focuses mainly on gene therapy (Griesenbach & Alton, 2008). Since CF is a single gene defect, gene therapy should in theory work. However, until this technology delivers a clinically useful method able to control the expressing gene stably in the correct organs, antimicrobial therapy is the best option.

1.1.3 Identification of CF pathogens

There are surprisingly few opportunistic pathogens that are able to infect the CF lung. Generally, *Staphylococcus aureus* and *Haemophilus influenzae* are most common in infants and young children. *P. aeruginosa,* which is the major CF pathogen, infects children and young adults, and later adult infection can be caused by members of the Bcc, *Stenotrophomonas maltophilia, Alcaligenes xylosoxidans*, non-tuberculous mycobacteria and fungi including *Aspergillus* spp. (Tummler & Kiewitz, 1999)

Once established in the CF lung, some of the pathogens become very problematic. These include mucoid *P. aeruginosa* and multi-drug resistant and highly transmissible strains of the Bcc. It is crucial that these isolates are correctly identified as misidentification can have detrimental consequences in terms of incorrect treatments, potential segregation and transplantation issues.

Identification of CF pathogens is normally based on sputum bacteriology. This can be challenging and may require the aid of reference laboratories. A combination of phenotypic, genotypic and biochemical tests are carried out to ensure correct identification, but even then it can be very difficult to identify certain isolates. An up to date knowledge of microbial taxonomy plays a major role in bacterial identification and developing genotyping methods to characterise individual strains for epidemiological studies. Today the gold standard genotyping methods are considered to be pulse-field gel electrophoresis (PFGE) and multi locus sequence typing (MLST). These are both time consuming and expensive to use and require analysis expertise.

1.2. The *Burkholderia cepacia* complex

Table 1: The *Burkholderia cepacia* complex

Genomovar I	***B. cepacia***
Genomovar II	***B. multivorans***
Genomovar III	***B. cenocepacia***
Genomovar IV	***B. stabilis***
Genomovar V	***B. vietnamensis***
Genomovar VI	***B. dolosa***
Genomovar VII	***B. ambifaria***
Genomovar VIII	***B. anthina***
Genomovar IX	***B. pyrrocinia***
Genomovar X	*B. ubonensis*
Genomovar XI	*B. latens*
Genomovar XII	*B. diffusa*
Genomovar XIII	*B. arboris,*
Genomovar XIV	*B. seminalis*
Genomovar XV	*B. metallica*

In this thesis, "Bcc" refers to Genomovar I-IX (in bold) as Genomovar X-XV have only recently been added to the complex and have not been previously investigated.

1.2.1 Taxonomy

B. cepacia is a Gram-negative bacterium which was first identified by Burkholder in 1950 as the causative agent of soft rot of onions (Burkholder, 1950). It was given the name *Pseudomonas cepacia* due to its phenotypic resemblance to *P. aeruginosa.*

With improved taxonomic methods *P. cepacia*, as well as closely related *Pseudomonas mallei* and *Pseudomonas pseudomallei,* were re-classified as *Burkholderia* (Yabuuchi *et al.*, 1992). Vandamme and colleagues then found that the species *B. cepacia* is in fact a group of genetically distinct species, initially referred to as genomovars (Vandamme *et al.*, 1997). This group, named the *Burkholderia cepacia* complex (Bcc) currently consists of 15 closely related species (Table 1) (Coenye *et al.*, 2003; Mahenthiralingam *et al.*, 2000; Vanlaere *et al.*, 2008). Since the identification of the last 6 species were published very recently, for the purpose of this thesis the term "Bcc" refers to the first 9 species of the complex.

1.2.2 Plant growth promotion, bioremediation and antifungal properties

Although the Bcc were originally described as plant pathogens, they also have many environmentally useful properties. The Bcc promotes growth of many important crops such as peas, maize, rice and wheat, and protects plants from fungal infections. They produce a variety of antifungal compounds such as cepacin, altercidins, pyrrolnitrin, cepacidins and siderophores (Berg *et al.*, 2005). On the other hand, a *Burkholderia* species was found to live as a symbiot inside the fungus *Rhizopus microsporus* and it was shown that a mycotoxin, believed to be produced by the fungus, was in fact produced by *Burkholderia* (Partida-Martinez & Hertweck, 2005).

Burkholderia species have demonstrated important bioremediation properties. For example, *B. vietnamiensis* G4 degrades trichloroethylene polluted ground water aquifers, *B. xenovorans* LB400 degrades polychlorinated biphenols and *B. phenoliruptrix* AC100 degrades 2,4,5-trichlorophenoxyacetate (O'Sullivan & Mahenthiralingam, 2005). As they are able to grow on a diverse range of carbon substrates they could be useful against oil and fuel industry contamination. Since these species are highly beneficial in the environment the US Environmental Protection Agency was asked to approve the use of members of the Bcc for bio control. This caused great debate due to the potential clinical hazard to immuno-compromised individuals. Early arguments were based on the premise that environmental and clinical Bcc were different. However, many clinical isolates of the

Bcc are in fact identical to strains found in the environment (Holmes *et al.*, 1998), and as the Bcc are not found in the commensal flora, they are likely to be directly acquired from the environment or nosocomially. The Bcc have been found in river water, in the rhizosphere, on onions and maize, but also in pharmaceutical solutions, detergents, on hospital equipment, in shampoo, cosmetics and toiletries as well as in industrial settings (Mahenthiralingam *et al.*, 2008). They can survive for long periods of time in solutions with high antibiotic concentrations or with minimal nutrients such as saline bags used in hospitals.

1.2.3 Clinical manifestations

The Bcc primarily infect patients with CF and chronic granulomatous disease (CGD). The outcome of CF and CGD is in both cases an immuno-compromised lung environment. CGD is caused by mutations in genes encoding subunits of the superoxide-generating NADPH oxidase in phagocytes, rendering these cells unable to perform oxidative killing (Heyworth *et al.*, 2003). In addition, Bcc are resistant to the other phagocytic killing mechanisms, including non-oxidative killing by cationic AMPs.

The clinical significance of *B. cepacia* infection in CF patients was first described in 1984 by Isles and colleagues, and has since emerged as a major CF pathogen (Isles *et al.*, 1984). The worst-case scenario is the onset of "cepacia syndrome" – a fatal necrotizing pneumonia with bacteraemia that occurs in 20% of all infected CF patients and which is very difficult to treat. In fact, there have only been three successful cases to date (Kazachkov *et al.*, 2001; Weidmann *et al.*, 2008) (Grimwood and Tweed, personal communication).

Within the Bcc, *B. cenocepacia* and *B. multivorans* are the most prevalent species in CF infections (Govan *et al.*, 2007). However, with the exception of *B. ubonensis*, all Bcc species have been recovered from CF lungs. The clinical outcome varies to some extent depending on species, and strains within a species. For example, regardless of strain, *B. cenocepacia* is associated with rapid decline in lung function and is the

species mostly associated with the "cepacia syndrome", whereas, *B. pyrrocinia, B. anthina* and *B. ambifaria* are rarely isolated and have not been shown to have the same detrimental effect as *B. cenocepacia* and *B. multivorans* (Reik *et al.*, 2005). Although *B. multivorans* is not considered to be as virulent as *B. cenocepacia*, some strains of *B. multivorans* have been responsible for serious outbreaks and multiple fatalities (Whiteford *et al.*, 1995). The severity of infection is thought to be related to the ability of the Bcc bacteria to invade respiratory epithelial cells and cause sepsis, which is more common for *B. multivorans* and *B. cenocepacia* (Keig *et al.*, 2002). However, *B. stabilis* can invade epithelial cells without any clinical manifestation (Schwab *et al.*, 2002).

Some Bcc strains have been shown to be particularly transmissible among patients. Outbreaks have mainly been associated with three distinct *B. cenocepacia* epidemic clones: the ET-12 clone, the PHDC clone and the Midwest clone, and particular strains of *B. multivorans*. The ET-12 lineage caused the largest epidemics in Canada and Europe in the late 1980s and throughout the 1990s (Govan *et al.*, 1993). Spread probably occurred at CF patient summer camps and from socialising in hospitals. The route of spread is thought to occur by aerosol droplet and direct physical contact or contaminated surfaces, or from contaminated disinfectants or the environment. Segregation of patients has been the only successful method to keep Bcc from spreading, a method with huge social and psychological implications for the patients (Govan *et al.*, 2007).

B. cenocepacia has been the most problematic species of the Bcc so far. Apart from being one of the most prevalent and most transmissible species, it is also the most difficult one to treat, and has been shown to lead to the highest post-transplant mortality (Murray *et al.*, 2008).

1.2.4 Putative virulence factors and survival mechanisms

The Bcc are known to have large genomes of 6-9 Mb distributed between multiple replicons. To date, over 30 *Burkholderia* genome sequencing projects have been

undertaken. The average size of each genome is 7.5 Mb containing approximately 7000 genes out of which 10% or more is foreign DNA acquired from horizontal gene transfer often associated with genomic islands, prophages and insertion sequences (Holden *et al.*, 2008; Mahenthiralingam *et al.*, 2008). A very useful website, www.burkholderia.com, currently contains 20 genomes with clinical and environmental isolates. A recent addition was the genome of the ET-12 isolate *B. cenocepacia* J2315 which was recently annotated and contains 3 chromosomes and a large plasmid amounting to 8 Mb (Holden *et al.*, 2008). This strain was isolated during the ET-12 outbreak in Edinburgh in 1989 and is the type strain for this clonal lineage of transmissible strains (Govan *et al.*, 1993). Studying the genomes of the Bcc species reveals many putative virulence factors, none of which have been proven to be directly responsible for the deterioration of the CF lung. Evidence from various model systems (mouse, rat, plant and nematode) has suggested the importance of individual virulence factors, but the results depend on the infection model used (Bernier *et al.*, 2003). In addition, studies of Bcc infections in CF patients also suggest a key role of host–pathogen interactions, since clinical outcome in individual patients cannot be predicted even during epidemic outbreaks when multiple patients are infected by the same strain (Govan *et al.*, 1993). However, various putative virulence factors have been investigated by a number of laboratory groups, and their roles are listed in Table 2 and summarised below.

To control expression of a variety of virulence factors and to adapt to different environments many bacteria use two-component regulatory systems (TCS) and quorum sensing (QS). Members of *Burkholderia* species contain amongst the highest number of two-component systems of any bacterial species (Alan Brown, personal communication). None of these have been looked at in detail, and little is known about *Burkholderia* virulence regulation. However, QS has been shown to play a role in the virulence and versatility of the Bcc and is involved in onion pathogenicity of *B. cepacia* ATCC25416 (Venturi *et al.*, 2004), and swarming motility, siderophore production and biofilm formation of *B. cenocepacia* clinical isolates (Huber *et al.*, 2001; Lewenza *et al.*, 1999; Lewenza & Sokol, 2001)). Interestingly, Bcc have been

shown to respond to *P. aeruginosa* quorum sensing molecules, and the two can co-exist in biofilms *in vitro* (Riedel *et al.*, 2001).

Exopolysaccharide (EPS) production and biofilm formation have been shown to be important in *P. aeruginosa* infections, and a role for EPS in the Bcc has been investigated recently. Bcc EPS had been shown to be involved in persistence in the lung (Chung *et al.*, 2003; Conway *et al.*, 2004), interactions with antimicrobial peptides (Herasimenka *et al.*, 2005) and the ability to scavenge reactive oxygen species and inhibit neutrophil chemotaxis (Bylund *et al.*, 2006). Eight different putative EPS gene cluster were found in the *B. cenocepacia* J2315 genome (Holden *et al.*, 2008), where of the best characterised is the conserved *bce* gene cluster (Moreira *et al.*, 2003). The *bce* genes encode enzymes for the biosynthesis of cepacian, which is a highly branched heptasaccharide repeating unit consisting of rhamnose, mannose, galactose, glucose and glucuronic acid (Fig. 2 (B) (Cescutti *et al.*, 2000)). Cepacian is the main EPS produced by the Bcc, although three additional EPSs have been isolated from some species (Cerantola *et al.*, 1996; Chiarini *et al.*, 2004).

The Bcc express a number of secreted virulence factors, for example haemolysins, proteases and lipases. In addition, four types of siderophores are produced: salicylic acid, ornibactin, pyochelin, and cepabactin (Mohr *et al.*, 2001). The Bcc have also been shown to have mucin-sulfatase activity, which enables them to degrade mucins for carbon sources to survive in the mucus (Schwab *et al.*, 2002).

The Bcc have been shown to be able to adhere to mucins and cellular receptors via pili and adhesins. The CblA cable pilus and the 22 kDa adhesin have been the most studied to date. The CblA is mainly associated with epidemic strains, and is in fact one of the ET-12 epidemic strain markers together with the genomic island associated *Burkholderia cepacia* epidemic strain marker (BCESM) (Mahenthiralingam *et al.*, 1997).

There is increasing evidence that epithelial cell invasion plays an important role in Bcc lung infections, which could explain the bacteraemia seen in association with the

capacia syndrome. Studies suggest that all members of the Bcc are capable of cell invasion, although, interestingly, *B. multivorans* and *B. cenocepacia* have generally been shown to be more invasive than the other species of the complex (Keig *et al.*, 2002).

Table 2: Putative virulence factors of the Bcc

Virulence trait	Features	References
Two-component regulatory systems (TCS)	Burkholderia species contain amongst the highest number of TCSs of any bacterial species	(Alan Brown, personal communication)
Quorum sensing (QS)	CepIR is conserved within Bcc, and BviIR is unique in *B. vietnamiensis;* Can respond to *P. aeruginosa* QS molecules and co-exist in biofilms *in vitro*	(Lewenza *et al.*, 1999; Malott & Sokol, 2007; Riedel *et al.*, 2001)
Flagella	*fliC* mutants show reduced invasiveness and *fliG* mutants how increase survival in rat agar lung infection model; immuno-stimulatory via TLR-5	(Tomich *et al.*, 2002; Urban *et al.*, 2004)
Adhesins and pili	22 kDa adhesin and CblA cable pilus	(Cheung *et al.*, 2007)
Transmissibility	*Burkholderia cepacia* epidemic strain marker (BCESM) and CblA	(Mahenthiralingam *et al.*, 1997)
Cell invasion and intracellular survival	Can survive in macrophages and amoeba; *B. stabilis, B. multivorans* and *B. cenocepacia* more invasive; survive using superoxide dismutase (SOD), peroxidases, catalases, nitric oxide detoxification	(Holden *et al.*, 2008; Lamothe *et al.*, 2004; Lamothe *et al.*, 2007; Lefebre & Valvano, 2001; Moura *et al.*, 2008; Valvano *et al.*, 2005)
EPS	cepacian biosynthesis and export cluster; 7 additional putative EPS gene cluster	(Holden *et al.*, 2008; Moreira *et al.*, 2003)
LPS	Unusual lipid A structure and inner core has Ko-Kdo; constitutive L-Ara4N modification, very immuno-stimulatory and is not neutralised by antimicrobial peptides	(Isshiki *et al.*, 1998; Shaw *et al.*, 1995; Shimomura *et al.*, 2003; Silipo *et al.*, 2007)
Antimicrobial resistance	Inherently resistant to all classes of antibiotics and antimicrobial peptides	(Holden *et al.*, 2008; Mahenthiralingam *et al.*, 2005)
Secretion	Type 1, II, III, IV, V and VI secretion systems	(Holden *et al.*, 2008)
Haemolysin	Induces degranulation and induces cell death in phagocytes	(Hutchison *et al.*, 1998)
Zinc metalloproteases	ZmpA is porteolytically active against type IV collagen, fibronectin, gamma interferon and neutrophil α-1 protease inhibitor	(Kooi *et al.*, 2005)
Siderophores	Salicylic acid, ornbactin, pyochelin and cepabactin	(Mohr *et al.*, 2001)

Members of the Bcc have been shown to survive within epithelial cells and macrophages, as well as amoeba, suggesting a potential environmental reservoir (Lamothe *et al.*, 2004; Valvano *et al.*, 2005). The Bcc can survive in macrophages despite the oxidative burst and they have been shown produce enzymes such as superoxide dismutase (SOD), catalase and catalase-peroxidase which contribute to resistance to reactive oxygen intermediates (Lefebre & Valvano, 2001).

Flagella have also been shown to be involved in invasion of epithelial cells (Tomich *et al.*, 2002) as a *fliG* mutant shows reduced invasiveness. However, a major role for flagella appears to be in the induction of the host immune response. A *fliC*II mutant of *B. cenocepacia* K56-2 survived a rat agar lung infection model whereas the wild type showed 40% mortality. Wild type flagella were also shown to directly stimulate interleukin-8 (IL-8) and NFκB through Toll-like receptor 5 (TLR5) (Urban *et al.*, 2004).

The main Bcc virulence factor proposed to induce immuno-stimulation is lipopolysaccharide (LPS). Bcc LPS has been shown to be as inflammatory as *Escherichia coli* and *Salmonella* LPS, except in IL-1β induction (Shimomura *et al.*, 2001). However, a study by Shimumura *et al* showed that *B. cepacia* LPS has an unusual interaction with the cationic AMP Polymyxin B (PMB). It binds tightly but is not neutralised like *Salmonella* LPS, instead IL-1β induction is elevated (Shimomura *et al.*, 2003). The LPS from the Bcc has also been shown to be four to five times more endotoxic and induce nine times more tumour necrosis factor (TNF) than *P. aeruginosa*, and a similar pattern was observed for IL-8 induction (Reddi *et al.*, 2003; Shaw *et al.*, 1995). The structure of *B. cenocepacia* J2315 LPS was recently determined (Fig. 1) and, together with studies of other Bcc species, suggests the common lipid A structure is a β-1-6-linked disaccharide of glucosamine, phosphorylated at position 1 and 4' with 4-amino-4-deoxy-*β*-L-arabinose (L-Ara4N) attached to the 1-phosphate, and acylated at the 2, 3, 2', 3' positions, with a secondary myristate on the distal glucosamine (De Soyza *et al.*, 2008; Silipo *et al.*, 2005; Silipo *et al.*, 2007). The inner core consists of a *Burkholderia* species specific

trisaccharide of L-Ara4N-(1→8)-D-*glycero*-α-D-*talo*-oct-2-ulosonic acid-(2→4)-3-deoxy-D-*manno*-oct-2-ulosonic acid (Ko-Kdo) which is linked to the distal glucosamine (Kdo-(1→6)-Glc*p*N) (Fig 4, (Gronow *et al.*, 2003; Isshiki *et al.*, 1998; Silipo *et al.*, 2007). The rest of the core is similar to that found in enterobacteria and contains L-α-D-Hep*p*-(1→7)-L-α-D-Hep*p*-(1→3)- [β-D-Glc*p*- (1→4)]-L-α-D-Hep*p* linked to the Kdo (1→5) (Isshiki *et al.*, 2003; Silipo *et al.*, 2007)).

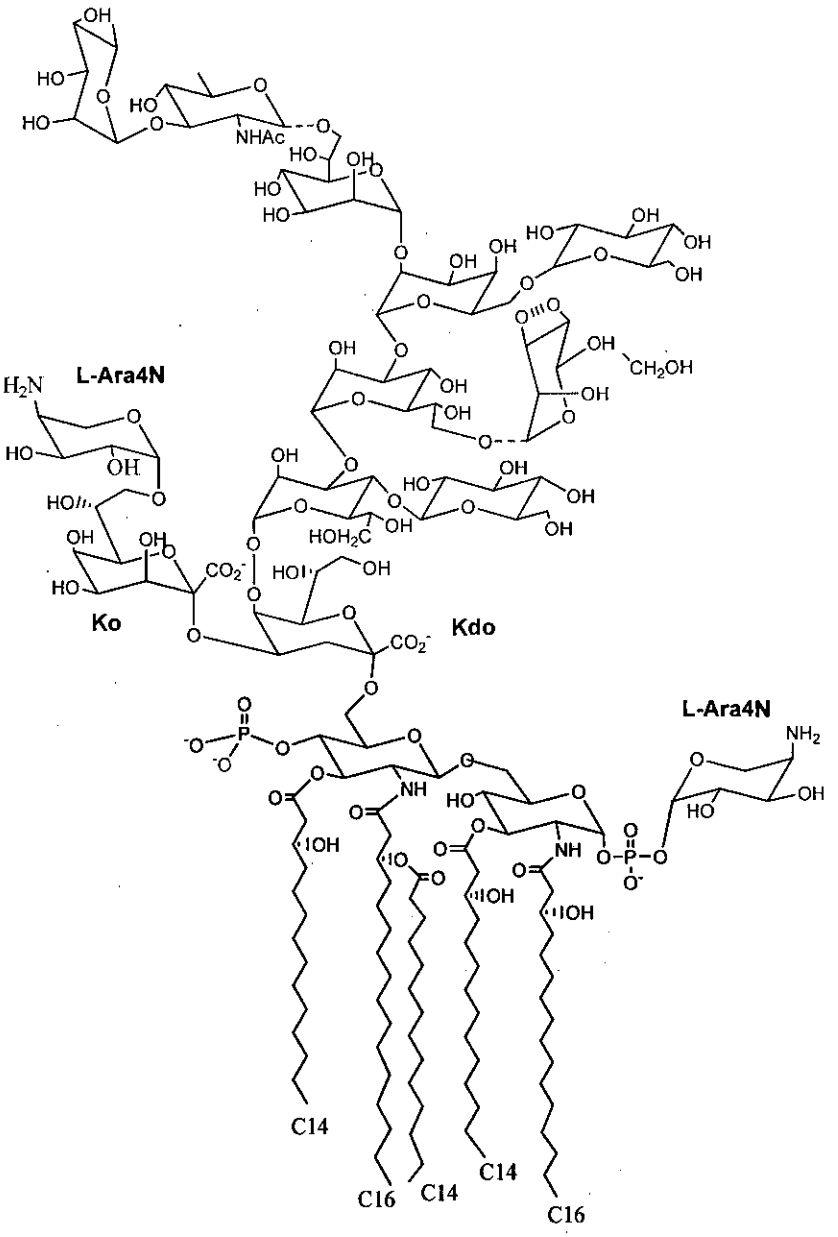

Fig. 1: The structure of the LPS from *B. cenocepacia* J2315 (Silipo *et al.*, 2007).

The O-antigen repeat of *Burkholderia cepacia* strain ASP B 2D was shown to be →2)-β-D-Rib*f*-(1→6)-α-D-Glc*p*-(1→ (Leone *et al.*, 2006), however, at least 16 different serotypes have been observed for the Bcc (Mahenthiralingam *et al.*, 2005) but with no correlation with genomovar status (Kenna *et al.*, 2003). The immuno-stimulatory abilities of the different genomovars have been compared by various groups, and although all species induce a similar response, some variations between and within the genomovars have been observed (De Soyza *et al.*, 2004; Moura *et al.*, 2008). Although many studies hint at clinical epidemic strains having higher endotoxicity than environmental strains, it has never been confirmed. The role of LPS of the Bcc is not only as an endotoxin, but also for membrane integrity and resistance mechanisms, in particular to AMPs, which will be discussed in detail below.

In addition to AMPs, the Bcc are resistant to practically all classes of clinically useful antibiotics. A striking illustration of this is *B. multivorans* ("eater of everything") which can ~~to~~ utilize Penicillin G as a sole nutrient (Beckman & Lessie, 1979). Resistance is species specific, with clinical isolates generally exhibiting broader resistance than environmental isolates. The genome of J2315 contains at least 4 β-lactamases and six different types of efflux systems (Holden *et al.*, 2008).

In summary, Bcc infection of the CF lung involves a complicated mixture of a variety of virulence factors and adaptation mechanisms. All virulence factors appear to some extent to be strain specific which makes it difficult to generalise for a species, nevertheless for the complex. The outcome of disease can differ enormously depending on what strain of Bcc is involved, but is also influenced by host factors. However, the main problem of Bcc infections is without question the virtually untreatable chronic inflammatory airway infection which leads to the fatal deterioration of the lung, and two likely virulence factors responsible for this are EPS for persistence and LPS for inflammation.

1.3. Exopolysaccharides

1.3.1 Role of bacterial exopolysaccharides

EPSs are produced by both Gram-positive and Gram-negative bacteria and generally exist in the form of capsules or slime, often associated with biofilms. Many bacterial species are believed to exist naturally in biofilms. Biofilms are often associated with nosocomial infections, for example, by biofilms forming on catheters and artificial hips (Mah & O'Toole, 2001). Many pathogenic bacteria use biofilm formation as a virulence factor, for example, *Streptococcus mutans* biofilms form dental plaque which eventually results in dental caries, and *Pseudomonas aeruginosa* exists as biofilms in the CF lung (see below). EPS capsules also contribute to virulence, and some examples of encapsulated bacteria are *Haemophilus influenzae type B, Streptococcus pneumoniae, Klebsiella pneumoniae, Neisseria meningitides* and *Burkholderia* sp. The main role of EPS during a bacterial infection is in protection against phagocytosis and antimicrobial agents, making it hard to treat bacteria once they convert to a mucoid phenotype.

However, there are also many industrial applications for extracted bacterial EPS, for example, as gelling agents, emulsifiers, heavy metal removers, or in enhanced oil recovery (Kumar *et al.*, 2007). As well as theses beneficial properties, there are also medicinal uses for EPS in anti-tumour, antiviral and arthritis treatments (Kumar *et al.*, 2007).

1.3.1 *Pseudomonas aeruginosa* alginate

It is well established that production of the EPS alginate is a main virulence factor of *P. aeruginosa*. In the CF lung, alginate forms complex biofilms in association with human mucin and neutrophil DNA, which reduce bacterial growth rate and act as a direct barrier against phagocytosis and opsonisation, and are involved in immuno-stimulation, adhesion and resistance to AMPs and reactive oxygen species (Govan & Deretic, 1996). Once *P. aeruginosa* converts to this mucoid phenotype it is associated

with repeated pulmonary exacerbations and decreased life expectancy, and is virtually impossible to eradicate. Alginate is a linear co-polymer of (1→4) linked β-D-mannuronic acid and α-L-guluronic acid ((Govan & Deretic, 1996) Fig. 2 (A)). Its biosynthesis overlaps with LPS biosynthesis, and this may explain why a loss of O-antigen is observed in mucoid isolates (Govan & Deretic, 1996). Alginate production can be induced in the CF lung but, with the exception of chronic bronchiectasis, is not generally observed during other *P. aeruginosa* infections (Govan & Deretic, 1996). Interestingly, variations in mucoidy are observed when bacteria are cultured on different media. For example, a strain can be mucoid on *Pseudomonas* Isolation Agar (PIA; Difco) but revert when grown on nutrient agar (Columbia Based agar, Oxoid), hence the media commonly used to identify *P. aeruginosa* is PIA (Govan & Deretic, 1996; Pugashetti *et al.*, 1982). Recently, Marvin Whitely and colleagues analysed sputum samples from CF patients and have developed a synthetic CF sputum medium (SCFM; (Palmer *et al.*, 2007)). They compared growth on SCFM with growth in sputum and found no significant differences in phenotype. This highlights the importance of the choice of virulence models and different media. The ability to use "host based" media should provide a more informative tool in understanding the mechanisms of CF lung disease.

1.3.2 *Burkholderia* exopolysacharides

EPS production is so far only a putative virulence factor for the Bcc. Bcc EPS in the form of mucoid colonial morphotypes is rarely seen in laboratory cultures, and no correlation has been observed between mucoidy and deterioration of the lung. However, Bcc EPS has been associated with altered clearance in a mouse model of infection (Chung *et al.*, 2003; Conway *et al.*, 2004), and EPS-deficient Bcc mutants displayed reduced mortality within a CGD mouse model (Sousa *et al.*, 2007). Similarly, a role for EPS in persistence in human airways is suggested by its capacity to scavenge reactive oxygen species and inhibit neutrophil chemotaxis (Bylund *et al.*, 2006). Bcc EPS has also been involved in interactions with antimicrobial peptides, although not as efficiently as *P. aeruginosa* alginate (Herasimenka *et al.*, 2005), and the formation of thick biofilms (Cunha *et al.*, 2004). Peeters *et al.* showed that Bcc

grown in biofilms are more resistant to antimicrobial compounds than planktonic bacteria (Peeters *et al.*, 2008). Recent studies (Richau *et al.*, 2000; Zlosnik *et al.*, 2008) have also challenged the previous belief that mucoid, EPS-producing colonial morphotypes of Bcc are rare in both environmental and clinical isolates (Govan & Deretic, 1996).

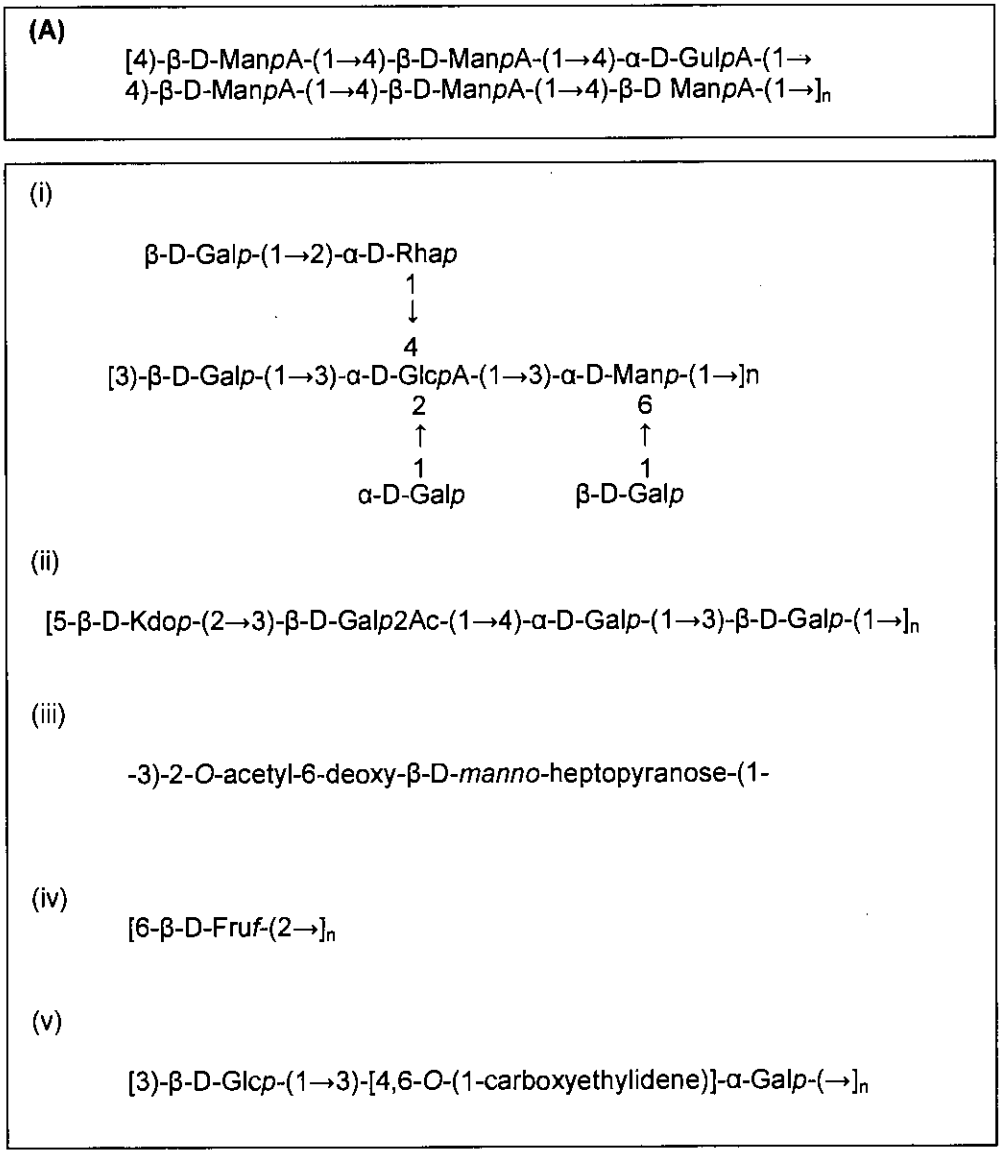

Fig. 2: Exopolysaccharides of the Bcc and *P. aeruginosa*. (A) *P. aeruginosa* alginate (Herasimenka *et al.*, 2005). (B) Bcc EPS: (i) cepacian (PSII) (Cerantola *et al.*, 1999; Cescutti *et al.*, 2000); (ii) homologous to main capsular polysaccharide of *B. pseudomallei* (Masoud *et al.*, 1997); (iii) *B. pseudomallei* and *B. mallei*

Studies have shown that mucoid Bcc isolates mostly synthesize one type of EPS in the form of a highly branched heptasaccharide repeating unit consisting of rhamnose,

mannose, galactose, glucose and glucuronic acid 1:1:3:1:1 (Fig. 2 (B); (Cescutti *et al.*, 2000). This EPS, now referred to as cepacian, was the second Bcc EPS whose structure was determined and was originally named PSII (Cerantola *et al.*, 1999). PSI was the first Bcc EPS structure with a repeating unit of equal amounts of glucose and galactose with pyruvate as a substituent (Fig. 2 (B) (Cerantola *et al.*, 1996)). The cepacian biosynthetic enzymes are encoded by the conserved *bce* gene cluster, and the biosynthetic pathway, as well as many of the enzymes have been well characterised (Ferreira *et al.*, 2007; Moreira *et al.*, 2003; Sousa, 2007; Videira *et al.*, 2005). In addition to cepacian and PSI, two other EPS have been isolated from the Bcc. One of these has previously been found in *B. pseudomallei,* which produces capsular EPS that have been shown to be involved in persistence and resistance to the host immune system (Reckseidler-Zenteno *et al.*, 2005; Reckseidler *et al.*, 2001). The main EPS produced by *B. pseudomallei* is a linear unbranched polymer of repeating units of galactose (KDO) and O-acetyl 3:1:1 (Fig. 2 (B) (Masoud *et al.*, 1997)). In addition, a gene cluster, *wcb*, was discovered in *B. mallei* that encodes the capsular EPS referred to as Type I O-PS (Fig. 2 (B) (DeShazer *et al.*, 2001)), also produced by *B. pseudomallei,* and was previously believed to be part of the O-antigen (Reckseidler *et al.*, 2001). The *wcb* gene cluster was recently found in *B. cenocepacia* J2315, but contained an insertion sequence in *wcbO*, encoding a putative EPS biosynthesis/export protein (Parsons *et al.*, 2003). This gene cluster was found on a genomic island on some, but not all, species of the Bcc. In addition to these EPSs, the common bacterial EPS levan has been found in members of the Bcc (Fig. 2 (B); (Chiarini *et al.*, 2004; Reckseidler *et al.*, 2001)). Finally, there are an additional 3 putative EPS gene clusters in the *B. cenocepacia* J2315 genome that have not been investigated (Holden *et al.*, 2008).

Although a potentially important virulence factor, the prevalence, exact role and contribution of Bcc EPS to CF lung disease is still not clear. Many different media have been used to enhance EPS production *in vitro*. The addition of glycerol or mannitol has been shown to increase EPS production of the Bcc in the laboratory (Sage *et al.*, 1990; Zlosnik *et al.*, 2008), but it is not clear if this reflects what occurs *in vivo*.

1.4. Lipopolysaccharides

1.4.1 Role of lipopolysaccharides in Gram-negative bacteria

LPS, or endotoxins, are major components of the outer membrane of most Gram-negative bacteria (Fig. 3), and are required for an intact cell envelope, resistance mechanisms and interactions with the host immune-system. The term "endotoxin" was coined by Richard Pfeiffer, who described a heat stable non-protein, non-secreted toxin of *Vibrio cholerae* that was still active in killed bacterial suspensions used for immunisation (Pfeiffer, 1892).

LPS consist of a hydrophobic anchor, lipid A, a non-repeating core oligosaccharide and often a distal O-antigen polysaccharide (Fig. 3). A strain containing O-antigen is referred to as "smooth", whereas a strain without O-antigen is "rough", originally based on their phenotypic appearance on agar plates. Mutants have been created that display LPS without both O-antigen and the outer core and these are referred to as "deep-rough" strains. These deep-rough strains contain the minimal required LPS for growth in most Gram-negative bacteria (Belunis *et al.*, 1995), although hypersensitive mutants lacking all core sugars have been isolated in *E. coli* (Meredith *et al.*, 2006). The lipid A structure is highly conserved among Gram-negative bacteria, whereas the outer core and O-antigen are variable. It is thought that O-antigen is not required for growth but has a protective role involved in complement neutralisation, phage interaction and serum resistance. Lipid A, on the other hand, is essential for survival and is an important structural component of the outer membrane. It is also important for immuno-stimulation and resistance to detergents and AMPs.

LPS is responsible for the fever symptoms during a Gram-negative bacterial infection. This is due its very potent immuno-stimulatory properties, which can lead to a dramatic induction of an inflammatory response that, if not regulated, will lead to toxic shock and sepsis. By preparing synthetic lipid A, Shiba and colleagues proved that the lipid A was the main immuno-stimulatory component of the LPS (Tanamoto *et al.*, 1984). This synthetic lipid A was shown to have identical endotoxic activities

to natural *E. coli* lipid A, and activity was shown to depend on phosphate groups and fatty acyl moieties (Galanos *et al.*, 1985).

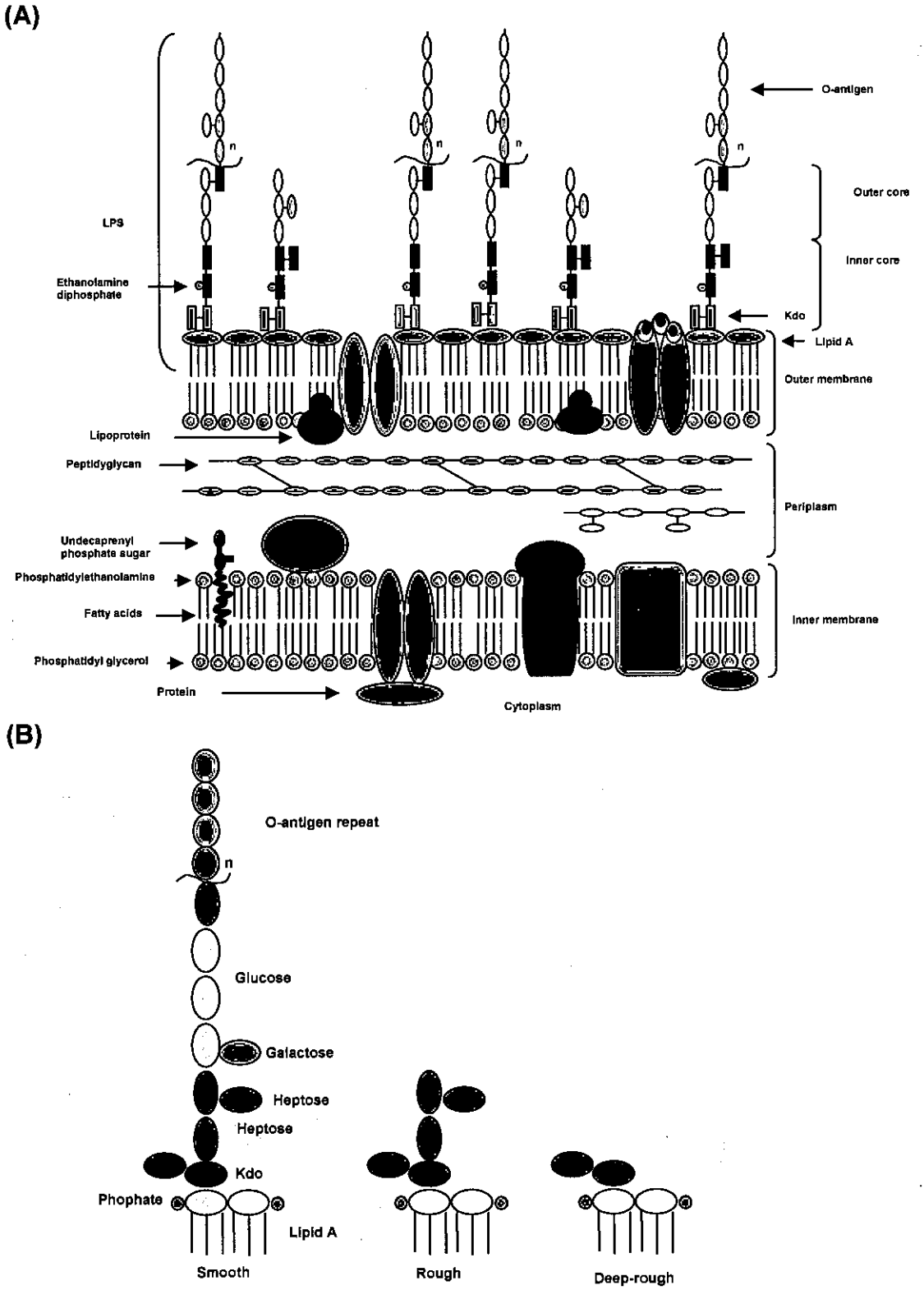

Fig. 3: **(A)** Schematic outer-membrane of *E. coli* and **(B)** lipopolysaccharide structures.

Lipid A generally interacts with the host immune system via TLR-4 receptors on innate immune cells, although *B. pseudomallei, Porphyromonas gingivalis* and *Leptospira interrogans* LPS have been associated with TLR-2 (Hirschfeld *et al.*, 2001; Werts *et al.*, 2001; Wiersinga *et al.*, 2007). The exact molecular details of the recognition of LPS and its mechanism of stimulation are not known, but a working model has been postulated: a LPS binding protein (LPB) in serum delivers LPS to CD14, which inserts the LPS into the TLR-4/MD-2 receptor complex. The LPS can then induce dimerisation of TLR-4 which activates the complex. This leads to activation of signalling cascades, such as the MAP kinase and NFκB-inducing cascades, via myeloid differentiation factor 88 (MyD88) and IL-1 receptor associated kinase (IRAK), which results in the production of an array of inflammatory cytokines and chemokines (Beutler, 2009; Erridge *et al.*, 2002).

An optimum core LPS structure for TLR-4 activation is a hexa-acylated diphosphorylated glucosamine disaccharide with fatty acyl chain lengths of C12-14, as illustrated by *E. coli* Kdo_2-lipid A (Fig. 6). The length and number of fatty acyl chains, as well as the presence or absence of phosphate groups, affect endotoxicity of the LPS isolated from other organisms. Some lipid A analogues, usually with fewer acyl chains, are in fact potent TLR4/MD2 antagonists. A study by Schromm et al. showed that a hexa-acylated lipid A with two phosphates was a better agonist than with one phosphate, and that penta or tetra acylated lipid A was antagonistic (Schromm *et al.*, 2000). Interestingly, the lipid A of the species that have been associated with TLR-2, for example *B. pseudomallei* and *Leptospira interrogans*, have less agonistic structures which may not be recognised by TLR-4 (Que-Gewirth *et al.*, 2004; Wiersinga *et al.*, 2007).

LPS also plays a major role in AMP resistance. Production of AMPs is part of the innate immune response in most plants and animals (Zasloff, 2002). Humans produce various different types, for example: defensins, cathelicidins and thrombocidins. These have been shown to recognize and inactivate microbial pathogens, as well as recruiting leukocytes and other cell types (by chemotaxis) to the site of infection and activating the adaptive immune response (Durr & Peschel, 2002).

In addition, many AMPs can bind and neutralize LPS during infection, hence inhibiting the cytokine response and the risk of endotoxic shock (Rosenfeld *et al.*, 2006). Their cationic and hydrophobic properties enable these peptides to disrupt the bacterial membrane by creating pores or leaks, leading to cell lysis (Brogden, 2005; McPhee & Hancock, 2005). Although, some pathogens can acquire resistance or are inherently resistant to AMPs, resistance is uncommon amongst pathogenic organisms, but is seen to some extent in commensal organisms. It has been proposed that these organisms provide protection by chronically stimulating the epithelia to express AMPs at levels that kill pathogens (Boman, 2000).

With increasing evidence of bacterial resistance, the natural product cationic AMP polymyxin (produced by *Paenibacillus polymyxa*) and its synthetic derivative colistin, have been useful clinically despite being toxic. Polymyxin is the main AMP used in research as it is a good model for AMPs and cheap to produce. However, to isolate and overproduce human, non-toxic AMPs would be ideal, and although it is technically difficult and expensive at the moment (Vargue, Morrison *et al.* in press) improvement in synthetic recombinant techniques should allow access to a range of novel peptides for future analysis. For example, one of the most cationic AMPs, human β-defensin 3 (HBD-3), has been shown to kill a broad spectrum of pathogens at micromolar concentrations including *P. aeruginosa*, multi-resistant *Staph. aureus* (MRSA) and vancomycin-resistant *Enterococcus faecium* (VRE) (Garcia *et al.*, 2001; Harder *et al.*, 2001). Garcia and colleagues claimed HBD-3 was active against the Bcc, but a conflicting, in-depth study was published using 23 different Bcc strains, all of which were highly resistant to HBD-3 (Sahly *et al.*, 2003). Importantly, all members of the Bcc remain uniquely resistant to all classes of AMPs.

A large number of studies have shown that AMP resistance occurs due to various chemical modifications of the lipid A that, in most cases, lead to neutralisation of the normally negatively-charged outer membrane. The different modifications are discussed in section 1.4.3.

1.4.2 Lipid A biosynthesis and transport

The *E. coli* lipid A is the best studied to date and provides an excellent model to understand molecular details involved in the conversion of a basic glucose precursor into the lipid core. The core LPS, Kdo_2-lipid A, is synthesised by 9 constitutively-expressed enzymes found in the cytoplasm and on the cytoplasmic face of the inner membrane (Fig. 4). This is referred to as *"the Raetz pathway"* (after Professor Christian Raetz, Duke University, North Carolina, USA, who has led this field for over 30 years) and homologues of most of these enzymes are found in all LPS-containing bacteria (Raetz & Whitfield, 2002; Raetz *et al.*, 2007).

Lipid A biosynthesis begins in the cytoplasm with the acylation of UDP-N-acetylglucosamine (UDP-GlcNAc) with R-3-hydroxymyristate by LpxA (Anderson *et al.*, 1993), followed by deacetylation of UDP-3-O-(acyl)-GlcNAc by LpxC (Young *et al.*, 1995) and a second fatty acyl chain is added by LpxD to form UDP-2,3- diacyl-GlcN (Kelly *et al.*, 1993). The peripheral membrane protein LpxH cleaves the pyrophosphate linkage of the UDP moiety to form 2,3-(diacyl)-GlcN-1-phosphate, also known as lipid X (Babinski *et al.*, 2002a; Babinski *et al.*, 2002b). LpxB then condenses lipid X with UDP-2,3- diacyl-GlcN, releasing UDP and creating the β,1'-6-linked disaccharide backbone (Radika & Raetz, 1988). The inner membrane protein LpxK adds a 4' phosphate generating the lipid A antagonist precursor lipid IV_A (Garrett *et al.*, 1997). Next the bifunctional enzyme KdtA adds two Kdo molecules (Belunis & Raetz, 1992; Clementz & Raetz, 1991), and LpxL and LpxM add secondary lauroyl and myrositoyl residues to the distal glucosamine unit (Clementz *et al.*, 1996; Clementz *et al.*, 1997). The complete product is referred to as Kdo_2-lipidA.

Though the overall pathway and the enzymes catalysing each step are generally conserved, there are slight variations between bacterial species. For example, the length of fatty acyl chains incorporated by LpxA can vary between C10 and C14 in different organisms (Anderson *et al.*, 1993; Odegaard *et al.*, 1997; Wyckoff *et al.*, 1998), and some bacteria lack LpxM and/or LpxL. Lack of LpxL can be compensated by the expression of an additional homologue LpxP, which incorporates palmitate

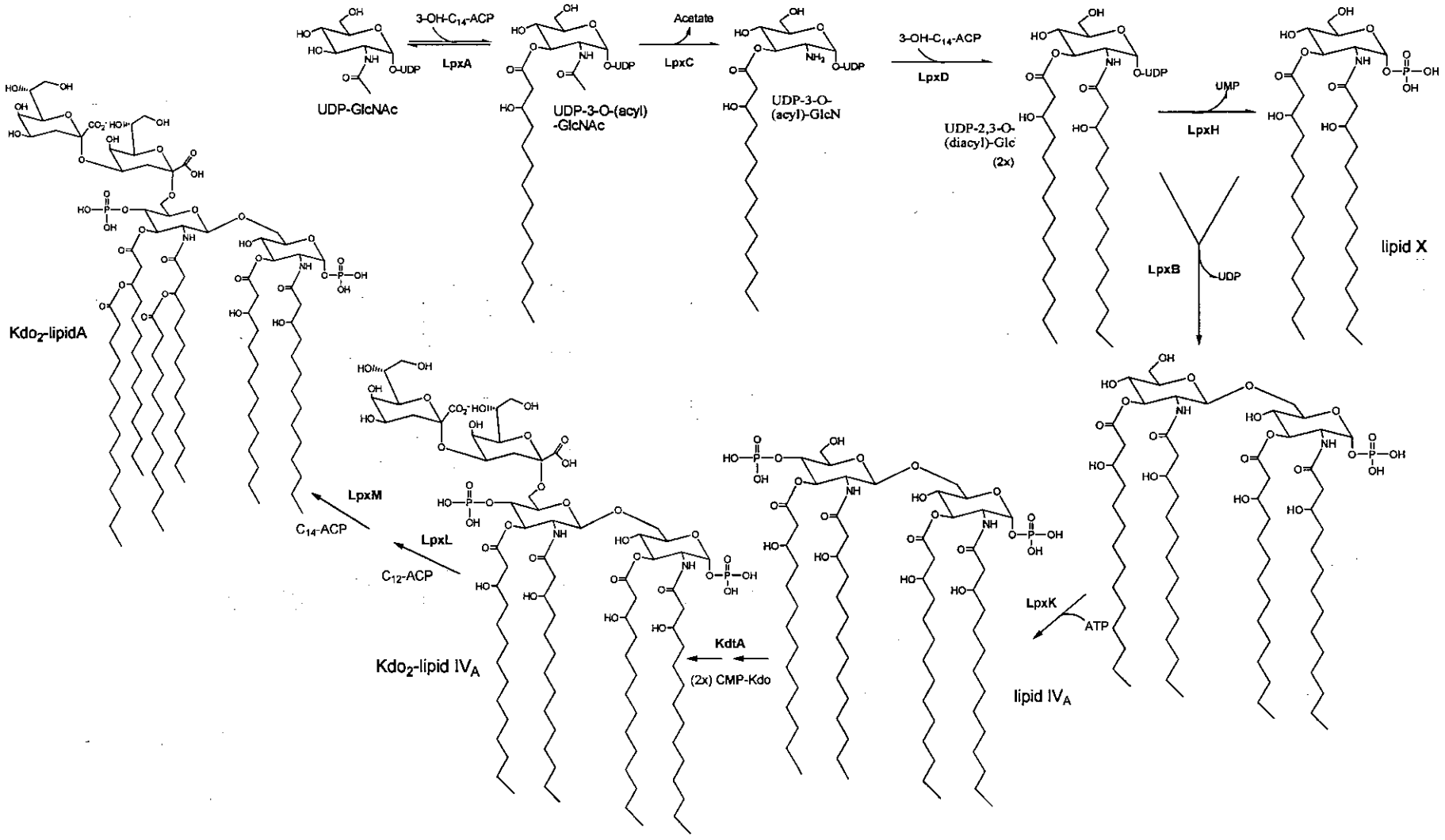

Fig. 4: The Raetz pathway: biosynthesis of Kdo2-lipid A in *E. coli*. Adapted from (Raetz *et al.*, 2007).

(C16) instead of laurate (C12) (Carty *et al.*, 1999; Montminy *et al.*, 2006). There are also differences in the Kdo incorporation, as some bacteria, for example, *Helicobacter pylori, Haemophilus influenzae* and *Vibrio cholerae* incorporate a single Kdo sugar (White *et al.*, 1997), and the LPS from other species contain a Ko molecule instead of a second Kdo, such as *Acinetobacter, Ralstonia* and members of the *Burkholderia species* (Vinogradov *et al.*, 1997; Zdorovenko *et al.*, 2008).

Because lipid A is an essential component of the outer membrane, the lipid A biosynthetic enzymes have been suggested as valid antibacterial drug targets. Interestingly, an LpxC inhibitor, CHIR-090, has shown potency against LpxC orthologues in *N. meningitidis, H. pylori, P. aeruginosa* and *E. coli* at nanomolar concentrations (Barb *et al.*, 2007).

Once synthesis of the Kdo_2-lipidA is complete, it is then transported across the inner membrane by the ABC transporter MsbA (Fig. 5). This transporter is essential and *msbA* knockouts in *E. coli* are lethal (Karow & Georgopoulos, 1993). Its essentiality and role as an LPS "flippase" was shown by Raetz and co-workers by creating a temperature sensitive point-mutant of the *E. coli msbA,* WD2, which is rapidly inactivated at 44 °C (Doerrler *et al.*, 2001). This mutant showed ~90% inhibition of lipid transport to the outer membrane by pulse-labelling and inner-membrane invaginations were observed by electron microscopy. Interestingly, lipid A modifications, believed to occur on the periplasmic face of the inner membrane, were also inhibited and these results further supported the role of MsbA as an inner membrane transporter. In addition, over-expression of MsbA can overcome LPS defects, such as Kdo-deficiency or under-acylation (Meredith *et al.*, 2006; Zhou *et al.*, 1998).

Once flipped to the periplasmic side of the inner membrane, the core and O-antigen are ligated to the lipid A and various species specific modifications can occur. These modification systems are discussed in detail in section 1.4.3.

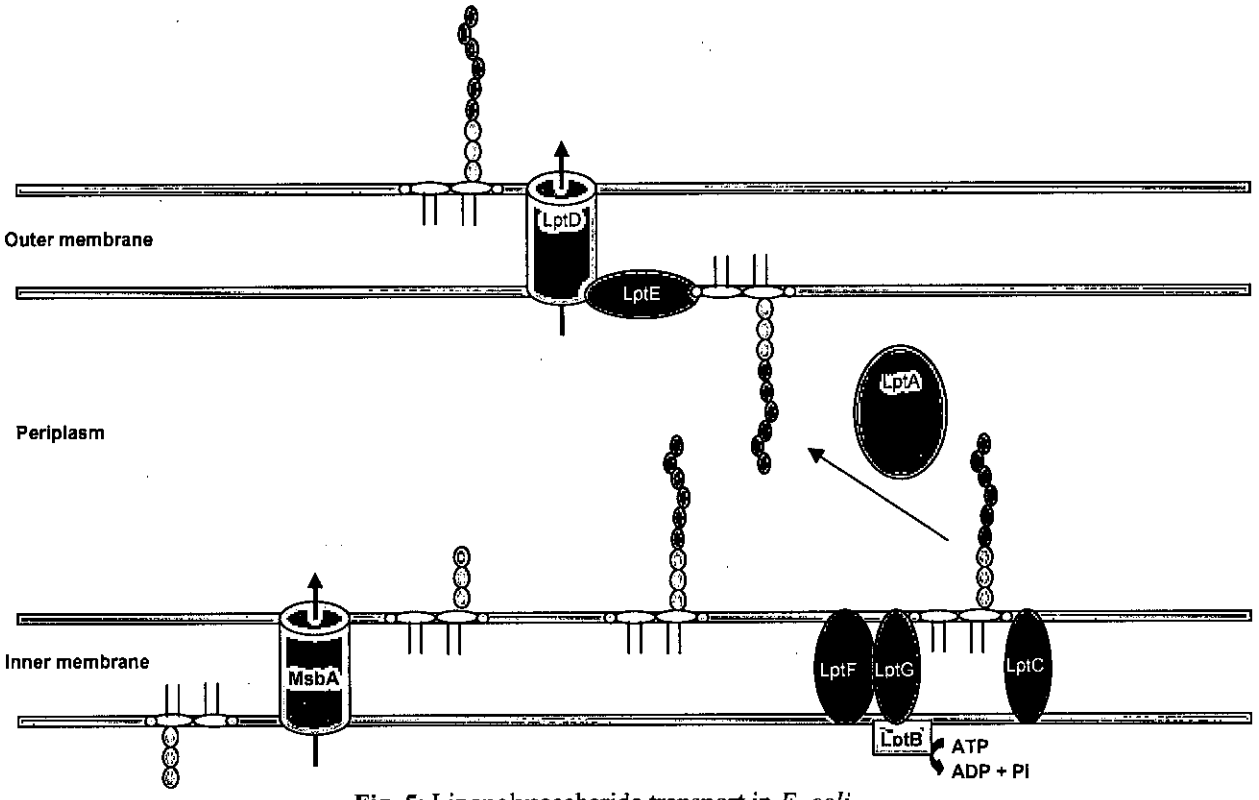

Fig. 5: Lipopolysaccharide transport in *E. coli*

It is still not fully understood how the hydrophobic lipid A is transported across the periplasm to the outer membrane. It was believed that so called Bayer bridges would form, providing contact sites between the inner and outer membrane (Bayer, 1968), however, these structures observed by electron microscopy could have been due to cell fixation method. A study by Sperandeo and co-workers described an ABC transporter system in *E. coli*, involving LptA and LptB (Sperandeo *et al.*, 2007), which showed similarity to the Lol system that transports lipoproteins across the periplasm (Tokuda & Matsuyama, 2004). *lptA* and *B* are co-transcribed in an operon which also contains *kdsC* and *D*, involved in Kdo biosynthesis (Sperandeo *et al.*, 2007). Conditional mutants, using an arabinose inducible promoter, showed growth depletion after 6 generations, and electron micrographs showed accumulation of membranous materials. This was confirmed by isopycnic sucrose density gradient centrifugation, after growing the mutants in N-acetyl[^{3}H]glucosamine, which revealed that the LPS did not reach the outer membrane, and accumulated in the periplasm (Sperandeo *et al.*, 2007). Raetz and co-workers recently showed that a temperature sensitive *lptA* mutant is completely defective in LPS export (Ma *et al.*, 2008). These

results indicate that LptA and B are both essential for *E. coli*. Another recent study showed that LptA is a periplasmic lipid A-specific binding protein (Tran *et al.*, 2008). Tran and co-workers suggest that to transport the lipid A to the outer membrane LptA and B work together with LptC, F and G as an "ATP-transporter" (Fig. 5). It is believed that LptB provides energy by hydrolysing ATP and LptB/F/G and possibly LptC release the LPS molecule from the inner membrane. Thereafter LptA binds lipid A and functions as a chaperone to transfer the LPS across the periplasm. Outer membrane proteins LptD and LptE then flip the LPS to the outer leaflet of the bacteria.

1.4.3 Lipopolysaccharide modification systems

Microbes have evolved various ways to evade the mammalian immune system as well as escape the pressure of antibiotic therapy. These avoidance/resistance strategies have been shown to be directly linked to their ability to covalently modify their lipid A core and outer structure. In most Gram-negative bacteria, for example *E. coli* and *Salmonella typhimurium*, a majority of these modifications are controlled by the TCSs PhoP/Q and PmrA/B.

A TCS consists of an inner membrane bound histidine kinase (PhoQ or PmrB) with an external loop to sense the periplasm, and a cytoplasmic response regulator (PhoP or pmrA) (Gunn, 2008). PmrA/B can be activated by PhoP/Q, but can also induce modifications independently (Soncini, 1996). Interestingly, *Francisella tularensis pmrA* exists as an orphan gene without a co-transcribed *pmrB* locus, but is still able to control modifications (Mohapatra *et al.*, 2007). These systems can be activated by growth of the bacteria in, for example, high Fe^{3+}, low Mg^{2+} and acidic pH (Groisman *et al.*, 1997; Wosten *et al.*, 2000).

Under repressed conditions, for example high Mg^{2+} and neutral pH, the acidic residues of the histidine kinase periplasmic sensor domain are bound to Mg^{2+} or other divalent cations. However, under acidic conditions or under Mg^{2+} limited conditions, it is thought that the lack of divalent cations bound to the sensor domain triggers a

conformational change where a conserved histidine is autophosphorylated and the phosphate is transferred to a conserved aspartate in the N-terminus of the response regulator, which then binds to specific recognition sites at promoters of regulated genes (Bader *et al.*, 2005; Gunn, 2008). These genes can modify the lipid A by adding positively charged L-Ara4N, phosphoethanolamine (PET) and/or adding/removing fatty acyl (FA) chains depending on growth conditions.

Acidic pH and a Mg^{2+} limiting environment are thought to be present inside macrophages, and it has been speculated that *Salmonella* have evolved to modify its LPS to be able to reside within macrophages. It has recently been shown that *S. typhimurium* grown inside RAW264.7 macrophages in the presence of ^{32}P, produced labelled lipid A that was extensively modified with L-Ara4N, PET, 2-hydroxymyristate and/or palmetate moieties (Gibbons *et al.*, 2005).

Bader and colleagues recently provided evidence that PhoQ can be directly activated by AMPs (Bader *et al.*, 2005). They propose that AMPs bind to the phosphate groups of the lipid A by displacing divalent cations to interact with the acidic residues of PhoQ. Bader *et al* showed that AMPs can displace divalent cations at low and intermediate Mg^{2+} levels, but not at high concentrations, suggesting that AMPs have evolved to compete with the divalent cations of the bacterial outer membrane. However, when the phosphate groups of lipid A are modified with, for example, positively charged L-Ara4N or PET, AMPs can no longer interact with PhoQ, rendering the bacteria resistant.

These modifications may also help control the electrostatic interactions of the outer membrane that would be disrupted upon depletion of divalent cations, that would normally bridge neighbouring negatively charged molecules (Bader *et al.*, 2005). Under Mg^{2+}-limiting conditions, modifications of the outer membrane allow the normally LPS-bound Mg^{2+} to be used for other cellular needs.

In contrast to enteric bacteria, it is possible that environmental non-pathogenic, or opportunistic bacteria, that would not have encountered AMPs of the immune system,

have evolved to adapt to low Mg^{2+} in aquatic environments, or high Fe^{3+} and aluminium concentrations in the soil, and are therefore able to resist AMPs. In addition, *Paenibacillus polymyxa*, the producer of the cyclic AMP PMB (Paulus & Gray, 1964), is a soil bacterium suggesting a need for other soil organisms to develop resistance to harmful secreted natural products.

Different bacteria have evolved to modify their lipid A in different ways, some of which are shown in Fig. 6.

The addition to positively charged L-Ara4N residues to the 1 or 4' phosphate position of the lipid A glucosamine disaccharide is associated with AMP resistance in many Gram-negative bacteria. In contrast, PET addition only appears to play a role in resistance in some pathogens, particularly those unable to synthesise L-Ara4N, for example *N. meningitides* (Tzeng *et al.*, 2005). Modification by PET is most probably involved in membrane stability, but does contribute to AMP resistance to some extent.

There are 6 different putative PET transferases encoded in *E. coli* (Raetz & Whitfield, 2002), and three of these have been identified. These catalyse the transfer of PET to the 1 and 4' phosphates (by EptA), the distal Kdo molecule (EptB) and on heptose sugars (CptA) of the core (Kanipes *et al.*, 2001; Lee *et al.*, 2004; Reynolds *et al.*, 2005; Tamayo *et al.*, 2005; Trent & Raetz, 2002). EptA has been shown to be regulated by PhoP/Q, however, EptB is induced by high Ca^{2+} concentrations, and *cptA* is constitutively expressed. Knocking out *eptA* has no significant effect on AMP resistance in *Salmonella*, but that could be because L-Ara4N is still produced in these mutants. Knocking *eptB* out in a deep-rough *E. coli* strain WBB06 results in hypersensitivity to Ca^{2+}, which could be suppressed by excess Mg^{2+}(Reynolds *et al.*, 2005). This shows that modification of the Kdo by PET is protective in a heptose deficient mutant, and that PET modifications in *E. coli* and *Salmonella* could play a major role in membrane permeability and serum resistance, as serum contains around 1 mM Ca^{2+}.

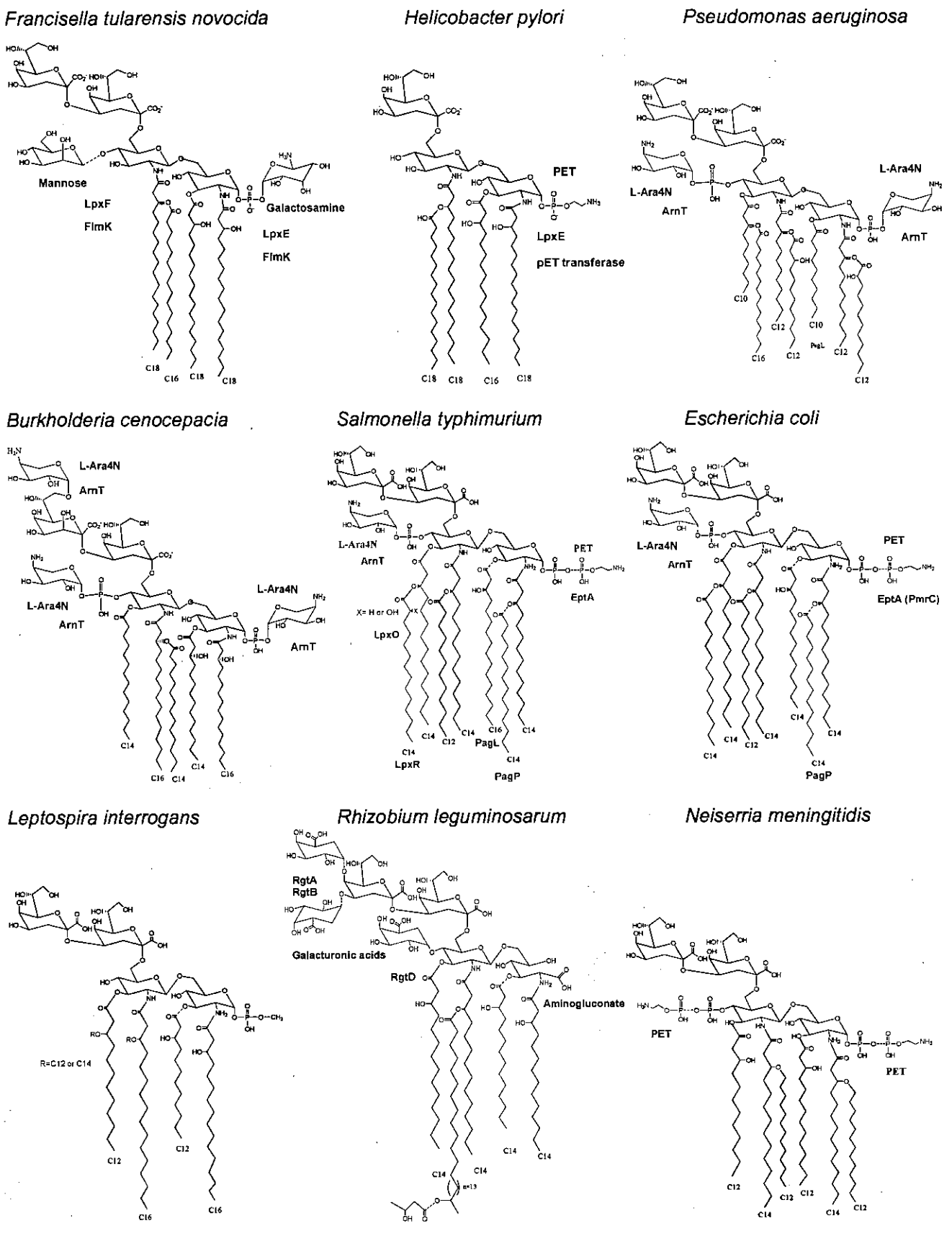

Fig. 6: Lipid A modifications in various Gram-negative bacteria. Blue structures can be added, and green structures removed, by various modification enzymes, shown in orange. The Ko of *Burkholderia cenocepacia* is shown in red.

Many species-specific peculiarities have been observed. For example, *N. meningitidis* lipid A is heavily modified with PET and is intrinsically resistant to AMPs even though it is unable to produce L-Ara4N, indicating a role for PET in AMP resistance in this organism (Tzeng *et al.*, 2005). It is unclear how these PET modifications are regulated.

Rhizobium leguminosarum, F. tularensis and *H. pylori* can remove a phosphate group instead of modifying it with positively charged groups (Karbarz *et al.*, 2003; Price *et al.*, 1995; Tran *et al.*, 2006; Vinogradov *et al.*, 2002). LpxE removes the 1 phosphate and LpxF the 4' phosphate. In *H. pylori*, removal of the 1 phosphate is followed by the addition of PET directly to the C-1 of the glucosamine (Tran *et al.*, 2004). Knocking LpxE out resulted in complete sensitivity to PMB indicating the need for dephosphorylation before PET addition (Tran *et al.*, 2006).

Some organisms can modify their lipid A with molecules other than PET and L-Ara4N. For example *Leptospira interrogans* methylates the 1 phosphate using S-adenosyl methionine (SAM) (Boon Hinckley *et al.*, 2005), and *F. tularensis* adds a galactosamine on the 1 phosphate and can add mannose directly to the 4'-C (Kanistanon *et al.*, 2008). *R. leguminosarum* lacks both phosphate groups and sometimes adds galacturonic acid on the 4'-C and the distal Kdo (Kanjilal-Kolar *et al.*, 2006; Kanjilal-Kolar & Raetz, 2006).

Many Gram-negative bacteria also modify their lipid A by adding or removing fatty acyl chains. The number and length of FA chains are important for both membrane stability and immuno-stimulation. For example, an increase in amide-linked acyl chains could provide further stability to the outer membrane under harsh conditions. *Salmonella* and *E. coli* will normally add palmitate (C16) by the PhoP/Q-induced palmitoyl-transferase PagP (Bishop *et al.*, 2000). Salmonella can also induce the esterase PagL which removes the 3-O-acyl chain (Kawasaki *et al.*, 2004), and under conditions of high Ca^{2+}, induce the deacylase LpxR which hydrolyses off the 3'-O-acyloxoacyl residue of lipid A (Reynolds *et al.*, 2006), possibly to evade recognition by the immune system. Many organisms have evolved to produce under-acylated LPS

to evade an immune response. For example, *H. pylori* and *F. tularensis* mostly have tetra-acylated LPS (Shaffer *et al.*, 2007; Stead *et al.*, 2008).

Interestingly, *Pseudomonas aeruginosa* has been shown to change its FA modification of its lipid A during CF infection (Ernst *et al.*, 2006). Environmental strains or strains from early/mild infection have penta or hexa-acylated LPS. Under these conditions PagL removes the 3-OH C10. However, this deacylase activity is lost during severe CF infection and hexa or hepta-acylated LPS is produced, increasing the inflammatory properties and causing more damage to the lung. This hepta-acylated CF LPS can be re-produced outside the CF lung by culturing the bacteria under Mg^{2+} limiting conditions (Ernst *et al.*, 2006).

A contradictory example to the theory that lipid A with fewer FAs are less immuno-stimulatory is Bcc LPS. Only penta or tetra-acylated Bcc LPS has ever been isolated, which is still highly immuno-stimulatory (De Soyza *et al.*, 2008; Ierano *et al.*, 2008; Silipo *et al.*, 2005; Silipo *et al.*, 2007).

Lipid A modifications are important for the bacteria to survive, but additional core and O-antigen modification can also contribute. Deep-rough mutants of *E. coli* are hyper-sensitive to AMPs and detergents, and a heptose-less *B. cenocepacia* mutant SAL-1 is not sensitive, but significantly less resistant to PMB (Loutet *et al.*, 2006), indicating a protective role for the core. In *E. coli* these heptose sugars of the core can be further phosphorylated by WaaP and WaaY (Yethon *et al.*, 1998). Addition of these negative charges on the inner core allows bridging of neighbouring LPS molecules by divalent cations, resulting in less fluid and more stable membrane. PmrA has also been shown to regulate resistance to complement killing by increasing O-antigen (Delgado *et al.*, 2006).

Interestingly, members of the Bcc and *Ralstonia sp.* do not phosphorylate their core (Zdorovenko *et al.*, 2008). Instead, the Bcc are extensively decorated with L-Ara4N (De Soyza *et al.*, 2008; Gronow *et al.*, 2003; Silipo *et al.*, 2007) which has been

shown to be not only essential for resistance but uniquely also for survival (Ortega *et al.*, 2007).

1.4.4 Aminoarabinose biosynthesis

L-Ara4N modification is an important resistance mechanism in many Gram-negative bacteria, and is directly associated with protection from AMP killing. In the majority of bacteria, for example *E. coli* and *Salmonella*, this resistance mechanism is regulated by PmrAB and can be switched on or off by various stimuli; however, some bacterial species, such as members of the Bcc, are constitutively modified with L-Ara4N and inherently resistant to AMPs.

In *E. coli* and *Salmonella*, the genes encoding the L-Ara4N biosynthetic enzymes are, with the exception of Ugd, found in an operon divided into two transcriptional units: *arnBCAD/arnTFE* (Fig. 7; (Breazeale *et al.*, 2002; Gunn *et al.*, 1998)). This locus was originally named the *pmr* locus because of its link to PMB resistance, but is now referred to as the *arn* locus due to its role in L-Ara4N biosynthesis. Homologues of these genes have been identified in the *B. cenocepacia* J2315 genome, however, the genetic organisation of the main locus is different, with the genes transcribed: *arnTG/arnBCA$_1$A$_2$D* (Fig. 7; (Ortega *et al.*, 2007)).

In *E. coli* and *Salmonella*, L-Ara4N biosynthesis (Fig. 7; (Raetz *et al.*, 2007; Yan *et al.*, 2007)) begins with the oxidation of UDP-glucose to UDP–glucuronic acid by UDP-glucose dehydrogenase (Ugd). The C-terminal domain of ArnA then catalyses the oxidative carboxylation of UDP-glucuronic acid to UDP-4-ketopenose (Breazeale *et al.*, 2002), which is converted to UDP-β-L-Ara4N by the transaminase ArnB (Breazeale *et al.*, 2003). Then the N-terminal domain of ArnA uses *N*-10-formylterahydrofolate to *N*-formylate UDP-β-L-Ara4N, which is selectively transferred to undecaprenyl phosphate (Upp) by ArnC (Breazeale *et al.*, 2005). The Upp-L-Ara4-formyl-*N* is deformylated by ArnD, and the product Upp-L-Ara4N is then flipped across the inner membrane by the heterodimeric flippase ArnE/F (Yan *et*

al., 2007), and the L-Ara4N is finally transferred from the Upp-L-Ara4N to lipid A by the L-Ara4N transferase ArnT (Trent *et al.*, 2001).

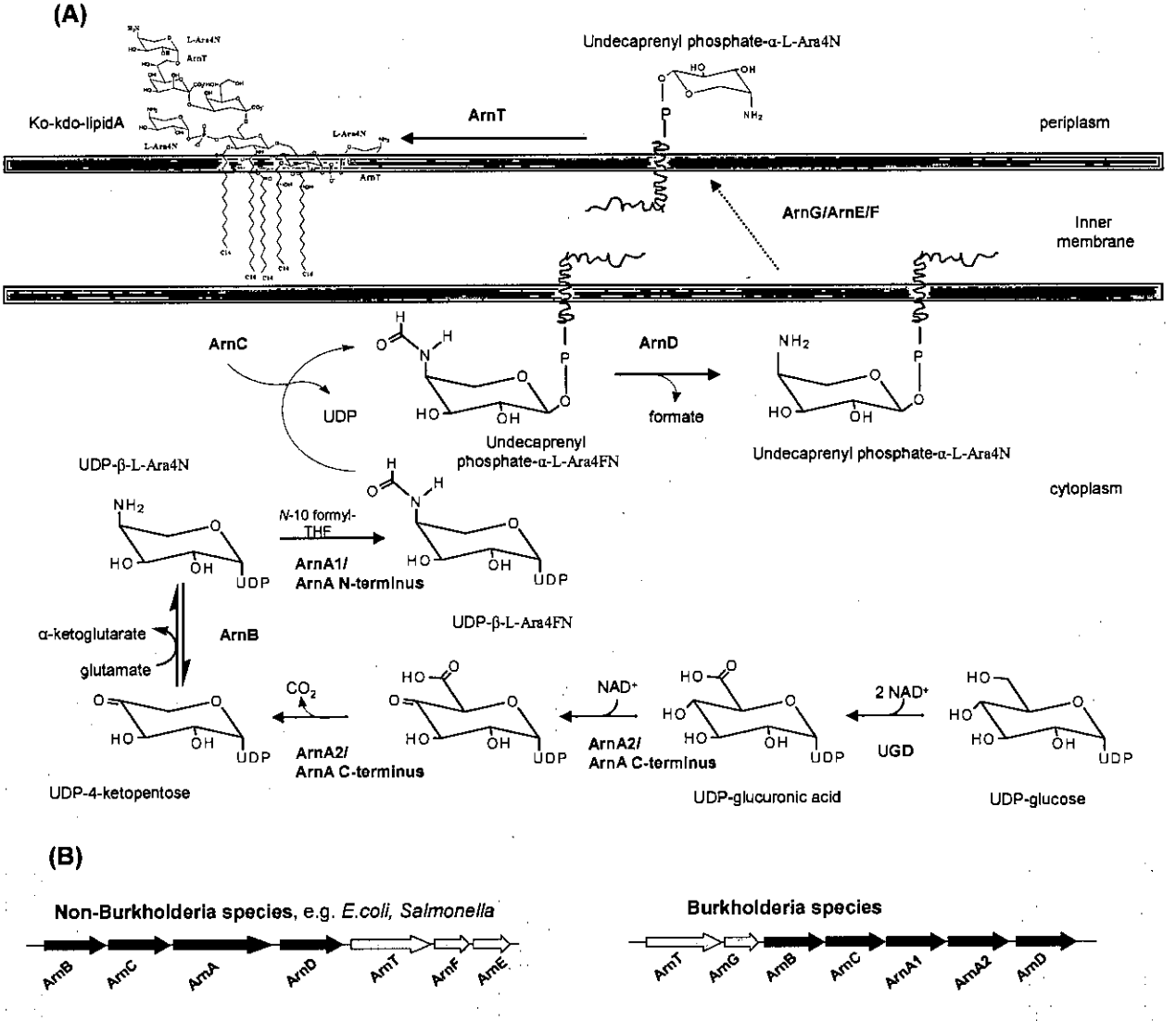

Fig. 7: Aminoarabinose biosynthesis (Yan *et al.*, 2007; Ortega *et al.*, 2007). **(A)** Proposed aminoarabinose biosynthetic pathway of *E. coli* (blue/black) vs. Bcc (red/black): **(B)** genetic organisation of the *arn* locus of non-*Burkholderia* species vs. *Burkholderia* species.

None of these enzymes have been characterised in *Burkholderia*, although *in silico* analysis suggests a similar pathway, but with some differences (Fig. 7). For example, ArnA, which is a bifunctional enzyme in *E. coli,* appears to be two separate enzymes in *B. cenocepacia*, ArnA1 and 2. In addition, it is likely that the flippase, which is a hetereodimer of ArnEF in *E. coli*, is a homodimer of ArnG in *B. cenocepacia*.

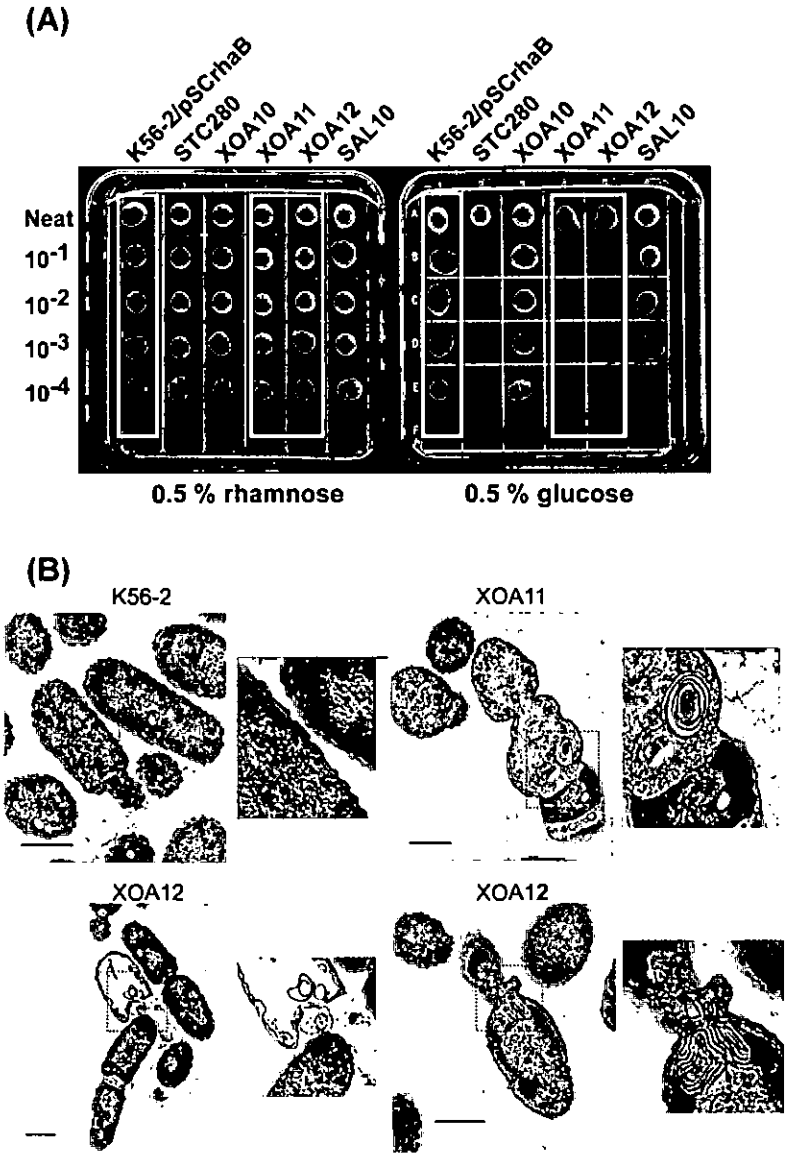

Fig. 8: Effect of conditional mutagenesis of the *arn* gene cluster (Ortega *et al.*, 2007). **(A)** Conditional lethal phenotype of strains XOA11 and XOA12 on M9 agar plates supplemented with 0.5% (w/v) rhamnose or 0.5% (w/v) glucose; **(B)** Transmission electron microscopy of strains K56-2, XOA11, and XOA12 after 8 h under non-permissive conditions.

In *E. coli* and *Salmonella*, knock outs of any of the above genes results in loss of resistance to PMB (Gunn *et al.*, 1998; Yan *et al.*, 2007). To prove the involvement of the *arn* locus in *B. cenocepacia* in AMP resistance, insertional inactivation attempts were carried out but none of the knock out strains survived (Ortega *et al.*, 2007). To investigate this further, Ortega and colleagues (in a collaboration between the Valvano, Govan and Campopiano laboratories) created conditional mutants of *B. cenocepacia* K56-2 by inserting a rhamnose inducible promoter upstream of ArnT

(XOA11) and ArnB (XOA12). Under permissive conditions (in presence of rhamnose), where the promoter is induced to transcribe the gene, the mutants behaved like wild type, but under non-permissive conditions (in presence of glucose), where the gene is not expressed, the conditional mutants displayed a significant loss in viability along with visible cell envelope defects (Fig. 8). Uniquely, this indicates that L-Ara4N synthesis is essential for viability of *B. cenocepacia* and provides an important potential Achilles heel for improved treatment of Bcc infections.

1.5. Aims

1.5.1 Exopolysaccharide investigation

Since the first description of pathogenicity of the Bcc was based on sour skin rot of onion bulbs, initial studies focused on growth on onion tissue extracts to investigate the "natural phenotype" of these organisms. Many strains of the different Bcc species are capable of infecting onions, some causing a stinky brown rot whereas others produce a colourless, slimy pathophysiology. To investigate the ability to grow on onions, "onion agar" was created by adding a homogenised, filtered onion extract to bacteriological agar. Interestingly, all strains tested were able to grow when this plant substrate was provided as the sole nutrient; in addition, many Bcc isolates, previously classified as nonmucoid, produced copious amounts of EPS.

The aim of this section was to investigate EPS production in all species of the Bcc in response to the onion substrate; to identify the onion component that induced the mucoid phenotype; and investigate the involvement of putative EPS gene clusters.

1.5.2 Lipopolysaccharides and AMP Resistance

1.5.2.1 Lipopolysaccharide extraction and analysis

The LPS from the Bcc is chemically and biologically unusual. It has a tetra or penta acylated lipid A which has Kdo-Ko attached at position 6 of the distal glucosamine, and Ara4N attached to one or both phosphates and to the Ko. In addition, it has a non-phosphorylated core. Its structure would suggest that *Burkholderia* LPS should not be immuno-stimulatory; however, LPS from members of the Bcc have been shown to be as immuno-stimulatory as *E. coli* LPS (De Soyza *et al.*, 2004; Zughaier *et al.*, 1999). Since the chronic inflammation in the airways is a main problem in CF infections, understanding the unique character of Bcc LPS is important.

Our overall goals of this thesis were to characterise the unusual chemical and biological properties of the LPS from the Bcc. The aim in this section was to isolate smooth, rough and deep-rough LPS of *B. cenocepacia* ET-12 strains and analyse them by gel electrophoresis and different staining methods.

1.5.2.2 UDP-glucose dehydrogenase

Uniquely, amongst Gram-negative bacteria, the enzymes of the L-Ara4N biosynthetic pathway are essential for *B. cenocepacia* viability, which suggests these enzymes could be potential targets for specific antimicrobial agents.

The synthesis of UDP-L-Ara4N begins with the conversion of UDP-glucose to UDP-glucuronic acid catalysed by the enzyme UDP-glucose dehydrogenase (Ugd). Two *P. aeruginosa* Ugd enzymes were recently characterised and shown to be involved in L-Ara4N and EPS biosynthesis (Hung *et al.*, 2007). The authors suggest Ugd as a potential drug target which will decrease the organism's impermeability and hence provide access to other drugs.

The genome of *B. cenocepacia* J2315 contains three predicted *ugd* genes: $ugd_{BCAL2946}$, $ugd_{BCAM0855}$ and $ugd_{BCAM2034}$. In collaboration with Slade Loutet (University of Western Ontario, London, Canada) these three *ugd* genes were each insertionally inactivated to generate independent mutant strains. Only inactivation of $ugd_{BCAL2946}$ resulted in increased sensitivity to polymyxin B. This sensitivity could be overcome when either $ugd_{BCAL2946}$ or $ugd_{BCAM0855}$ but not $ugd_{BCAM2034}$ were expressed from plasmids. A conditional $ugd_{BCAL2946}$ mutant was created in a $\Delta ugd_{BCAM0855}$ background, and under repressive conditions, growth of the conditional mutant was significantly impaired; however, growth could be rescued by either $ugd_{BCAL2946}$ or $ugd_{BCAM0855}$, but not $ugd_{BCAM2034}$, expressed *in trans* (Loutet *et al.*, 2009).

The aim of this section was to purify and biochemically characterise the three putative Ugd enzymes and investigate their Ugd activity *in vitro*.

1.5.2.3 Aminoarabinose transferase

The last enzyme of the L-Ara4N biosynthetic pathway is the inner membrane protein aminoarabinose transferase, ArnT, which catalyses the transfer of L-Ara4N from undecaprenyl phosphate to the lipid A. There is only one clear putative ArnT in the *B. cenocepacia* J2315 genome rendering this enzyme a good drug target.

In this part of the work, the aim was to clone, express and purify recombinant *B. cenocepacia* ArnT. In addition, it was hoped to biochemically characterise this important Bcc enzyme.

Chapter 2: General Materials and Methods

2.1. Materials

2.1.1 Solutions and Buffers

Polymyxin B stock (10 mg ml^{-1}): one hundred mg polymyxin B sulfate (Calbiochem) was dissolved in 10 ml dH_2O and filter-sterilised through a 0.2 μm filter (Micropore). Final Polymyxin B concentrations are specified in different methods.

Trimethoprim stock (50 mg ml^{-1}): one hundred mg trimethoprim (Sigma) was dissolved in 2 ml DMSO and filter-sterilised through a 0.2 μm filter. Trimethoprim was used at a final concentration of 50 μg ml^{-1} unless otherwise stated.

Tetracycline stock (5 mg ml^{-1}): 50 mg tetracycline (Sigma) dissolved in 10 ml 70% (v/v) ethanol and filter-sterilised through a 0.2 μm filter. Tetracycline was used at a final concentration of 25 μg ml^{-1} unless otherwise stated.

Gentamycin stock (50 mg ml^{-1}): 500 mg gentamycin (Sigma) dissolved in 10 ml dH_2O and filter-sterilised through a 0.2 μm filter. Gentamycin was used at a final concentration of 50 μg ml^{-1} unless otherwise stated.

Kanamycin stock (30 mg ml^{-1}): 300 mg kanamycin (Sigma-Aldrich) dissolved in 10 ml dH_2O and filter-sterilised through a 0.2 μm filter. Kanamycin was used at a final concentration of 30 μg ml^{-1} unless otherwise stated.

Ampicillin stock (100 mg ml^{-1}): one gram ampicillin sodium salt (Fluka-BioChemika) dissolved in 10 ml dH_2O and filter-sterilised through a 0.2 μm filter. Ampicillin was used at a final concentration of 100 μg ml^{-1} unless otherwise stated.

IPTG (isopropyl-β, D-thiogalactopyranoside; Apollo Scientific LTD): a 100 mM stock solution was prepared and filter-sterilised through a 0.2 μm filter. It was stored at 2-8 °C and used at a final concentration of 1 mM unless otherwise stated.

SDS (sodium dodecyl sulfate) sample buffer (2x): one ml of 1.5 M Tris (Trizma Base, Sigma), pH 8.0, 2 ml 100% (v/v) glycerol (Fisher Scientific), 2 ml 0.05% (w/v) bromophenol Blue (Sigma), 1.6 ml 10% (w/v) SDS (Sigma) and 0.4 ml β-mercaptoethanol (Sigma) were mixed and stored at room temperature.

SDS running buffer: 1xTGS buffer was made up in dH_2O (10 x stock, Bio-Rad) containing 25 mM Tris, pH 8.3, 192 mM glycine and 1% (w/v) SDS.

SDS stain: one gram Brilliant Blue R250 (Sigma), 400 ml methanol (Fisher Scientific), 100 ml acetic acid (Fisher Scientific) and 500 ml dH_2O were mixed and stored at room temperature.

SDS destain: 400 ml methanol, 100 ml acetic acid and 500 ml dH_2O were mixed and stored at room temperature.

TAE (Tris-Acetic acid-EDTA): 1xTAE buffer was made up in dH_2O (50 x stock, Bio-Rad) containing 40 mM Tris-HCl, 20 mM acetic acid and 1.0 M EDTA, adjusted to pH 8.3.

Ethidium Bromide (Sigma): a stock solution of 10 mg ml^{-1} was made up in dH_2O, and used at a final concentration of 5 μg ml^{-1}. The solution was stored at 2-8°C.

Saline: eight and a half grams of NaCl was dissolved in 1 litre dH_2O and sterilised by autoclaving at 121 °C for 15 minutes.

Transfer buffer (Western Blot): 25 mM Tris (Sigma), 150 mM glycine (Fisher Scientific), 10% (v/v) methanol (Fisher Scientific) in dH_2O

PBS (phosphate buffered saline): One phosphate buffered saline tablet (Dubelco A, Oxoid) was dissolved in 100 ml dH_2O and autoclaved at 121 °C for 15-20 minutes.

Binding buffer: 20 mM Tris (Sigma), 500 mM NaCl (Fischer Scientific), 5 mM Imidazole (Sigma), pH 7.5 in dH_2O.

Elution buffer: 20 mM Tris, 500 mM NaCl, 500 mM Imidazole, pH 7.5 in dH_2O.

2.1.2 Media

All liquid media and solid agars were autoclaved at 121 °C for 15-20 minutes.

Nutrient agar (NA): 15.6 g Columbia based agar (Oxoid) was dissolved in 1 L dH_2O.

Nutrient broth (NB): 25 g Nutrient Broth No2 (Oxoid) and 5 g yeast extract (DIFCO Laboratories) was dissolved in 1 L dH_2O.

Pseudomonas isolation agar (PIA): 45 g of *Pseudomonas* isolation agar (Difco) was dissolved in 1 L of dH_2O containing 20 ml of glycerol.

Isosensitest agar (ISA): 31.4 g Isosensitest agar (Oxoid) was dissolved in 1 L dH_2O.

Isosensitest broth (ISB): 23.4 g Isosensitest broth (Oxoid) was dissolved in 1 L dH_2O.

Luria Bertani (LB) agar: 35 g LB agar (Sigma) was dissolved in 1 L dH_2O.

LB broth: 10 g Bacto tryptone (Biogene), 5 g yeast extract (Fluka-BioChemika), 10 g NaCl (Fisher Scientific) was dissolved in 1 L dH_2O and adjusted to pH 7.5.

2YT broth: 16 g peptone, 10 g yeast extract and 5 g NaCl was dissolved in 1 L dH_2O and adjusted pH to 7.5.

S-Gal/LB/Amp plates: a pack of S-Gal™/LB Agar Blend (Sigma) was dissolved in 500 ml dH_2O. After autoclaving, ampicillin was added just before pouring the plates.

SOB (super optimal broth) medium: 20 g Bacto Tryptone (Biogene), 5 g Bacto Yeast Extract (Fluka-BioChemika) and 0.5 g NaCl (Fisher Scientific) was dissolved in 1 L dH_2O, adjusted to pH 7.5. After autoclaving, 2.5 mM KCl, 10 mM $MgCl_2$ and 10 mM $MgSO_4$ was added.

SOB agar: 20 g Bacto Tryptone (Biogene), 5 g Bacto Yeast Extract (Fluka-BioChemika) and 0.5 g NaCl (Fisher Scientific) was dissolved in 1 L dH_2O, adjusted to pH 7.5, then Bacteriological Agar (Oxoid) was added at 1.5% (w/v). After autoclaving, 2.5 mM KCl, 10 mM $MgCl_2$ and 10 mM $MgSO_4$ was added.

SOC (SOB with catabolite repression) medium: 20 g Bacto tryptone, 5 g yeast extract, 2 ml 5M NaCl, 2.5 ml 1M KCl (Fisher Scientific), 10 ml 1 M $MgCl_2$ (Fisher Scientific), 10 ml 1M $MgSO_4$ (Fisher Scientific), 20 ml 1 M glucose (Fisher Scientific), in 1 L dH_2O, adjusted to pH 7.5.

2.1.3 Instruments

DNA thermal cyclers for PCR amplification (Techne/Techgene, Applied Biosystems or Perkin Elmer), gel tanks for SDS-PAGE and DNA gel electrophoresis (Bio-Rad, Flowgen, Anachem), centrifuges (DuPont Instruments, Denley), FPLC: Äkta Basic100 (Amersham Biosciences), Cary 50 UV-Vis spectrophotometer (Varian), multipoint inoculator (Denley), sonicator (Soniprep 150) and electroporator (EasyjecT Plus, EQUIBIO, Flowgen), freeze drier (Edwards), rotary evaporator (Büchi B-480), heating block (Grant Instruments Ltd), sonicator bath (Sonicor).

2.1.4 Bacterial Strains and plasmids

All *E. coli* strains and plasmids used in this study are specified in Table 3.

Table 3: *E. coli* strains and plasmids.

Strain name	Relevant characteristics	Source/Reference
JM109	*end*A1, *rec*A1, *gyr*A96, *thi*, *hsd*R17 (r_k^-, m_k^+), *rel*A1, *sup*E44, Δ(*lac-pro*AB), [F′ *tra*D36, *pro*AB, *laq*I^{q}ZΔM15]	Promega
Top10^{TM}	F- *mcr*A Δ(*mrr-hsd*RMS-*mcr*BC) φ80*lac*ZΔM15 Δ*lac*X74 *rec*A1 *ara*D139 Δ(*araleu*) 7697 *gal*U *gal*K *rps*L (StrR) *end*A1 *nup*G	Invitrogen
DH5α	F- φ80*lac*ZΔM15 Δ(*lac*ZYA-*arg*F)U169 *rec*A1 *end*A1 *hsd*R17(rk-, mk+) *pho*A *sup*E44 *thi*-1 *gyr*A96 *rel*A1 λ-	Invitrogen
HMS174 (DE3)	K-12 derivative, F$^-$ *recA1 hsdR*(r_{K12}^- m_{K12}^+) (DE3) (Rif^R)	Novagen
BL21 (DE3)	B834 derivative, F$^-$ *ompT hsdS*$_B$(r_B^- m_B^-) *gal dcm* (DE3)	Novagen
BLR (DE3)	BL21 derivative F$^-$ *ompT hsdS*$_B$(r_B^- m_B^-) *gal dcm* (DE3) Δ*(srl-recA)306*::Tn*10* (Tet^R)	Novagen
Rosetta (DE3),	BL21 derivative , F$^-$ *ompT hsdS*$_B$(r_B^- m_B^-) *gal dcm* (DE3) pRARE (Cam^R)	Novagen
C41 (DE3)	BL21(DE3) derivative F$^-$ *ompT hsdS*$_B$ (r_B^- m_B^-) *gal dcm* (DE3)	(Miroux & Walker, 1996)
C43 (DE3)	C41 (DE3) derivative, expressing F-ATPase gene	(Miroux & Walker, 1996)
GT115	*F*$^-$ *mcr*A Δ(*mrr-hsdRMS-mcr*BC) 80*lac*ZΔM15 Δ*lacX*74 *rec*A1 *end*A1 Δ*dcm, uiad(MluI)::pir-116, sbcC-sbcD*	InvivoGen
MG1655	K-12 wild type, F$^-$, lambda$^-$, rph-1	Coli Genetics Stock Centre
WBB06	W3110 K-12 derivative *δ(rfa*CF)::*tet*σ	(Brabetz *et al.*, 1997)
AY103	W3110, *pmrA*^{c}, Δ*arnT*::*kan*, (Kan^R)	(Yan *et al.*, 2007)

Plasmid name	Relevant characteristics	Source/Reference
pGEM T-Easy	Cloning vector; Ap^r	Promega
pET28a	Expression vector, Kan^R	Novagen
pET22b	Expression vector, Amp^R	Novagen
pTrc99a	*trcP* vector, *lacI*^{q}, pUC18 *Eco*RI-*Hind*III polylinker region, Amp^R	(Amann *et al.*, 1988)
pRK2013	RK2 derivative, Km^r *mob*$^+$ *tra*$^+$ ColE1	(Figurski & Helinski, 1979)
pDA-17	*ori*pBBR1, Tet^R, *mob*+, *Pdhfr*, FLAG epitope	(Flannagan *et al.*, 2007)
pSCRhaB3	*ori*$_{pBBR1}$ *rhaR rhaS* P_{rhaB} Tp^r *mob*$^+$	(Cardona & Valvano, 2005)
pGPΩTp	*ori*R6K, ΩTp^r cassette, *mob*$^+$	(Ortega *et al.*, 2007)

All Bcc isolates are from the Edinburgh CF Microbiology Laboratory strain repository, unless otherwise specified. Strain names and sources are specified further for each method below.

2.2. Molecular biology: Competent cells

2.2.1 Chemically competent cells prepared by the $CaCl_2$ method

One hundred ml of LB broth, supplemented with appropriate antibiotics, was inoculated with 1 ml of overnight culture and grown at appropriate temperatures to an OD_{600} of 0.6. They were then cooled down quickly on ice, and transferred to a pre-cooled falcon tube and pelleted at 6000 x g for 10 minutes at 4 °C. The pellet was resuspended in ice cold 10 mM Tris (pH 8.0) with 50 mM NaCl and pelleted again. The pellet was resuspended in half the original volume of 30 mM $CaCl_2$ and incubated on ice for 20 minutes. The cells were pelleted and finally resuspended in one twentieth of the original volume of 30 mM $CaCl_2$. The cells were prepared in 200 µl aliquots and frozen in liquid nitrogen to be stored at -80 °C.

2.2.2 Electro-competent cells

Two hundred ml of 2YT broth, supplemented with 5 mM $CaCl_2$ and appropriate antibiotics, was inoculated with 2 ml of overnight culture. The cells were grown at appropriate temperatures until an OD_{600} of 0.6. They were then cooled down quickly on ice, and transferred to a pre-cooled falcon tube and pelleted at 6000 x g for 10 minutes at 4 °C. The pellet was washed 3 times in ice cold sterile dH_2O. The pellet was transferred to a 10 ml falcon tube and washed with sterile dH_2O containing 10 % (v/v) glycerol. Finally, the pellet was resuspended in an equal volume of sterile dH_2O containing 10 % (v/v) glycerol. Aliquots of 200 µl were prepared and frozen in liquid nitrogen to be stored at -80 °C.

2.3. Molecular biology: DNA manipulation

2.3.1 Alkaline lysis extraction of bacterial chromosomal DNA

Two to three bacterial colonies were scraped from a plate and mixed into 20 µl lysis buffer (2.5 ml 10% (w/v) SDS (Sigma), 5 ml 1 M NaOH (Fisher Scientific), 92.5 ml MilliQ H_2O) in an Eppendorf tube, then heated to 95 °C for 15 minutes. After a quick spin in a centrifuge, 180 µl milliQ water was added. It was centrifuged for 5 minutes at 10 000 x g, then stored at –20 °C.

2.3.2 Polymerase chain reaction (PCR) amplification

All primers used in these studies were purchased from SigmaGenosys and are listed in Table 4. PCR reagents, programmes and the instruments used are described in the relevant methods.

Table 4: Primers used in this study.

General Primers	Primer Sequence 5' - 3'
BCR1	TGACCGCCGAGAAGAGCAA
BCR2	CTCTTCTTCGTCCATCGCCTC
BCRG3A1	GCTCGACGTTCAATATGCC
BCRG3A2	TCGAGACGCACCGACGAG
BCESM 1	CCACGGACGTGACTAACA
BCESM 2	CGTCCATCCGAACACGAT
cblA 1	CCAAAGGACTAACCCA
cblA 2	ACGCGATGTCCATCACA
Sequencing pCR2.1 For	CAGCAAACAGCTATGAC
Sequencing pCR2.1Rev	GTAAAACGACGGCCAG
Sequencing pGEM For	TAATACGACTCACTATAGGG
Sequencing pGEM Rev	ATTTAGGTGACACTATAGAA
Sequencing pET For	TTAATACGACTCACTATAGGG
Sequencing pET Rev	CTAGTTATTGCTCAGCGGT

Table 4 continued...

Chapter 3 Primers	Primer Sequence 5' - 3'
Bamb_5549 For	CGCAGCCAGAAGATACAGGT
Bamb_5549 Rev	TCGAGCGTGTAGAGCTTGC
Bamb_3621 For	TCGTCGCACAGCAGCATT
Bamb_3621 Rev	CACTTCGCCGTCCAGATAGA
bceB Δ11bp For	TGAAGGCGGTSGCGATCGTC
bceB Δ11bp Rev	TCGATSCGCACGTCGTCGAG
bceB short For (*Nde*I)	AGC*CATATG*TTGAGCGTGCTGGCGAGAGTCATGAT
bceB long For (*Nde*I)	*CATATG*CGGCACGGGCTGCACAAGGAGCTGTTCGG
bceB no stop Rev (*Xho*I)	TAATG*CTCGAG*GTACGCGTTGCTGCCGGTGAAGC
bceB 6 His Rev (*Xba*I)	*TCTAGA*CAACTCAGCTTCCTTTCGGGCTTTGTTAGC
KO *bceB* For (*Xba*I)	*TCTAGA*GTTCGGCAAACGCCTGTTCAAAGA
KO *bceB* Rev (*Eco*RI)	*GAATTC*CCGACTGGTGAAAGCTGAAACTCATC
RSF1300	TAACGGTTGTGGACAACAAGCCAGGG
wcbO For	ATGAGTCGTTCTTTCCTTGC
wcbO Rev	ACATGCTTGCGTTGGTCG

Chapter 4 Primers	Primer Sequence 5' - 3'
arnT For C-term His (*Nco*I)	GGCTGAAAAC*CCATGG*ACGATACGCCGTCG
arnT Rev C-term His (*Xho*I)	GGGAGGCG*CTCGAG*CGATTGCGGTTTCTCG
arnT For N-term His (*Nde*I)	ACAACCAACAGGCTGAAAA*CATATG*AACGA
arnT Rev N-term His (*Xho*I)	GGGTTCATG*CTCGAG*GCGTCCTTACGATTG
arnT Nterm6 His For1 (*Nco*I)	AGAAGGAGATATA*CCATGG*GCAGCAGCCAT
arnT Nterm6 His For2 (*Eco*RI)	ACTTTAAGAAGGA*GAATTC*CCATGGGCAGCAG
arnT Nterm6 His Rev (*Hind*III)	CTCGAGGC*AAGCTT*ACGATTGCGGTTTCT
arnT Cterm6His Rev (*Hind*III)	*AAGCTT*TGTTAGCAGCCGGATCT
pmrK For	CTGACGTTCGCGTGGTTC
pmrK Rev	GGCCCATCAGGTTCCAGT
ugd bcal2946 For (*Nde*I)	AGTACCGGAACA*CATATG*AAAATCACCATC
ugd bcal2946 Rev (*Bam*HI)	TCGCGAAGA*GGATCC*ATCGTAGGTTCAGCC
ugd bcam0855 For (*Nde*I)	AGGGGTCCGACA*CATATG*AATCTGACTATC
ugd bcam0855 Rev (*Xho*I)	*CTCGAG*TGACGGAAAACGGGTTACGCGCTG
ugd bcam2034 For (*Nde*I)	GTCACAAGCCACCCAGGGGAACA*CATATG*A
ugd bcam2034 Rev (*Bam*HI)	TCAAGGTC*GGATCC*TCAGTGCTGAAGCAG

2.3.3 Gel electrophoresis of DNA

To prepare a 1% (w/v) agarose gel, 1 g agarose (Fisher Scientific) was added to 100 ml 1xTAE buffer and heated in a microwave until totally dissolved. The solution was cooled to ca 60 °C before the addition of ethidium bromide. The gel was poured into a casting mould and allowed to set at room temperature. Alternatively, precast 1.2 or 4 % E-gels (Invitrogen) were used.

The PCR products were prepared by adding 5x loading buffer (Bioline) and were then added to the wells, alongside either a 1 kb Plus DNA ladder (Invitrogen), 50 kb DNA ladder (Invitrogen) or Hyperladder I (Bioline). The gel was run at 100 V until markers showed sufficient separation, or according to manufacturers' instructions for the E-gels. The bands were visualised using a UV lamp (Uvitec) or a Gel Doc (Bio-rad).

DNA purification from the agarose gel was carried out following a QIAprep® Gel Extraction kit from Qiagen.

2.3.4 Cloning

Three µl gel purified PCR product was ligated with 1 µl pGEM® T-Easy in 5 µl 2x ligation buffer and 1 µl T4 DNA ligase (Promega). It was left overnight at 4 °C or for 3 hours at room temperature.

Two µl of the ligated product was then transformed into 50 µl *E. coli* JM109 cells. After the cells had defrosted on ice, the ligation product was added and incubated on ice for 30 minutes. The mix was then heat shocked at 42 °C for 30 s, then put back on ice for 2 min. To this, 250 µl SOC media was added and the cells were grown for 1 hour at 37 °C with shaking at 200 rpm. The cells were spread on S-Gal/LB/Amp plates and incubated at 37 °C over night.

Viable (white) colonies were picked, based on blue/white screening, into LB/Amp broth and grown overnight at 37 °C at 200 rpm.

Plasmid DNA purification from the overnight cultures was carried out using a QIAprep® Spin Mini-Prep kit from Qaigen according to the manufacturer's instructions.

2.3.5 Restriction Digests

The restriction enzymes used in this study were: *Eco*RI, *Nco*I, *Nde*I, *Xba*I, *Hind*III, *Bam*HI, *Hae*III and *Xho*I (all purchased from New England Biolabs, NEB).

For a small scale restriction digest, 8 µl DNA was mixed with 0.5 µl of each restriction enzyme required and 1 µl 10 x buffer relevant to the restriction enzymes used. The mixture was incubated at 37 °C for 3 hours, then analysed by agarose gel electrophoresis.

For a large scale restriction digest, 43 µl of plasmid DNA was mixed with 1 µl of each restriction enzyme required and 5 µl 10 x buffer relevant to the restriction enzymes used. After incubation at 37 °C for 3 hours the samples were analysed by agarose gel electrophoresis followed by a gel extraction.

2.3.6 DNA Sequencing

The DNA sequencing of clones was carried out by a PCR-based method using BigDye®Terminator v3.1 (Applied Biosystems). Samples were prepared in a 0.5 ml PCR tube: 5 µl plasmid DNA, 1 µl forward or reverse primer, 2 µl BigDye and 2 µl 5x sequencing buffer. The reaction was cycled 30 times at 94°C for 30 s, 45°C for 15 s and 60°C for 4 minutes. The reaction was then submitted to the ICMB (Institute for Cell and Molecular Biology, University of Edinburgh) service for sequencing analysis. Fluorescent DNA sequence chromoatograms were analysed using VectorNTI software (Invitrogen).

2.3.7 Electroporation

Aliquots of electro-competent cells and plasmid DNA were thawed on ice. Two µl DNA was placed in a 0.2cm cuvette (Sigma-Aldrich), and then ~100 µl cells were added. The cuvette was dried and placed in the electroporator and the cells were subjected to electroporation (2500V, 25µF, 99 Ω). Five hundred µl SOC was added immediately and the mixture was transferred to a sterile Eppendorf tube. The mixture was left shaking at 30 °C for 1 hour, then spread onto antibiotic containing LB agar plates and incubated overnight at 30°C.

2.3.8 Tri-parental mating

The recipient strain was grown on an LB plate overnight at optimal temperature. An *E. coli* DH5α helper strain carrying pRK2013 and the *E. coli* donor strain carrying the plasmid to be conjugated were streaked onto SOB agar plates with appropriate antibiotic selection and incubated at 37°C overnight. The recipient strain was then grown overnight in LB broth, and the donor and helper strains were grown in SOB media with antibiotics.

The cells were pelleted at 6000 x g for 15 minutes. The donor and helper strains were each resuspended in 3 ml PBS, and 1 ml of each was used to resuspend the recipient strain. The cells were pelleted together and washed in 2 ml PBS and then resuspended in 2 ml LB broth. A sterile 2 µm filter was placed on an SOB plate and left for 10 minutes. 100 µl of the neat bacterial mixture was added to the filter paper, and the plate was incubated upright overnight at optimum temperature. The filter paper was then placed in a sterile universal tube containing 10 ml LB broth. After quickly vortexing, 100 µl of the eluted bacterial mixture was spread onto LB plates containing antibiotics to select for the recipient containing the donor plasmid.

2.3.9 Insertional inactivation of Bcc genes.

Insertional inactivation of *B. cenocepacia* K56-2 genes was performed using suicide vector pGPΩTp, as described previously by Flannagan *et al.* (Flannagan *et al.*, 2007). A 300 bp PCR-amplified internal fragment from the target gene, flanked by *Xba*I and *Eco*RI sites, was cloned into pGPΩTp. *E. coli* GT115 cells were transformed with the resulting mutagenesis plasmid, and were used to conjugate the plasmid into a wild-type strain of the Bcc by triparental mating. Colonies were verified by PCR using the forward primer for the insert and the reverse plasmid specific primer RSF1300.

2.4. Molecular biology: Protein Expression and purification

2.4.1 Protein expression

Six µl DNA product from 2.3.4 was ligated with 2 µl of an expression vector, such as pET28a or pET22b (which had been digested by the same restriction enzymes), in 1 µl 10 x buffer (NEB) and 1 µl T4 DNA ligase (NEB). It was left overnight at 4 °C. The ligation product was transformed into TOP10^{TM} cells or DH5α cells as described in Method 2.2.4. The cells were plated on LB antibiotic selection plates overnight at 37 °C. Colonies were picked and grown overnight in LB broth, containing appropriate antibiotics, and plasmid DNA was prepared by Miniprep (Qiagen). A small-scale restriction digest was carried out to assess the success of the ligation.

For expression, the plasmid DNA was used to transform *E. coli* (DE3) cells (Table 1). They were plated on LB antibiotic selection plates, and then grown in LB broth, containing appropriate antibiotics, until OD_{600} of 0.5 - 1.0. Approximately 1 ml broth was enough for a small-scale induction. Half of the cells were induced with IPTG and left for 3 hours, the other half were used as un-induced controls. The cells (500 µl) were pelleted by centrifugation at 5000 x g and used for analysis by SDS-PAGE (see 2.4.4). Large-scale inductions required 6 litres of broth. Cells were induced with

IPTG for 3 hours and pelleted by centrifugation at 5000 x g. The pellet was kept at – 20 °C until needed for purification.

2.4.2 Protein purification: immobilised metal affinity chromatography (IMAC)

The *E. coli* cell pellet was resuspended in binding buffer containing a tablet of protease inhibitor cocktail (Roche). The cells were sonicated on ice, 30 seconds on/30 seconds off, for 10 minutes, followed by centrifugation at 25000 x g for 30 minutes at 4 °C. The supernatant was filtered through a 0.45 μm filter. An ÄKTA Basic instrument fitted with a 5 ml HisTrap™ (Nickel resin, GE Healthcare) column was used to isolate the enzymes from the filtered cell free extract following manufacturer's instructions. The enzymes were eluted in 10 ml fractions using an increasing gradient of elution buffer, and the fractions of interest were analysed by SDS-PAGE.

2.4.3 Protein purification: size exclusion chromatography

The enzymes were further purified by size exclusion chromatography using a HiPrep 26/60 Sephacryl S-200 column (GE Healthcare) following manufacturer's instructions. The calibrated column was equilibrated with 150 mM NaCl and 20 mM Tris, pH7.5, then 5 ml of concentrated protein sample was injected and eluted at 2 ml per minute. The molecular weights of the enzymes were estimated from their column elusion volumes and by non-denaturing gel electrophoresis (10% Novex® Tris-Glycine Pre-Cast Gels, Invitrogen), following the manufacturer's instructions.

The protein concentration was determined by a BCA assay (Pierce) following the manufacturer's instructions.

2.4.4 Calibration of Sephacryl S-200 column

Calibration was carried out using high molecular weight (HMW) and low molecular weight (LMW) calibration kits from GE Healthcare, following manufacturer's instructions. Briefly, the column was equilibrated with 150 mM NaCl and 20 mM Tris, pH7.5. First, 1 mg ml^{-1} Blue Dextran 2000 was run alone, and its elution volume was noted as the void volume, V_0. Second, a mixture of high molecular weight standards (5 – 20 mg ml^{-1} each) were run and the elution volumes, V_e, noted. Finally, the low molecular weight standards (5 – 20 mg ml^{-1} each) were run. The K_{av} was caculated as $V_e - V_0/V_t - V_0$, where V_t is the total volume of the column (320 ml). K_{av} was plotted against log(molecular weight) of each standard. The molecular weights of unknown samples were read from the graph.

2.4.5 SDS-PAGE

SDS-PAGE mini gels (15% (v/v) acrylamide) were made, using the Mini-Protean 3 system (Bio-Rad), as follows; 5 ml 30% (v/v) acrylamide (Bio-Rad), 2.185 ml dH_2O, 2.5 ml 1.5 M Trizma (Sigma), pH 8.8, 100 µl 10% SDS, 15 µl *N,N,N,*N-tetramethyl-ethane-1,2-diamine (TEMED) (Fluka-BioChemika) and 200 µl ammonium persulfate (APS) (100 mg ml^{-1}, Fluka-BioChemika) were mixed to make the running gel. After the running gel had set, the 4% (v/v) acrylamide stacking gel was made by mixing 1.35 ml 30% (v/v) acrylamide, 5.8 ml dH_2O, 2.5 ml 0.5 M Trizma, pH 6.8, 100 µl 10% (w/v) SDS, 15 µl TEMED and 200 µl APS (100 mg ml^{-1}).

Protein samples were denatured by the addition of 2 x SDS sample buffer and water to the cell pellets and boiling for 10 minutes. They were then loaded onto the gel along side either LMW marker (GE Healthcare), ColourPlus pre-stained marker (NEB) or SeeBlue®Plus2 pre-stained marker (Invitrogen) and run in SDS running buffer at 200V and 180 mA for 1 hour.

Gels were stained using SDS stain for one hour whilst gently shaking at 37 °C. The bands were visualised by destaining the gel in SDS destain for one hour at 37 °C.

2.4.6 Western Blot

After SDS-PAGE, the gel was cut so that only the lanes of interest were present. A piece of nitrocellulose membrane (Hybond™-ECL™, Amersham) was cut 0.5 cm longer and wider than the gel. Both the gel and the membrane were put in transfer buffer for 10 minutes at room temperature whilst agitated. Six pieces of filter paper (Whatman) were cut 0.5 cm longer and wider than the membrane. Three pieces were soaked in transfer buffer and placed on top of each other in the Trans-Blot®SD Semi-Dry Transfer Cell (Bio-Rad), the membrane was placed on top of the filter papers followed by the gel. The remaining 3 filter pieces were soaked and placed on top of the gel. The gel was blotted for 30 minutes at 15 V and 5.5 x width x length of the gel in mA. The membrane was placed in blocking solution (25 ml 1 x PBS, 0.01% (v/v) tween 20, 5 % (w/v) dried skimmed milk) over night at 4 °C whilst agitated.

The blocking solution was poured off and the membrane was covered in washing solution (PBS, 0.01% tween 20) and washed 3 x 5 min, followed by 2 x 10 min whilst agitated. After that, an anti-His antibody solution [30 ml PBS, 0.01% (v/v) tween 20, 5% (w/v) dried skimmed milk, 2.5 µl anti-His antibody (GE Healthcare)] was added and left for 1 hour at room temperature whilst agitated. The membrane was washed again 3 x 5 min, 2 x 10 min, followed by incubation of the anti-IgG antibody solution [30 ml PBS, 0.01% (v/v) tween 20, 5% (w/v) dried skimmed milk, 2.5 µl anti-mouse IgG-Hrp-linked antibody (Cell Signalling Technology, Inc)], then washed again 3 x 5 min, 2 x 10 min, then dried on filter paper (Whatman) before it was basted with ECL Plus Western Blotting Detection System (GE Healthcare). It was dried again then covered in cling film before it was developed using KODAK BioMax XAR film in a Hypercassette™ (Amersham) for 30 s, 2 min, 5 min and 10 min.

The above method, with a few modifications, was also used detect biotinylation. Superblock (Pierce) was used instead of blocking solution for overnight incubation. Instead of the antibody solutions, 0.5 µl streptavidin-Hrp (BD Biosciences) was

added to 25 ml Superblock. The washing steps were extended to 2 x 5 min, 2 x 10 min, 1 x 30 min.

2.4.7 Protein assays

Cary 50 UV visible spectrophotometers (Varian) were used to assay protein concentrations and activities, the concentration and kinetics programmes were used respectively. Origin 6.1 software was used to analyse any activity data.

2.4.8 Liquid chromatography-electrospray ionisation mass spectrometry (LC-ESI-MS) of proteins

Molecular weight of purified proteins was determined by LC-ESI-MS, carried out by David Clarke and Gareth Morrison, School of Chemistry, University of Edinburgh.

Mass spectrometry was performed on a MicroMass Platform equipped with an electrospray ion source. The spectrometer cone voltage was ramped from 40 to 70 volts and source temperature set to 140 °C. Protein samples were separated with a Waters HPLC 2690 with a Jupiter C5 reverse phase column (5 μm, 250 x 4.6 mm, Phenomenex) directly connected to the spectrophotometer. Proteins were eluted from the column with a 5-95% acetonitrile gradient using an acetonitrile/water/0.01% (v/v) trifluoroacetic acid (TFA) solvent system (flow rate 0.4 ml/min). The total ion count in the range 500 to 2000 m/z was scanned at 0.1 s intervals. The scans were accumulated, the spectra combined and the molecular mass was determined by the MaxEnt and Transform algorithms of the Mass Lynx software (MicroMass).

2.5. Molecular biology: RNA manipulation

2.5.1 RT-PCR

RNA was extracted from mid-log phase cultures (RNeasy® Protect Bacteria Mini Kit; Qiagen) and DNase I-treated (RNase-free DNase set; Qiagen), prior to reverse

transcription with 1.5 μg RNA template, random primers and SuperScript III Reverse Transcriptase (RT; Invitrogen). cDNAs and corresponding non-RT controls were used as template in PCR reactions.

2.6. Minimum Inhibition Concentration (MIC) assay

The method used follows that of Andrews, 2001 (Andrews, 2001): Bacterial strains of interest, and control stains[1] *Pseudomonas aeruginosa* NTCTC 10662, *Escherichia coli* NTCTC 10418 and *Staphylococcus aureus* NTCTC 6571, were grown over night on a nutrient agar plate at 37 °C, followed by overnight subcultures in nutrient broth at 37°C. The bacterial cultures were diluted in saline: Gram-negative bacteria 1:500 and Gram-positive bacteria 1:100. Two μl (approximately 10^4 cfu) of each strain was spotted onto antibiotic plates using a multipoint inoculator. The plates were prepared according to Table 5. For example, for a plate with a final concentration of 64 μg ml^{-1}, 0.128 ml of a 10 mg ml^{-1} antibiotic stock was added to 20 ml ISA.

Table 5: Concentration of antibiotic stock; Amount of antibiotic added; Concentration in 20ml ISA

10 μg ml^{-1}			100 μg ml^{-1}				1 mg ml^{-1}			10 mg ml^{-1}			
0.12 ml	0.25	0.5	0.1	0.2	0.4	0.8	0.16	0.32	0.64	0.128	0.256	0.512	1.024
0.06 μg ml^{-1}	0.12	0.25	0.5	1	2	4	8	16	32	64	128	256	512

The inoculated plates were incubated overnight at 37 °C. The MIC value is interpreted as the lowest concentration of an antibiotic where all visible growth is inhibited.

[1] Kindly donated by Ahmed Hamouda, Molecular Chemotherapy, University of Edinburgh

Chapter 3: Exopolysaccharide Investigation

3.1. Materials and methods

3.1.1 Bacterial strains and culture conditions

Bcc isolates used in this study are described in Table 6, and include 16 isolates from the two published Bcc strains panels (Coenye *et al.*, 2003; Mahenthiralingam *et al.*, 2000b). Additional Bcc strains investigated included *B. pyrrocinia* BTS7, *B. cenocepacia* BTS2, as well as 19 *B. multivorans*, 14 *B. cenocepacia* IIIA and 11 *B. cenocepacia* IIIB isolates from the Edinburgh CF Microbiology Laboratory (ECFML) collection. Isolates were recovered from storage at -80 °C by subculture on nutrient agar (NA; Columbia base agar, Oxoid) and subsequently grown on media composed of 1.5% (w/v) bacteriological agar (Oxoid) containing 2% (w/v) sugars and fractions from various isolation methods below. All clinical *P. aeruginosa* strains used were from the ECFML collection, and were sub-cultured onto *Pseudomonas* isolation agar (PIA; Difco) or NA before grown on sugar media.

Sugars and other related chemicals were purchased from: Sigma-Aldrich, BDH AnalaR, MP Biochemicals, Fluka BioChemika, or Acros Organics.

3.1.2 Onion maceration

Peeled white onion (Sainsbury's, Edinburgh, UK) slices were placed in Petri dishes and inoculated with stationary phase Bcc cultures (10^6 cfu) that had been cultured overnight in 2.5% (w/v) nutrient broth No 2 (Oxoid) with 0.5% (w/v) yeast extract. The onions were incubated at 30 °C for 5 days. The results were assessed by eye, and onion maceration recorded as positive or negative.

3.1.3 Onion extract agar

Peeled white onions (1 kg) were chopped, homogenised in a blender at room temperature, and filtered through muslin. The filtrate was filter-sterilized through a 0.22 μm filter and lyophilised to give a yellow sticky powder (typical yield 62 g). Twenty grams of lyophilised onion extract and 15 g bacteriological agar were made up to 1 litre distilled H_2O, and then autoclaved at 121 °C for 15 min. Strains were subcultured onto onion agar and incubated for 72 hours at 30 °C. Mucoidy was recorded on a scale ranging from nonmucoid (-) to very mucoid (+++).

Concentration effects were investigated by incorporating onion extract into agar at final concentrations ranging from 0.25 μg ml^{-1} to 5 mg ml^{-1}.

3.1.4 Sugar agar

Sugar agar contained 20 g of the sugar of interest, 2 g yeast extract, and 15 g bacteriological agar dissolved in 1 litre distilled H_2O (Sage *et al.*, 1990). The sugars used were as follows: D-fructose, D-galactose, D-mannitol, D-glucose, glycerol, lactose, L-rhamnose, D-mannose, maltose, sucrose, *myo*-inositol, ribitol (adonitol), and D-glucitol (sorbitol). The fructan polysaccharide inulin was also tested.

As a control isolates were grown on bacteriological agar containing 0.2% (w/v) yeast extract alone.

3.1.5 Reverse-phase chromatography

Twenty millilitres of onion extract, 2% (w/v) in distilled H_2O, was loaded onto a pre-packed C8 column (10 g/60.0 ml, Varian, Anachem) and bound material was eluted stepwise using 3 concentrations of methanol (20% (v/v), 50% (v/v) and 80% (v/v); Fisher Scientific). Each fraction was lyophilised, dissolved in distilled H_2O and incorporated into 1.5% (w/v) bacteriological agar.

3.1.6 Ethyl acetate partitioning

To separate any lipids, non-polar, non-acidic and polar compounds, the resolubilised onion extract was brought to pH 7.0 using NaOH and partitioned against ethyl acetate (Fisher Scientific) at 1:1 (v/v). The phases were separated, and the aqueous phase was brought to pH 2.0 using HCl and the extraction was repeated. Following both extractions, the organic and aqueous layers were evaporated or lyophilised respectively, and then redissolved in distilled H_2O, pH adjusted to 7.0, and incorporated into 1.5% (w/v) bacteriological agar.

3.1.7 Acid hydrolysis.

The aqueous phase residue of the ethyl acetate partitioned onion extract was redissolved in distilled H_2O (50 mg ml^{-1}) and was hydrolysed in 2 M TFA (Sigma) at 60 °C or 120 °C for 1 h.

3.1.8 Paper electrophoresis

To fractionate the extract based on the presence or absence of functional groups, the freeze-dried aqueous phase of the onion extract was weighed and resuspended in distilled H_2O to a final concentration of 50 mg ml^{-1}. One millilitre was loaded at a centre origin of a Whatman No.1 paper (57×42 cm). The following standards were added in the margins of the paper: glucose 6-phosphate, glucose, glucosamine, methyl green (Sigma) and orange G (BDH). Electrophoresis was conducted at 1 kV for 20 min, in volatile buffers at pH 2.0 or 6.5 with white spirit or toluene as coolant (Fry, 2000). The chromatograms were left to dry overnight in a fume cupboard.

3.1.9 Paper chromatography

One millilitre aliquots of each of the redissolved aqueous phase of the onion extract and the TFA hydrolysed samples (50 mg ml^{-1}) were chromatographed on Whatman No1 paper alongside markers [ferulic acid, rhamnose, glucose, lactose, mannose,

galactose, fructose, mannitol, and glycerol] in butan-1-ol:acetic acid:water (12:3:5) for up to 60 h. The chromatograms were left to dry overnight in a fume cupboard.

3.1.10 Staining and elution methods

Electrophoretograms and chromatograms were stained with silver nitrate to reveal monosaccharides, oligosaccharides, alditols, saccharinic acids and phenols (Fry, 2000). Briefly, the chromotograms were dipped in solution 1 (prepared by dissolving 0.2 g $AgNO_3$ (Sigma) in 0.4 ml dH_2O, which was added to 26 ml acetone (Fisher Scientific) whilst rapidly stirring) and air dried for 15 minutes, then covered in solution 2 (1.25 ml 10 M NaOH mixed with 100 ml ethanol) and air dried for 15 minutes, this process was repeated a second time. The chromatograms were then placed in a water bath and washed with running water for 2 hours. Stained sugars appear brown.

To reveal monosaccharides and reducing disaccharides, the chromatograms were stained with aniline hydrogen phthalate (Fry, 2000). Briefly, a stock solution was prepared by mixing 16 g phthalic acid (Sigma) in 490 ml acetone, 490 ml diethylether (Fisher Scientific) and 20 ml dH_2O. One hundred ml of the stock solution was mixed with 0.5 ml aniline (Fisons), and used to cover the chromatograms. The chromatograms were left to dry, and then placed in an oven at 105 °C for 5 minutes. Uronic acids stain orange, hexoses brown, pentoses dull-red, and reducing disaccharides are stained in various colours.

The paper strips of interest from both methods were eluted by a syringe method with distilled H_2O (Eshdat & Mireman, 1972). Briefly, 2 cm wide strips were cut along the chromatogram, and rolled up tightly to fit into a 5 ml syringe, which was placed in a 15 ml Falcon tube. Five hundred µl dH_2O was added at the time (2 ml in total) and the sugars were eluted by centrifugation at 2600 rpm. The eluted material was incorporated into 1.5% (w/v) bacteriological agar with 0.2% (w/v) yeast extract.

3.1.11 High-performance anion-exchange chromatography with pulsed amperometric detection (HPAE–PAD).

The HPAE-PAD was carried out by Ben R. Mewburn (Edinburgh Cell Wall Group, Institute of Molecular Plant Sciences, University of Edinburgh).

Twenty microlitres each of the aqueous phase of the onion extract and the TFA-hydrolysed samples (0.1 mg ml^{-1}) were analysed by HPAE–PAD (Dionex). The system consisted of an AS3500 autosampler, GP40 gradient pump, ED40 electrochemical detector, and PC10 pneumatic controller. The amperometry detector cell contained a gold electrode and a pH-Ag|AgCl combination reference electrode. CarboPac MA-1, PA-1, and PA-100 columns and guard columns were used for the separation of alditols, monosaccharides, and oligosaccharides respectively. Eluents, degassed by bubbling with helium, were as follows. MA-1: 600 mM NaOH at 0.4 ml min^{-1} (isocratic); PA-1: 20 mM NaOH for 3 min, then H_2O for 32 min, then a 0→200 mM NaOH gradient over 10 min (all at 1.0 ml min^{-1} with post-column addition of base); PA-100: 100 mM NaOH throughout, supplemented with a 0→200 mM NaOAc gradient over 30 min, then 200→800 mM NaOAc over 10 min (all at 1.0 ml min^{-1}). Analytes were identified by comparison of retention times to those of standards (D-glucose, D-fructose, D-galactose, D-mannose, L-rhamnose, arabinose, xylose, fucose, D-ribose; lactose, sucrose, cellobiose, mix: maltose, maltotriose, maltotetraose, maltopentaose, maltohexose, maltoheptaose; D-glucitol, perseitol, xylitol, D-mannitol, D-galactitol, ribitol, arabinitol, *myo*-inositol, erythritol) and quantified by integration of peak area with Chromeleon software (Dionex).

3.1.12 Investigation of conserved EPS gene clusters in Bcc species.

The genome analysis was carried out by Alan R. Brown (CF Group, Centre for Infectious Diseases, University of Edinburgh).

Genome sequences representing five Bcc species were examined to determine if two previously published EPS gene clusters within *B. cenocepacia* J2315, the *bce* gene

cluster (Moreira *et al.*, 2003) and the *wcb* gene cluster (Parsons *et al.*, 2003), are conserved across the Bcc. The amino acid sequences for every open-reading frame (ORF) within each of the two gene clusters within *B. cenocepacia* J2315 (genome sequence available at the Wellcome Trust Sanger Institute; http://www.sanger.ac.uk/) were used to search by TBLASTN the following Bcc genome sequences: *B. ambifaria* AMMD, *B. vietnamiensis* G4, *B. multivorans* ATCC17616, *Burkholderia* sp. 383. (all sequences are available at the US Department of Energy Joint Genome Institute; http://www.jgi.doe.gov/) and *B. dolosa* AU0158 (available at The Broad Institute; http://www.broad.mit.edu/). TBLASTN searches were performed using default parameters (BLOSUM 62, Word size 3).

3.1.13 RT-PCR analysis of EPS biosynthetic gene clusters

The RT-PCR analysis was carried out by Alan R. Brown and Roseanna Hennessey (CF Group, Centre for Infectious Diseases, University of Edinburgh).

The EPS-producing strain, *B. ambifaria* AMMD, was cultured in 0.2 % (w/v) yeast extract with or without supplementation with 2 % (w/v) mannitol. RNA was extracted from mid-log phase cultures (RNeasy Protect Bacteria Mini Kit; Qiagen) and DNase I-treated (RNase-free DNase set; Qiagen), prior to reverse transcription with 1.5 μg RNA template, random primers and SuperScript III Reverse Transcriptase (Invitrogen). cDNAs and corresponding non-RT controls were used as template in PCR reactions specific for two distinct *wza* homologues (Bamb_5549 and Bamb_3621) located within two separate putative EPS biosynthetic gene clusters.

3.1.14 PCR analysis of *wcbO* gene.

The *wcbO* gene is found in the *wcb* gene cluster, previously described by Parsons *et al.* (Parsons *et al.*, 2003). Parsons and colleagues report an *IS407*–like insertion sequence within the *B. cenocepacia* J2315 *wcbO* and they suggest it may be the reason *B. cenocepacia* J2315 is unable to produce EPS. A PCR assay was set up using the previously published *wcbO* primers (Parsons *et al.*, 2003). Genomic DNA

from strains to be tested was prepared as described in 2.3.1. PCR reactions were performed in a 25 µl volume containing 2 µl genomic DNA, 300 nM forward and reverse primer (*wcbO* For, Rev), 260 µM of each dNTP, 4% (v/v) DMSO, 1 U Gold Taq polymerase (Biogene) and appropriate manufacturer's reaction buffer. Thermal cycling was performed using the following parameters: 94 °C 3 min; 30 cycles of 95 °C (1 min), 50 °C (1 min) and 72 °C (10 min); 72 °C 10 min. PCR products were electrophoresed on a 1.2 % E-Gel alongside a 1 kb Plus DNA ladder and visualised by UV illumination. The *B. cenocepacia* J2315 *wcbO* gene sequence harbouring the *IS407*–like insertion yields a PCR product of 1.65 kb, compared to 400 bp for wild type *wcbO*.

3.1.15 PCR analysis of *bceB* gene.

The *bceB* PCR assay was developed by Alan R. Brown (CF Group, Centre for Infectious Diseases, University of Edinburgh).

Using the *bceB* gene sequence of *B. cenocepacia* J2315, *bceB* homologues were identified within the publicly-available genome sequences of *B. ambifaria* AMMD, *B. cepacia* sp. 383, *B. cenocepacia* AU1054, *B. cenocepacia* HI2424, *B. cenocepacia* PC184, *B. vietnamiensis* G4 and *B. dolosa* AU0158. The eight gene sequences were aligned, and PCR primers flanking the location of the previously described 11-bp deletion in *B. cenocepacia* J2315 (Moreira *et al.*, 2003) were designed based on conserved regions across the eight aligned sequences (*bceB* Δ11bp For and Rev). Genomic DNA from strains to be tested was prepared as described in 2.3.1. Two microlitres of supernatant containing genomic DNA was used as template in PCR assays. PCR reactions were performed in a 50 µl volume containing 300 nM forward and reverse primer, 1.5 mM $MgCl_2$, 260 µM of each dNTP, 4% (v/v) DMSO (Sigma), 1 U Taq polymerase (Invitrogen) and appropriate manufacturer's reaction buffer. Thermal cycling was performed using the following parameters: 94 °C 3 min; 40 cycles of 94 °C (30 s), 60 °C (30 s) and 72 °C (30 s); 72 °C 10 min. PCR products were electrophoresed on a 4 % E-Gel alongside a 1 kb Plus DNA ladder and visualised by UV illumination. The *B. cenocepacia* J2315 *bceB* gene sequence harbouring the 11-bp deletion yields a PCR product of 140 bp, compared to 151 bp from the wildtype sequence found in *B. cenocepacia* IST 432 (Videira *et al.*, 2005).

3.1.16 PCR analysis of BCESM and *cblA* gene

Isolates of the *B. cenocepacia* ET12 lineage uniquely harbour both of the putative epidemic strain markers BCESM and the *cblA* gene. PCRs were performed as described previously (Mahenthiralingam *et al.*, 1997; Sajjan *et al.*, 1995). Briefly, two microlitres of genomic DNA was used as template in PCR assays. PCR reactions were performed in a 25 µl volume containing 300 nM forward and reverse primer (*cblA* 1 and 2, BCESM 1 and 2), 260 µM of each dNTP, 4% (v/v) DMSO, 1 U Gold Taq polymerase (Biogene) and appropriate manufacturer's reaction buffer. Thermal cycling was performed using the following parameters: BCESM, 30 cycles of 94 °C (1 min), 63 °C (1 min) and 72 °C (2 min) followed by a final extension at 72 °C for 10 min; *cblA*, 3 min 95, then 30 cycles of 94 °C (1 min), 55 °C (1 min), 72 °C (1 min), followed by a 10 min extension at 72 °C. PCR products were electrophoresed on a 1.2 % E-Gel alongside a 1 kb Plus DNA ladder and visualised by UV illumination.

3.1.17 Expression of recombinant BceB in *E. coli.*

Genomic DNA from *B. cenocepacia* PC184, containing a wild type *bceB* gene, was prepared as described in 2.3.1. A long (1440 bp) and a short (1380 bp) version of the *bceB* gene, both flanked by *Nde*I and *Xho*I sites and no stop codon, was PCR-amplified, using 2 puReTaq™ Ready-To-Go PCR beads (Amersham), 5 µl of each primer (*bceB* short For or *bceB* long For, with *bceB* no stop Rev), 1 µl genomic DNA and 39 µl dH_2O. Samples were amplified for 30 cycles: 95 °C 1 min, 60 °C 1 min, and 72 °C 2 min; with a final 10-min extension at 72°C. The genes were electrophoresed on a 1% agarose gel, and gel extracted using QIAprep® Gel Extraction kit from Qiagen. The *bceB* long and *bceB* short genes were cloned into pGEM as described in 2.3.4. After restriction digests and sequencing analysis, the genes were cloned into pET28a (to use as a template for PCR in 3.1.17) and pET22b vectors, yielding C-terminal 6His tags (see 2.4.1.).

Expression in *E. coli* C41 (DE3) was carried out as in 2.4.1. using the plasmids pET22b/*bceB* long and short, selected on ampicillin, and visualised by Western Blot (see 2.4.6). BceB long is 55041.55 Da and BceB short is 52486.44 Da.

Two PCR reactions were set up using pET28a/bceB long and short as templates, using 2 puReTaq™ Ready-To-Go PCR beads (Amersham), 5 µl of each primer (*bceB* short For or *bceB* long For, with *bceB* 6 His Rev), 1 µl genomic DNA and 39 µl dH_2O. Samples were amplified for 30 cycles: 95 °C 1 min, 60 °C 1 min, and 72 °C 2 min; with a final 10-min extension at 72°C. The *bceB* long (1506 bp) and short (1446 bp) genes, flanked by *Nde*I and *Xba*I, were now amplified with the 6 His tag. The genes were electrophoresed on a 1% agarose gel, and gel extracted using QIAprep® Gel Extraction kit from Qiagen. The *bceB* long 6His and *bceB* short 6His genes were again cloned into pGEM as described in 2.3.4. After restriction digests and sequencing analysis, the genes were cloned into pSCRhaB3 (as described in see 2.4.1.) and selected on trimethoprim.

Expression in *E. coli* DH5α was carried out using pSCRhaB3/*bceB* long 6His and *bceB* short 6His, and visualised by SDS-PAGE (see 2.4.5.) and Western Blot.

3.1.18 Complementation of *ΔbceB*.

Complementation was attempted using the rhamnose-inducible pSCRhaB3 vector as described previously by Ortega and colleagues (Ortega *et al.*, 2005). *E. coli* DH5α was transformed with pSCRhaB3/ *bceB* long 6His or *bceB* short 6His and selected on trimethoprim plates to become donors for triparental mating. In addition, the helper strain was prepared by transforming *E. coli* DH5α with helper plasmid pRK2013, selected on kanamycin plates, and the recipient strains *B. cenocepacia* K56-2 and BC7 were streaked onto a gentamycin plate. Triparental mating was carried out as described in 2.3.8, and *B. cenocepacia* K56-2 and BC7 containing a wild type *bceB* on pSCRhaB3 were selected on trimethoprim and gentamycin. Complementation was investigated by streaking successful colonies on onion and mannitol agar plates.

B. cenocepacia species determination was carried out by *B. cenocepacia* III-A *recA* PCR (see 3.1.19).

3.1.19 RT-PCR analysis of *bceB* expression

Overnight cultures of *E. coli* Top10 cells transformed with either empty pSCRhaB3 or with pSCRhaB3/*bceB* and overnight cultures of *B. cenocepacia* K56-2, with either pSCRhaB3, pSCRhaB3/*bceB* or without plasmid, was sub-cultured into fresh LB media containing either 1 % (w/v) glucose or rhamnose. RNA was extracted from mid-log phase cultures (RNeasy Protect Bacteria Mini Kit; Qiagen) and DNase I-treated (RNase-free DNase set; Qiagen), prior to reverse transcription with 1.5 µg RNA template, random primers and SuperScript III Reverse Transcriptase (Invitrogen). cDNAs and corresponding non-RT controls were used as template in PCR reaction amplifying *bceB* following the protocol in 3.1.15 using *bceB* Δ11bp For and Rev primers.

3.1.20 Insertional inactivation of *bceB* in *B. ambifaria* AMMD

The insertional inactivation was carried out in collaboration with Alan R. Brown (CF Group, Centre for Infectious Diseases, University of Edinburgh).

Insertional inactivation of *bceB* was performed using the pGPΩTp suicide vector, essentially as described previously (Flannagan *et al.*, 2007). In brief, a 300-bp fragment internal to the *bceB* ORF of *B. ambifaria* AMMD and flanked by *Xba*I and *Eco*RI sites was PCR-amplified (using KO *bceB* For and Rev primers) and ligated into the corresponding sites in pGPΩTp following appropriate restriction. The resulting plasmids were transformed into *E. coli* GT115 competent cells (InvivoGen, San Diego USA) and subsequently introduced into *B. ambifaria* AMMD by triparental mating. Any resulting exconjugants were selected using gentamicin (50 mg ml^{-1}) and trimethoprim (100 mg ml^{-1}), and mutants identified by PCR using a chromosomal-specific primer in conjunction with the vector-specific primer RSF1300 (Flannagan *et al.*, 2007). *B. ambifaria* species determination was carried out by *recA* PCR and RFLP analysis (see 3.1.21).

3.1.21 Species determination by *recA* PCR and RFLP

recA PCR and restriction fragment length polymorphism (RFLP) are routinely used in reference laboratories to identify, and also distinguish between, Bcc isolates (Mahenthiralingam *et al.*, 2000a). The BCR1 and 2 primers amplify a Bcc specific region of the *recA* gene, whereas BCRG3A1 and 2 are specific to the *B. cenocepacia* III-A *recA* gene. PCR reactions were performed in a 25 µl volume containing 300 nM forward and reverse primer, 260 µM of each dNTP, 1 U Taq DNA polymerase (Qiagen) with Q solution and appropriate manufacturer's reaction buffer. Thermal cycling was performed using the following parameters: 30 cycles of 94 °C (30 s), 58 °C (BCR)/62 °C (BCRG3A) (45 s), 72 °C (1 min), followed by a 10 min extension at 72 °C. PCR products were analysed by electrophoresis on a 1.2 % E-Gel alongside a 1 kb Plus DNA ladder and visualised by UV illumination. BCR 1 and 2 amplifed a 1 kb product, whereas BCRG3A 1 and 2 amplifed a 278 bp product.

RFLP was carried out using 10 µl *recA* PCR product, 7 dH2O, 1 µl buffer 2 (NEB), and 1 µl *Hae*III (NEB). The mixture was incubated overnight or for 3 hours at 37 °C, after which it was run on a 4% E-gel alongside a 50 kb DNA ladder and visualised by UV illumination.

3.2. Results

3.2.1 Exopolysaccharide production on onion agar

When a lyophilised onion extract was incorporated into agar at 2% (w/v) as the sole nutrient, members of the Bcc were not only able to grow, but the majority of isolates also produced copious amounts of exopolysaccharide, as typified by *B. ambifaria* AMMD (Fig. 9). This "mucoid" phenotype is not observed when the Bcc are cultured on *Burkholderia cepacia* media (Mast Diagnostics), nutrient agar and other common laboratory media. Different concentrations of onion extract, ranging from 0.25 μg ml^{-1} to 5 mg ml^{-1}, were tested, and EPS production was observed in all cases. Induction of EPS biosynthesis on onion agar was observed in all Bcc species investigated, but was not observed in all strains within a species (Tables 6-9). The exception was the single strain of *B. stabilis* available for testing. Of particular interest was the failure of the virulent *B. cenocepacia* ET12 representatives J2315, K56-2 and BC7 to produce EPS on any media tested.

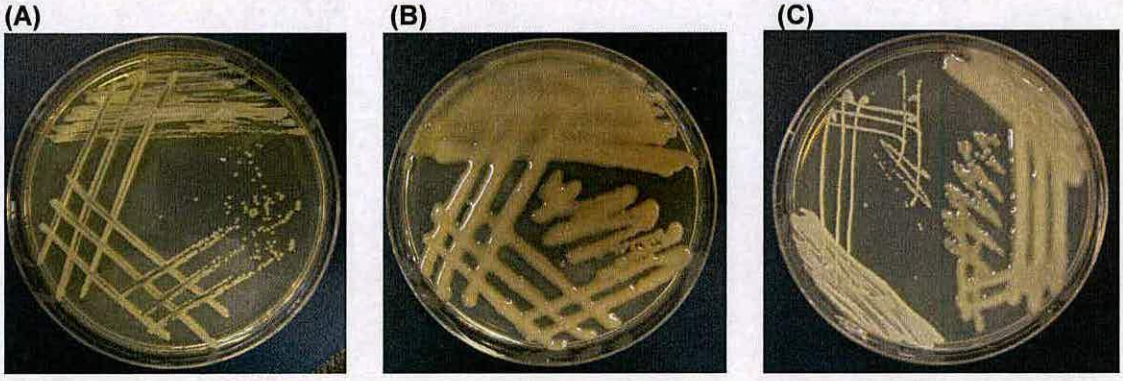

Fig. 9: Growth of *Burkholderia ambifaria* AMMD on **(A)** nutrient agar (nonmucoid); **(B)** onion agar (mucoid), and **(C)** comparison of AMMD *bceB* mutant (left) and AMMD wild type (right) on mannitol agar.

Interestingly, there was no correlation between induction of Bcc EPS on onion agar and the ability of individual Bcc strains to cause maceration of onion bulbs (Table 6). Maceration by *B. cepacia* ATCC25416 is illustrated in Figure 10.

Table 6: Exopolysaccharide biosynthesis of *Burkholderia cepacia* complex species when grown on agar supplemented with various substrates.

Species	Strain	Source	Maceration of onions	YE	Onion	Glucose	Sucrose	Fructose	Inulin	Glycerol	Mannitol	Glucitol	Ribitol	Inositol	Mannose
B. cepacia	ATCC25416	Onion	Yes brown	-	++	-	++	+++	-	+++	+++	+++	+++	+++	+
B. cepacia	CEP509	CF	No	-	-	-	+	++	+	++	++	+	+	+	-
B. multivorans	C1576	CF	No	-	++	-	+	+++	+	++	+++	+++	+++	+++	-
B. multivorans	ATCC 17616	Soil	§	-	++	-	+	+++	+	++	+++	+++	+++	+++	-
B. cenocepacia	J2315*	CF	Yes brown	-	-	-	-	-	-	-	-	-	-	-	-
B. cenocepacia	K56-2*	CF	No	-	-	-	-	-	-	-	-	-	-	-	-
B. cenocepacia	BC7*	CF	§	-	-	-	-	-	-	-	-	-	-	-	-
B. cenocepacia	PC184	CF	§	-	++	-	+	++	+	+	++	+	+	+	-
B. cenocepacia	BTS2	CF	§	-	++	-	+	++	+	+	++	++	+	++	-
B. stabilis	LMG14294	CF	§	-	-	-	-	+	-	-	+	-	-	-	-
B. vietnamiensis	LMG10929	Rice	No	-	+++	-	++	+++	+	+++	+++	+	-	+++	++
B. vietnamiensis	PC259	CF	No	-	++	-	+	+++	+	++	+++	+	-	-	-
B. dolosa	E12	CF	Yes green	-	++	-	-	+++	-	++	++	-	+	+++	-
B. ambifaria	AMMD	Soil	No	-	+++	-	+	+++	+	+++	+++	+++	+++	+++	-
B. anthina	W92^T	Soil	No	-	+++	-	-	+++	+	+++	+++	+++	+++	+++	++
B. anthina	C1765	CF	No	-	+	-	-	+++	-	+++	+++	-	+++	+	+
B. pyrrocinia	BTS7	CF	§	-	+++	-	+	+++	+++	+++	+++	+++	+++	+++	+
B. pyrrocinia	C1469	CF	Yes slimy	-	++	-	++	++	+	++	+++	+++	+++	++	-

All strains tested are from the two published Bcc panels (Coenye *et al.*, 2003; Mahenthiralingam *et al.*, 2000) except BTS2 and BTS7 that were donated by Paola Cescutti, University of Trieste, Italy. EPS production was scored on a scale from – (no EPS) to +++ (very mucoid). Mucoid growth described as +++ is shown in Figure 1b. *ET12 isolates. § Not tested for maceration. YE, yeast extract agar.

Table 7: EPS production and *bceB*, BCESM & *cblA* PCR results for clinical isolates of *B. cenocepacia* IIIA.

	EPS PRODUCTION IN RESPONSE TO GROWTH ON ONION EXTRACT AND ALCOHOL SUGARS										PCR RESULTS		
Strain	**Onion**	**Sucrose**	**Fructose**	**Inulin**	**Glycerol**	**Mannitol**	**Glucitol**	**Ribitol**	**Inositol**	**Mannose**	***bceB***	**BCESM**	***cblA***
E3097	-	-	-	-	-	-	-	-	-	-	Δ 11bp	+	+
E3051	-	-	-	-	-	-	-	-	-	-	wt	-	-
E3046	++	+	++	-	++	+++	+++	+++	++	-	wt	-	-
E3042	+	+	-	-	+	+	+	+	-	-	wt	-	-
E1913	-	-	-	-	-	-	-	-	-	-	Δ 11bp	+	+
E1217	++	+	+++	-	+	++	++	+++	++	-	wt	-	-
E1197	-	-	-	-	-	-	-	-	-	-	Δ 11bp	+	+
E1189	-	-	-	-	-	-	-	-	-	-	Δ 11bp	+	+
E1150	+++	-	+++	-	-	++	++	+++	++	-	wt	-	-
E1073	-	-	-	-	-	-	-	-	-	-	Δ 11bp	+	+
E1001	+++	+	++	-	+	++	++	++	++	-	wt	+	-
E946	+++	+	++	-	-	++	++	++	+	-	wt	-	-
E938	-	-	-	-	-	-	-	-	-	-	Δ 11bp	+	+
E937	+++	+++	+++	-	++	+++	+++	+++	+++	-	wt	-	-

EPS production was scored on a scale from - (no EPS) to +++ (highly mucoid). *bceB* PCR: 'Δ 11bp' denotes the presence of an 11 bp deletion as judged by size of the observed PCR product compared to wildtype (wt) sequence. With the exception of isolate E3051, all non-EPS producing *B. cenocepacia* IIIA isolates studied appear to harbour the 11 bp deletion. *B. cenocepacia* IIIA isolates were also assessed for the presence of the epidemic strain markers, BCESM and *cblA*. These analyses revealed the 11 bp deletion within *bceB* to be a conserved feature of isolates of the ET12 lineage (positive for both epidemic markers).

Table 8: EPS production and *bceB* PCR results for clinical isolates of *B. multivorans*.

	EPS PRODUCTION IN RESPONSE TO GROWTH ON ONION EXTRACT AND ALCOHOL SUGARS										
Strain	**Onion**	**Sucrose**	**Fructose**	**Inulin**	**Glycerol**	**Mannitol**	**Glucitol**	**Ribitol**	**Inositol**	**Mannose**	***bceB* PCR**
E3221	+	-	-	-	-	++	+	+++	++	-	wt
E3218	+	-	-	-	-	-	-	-	-	-	wt
E3215	++	-	-	-	+	-	-	-	-	-	wt
E3187	++	-	-	-	-	+	+	+++	++	-	wt
E3155	+	-	+	-	-	++	++	++	++	-	wt
E3142	-	-	-	-	-	-	-	-	-	-	wt
E3103	++	-	+	-	+	++	+++	+++	+++	-	wt
E2989	+	-	+	-	-	+	++	++	++	-	wt
E2964	-	-	-	-	-	-	+++	+++	+++	-	wt
E2972	+	-	++	-	+	++	++	+++	+++	-	wt
E2858	+	-	-	-	-	-	-	+++	+	-	wt
E2785	-	-	-	-	-	-	-	-	-	-	wt
E2779	++	-	+	-	-	++	++	+	++	-	wt
E2739	+	-	-	-	-	+	+	-	-	-	wt
E2633	++	-	+	-	-	++	++	++	++	-	wt
E2608	-	-	-	-	-	-	-	-	-	-	wt
E2525	-	-	-	-	-	-	-	-	-	-	wt
E2228	+	-	-	-	-	+	+	+	+	-	wt
E2499	+	-	-	-	-	-	-	-	+	-	wt

EPS production was scored on a scale from - (no EPS) to +++ (highly mucoid). All *B. multivorans* isolates studied harboured a *bceB* PCR product consistent with the wildtype (wt) sequence, irrespective of their EPS status.

Table 9: EPS production and *bceB* PCR results for clinical isolates of *B. cenocepacia* IIIB.

	EPS PRODUCTION IN RESPONSE TO GROWTH ON ONION EXTRACT AND ALCOHOL SUGARS										
Strain	**Onion**	**Sucrose**	**Fructose**	**Inulin**	**Glycerol**	**Mannitol**	**Glucitol**	**Ribitol**	**Inositol**	**Mannose**	***bceB* PCR**
E3043	+++	-	-	-	+	++	++	+	-	-	wt
E2854	++	-	++	+	+	++	++	+++	+	-	wt
E2836	+++	+	+++	+	+++	+++	+++	+++	+++	-	wt
E2685	++	-	+	-	+	++	++	+++	+	-	wt
E2398	+++	-	+++	++	+++	+++	+++	+++	+++	-	wt
E2101	+++	+	+++	+	+	+++	+++	+++	+++	-	wt
E1974	-	-	-	-	-	-	-	-	-	-	wt
E1673	+++	+	+++	+	+++	+++	+++	+++	+++	-	wt
E1601	-	-	-	-	-	-	+	-	-	-	wt
E1123	-	++	-	-	-	-	-	-	-	-	wt
E1003	+++	++	+++	+	+++	+++	+++	+++	+++	-	wt

EPS production was scored on a scale from - (no EPS) to +++ (highly mucoid). All *B. cenocepacia* IIIB isolates studied harboured a *bceB* PCR product consistent with the wildtype (wt) sequence, irrespective of their EPS status.

(A) (B)

Fig. 10: Onion maceration by *B. cepacia* ATCC25416. **(A)** control onion and **(B)** onion infected by *B. cepacia* ATCC25416.

For comparison, clinical *P. aeruginosa* strains, either mucoid on both PIA and nutrient agar or non-mucoid, were grown on onion and mannitol agars. However, the choice of agar had no significant effect on phenotype (Table 10).

Table 10: EPS biosynthesis of clinical isolates of *P. aeruginosa*.

Strain	Nutrient agar	PIA	Mannitol agar	Onion agar
E14	(+)	+	(+)	(+)
E15	+	+	+	+
E16	+	+++	+++	+++
E24	+	++	++	++
E25	(+)	+	+	(+)
E29	+	+++	+++	+++
E36	(+)	++	+++	+
E48	(+)	+++	++	+
E55	+	+	++	+
E64	+	+++	+++	+++
E81	+++	+++	+++	+++
E9	-	-	-	-
E22	-	-	-	-
E23	-	-	-	-
E32	-	-	-	-
E37	-	-	-	-
E39	-	-	-	-
E49	-	-	-	-
E56	-	-	-	-
E60	-	-	-	-

Clinical isolates of *P. aeruginosa* were grown on NA, PIA, mannitol and onion agars. EPS production was scored on a scale from - (no EPS) to +++ (highly mucoid).

3.2.2 Investigating the onion factor

Attempts were made to identify the "onion factor" responsible for EPS biosynthesis by use of standard biochemical methods for extracting and fractionating phytochemicals. The causative factor was retained on drying *in vacuo*, and remained in the aqueous phase after partition with ethyl acetate at pH 7.0 and pH 2.0 discounting the role of lipids. Reverse-phase chromatography was carried out but only the flow through was biologically active suggesting the active component is not hydrophobic. A proteinaceous factor was also ruled out by the fact that there were no bands by SDS-PAGE analysis (data not shown) and the extract was still active after incubation at 70 °C for 15 minutes, which would have denatured most polypeptides. Attention was then turned to the carbohydrate content of onion extract. After preparative paper electrophoresis in buffers at pH 2.0 and 6.5 (Fig. 11), the only biological active material recovered from paper strips co-migrated with the glucose standard, indicating the absence of ionisable functional groups such as phosphate, acid or amine. Based on staining methods and paper elution, analytical paper chromatogography revealed the likely causative agent to be glucose, fructose, sucrose, galactose, or mannose (Fig. 12).

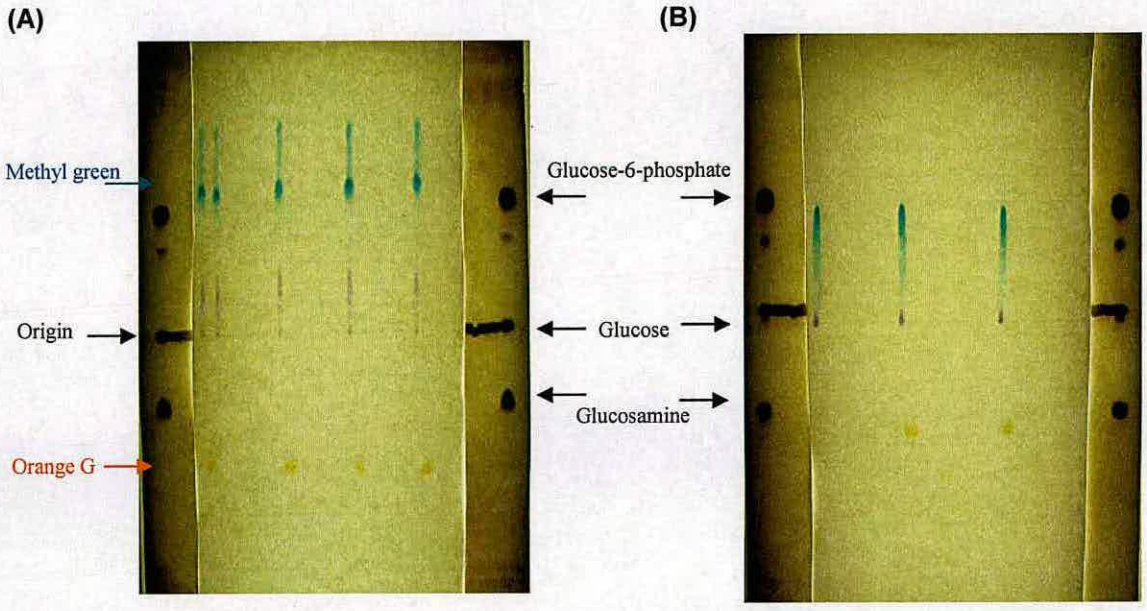

Fig. 11: Paper electrophoretograms of onion extract. **(A)** pH 2.0 in white spirit; and **(B)** pH 6.5 in toluene. Edges have been silver nitrate stained to illustrate the migration of the extract. Methyl Green and Orange G were used as markers to see how far the solvent front had migrated.

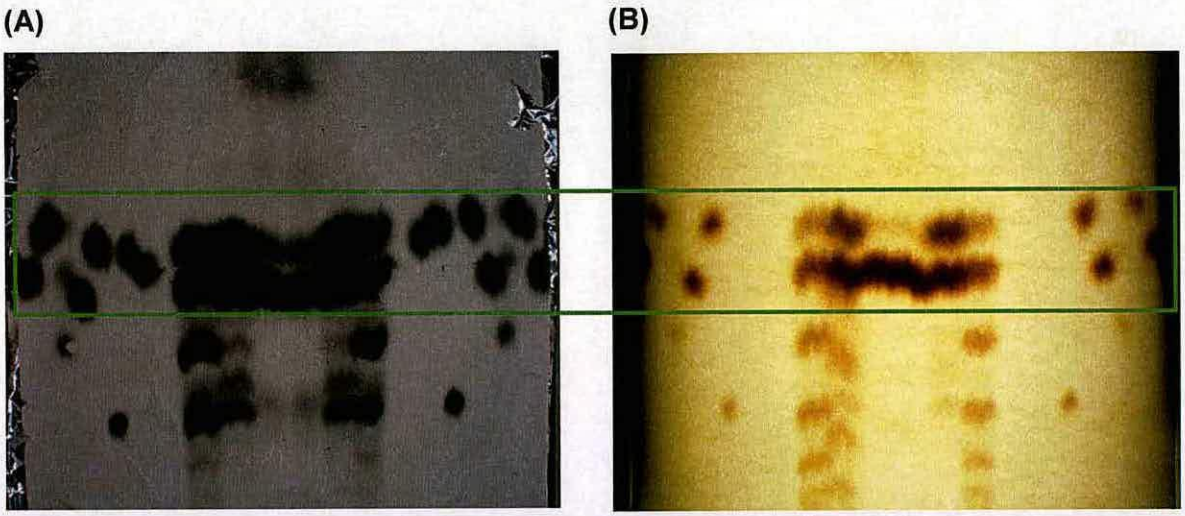

Fig. 12: Paper chromatograms run in butan-1-ol:acetic acid:water (12:3:5) for 50 hours, **(A)** silver stained, **(B)** aniline hydrogen phthalate stained. Order of samples on both chromatograms: glucose, fructose, sucrose, galactose, mannose, lactose, mannitol, sorbitol, glycerol, inulin, onion, TFA 60°C, TFA 120°C, TFA 120°C, TFA 60°C, onion, inulin, glycerol, sorbitol, mannitol, galactose, sucrose, fructose, glucose. The green box indicates the mucoid inducing area.

Further analysis using HPAE-PAD chromatography (Fig. 13) confirmed the major carbohydrate components to be sucrose, glucose, fructose and fructans. The HPAE-PAD chromatograms in Fig. 13 show characteristic peaks of glucose, fructose and sucrose. Sucrose breaks down to fructose and glucose upon mild hydrolysis, as do the fructans to fructose. Fructose breaks down under complete hydrolysis whilst glucose remains stable. The ability of these and related compounds to stimulate EPS biosynthesis in Bcc was then investigated (Table 6). Glycerol and mannitol were also included as these sugar alcohols have previously been noted to enhance EPS biosynthesis in *Pseudomonas aeruginosa* (Whitchurch *et al.*, 1996) and the Bcc (Sage *et al.*, 1990). Glucitol was included because of its close degradative relationship with fructose and mannitol (Allenza *et al.*, 1982). These experiments showed that within a particular Bcc species, EPS biosynthesis was strain-specific and that the most potent inducers of EPS were fructose and all the alditols tested, most significantly mannitol and glucitol, as well as the cyclitol *myo*-inositol. Importantly, the profile of EPS biosynthesis production with these sugars was similar to that observed with onion extract (Table 6). EPS biosynthesis was not observed on agar containing yeast extract alone, nor in the presence of glucose (Table 6), galactose, lactose or maltose (data not shown) with any Bcc strains tested.

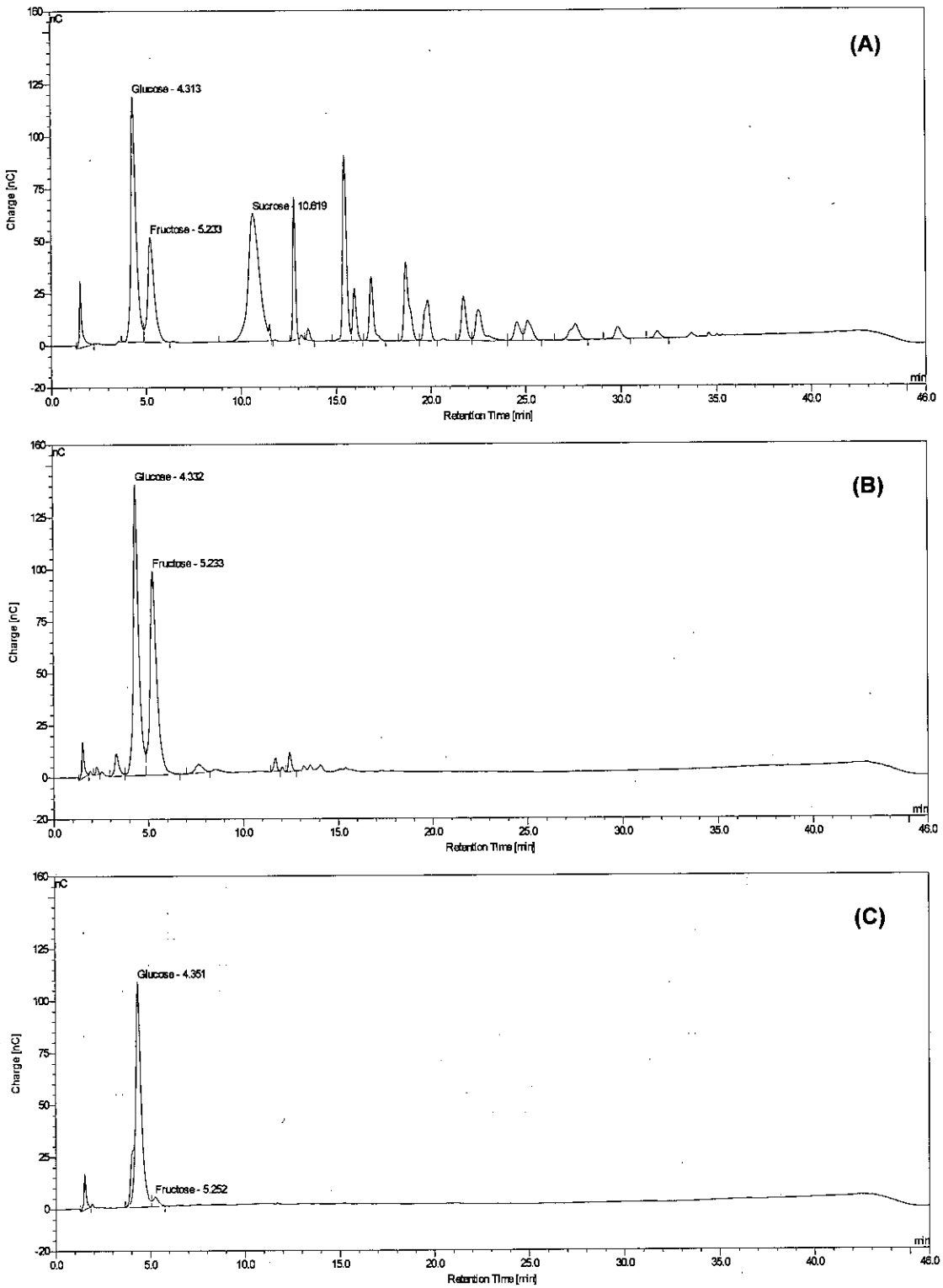

Fig. 13: HPAE-PAD chromatograms. Carbopac PA-100 column separation of sugars in onion extract. **(A)** crude onion extract; **(B)** onion extract hydrolysed by 2 M TFA 60°C 1 h; and **(C)** onion extract hydrolysed by 2 M TFA 120°C 1 h. Glucose, fructose and sucrose peaks were clearly identified based on standards (not shown), and hydrolysis pattern. Peaks with retention times between 12.0 to 36.0 min appear to be oligosaccharides of fructose based on their degradation to fructose under mild hydrolysis.

3.2.3 Molecular basis for lack of EPS biosynthesis in Bcc

With the exception of the single *B. stabilis* strain tested, all Bcc species were shown to be capable of producing EPS when grown on onion agar (Tables 6-9), suggesting the presence of a conserved EPS biosynthetic gene cluster. Consequently, genome sequences representing five Bcc species (*B. ambifaria*, *B. multivorans*, *B. vietnamiensis*, *B. dolosa* and *Burkholderia* sp. 383) were examined to determine if two putative EPS gene clusters within *B. cenocepacia* J2315, the *bce* gene cluster (Moreira *et al.*, 2003) and the *wcb* gene cluster (Parsons *et al.*, 2003), are conserved across the Bcc. The *wcb* gene cluster was found to be poorly conserved, with between one-third and one-half of J2315 ORFs having no direct homologues within the species examined (data not shown). Notably, within the EPS-producing *B. ambifaria* AMMD strain, over half of the J2315 *wcb*-associated ORFs have no homologues, and the remaining homologous ORFs are not organised within a gene cluster. In contrast, the *bce* gene cluster was conserved across all species examined, both in terms of sequence homology and organization of ORFs (Fig. 14).

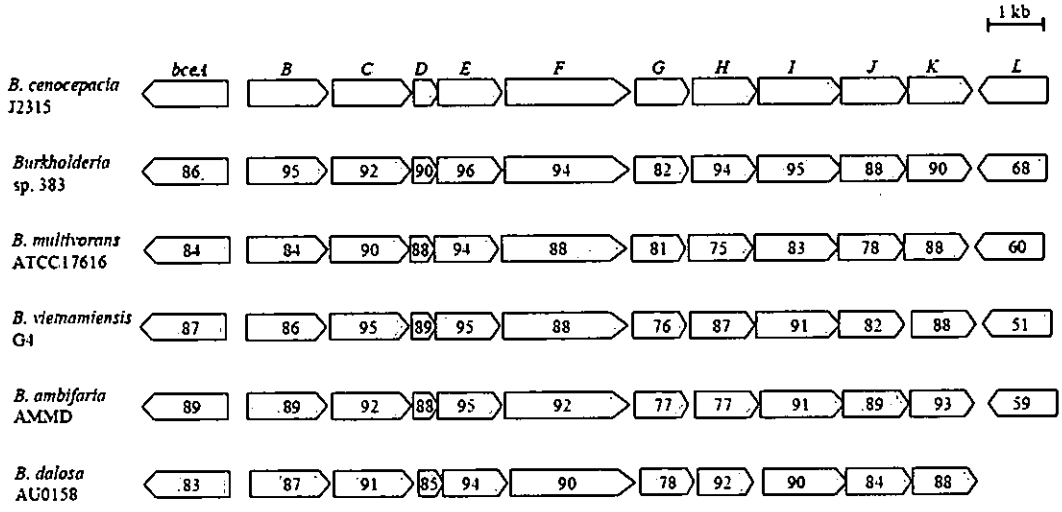

Fig. 14: Comparison of homology within *bce* gene cluster of representative Bcc species. Genetic organization of the *bce* gene cluster within *B. cenocepacia* J2315 is shown (Moreira *et al.*, 2003). The homologous genes from other Bcc genomes are present in the same order and orientation as observed within *B. cenocepacia* J2315, indicating a conserved gene cluster. The only exception is the *bce* gene cluster of *B. dolosa* AU0158, which lacks a homologue of BceL, a putative transporter protein. Numbers indicate the percentage identity to the *B. cenocepacia* J2315 proteins.

In the course of these genome comparisons, a third putative polysaccharide biosynthetic gene cluster was identified on chromosome 2 of *B. cenocepacia* J2315.

This cluster encodes two putative EPS transporter proteins (BCAM1330 and BCAM1331), an acyltransferase (BCAM1333), several glycosyltransferases (BCAM1335, BCAM1337, BCAM1338), a polysaccharide biosynthesis protein (BCAM1336) and a mannose-6-phosphate isomerase (BCAM1340). This cluster is conserved amongst several Bcc species, albeit to a lesser extent than the *bce* gene cluster (data not shown). In the EPS-producing *B. ambifaria* AMMD, this gene cluster maps to ORFs Bamb_3621 through to Bamb_3629.

To investigate which polysaccharide gene cluster is induced by growth on mannitol, the expression of representative genes from two distinct EPS gene clusters was assessed in *B. ambifaria* AMMD grown in the presence and absence of mannitol. The genes studied each encode homologues of the Wza EPS export protein: Bamb_5549 of the *bce* gene cluster (equivalent to *bceE*, BCAM0858 of *B. cenocepacia* J2315), and Bamb_3621 of the novel putative polysaccharide gene cluster described above (BCAM1330 of *B. cenocepacia* J2315). As shown in Figure 15, expression of Bamb_3621 was not observed under either growth condition. In contrast, expression of the *bceE* homologue (Bamb_5549) was clearly induced by the presence of mannitol. Consequently, we focused on the *bce* gene cluster to investigate why some Bcc isolates, most notably those of the *B. cenocepacia* ET12 lineage, failed to produce EPS under any growth conditions.

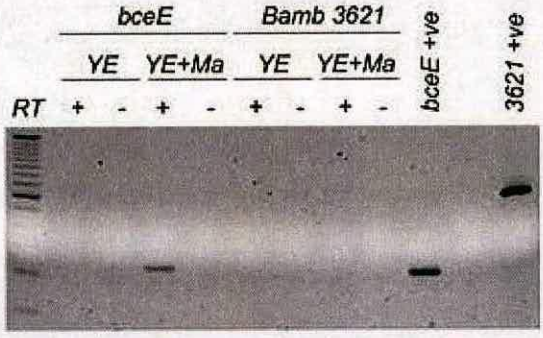

Fig. 15: Induction of the *bce* gene cluster by mannitol. RT-PCR analysis was performed to assess the expression of two distinct *wza* homologues (*bceE* and Bamb_3621) of *B. ambifaria* AMMD in the absence and presence of mannitol. Expression was assessed in yeast extract (YE) and yeast extract supplemented with 2% (w/v) mannitol. Only *bceE* expression was strongly induced by growth in YE+Mannitol. RT and non-RT reactions (+ / -) are shown alongside each other. Genomic DNA positive controls are shown for each gene (bceE +ve, 3621 +ve).

To confirm that the *IS407*-like insertion sequence in *wcbO,* described by Parsons *et al.*, is not the reason for lack of EPS production, a screen was set up using the PCR assay described by Parsons and colleagues (Parsons *et al.*, 2003). No correlation was found between the presence of the *IS407*-like insertion sequence within *wcbO* and lack of mucoidy, even within the ET-12 lineage (Fig. 16). In fact, most mucoid isolates tested did not appear to possess a *wcbO* gene at all.

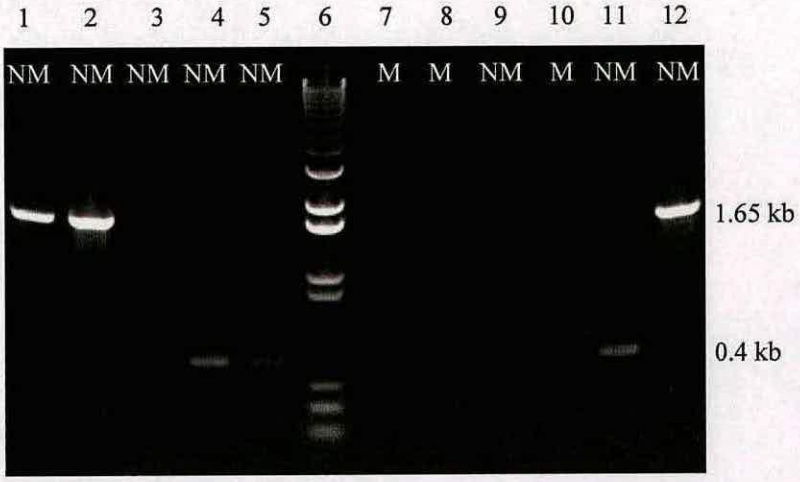

Fig. 16: PCR for the presence of *wcbO* and screen for the *IS407*-like sequence in *wcbO* in *B. cenocepacia* IIIA representatives. Lane 1, J2315; lane 2, E1189, lane 3, E3051; lane 4, E1073; lane 5, E1197; lane 6, 1 kb Plus ladder; lane 7, E1001; lane 8, E946; lane 9, E938; lane 10, E937; lane 11, K56-2; lane 12, J2315. The presence of the IS 407-like sequence in *wcbO* is seen in lane 1, 2 and 12 with a product of 1.65 kb, whereas a wild type *wcbO* yields a product at 0.4 kb (lane 4, 5 and 11). Note, some do not contain a *wcbO* gene (lane 3, 7, 8, 9, 10).

A PCR assay was then designed to screen isolates for an 11-bp deletion in the *bceB* gene which has been suggested to be responsible for loss of EPS production in the CF isolate *B. cenocepacia* J2315 (Moreira *et al.*, 2003). Of the panel of strains shown in Table 6, only the *B. cenocepacia* ET12 isolates J2315, K56-2 and BC7 were found to harbour the 11-bp deletion. This result prompted an examination of a panel of *B. cenocepacia recA* lineage IIIA strains containing both ET12 and non-ET12 isolates. There was a clear correlation between the 11-bp deletion and the presence of both *cblA* (cable pilus) and BCESM (*B. cepacia* epidemic strain marker), confirming this deletion is a conserved feature within the ET12 lineage (Fig. 17). In our study, with the exception of strain E3051, the presence of the deletion correlated with the lack of EPS production in all *B. cenocepacia* IIIA isolates examined (Fig. 17; Table 7).

Furthermore, the 11-bp deletion in the *bceB* gene was not observed in any *B. cenocepacia* IIIB or *B. multivorans* isolates studied (Tables 8 and 9).

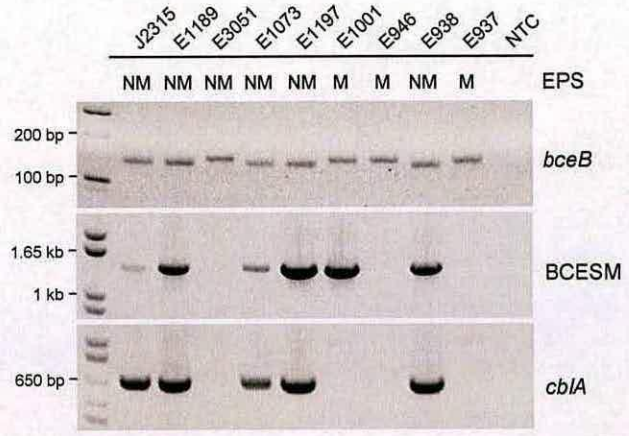

Fig. 17: *bceB* PCR analysis of representative *B. cenocepacia* IIIA isolates. For each isolate, EPS production is indicated as mucoid (M) or nonmucoid (NM) alongside PCR analysis of *bceB*, and the epidemic strain markers *cblA* and BCESM. All PCR products are pictured alongside the 1 Kb Plus DNA Ladder (Invitrogen). NTC – no template control. The *bceB* PCR assay yields a 151 bp product from wild-type sequence and a 140 bp product from sequence harbouring an 11-bp deletion (as previously reported within J2315). With one exception (E3051), lack of EPS production within *B. cenocepacia* IIIA isolates correlated with the 11-bp deletion within *bceB*. This deletion was only observed within strains that were positive for both *cblA* and BCESM, indicating it to be a conserved feature of the ET12 lineage.

To confirm the involvement of BceB in onion-induced EPS production, attempts were made to complement BceB function within *B. cenocepacia* K56-2 by introducing a wildtype *bceB* amplified from *B. cenocepacia* PC184 on a pSCRhaB3 plasmid, previously used for complementation of gene function in *B. cenocepacia* (Ortega *et al.*, 2005). Weak expression of 6 His-tagged *B. cenocepacia* PC184 BceB on a pET22b plasmid was detected in *E. coli* C41(DE3) cells (Fig. 18) by Western blot. These *E. coli* cells have previously been shown to support expression of membrane-bound proteins (Miroux & Walker, 1996). In addition, wild type *bceB* mRNA was being expressed in the *B. cenocepacia* K56-2 recipient containing pSCRhaB3/*bceB* (Fig. 19), however, we were unable to detect protein expression within *B. cenocepacia* K56-2 nor see a change in phenotype on sugar and onion agar. Consequently, we chose to disrupt the *bceB* ORF of an EPS-producer. Insertional inactivation of the *bceB* gene resulted in loss of EPS production in *B. ambifaria* AMMD when grown mannitol agar (Fig.9 (C)) and on onion agar (data not shown).

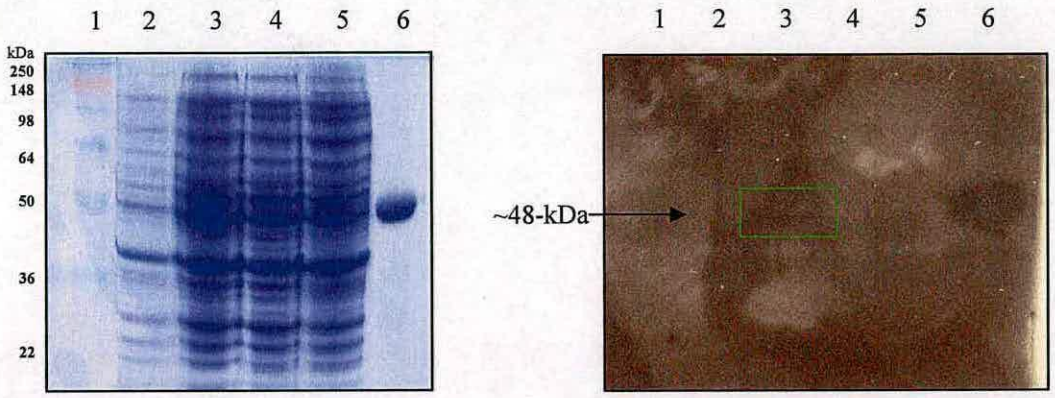

Fig. 18: Weak *B. cenocepacia* PC184 BceB expression in *E. coli* C41 (DE3). The order on both gels is as follows: lane 1, SeeBlue®Plus2 pre-stained marker; lane 2, BceB/C41 uninduced; lane 3, BceB/C41 induced; lane 4, BceB/C43 uninduced; lane 5, BceB/C43 induced; lane 6, SPT 6His +ve control. BceB appears at ~48-kDa, the gene sequence predicted a 52-kDa protein but BceB has a cleavable signal peptide at the N-terminal site resulting in a 48 Da product (Videira et al 2005).

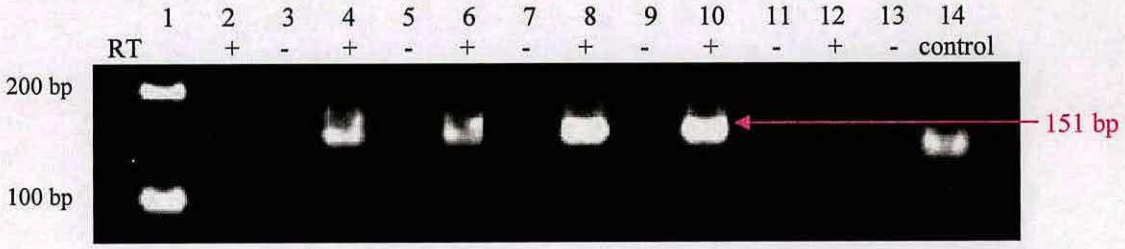

Fig. 19: RT-PCR expression of pSCRhaB3/*bceB* in *B. cenocepacia* K56-2. Lane 1, 1kb plus DNA marker showing only between 100 bp and 200 bp; lane 2 and 3, *B. cenocepacia* K56-2, RT + and -; lane 4 and 5, K56-2/pSCRhaB3 control rhamnose, RT +/-; lane 6 and 7, K56-2/pSCRhaB3 control glucose, RT +/-; lane 8 and 9, K56-2/pSCRhaB3/*bceB* rhamnose, RT +/-; lane 10 and 11, K56-2/pSCRhaB/ *bceB* glucose, RT +/-; lane 12 and 13, *B. cenocepacia* J2315, RT +/-; lane 14, J2315 DNA control. The *bceB* wild type yields a 151 bp product and *bceB* with an 11-bp deletion a 140 bp product.

3.3. Discussion

This study returned to the original Bcc host and found that Bcc isolates previously considered non-mucoid produce copious amounts of EPS when onion tissue is provided as the sole nutrient. This surprising observation not only highlights the metabolic potential of this group of organisms, but also revealed a putative virulence factor that would be missed on routine laboratory culture. Onion-induced EPS biosynthesis is not species-specific, and is exhibited by isolates of both clinical and environmental origin. Interestingly, mucoidy on onion agar does not correlate with onion maceration.

The onion components responsible for EPS induction are primarily the carbohydrates sucrose, fructose and fructans. Additionally, all alcohol sugars tested are able to induce EPS production, in particular mannitol and glucitol. The reasons why EPS biosynthesis is readily induced by onion extracts and, in particular, by fructose and the hexitol sugars mannitol and glucitol require further investigation. However, the similar profile of EPS induction shown by growth on fructose and alcohol sugars may be explained by consideration of the results of a previous study that investigated the initial steps of utilization of these sugars by the Bcc (Allenza *et al.*, 1982). It was found that growth of Bcc on fructose involves active transport into the cell followed by fructokinase conversion to fructose 6-phosphate then degradation via the Entner–Doudoroff pathway. Growth on mannitol and glucitol also requires this pathway following active uptake and intracellular oxidation to fructose. An ability to respond to inulin was confined to certain strains, all of which responded well to fructose. This suggests that the fructan polysaccharide was only active in bacteria that can hydrolyse it to fructose.

The ability of hexoses and hexitols, in particular mannitol, to enhance EPS biosynthesis in the Bcc has disturbing clinical implications for therapeutic intervention in CF. Recent attempts to improve airway clearance with hypertonic saline 5% (w/v) have been handicapped by the problem of salty taste and reservation concerning the salt-sensitive nature of most natural antimicrobial peptides, including

human defensins. Thus, attention has turned to the use of non-ionic osmolytes, including inhaled mannitol (Daviskas *et al.*, 2005; Robinson *et al.*, 1999; Wills, 2007), which is marketed as Bronchitol™ by Pharmaxis. In their study of the clinical use of Bronchitol™, Robinson and colleagues acknowledged that the majority of *P. aeruginosa* and Bcc isolates are able to utilize mannitol as a carbon and energy source. However, they felt that the nutritional influence of mannitol as a therapeutic osmolyte would be minimal given the abundance of other nutrients already present in CF respiratory secretions. In contrast, our study highlights the potential induction of virulence determinants during osmolyte therapy, and provides further justification for the continued exclusion of CF individuals known to be infected with Bcc from ongoing trials of inhaled mannitol (http://clinicaltrials.gov; identifier NCT00117208 and NCT00251056). Additionally, fructose and sugar alcohol levels are elevated in the serum, and possibly the airway secretions, of patients with CF related diabetes, indicating that the lung environment of these patients may enhance bacterial virulence (Reid & Bell, 2009).

Intriguingly, none of the *B. cenocepacia* ET12 lineage tested was able to produce EPS on any media tested. This was surprising as the lineage is considered to be the most virulent of the Bcc and EPS had been suggested as a putative virulence factor analogous to the characteristic transition to an alginate producing mucoid phenotype in *P. aeruginosa* (Govan & Deretic, 1996). Two previous studies proposed reasons for the lack of EPS production in *B. cenocepacia* J2315. Parsons and colleagues described an *IS407*-like insertion sequence within *wcbO*, encoding a putative polysaccharide biosynthesis/export protein, found in the *wcb* gene cluster (Parsons *et al.*, 2003); and Moreira and colleagues found an 11 bp deletion in *bceB*, encoding a glycosyltransferase, in the *bce* gene cluster (Moreira *et al.*, 2003). *In silico* analysis comparing available Bcc genome sequences, revealed that the *wcb* gene cluster is poorly conserved, and is in fact only present in some strains on a genomic island. Its role in onion-induced EPS biosynthesis can be further discounted by the lack of correlation between the presence or absence of the *IS407*-like insertion sequence and mucoidy. In contrast, the *bce* gene cluster is highly conserved among all Bcc species. Several of the encoded proteins in this particular cluster have been characterised

(Ferreira *et al.*, 2007; Sousa *et al.*, 2008; Sousa, 2007; Videira *et al.*, 2005), and it is thought to be involved in the biosynthesis of cepacian, the major and the best characterised EPS of the Bcc. In the present study, we obtained evidence for the role of this EPS in the onion-induced mucoid phenotype by demonstrating induction of the *bce* gene cluster by mannitol. We also found a clear correlation between the inability of representatives of the *B. cenocepacia* ET12 lineage to produce EPS and the presence of an 11 bp deletion within the *bceB* gene. Consistent with this correlation, insertional inactivation of *bceB* resulted in the loss of EPS production by *B. ambifaria* AMMD when grown on onion and mannitol media. However, mutations elsewhere within the *bce* gene cluster, or in other EPS-related gene clusters, must be responsible for the lack of EPS biosynthesis in *B. cenocepacia* strain E3051, and in other EPS-negative Bcc strains in our study which contain a wild type *bceB*. This could also explain our inability to generate an EPS producer by simple expression of a plasmid-encoded, wild-type *bceB* in a non-producer that contained the 11 bp deletion. Taken together, these interesting observations highlight the pivotal role of the *bce* gene cluster in onion-induced EPS biosynthesis, and suggest that the observed EPS is cepacian.

The role of Bcc EPS as a putative virulence factor is unclear. The influence of mannitol and other alcohol sugars on EPS production suggests that the prevalence of EPS in the Bcc may have been underestimated. In addition, given the variety of human, animal, plant and other models studied, the role of EPS may be influenced by the host involved and the route of inoculation. EPS has been associated with altered Bcc clearance in a mouse model of infection (Conway *et al.*, 2004), and EPS-deficient Bcc mutants displayed reduced mortality within a CGD mouse model (Sousa *et al.*, 2007). Similarly, a role for EPS in resistance of Bcc in human airways is suggested by its capacity to scavenge reactive oxygen species and inhibit neutrophil chemotaxis (Bylund *et al.*, 2006). In our study, EPS biosynthesis did not correlate with the ability to cause onion rot, which is perhaps to be expected since pectinases rather than EPS are likely to play the major role in the maceration of plant tissue. Cunha *et al.* did not observe a clear correlation between EPS biosynthesis *in vitro* and the ability of Bcc strains to establish chronic infections within the CF lung

(Cunha *et al.*, 2004). Recent evidence, however, suggests a possible and unexpected role for Bcc EPS in CF lung infection. Consistent with the findings of our study, Zlosnik *et al.* reported that isolates of *B. cenocepacia*, the most virulent Bcc species, are most frequently non-mucoid (Zlosnik *et al.*, 2008). They also observed a mucoid to non-mucoid conversion in sequential isolates of Bcc from chronically-infected CF patients. This loss of mucoidy *in vivo*, and its absence in the virulent *B. cenocepacia* ET12 lineage, provides an intriguing contrast with the characteristic non-mucoid to mucoid conversion observed with alginate-producing *P. aeruginosa*. The observations made by Zlosnik and colleagues suggest that Bcc EPS could be responsible for the persistence of Bcc in CF airways whilst loss of EPS leads to increased disease severity. Clearly, further analyses are required to explore the role of EPS production in the Bcc and what influence it has on the host/pathogen interaction.

Chapter 4: Lipopolysaccharides and AMP Resistance

4.1. Lipopolysaccharide methods

4.1.1 Bacterial strains and culture conditions

B. cenocepacia K56-2, J2315 and SAL-1 and *E. coli* WBB06 were recovered from storage at -80 °C by subculture on nutrient agar and grown at 37 °C; SAL-1 was selected on trimethoprim and WBB06 on tetracycline agar. The *E. coli ΔarnT* strain AY103 (Yan *et al.*, 2007), was recovered from storage at -80 °C by subculture on LB with kanamycin agar and grown at 30 °C.

E. coli WBB06 and AY103 were made electrocompetent as described in 2.2.2.

E. coli TOP10, *E. coli* BL21 (DE3), HSM174 (DE3), Rosetta (DE3), C41 (DE3) or C43 (DE3) were used for cloning and expression of recombinant proteins.

Kdo_2-lipid A, purified from *E. coli* WBB06 (Raetz *et al.*, 2006), was purchased from Avanti Polar Lipids.

4.1.2 Small-scale lipopolysaccharide extraction

Bacteria were grown overnight in nutrient broth at 37 °C. Five ml were centrifuged for 10 minutes at 13000 rpm. The pellet was resuspended in 0.75 ml dH_2O. 0.5 ml 90% phenol (Fisher Scientific) was added. The mixture was vortexed then heated to 65 °C for 15 minutes, vortexing every 5 minutes. It was then cooled on ice after which the layers were separated by centrifugation. Both layers were dialysed against water in 6000 – 8000 Dalton (Da) molecular weight cut off dialysis tubing (Spectra/Por, Spectrum) for 48 hours, with running water. The samples were then freeze dried, and resuspended in 100 µl DOC sample buffer (4ml of stock solution C (7.69 g Tris base (Sigma); 75 ml dH_2O; pH 6.8, made up to 100 ml with dH_2O); 5 mg

Bromophenol blue, 2 ml glycerol (Fisher Scientific), made up to 20 ml with dH_2O) and analysed by DOC-PAGE (see 4.1.4.).

4.1.3 Large-scale lipopolysaccharide extraction

Bacteria were grown in 4 L nutrient broth at 37 °C for 48 hours; the cells were harvested by centrifugation at 9000 g for 20 minutes. The pellet was resuspended in 70 ml chilled EDTA solution (0.05 M Na_2HPO_4 (Sigma), 0.005 M EDTA (Fisher Scientific), pH adjusted to 7.0). The mixture was sonicated (amplitude 10 microns) on ice for 30 seconds with a 1 minute pause, repeating 10 times. Then 15 mg lysozyme (Sigma) was added and stirred at 4 °C over night. The mixture was then heated to 37 °C for 20 minutes with frequent stirring. 4 mg DNase (Roche), 20 mg RNase (Roche) and 25 ml of 0.04 M $MgCl_2$ (Fisher Scientific) was added. The solution was then incubated at 37 °C for 10 minutes followed by incubation at 60 °C for 10 minutes. The mixture and 100 ml phenol were both heated to 65 °C; they were then added together in a fume hood and heated at 65 °C for 15 minutes with stirring. The mixture was then incubated on ice for 15 minutes and then centrifuged at 9000 x g for 20 minutes at 4 °C in new polypropylene centrifuge tubes. The water and phenol layers were each pipetted into a new centrifuge tube. 30 cm lengths of 3000-6000 Da molecular weight cut off dialysis tubing (Spectra/Por, Spectrum) were rinsed in dH_2O and then filled with each of the layers and dialysed against running dH_2O for 4 days. The dialysed samples were then centrifuged again at 9000 g, and then freeze-dried. Samples were then stored at – 20 °C until analysed by DOC-PAGE (see 4.1.4.).

4.1.4 DOC-PAGE

The DOC (deoxycholate) gels were made up using three solutions: Solution A, 30% Bis/Acrylamide (Bio-Rad); solution B, 1.5 M Trizma (Sigma), pH 8.8; and solution C, 500 mM Trizma, pH 6.8.

The running gel was prepared as follows: 6 ml Solution A, 2 ml Solution B, 2 ml dH_2O, 17.5 µl APS (Fluka) and 8.75 µl TEMED (Sigma) were mixed and loaded into glass plates. The stacking gel was made up of 0.66 ml Solution A, 1 ml Solution C, 3.34 ml dH_2O, 12.5 µl APS and 6.25 µl TEMED.

A running buffer was made up of 10.85 g glycine (Fisher Scientific), 2.25 g Tris base, 1.25g sodium deoxycholate (BDH), 500 ml dH_2O.

The gels were pre-run for 10 minutes at 30mA, then after loading run for 1 hour at 30mA. Gels were left in fixative (40% w/v ethanol, 5% acetic acid) overnight, or in fixative with 0.05% (w/v) alcian blue (Sigma).

4.1.5 Sodium-m-periodate silver staining

The gel was covered in 50 ml oxidiser (0.7% w/v sodium-m-periodate (Fisons) in fixative) for 10 minutes on shaker, then washed in water 5 x 5 minutes. It was then covered with stain solution (140 ml water, 280 µl 10.0 M NaOH (Fisher Scientific), 2 ml 28-30% ammonium hydroxide (Sigma), 1 g silver nitrate (Sigma) semi-dissolved in 5 ml water added drop wise) for no more than 10 minutes, and washed again 5 x 5 minutes. Developer (100 ml water, 50 µl formaldehyde (Sigma), 50 µl citric acid (Fisher Scientific)) was added until bands were visible, then a stop solution (100 ml water, 500 µl acetic acid) was added for exactly 1 minute. The gel was washed, and stored, in water.

Staining by alcian blue follows the protocol above, but without the initial oxidising step by sodium-m-periodate.

4.1.6 Negative staining

Negative staining was carried out as described previously (Castellanos-Serra & Hardy, 2006), with some modifications. After gel electrophoresis, the gel was washed 3 x 15 minutes in 30% (v/v) acetonitrile (Fisher Scientific). Then the gel was

incubated in 10 mM zinc sulfate (Sigma) for 15 minutes, after which the gel was washed in excess dH_2O for 30 seconds before adding a 0.2 M imidazole (Sigma) solution for 1-3 minutes. The gel was washed, and kept, in dH_2O. The bands were visualised by scanning the gel with a black cardboard background.

The bands of interest were excised and incubated in PBS, pH7.4, containing 100 mM EDTA di-sodium salt or 0.3 M glycine (Fisher Scientific) for 1-2 minutes, then washed in dH_2O for 2 x 5 minutes. The gel was crushed through a metal sieve and incubated in twice the crushed gel volume of 5% (v/v) triethylamine (Sigma-Aldrich) for 20 minutes. The eluted material was lyophilised.

4.1.7 Sulfo-NHS-biotinylation

LPS (100 μg) was solubilised in 1 ml sterile PBS using a heated sonicator bath for 10 minutes. 500 μl was kept as control, and 500 μl was incubated with 100 μl 10 mM *N*-hydroxysulfosuccinimide-biotin (Sulfo-NHS-biotin; Pierce) for 30 minutes at room temperature. Both the control LPS and the biotinylated LPS was lyophilised overnight, then resuspended in 100 μl DOC-sample buffer. Each sample (10 μl) was analysed on duplicate DOC gels (see 4.1.4.), one was silver stained as described in 4.1.5. and the other was used for streptavidin western blot (see 2.4.7).

4.2 Cationic antimicrobial peptide resistance

4.2.1 *In silico* analysis of UDP-glucose dehydrogenase (Ugd) and Aminoarabinose transferase (ArnT)

The Ugd PA2022 DNA and protein sequences from *P. aeruginosa* PA01, and the ArnT DNA and protein sequences from *E. coli* K12 strain MG1655 were used to BLAST the *B. cenocepacia* J2315 genome sequence available at the Wellcome Trust Sanger Institute (http://www.sanger.ac.uk/) and the NCBI genomic BLAST service (http://www.ncbi.nlm.nih.gov/sutils/genom_table.cgi) using TBLASTN and

TBLASTP. Protein sequence alignments were created using Vector NTI Advance™ Explorer and ClustalW software.

4.2.2 Cloning and expression of UDP-glucose dehydrogenases, *ugd*$_{BCAL2946}$, *ugd*$_{BCAM2034}$ and *ugd*$_{BCAM0855}$

The *B. cenocepacia* J2315 *ugd*$_{BCAL2946}$, *ugd*$_{BCAM2034}$ and *ugd*$_{BCAM0855}$ genes were amplified using 2 puReTaq™ Ready-To-Go PCR beads (Amersham), 5 µl of each primer (ugd bcal2946 For and Rev, ugd bcam2034 For and Rev, ugd bcam0855 For and Rev), 1 µl *B. cenocepacia* J2315 genomic DNA (prepared as in 2.3.1.) and 39 µl dH_2O. Samples were PCR-amplified for 30 cycles at 94 °C 1 min, 54 °C 1 min, and 72 °C 2 min, with a final 10 min extension at 72 °C. The amplified *ugd* PCR products (1398 bp for *ugd*$_{bcal2946}$, 1413 bp for *ugd*$_{bcam2946}$ and 1436 bp for *ugd*$_{bcam0855}$) were isolated from a preparative 1 % agarose gel and cloned using the pGEM®-T Easy vector system (see 2.3.4.). Positive clones were isolated and sequenced to confirm the fidelity of the PCR reaction. Restrictions enzymes *Nde*I and *Bam*HI were used to cut *ugd*$_{BCAL2946}$ and *ugd*$_{BCAM2034}$, and *Nde*I and *Xho*I to cut *ugd*$_{BCAM0855}$ to ligate with pET28a (cut with identical enzymes). The ligation mixtures were used to transform *E. coli* Top10 cells, and selected by kanamycin resistance. Plasmids were isolated and inserts of the correct size were confirmed by restriction digest analysis.

The resulting plasmids, pET-28a/*ugd*$_{BCAL2946}$, pET-28a/*ugd*$_{BCAM2034}$ and pET-28a/*ugd*$_{BCAM0855}$, were expressed in *E. coli* BL21 (DE3) or HSM174 (DE3) (see 2.4.1), each with an N-terminal 6His tag.

4.2.3 Purification of recombinant Ugd$_{BCAL2946}$ and Ugd$_{BCAM0855}$

To prepare recombinant Ugd proteins for biochemical analysis a large-scale culture (4 liters of LB supplemented with kanamycin) was performed with *E. coli* HMS 174 (DE3) transformed with pET-28a/*ugd*$_{BCAL2946}$ or pET-28a/*ugd*$_{BCAM0855}$. Each batch was grown to an OD_{600} of 0.6, and induced by addition of 0.5 mM IPTG (final concentration) for 3 h at 37 °C with shaking. Both Ugd$_{BCAL2946}$ and Ugd$_{BCAM0855}$

were highly over-expressed in soluble forms and cell-free extracts were prepared as described in 2.4.2.

An ÄKTA Basic instrument fitted with a 5 ml HisTrap™ (GE Healthcare) column was used to isolate the enzymes from the ultra-filtered cell free extracts. The buffers used were as follows: 500 ml binding buffer 20 mM Tris, 500 mM NaCl, 5 mM Imidazole, pH 7.5; 500 ml elution buffer: 20 mM Tris, 500 mM NaCl, 500 mM Imidazole, pH 7.5. The eluted His-tagged Ugd proteins were judged >90% pure by SDS-PAGE analysis after this step.

The enzymes were further purified by size exclusion chromatography, as described in 2.4.3., using a HiPrep 26/60 Sephacryl S-200 column (GE Healthcare). The calibrated column was equilibrated with 150 mM NaCl and 20 mM Tris, pH7.5. The molecular weights of the enzymes were estimated from their column elution volumes and by non-denaturing gel electrophoresis (10% Novex® Tris-Glycine Pre-Cast Gels, Invitrogen), following the manufacturer's instructions.

The subunit molecular weights were confirmed by LC-ESI-MS and were within 0.1 % of the theoretical values (see 2.4.8.).

The protein concentration was determined by a BCA assay (Pierce) and a typical yield was ~3 mg Ugd per litre of *E. coli* culture.

4.2.4 Purification of recombinant $Ugd_{BCAM2034}$

To prepare recombinant $Ugd_{BCAM2034}$ a large-scale culture (4 liters of LB supplemented with kanamycin) was performed with *E. coli* BL21 (DE3) transformed with pET-28a/$ugd_{BCAM2034}$. Each batch was grown to an OD_{600} of 0.6, and induced by addition of 0.2 mM IPTG final concentration for 16 h at 15 °C with shaking.

A 5 ml HisTrap™ column was attempted as described in 4.2.2. and some protein was isolated; however, this was not possible to repeat due to problems of insolubility of the enzyme.

To solubilise $Ugd_{BCAM2034}$ for purification the pellet was resuspended and homogenized in 5ml per g cell pellet in binding buffer containing 25 % (w/v) sucrose, 1 mM EDTA and a protease inhibitor tablet. Thirty mg lysozyme, 5 µl DNase and 5 mM $MgCl_2$ was added and the cells were left to stir for 1 hour at 4 °C. The cells were sonicated in ice for 10 minutes, 30 s on/30s off. Then 1 % (w/v) n-Dodecyl-ß-maltoside (DDM) and 20 % glycerol was added and the cells were incubated with mixing at 4°C for 1 hour before centrifugation at 14 000 rpm for 45 minutes. The supernatant was incubated with equilibrated nickel NTA agar beads for 3 hour. The beads were washed in elution buffer (20 mM Tris, pH7.5, 500 mM NaCl, 0.1 % (w/v) DDM, and 10 % glycerol) with 10 mM imidazole. Protein was eluted in elution buffer containing 20, 50, 100 or 200 mM imidazole. All fractions were analysed by SDS-PAGE, and fractions containing $Ugd_{BCAM2034}$ were concentrated to ~1 mg ml^{-1} and assayed for Ugd activity. The molecular weight of $Ugd_{BCAM2034}$ was estimated from size-exclusion chromatography, LC-ESI-MS and non-denaturing gel electrophoresis (as above).

4.2.5 *In vitro* Ugd activity assay

Ugd oxidizes UDP-glucose to UDP-glucuronic acid, and in the process also reduces 2 moles of NAD^+ to 2 moles of NADH. The molar extinction co-efficient of NADH is 6.220 $mM^{-1}cm^{-1}$ at 340 nm. A standard Ugd activity assay was set up using 200 µl H_2O, 100 µl purified Ugd (1 mg ml^{-1}), 200 µl buffer (100 mM Tris, pH 7.5), 250 µl NAD^+ (10 mM; Roche) at 25 °C. The reaction was initiated by the addition of 250 µl UDP-glucose (1 mM; Calbiochem) and the production of NADH was monitored at 340 nm on a Cary 50 UV visible spectrophotometer (Varian). Initial velocities were determined for UDP-glucose using concentrations ranging from 0 to 0.25 mM, and NAD^+ using concentrations ranging from 0 to 2.5 mM. To determine kinetic constants one substrate was held constant at the maximum concentration, while the

other was varied. The kinetic parameters (k_{cat}, K_m, V_{max}) were determined by non-linear regression from $V = V_{max}[S]^h/([S]^h + K_m^h)$ using Origin6.1 software.

Substrate specificity was investigated by replacing the substrate UDP-glucose with either: UDP-galactose, UDP-acetylglucosamine or GDP-mannose (Calbiochem), and performing the standard assay.

4.2.6 Cloning and expression of aminoarabinose transferase, ArnT

The *B. cenocepacia* J2315 *arnT* gene (BCAL1929) was amplified twice; first *arnT* was amplified without a stop codon: 2.5 U Herculase® Hotstart DNA Polymerase (Stratagene), 300 nM of each primer (*arnT* C-term His For and Rev,), 4 % DMSO, 200 µM each dNTP and 1 µl *B. cenocepacia* J2315 genomic DNA (prepared as in 2.3.1.) with appropriate manufacturer's reaction buffer, made up in 50 µl reactions.

The second reaction amplified *arnT* with a stop codon: 2.5 U Proofstart DNA polymerase (Qiagen), 1 µM of each primer (*arnT* N-term His For and Rev), 300 µM each dNTP and 1 µl *B. cenocepacia* J2315 genomic DNA (prepared as in 2.3.1.) with solution Q and appropriate manufacturer's reaction buffer, made up in 50 µl reactions.

Both samples were PCR-amplified for 30 cycles at 95 °C 1 min, 60 °C 1 min, and 72 °C 2 min, then 1 puReTaq™ Ready-To-Go PCR bead was added for a final 10 min extension at 72 °C. The amplified *arnT* PCR products (1680 bp for $arnT_{C\text{-}term}$, 1692 bp for $arnT_{N\text{-}term}$) were isolated from a 1% agarose gel and cloned using the pGEM®-T Easy vector system (see 2.3.4.). Positive clones were isolated and sequenced to confirm the fidelity of the PCR reaction. Restrictions enzymes *Nco*I and *Xho*I were used to cut $arnT_{C\text{-}term}$ and *Nde*I and *Xho*I to cut $arnT_{N\text{-}term}$ to ligate with pET28a (cut with identical enzymes). The ligation mixtures were used to transform *E. coli* Top10 cells, and selected by kanamycin resistance. Plasmids were isolated and inserts of the correct size were confirmed by restriction digest analysis.

The resulting plasmids, pET-28a/*arnT*$_{C\text{-term}}$ and *arnT*$_{N\text{-term}}$, were expressed in *E. coli* HSM 174 (DE3), BLR (DE3), Rosetta (DE3), C41 (DE3) or C43 (DE3) (see 2.4.1). Expression was visualised by western blot using anti-His antibodies as described in 2.4.6. (ArnT$_{C\text{-term}}$ at 63748.48 Da and ArnT$_{N\text{-term}}$ at 64845.64 Da). Large-scale inductions in *E. coli* C41 (DE3) or C43 (DE3) were set up using pET-28a/ *arnT*$_{N\text{-term}}$.

To prepare the *arnT* genes for cloning into an alternative expression plasmid, pTrc99a, two PCR reactions were set up using pET-28a/*arnT*$_{N\text{-term}}$ and *arnT*$_{C\text{-term}}$ as templates, using 2 puReTaq™ Ready-To-Go PCR beads (Amersham), 5 µl of each primer (either *arnT* C-term and *arnT* C-term6 His Rev, or *arnT* Nterm6 His For1 and *arnT* Nterm6 His Rev), 1 µl genomic DNA and 39 µl dH_2O. Samples were amplified for 30 cycles: 95 °C 1 min, 60 °C 1 min, and 72 °C 2 min; with a final 10-min extension at 72°C. The *arnT*$_{C\text{-term}}$ (1698 bp) and *arnT*$_{N\text{-term}}$ (1748 bp) genes, flanked by *Nco*I and *Hind*III, were now amplified with the 6 His tag. The genes were electrophoresed on a 1% agarose gel, and gel extracted using QIAprep® Gel Extraction kit from Qiagen. The *arnT*$_{C\text{-term}}$ and *arnT*$_{N\text{-term}}$ genes were again cloned into pGEM as described in 2.3.4. After restriction digests and sequencing analysis, the genes were cloned into pTrc99a (as described in see 2.4.1.) and selected on ampicillin.

4.2.7 RT-PCR of C-terminal ArnT expression

To double-check that *arnT*$_{C\text{-term}}$ was being expressed, RT-PCR was performed. *E. coli* strain BLR (DE3) were transformed with pET-28a/*arnT*$_{C\text{-term}}$; and *E. coli* TOP10 cells were transformed with pTrc99a/*arnT*$_{C\text{-term}}$. *B. cenocepacia* J2315 was used as a positive control. Overnight cultures were sub-cultured into fresh LB media and grown until an OD_{600} of 0.5, when half the *E. coli* cells were induced with IPTG (1mM final concentration). RNA was extracted from mid-log phase cultures (RNeasy Protect Bacteria Mini Kit; Qiagen) and DNase I-treated (RNase-free DNase set; Qiagen), prior to reverse transcription with 1.5 µg RNA template, random primers and SuperScript III Reverse Transcriptase (Invitrogen). cDNAs and corresponding non-RT controls were used as template in PCR reaction amplifying *arnT*. PCR

reactions were performed in a 25 µl volume containing 300 nM forward and reverse primer (*pmrK* For and Rev), 260 µM of each dNTP, 1 U Taq DNA polymerase (Qiagen) with Q solution and appropriate manufacturer's reaction buffer. Thermal cycling was performed using the following parameters: 35 cycles of 95 °C (30 s), 58 °C (30 s), 72 °C (1 min), followed by a 10 min extension at 72 °C.

4.2.8 Sulfo-NHS-biotinylation of *E. coli* WBB06/pTrc99a/*arnT*$_{C\text{-term}}$ LPS

Deep-rough *E. coli* WBB06 were transformed by electroporation (as in 2.3.7.) with pTrc99a/*arnT*$_{C\text{-term}}$ and clones were selected by tetracycline and ampicillin resistance. Overnight cultures were sub-cultured into fresh LB media and grown until an OD_{600} of 0.5 at 37°C, when half the *E. coli* cells were induced with IPTG (1mM final concentration). Small-scale LPS extractions of induced and uninduced cells were carried out (as in 4.1.2) followed by NHS-biotinylation and Western blot as described in 4.1.7.

4.2.9 Purification of ArnT

The *E. coli* C41 (DE3) or C43 (DE3) pellets expressing pET-28a/ *arnT*$_{N\text{-term}}$, were resuspended (5 ml per g cell pellet) in 25 mM Tris buffer (pH 8.0) and a tablet of protease inhibitor cocktail (Roche). The mixture was stirred briskly at 4°C for 30 minutes. This mixture was sonicated for 15 minutes (30 seconds on and 30 seconds off) and then centrifuged at 25000 x g for 30 minutes at 4°C to remove insoluble debris. The opaque supernatant was decanted and ultra centrifuged at 120000xg for 2 hours at 4°C. The resulting dense golden pellet was resuspended in a minimal amount of 25mM Tris buffer (pH 8.0) and frozen in 1 ml aliquots at -20°C.

Aliquots of enriched inner membranes were solubilised in 25 mM Tris buffer (pH 8.0) containing 500 mM NaCl, 1% (w/v) DDM and 20% (v/v) glycerol (resolubilisation buffer) at 4°C for 3 hours with gentle agitation. The extraction mixture was centrifuged for 30 minutes at 25000 x g and 4°C to remove any remaining unsolubilised material. TALON metal affinity resin (Clontech) was

washed three times in water and then three times in resolubilisation buffer. The extract supernatant was incubated with the equilibrated TALON resin for 1-2 hours at 4°C with gentle agitation. The resin was washed with 20 column volumes 10 mM imidazole. The protein was eluted with 25 mM Tris buffer with different concentrations of imidazole (20, 50, 100, 200 mM). All the fractions were collected for a SDS-PAGE and Western Blot.

4.2.10 ArnT assay in *E. coli* AY103 (*arnT::kan)*

The *E. coli arnT* knock-out mutant strain AY103 was made electrocompetent as described in 2.2.2. Aliquots of the cells were transformed by electroporation (as in 2.3.7.) with pTrc99a/$arnT_{C\text{-}term}$, pTrc99a/$arnT_{N\text{-}term}$ or pTrc99a/FbpA. As a positive control we used pTrc99a/FbpA which expresses a 33kDa ferric binding protein from *Neisseria gonorrhoeae* (cloned by Paul Bilton, School of Chemistry, University of Edinburgh). *E. coli* AY103, and *E. coli* AY103 containing pTrc99a/$arnT_{C\text{-}term}$, pTrc99a/$arnT_{N\text{-}term}$ or pTrc99a/FbpA sub-cultured onto LB agar plates containing either kanamycin (30 μg ml^{-1}), kanamycin and ampicillin (100 μg ml^{-1}), or polymyxin (10 μg ml^{-1}), the same strains were used to inoculate 10 ml LB broth overnight at 30 °C. The overnight cultures were used for small-scale LPS extractions, followed by sulfo-NHS-bioltinylation and western blot.

4.2.11 Complementation assay of *B. cenocepacia* XOA11 (*arnT* conditional mutant)

To clone the *B. cenocepacia arnT* gene into the pDA-17 plasmid suitable for expression in *B. cenocepacia* conditional *arnT* mutant XOA11 (Ortega *et al.*, 2007) it was amplified as follows. A PCR reaction was set up using pET-28a/$arnT_{N\text{-}term}$ as template, using 2.5 U Proofstart DNA polymerase (Qiagen):, 1 μM of each primer (*arnT* Nterm6 His For2 and *arnT* Nterm6 His Rev), 300 μM each dNTP and 1 μl *B. cenocepacia* J2315 genomic DNA (prepared as in 2.3.1.) with solution Q and appropriate manufacturer's reaction buffer, made up in 50 μl reactions. Thermal cycling was performed using the following parameters: 40 cycles at 95 °C 1 min, 55

°C 1 min, and 72 °C 2 min, then 1 puReTaq™ Ready-To-Go PCR bead was added for a final 10 min extension at 72 °C. The *arnT*$_{N\text{-term}}$ (1762 bp) gene, flanked by *Eco*RI and *Hind*III, was now amplified with the N-terminal 6 His tag. The genes were electrophoresed on a 1% agarose gel, and gel extracted using QIAprep® Gel Extraction kit from Qiagen. The *arnT*$_{N\text{-term}}$ gene was again cloned into pGEM as described in 2.3.4. After restriction digests and sequencing analysis, the genes were cloned into pDA-17 (as described in see 2.4.1.) and clones were selected by tetracycline resistance.

E. coli DH5α was transformed with pDA-17/*arnT*$_{N\text{-term}}$ and selected on tetracycline plates to become donors for triparental mating. In addition, the helper strain was prepared by transforming *E. coli* DH5α with helper plasmid pRK2013, selected on kanamycin plates, and the recipient strains *B. cenocepacia* conditional *arnT* mutant XOA11 was streaked onto a gentamycin/trimethoprim plate. Triparental mating was carried out as described in 2.3.8, and *B. cenocepacia* XOA11 containing a wild type *arnT* on pDA-17 was selected on tetracycline, trimethoprim and gentamycin, containing 0.5 % rhamnose. Complementation was investigated by streaking successful colonies on LB agar plates containing 0.5 % glucose.

4.3. Results

4.3.1 LPS extraction and analysis

Members of the *B. cenocepacia* ET-12 lineage have rough LPS with the exception of *B. cenocepacia* K56-2 which has smooth LPS. This was shown to be due to an insertion sequence in *wbxE*, encoding a glycosyl transferase involved in O-antigen biosynthesis, found in all ET-12 strains except K56-2 (Ortega *et al.*, 2005). Hence, the LPSs used in this section were isolated from the clonal ET-12 strains *B. cenocepacia* K56-2 and J2315. In addition, LPS from a deep-rough *B. cenocepacia* ET-12 mutant SAL-1 was investigated. The SAL-1 strain is heptose-less due to insertional inactivation of *hldD* and *hldA* genes, encoding a putative ADP-l-glycero-D-manno-heptose-6-epimerase and a putative D-beta-D-heptose 7-phosphate kinase, respectively (Loutet *et al.*, 2006). The LPS from these smooth, rough and deep-rough *B. cenocepacia* ET-12 strains were extracted using the hot phenol-water method yielding an aqueous and a phenol phase. Both phases were analysed by DOC-PAGE. A commercial *E. coli* Kdo_2-lipid A preparation (Avanti), isolated from deep-rough *E. coli* strain WBB06, was used as a control. *E. coli* WBB06 is also a heptose-less mutant, with mutations in heptosyltransferase genes *rfaC* and *rfaF* (Brabetz *et al.*, 1997), and its LPS has recently been fully characterised (Raetz *et al.*, 2006), making it an excellent model for comparison.

To visualise the LPS, the DOC gels were stained using different staining methods. Based on protein silver staining methods, sodium-m-periodate (smp) silver staining of LPS was developed by Tsai and Frasch in 1982 (Tsai & Frasch, 1982) and involves smp oxidation followed by ammoniacal silver nitrate incubation and citric acid/formaldehyde development. It is believed that the smp reacts with diol groups on polysaccharides to form reactive aldehydes with which the silver nitrate reacts to form a precipitate of silver (Fig. 20 (A)). Instead of using smp oxidation, the cationic dye alcian blue was added prior to silver staining. This combination is thought to reveal more negatively charged and hydrophilic residues (Fig. 20 (B)). However, based on the gels in Fig. 20, no significant differences were observed between the

two silver staining methods, although, smp silver staining produces a gel with a clearer background

.

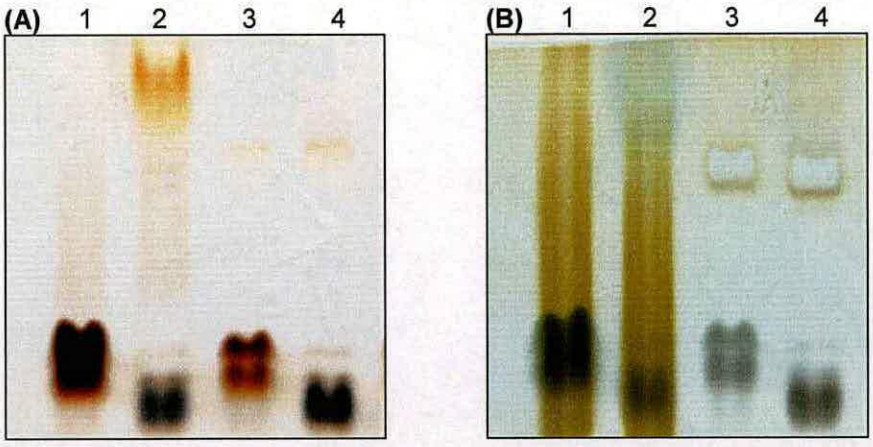

Fig. 20: DOC-gels illustrating smp-silver staining **(A)** vs alcian blue silver staining **(B)**. The sample order on both gels is as follows: lane1, *B. cenocepacia* J2315 aqueous phase; lane 2, *B. cenocepacia* K56-2 aqueous phase; lane 3, *B. cenocepacia* J2315 phenol phase; lane 4, *B. cenocepacia* K56-2 phenol phase.

Kropinski *et al* argued that smp silver staining does not stain polysaccharides but only lipid A and suggest possible Ag^{+} binding sites on the fatty acid chains (Kropinski *et al.*, 1986). Corzo *et al* added that only pre-treating with alcian blue allowed the visualisation of polysaccharides that would be missed by smp silver staining (Corzo *et al.*, 1991). It is likely that the lower (faster migrating) bands on a DOC-gel represent the lipid A and core, and, in smooth isolates, each rung up the characteristic ladder represents a lipid A-core molecule substituted with an increase of one additional O unit, and the spacing between rungs is determined by the size of the O unit. This gives rise to the characteristic, strain-specific O-antigen ladder banding pattern observed in LPS gels. However, from gel analysis alone one cannot fully determine LPS modifications present in different isolates. Therefore, a method of isolating and analysing the chemistry of individual bands would be very useful. During literature research for this project a new staining method was found. This is called "negative", or "reverse", staining and is based on an interaction between zinc and LPS (Castellanos-Serra & Hardy, 2006; Hardy & Castellanos-Serra, 2004). The gel was incubated with zinc sulfate and the zinc bound to the biomolecules negatively charged residues, for example phosphate groups or polyhydroxyls, then

imidazole was added to interact with unbound zinc ions leading to form the insoluble zinc imidazolate ($ZnIm_2$) which stains the whole gel, except the biomolecule, white (Fig. 21). The LPS appears as a clear zone and is observed against a black background. In effect, the LPSs are not chemically modified and remain "unstained". In addition, this method appears to be more sensitive than silver staining (Fig. 21).

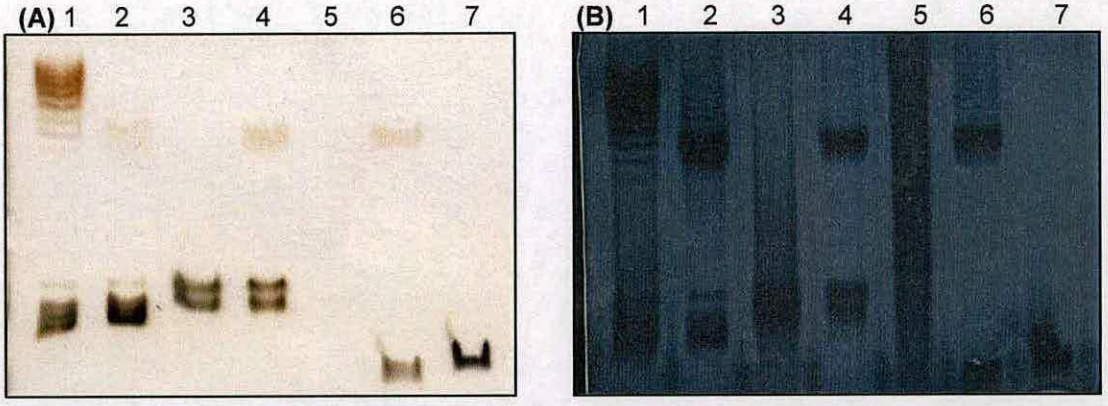

Fig. 21: DOC-gels illustrating smp-silver staining **(A)** vs negative (reverse) staining **(B)**. The sample order on both gels is as follows: lane 1, *B. cenocepacia* K56-2 aqueous phase; lane 2, *B. cenocepacia* K56-2 phenol phase; lane 3, *B. cenocepacia* J2315 aqueous phase; lane 4, *B. cenocepacia* J2315 phenol phase; lane 5, *B. cenocepacia* SAL-1 aqueous phase; lane 6, *B. cenocepacia* SAL-1 phenol phase; lane 7, *E. coli* Kdo_2-lipid A (Avanti). Two µg of each sample was loaded into the wells.

The different LPS bands can then be excised and the biomolecules recovered by first reversing the zinc fixation by EDTA incubation and then eluting from the gel with triethylamine. This method should, when optimised, recover ~80 % of the biomolecules, and the recovered material should still be intact and biologically active (Hardy & Castellanos-Serra, 2004). To optimise the recovery procedure in our hands we used Kdo_2-lipid A and SAL-1 LPS but we could only re-isolate a very small percentage of the initial material (data not shown). Time prevented a detailed study of the reverse-staining method but current work in the lab is aimed at optimising purification and analysis of Bcc LPS using this technique. With this method in hand, investigations into where AMPs bind to LPS can be carried out, as well as understanding which components and structures are immuno-stimulatory.

A recent study by Raetz and co-workers used *N*-hydroxysuccinimide-biotin (NHS-biotin; membrane permeable) and sulfo-NHS-biotin (membrane impermeable) to

show that Upp-L-Ara4N transport across the inner-membrane is defective in *pmrL* and *pmrM* mutants of *pmrA*^{c} strain MST100 compared to wild type (Hung *et al.*, 2007). They treated cell cultures with NHS-biotin or sulfo-NHS-biotin, followed by lipid extraction, TLC and ESI/MS analysis of Upp-L-Ara4N modification. In this study, attempts were made to detect any LPS species modified with L-Ara4N by directly labelling isolated LPS with sulfo-NHS-biotin. The sulfo-NHS-biotin reacts with primary amine groups of L-Ara4N (Fig. 22), and the biotinylated LPS can be detected by streptavidin using Western blotting. When applied to *B. cenocepacia* J2315, SAL-1 and *E. coli* Kdo_2-lipid A, only J2315 and SAL-1 are visible after blotting (Fig. 23) as would be expected. However, the band observed from the SAL-1 LPS is significantly higher (slower migrating) than the main band observed by smp silver staining, and suggests that the higher bands of the phenol phase of rough and deep-rough isolates observed mainly by alcian blue and negative staining may be important polysaccharide bands missed by some extraction and staining methods. This method may in future provide a useful tool for detecting L-Ara4N modified LPS by western blot.

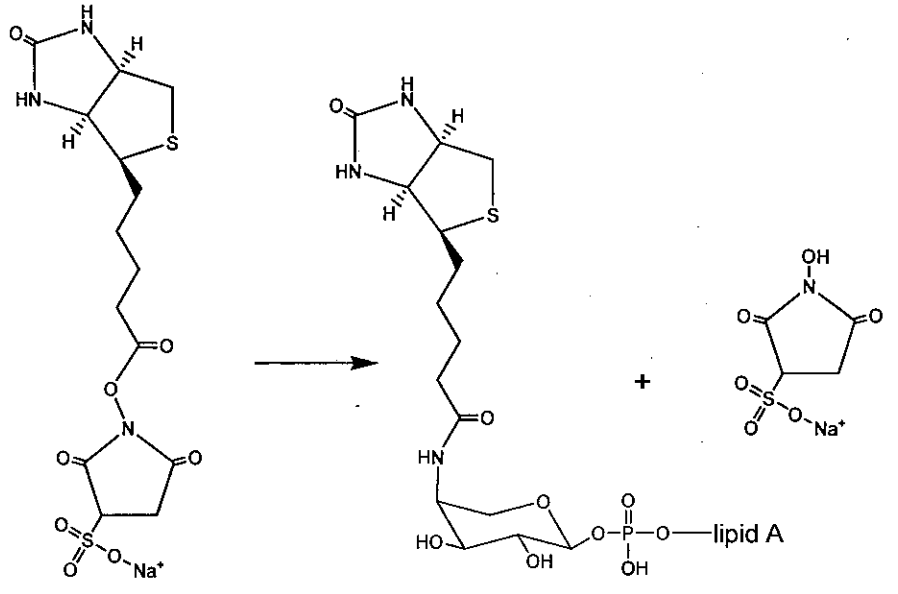

Fig. 22: Sulfo-NHS-biotin reacting with L-Ara4N-lipid A.

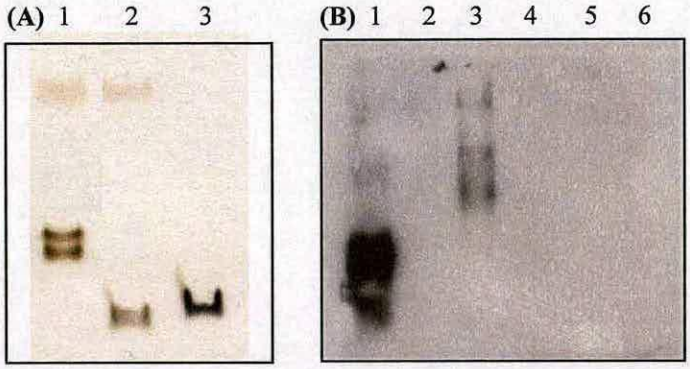

Fig. 23: Biotinylation of LPS. **(A)** Smp-silver stained DOC-gel: lane 1, *B. cenocepacia* J2315; lane 2, *B. cenocepacia* SAL-1; lane 3, *E. coli* Kdo_2-lipid A (Avanti). **(B)** Western blot of biotinylated LPS using streptavidin: lane 1, biotinylated *B. cenocepacia* J2315; lane 2, control *B. cenocepacia* J2315; lane 3, biotinylated *B. cenocepacia* SAL-1; lane 4, control *B. cenocepacia* SAL-1; lane 5, biotinylated *E. coli* Kdo_2-lipid A; lane 6, control *E. coli* Kdo_2-lipid A.

4.3.2 *in silico* genome analysis of *B. cenocepacia ugd* and *arnT*

The synthesis of UDP-L-Ara4N begins with the conversion of UDP-glucose to UDP-glucuronic acid catalysed by the enzyme UDP-glucose dehydrogenase (Ugd); and the last enzyme of the L-Ara4N biosynthetic pathway is the inner membrane protein aminoarabinose transferase, ArnT, which catalyses the transfer of L-Ara4N from Upp-L-Ara4N to the lipid A. In order to identify any putative homologs of these two enzymes in the *B. cenocepacia* J2315 genome, the Ugd PA2022 DNA and protein sequences from *P. aeruginosa* PA01, and the ArnT DNA and protein sequences from *E. coli* K12 strain MG1655 were used to BLAST the *B. cenocepacia* J2315 genome sequence available at the Wellcome Trust Sanger Institute and the NCBI genomic BLAST service using TBLASTN and TBLASTP.

Compared to *E. coli* MG1655 ArnT, there was no significant hit in the *B. cenocepacia* J2315 genome, but the three closest potential hits were *BCAL1199, BCAL1929* and *BCAL2370*, found on chromosome 1, with 8.2%, 22.3% and 14.8% amino acid identity respectively. *BCAL1199* is found in a six gene-cluster containing phage-related proteins (Fig. 24) and is not very likely to be an L-Ara4N transferase. *BCAL1929* and *BCAL2370* are found in a seven and an eleven gene-cluster respectively (Fig. 25 and 26), both encoding putative gycosyl transfereases, however,

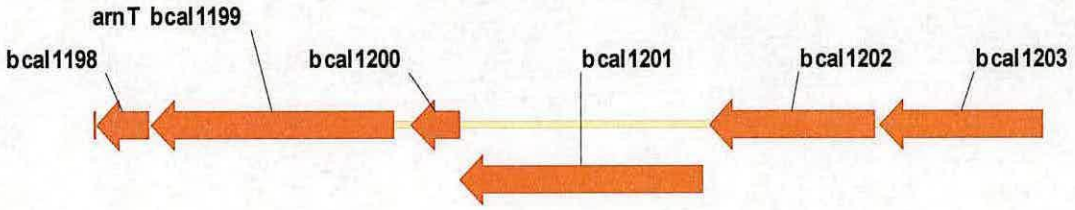

3889 bp

Fig. 24: Putative *arnT*$_{BCAL1199}$ gene cluster. BCAL1198, 1200, 1202 and 1203 encode hypothetical proteins; BCAL1199, a putative phage-related protein; and BCAL1201, a putative phage-related protein endonuclease-like protein.

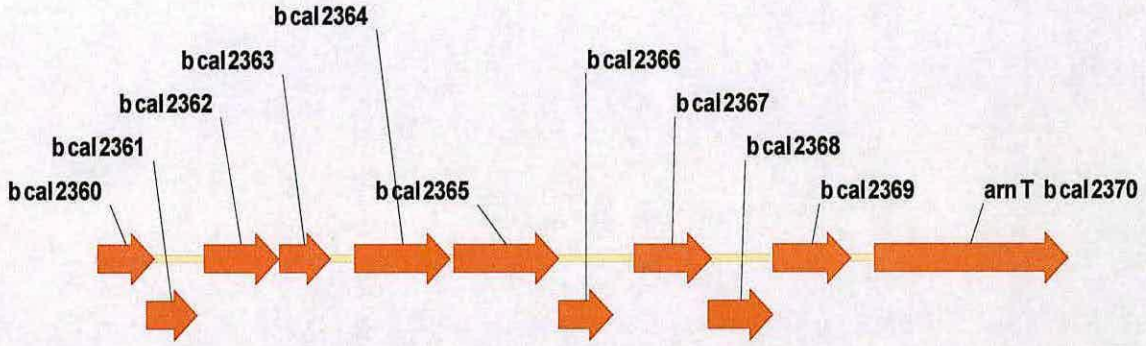

9488 bp

Fig. 25: Putative *arnT*$_{BCAL2370}$ gene cluster. BCAL2360 and 2361, encode putative sigma factors; BCAL2362, hypothetical protein; BCAL2363, RDD domain-containing protein; BCAL2364, metallophosphoesterase; BCAL2365, putative glycosyltransferase; BCAL2366, putative glycosyltransferase or putative kinase; BCAL2367, TetR family regulatory protein or putative decarboxylase; BCAL2368, TetR family regulatory protein or putative decarboxylase; BCAL2369, putative dehydrogenase; BCAL2370, glycosyltransferase.

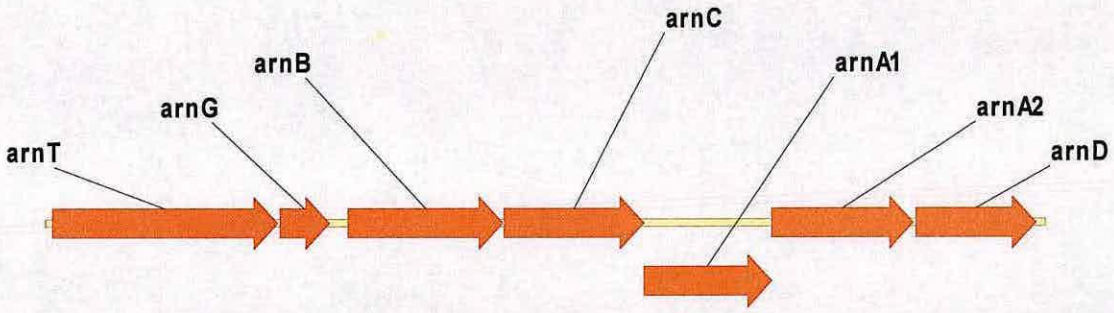

7401 bp

Fig. 26: Putative L-Ara4N biosynthetic gene cluster in *B. cenocepacia* J2315. *arnT*$_{BCAL1929}$, putative L-Ara4N transferase; *arnG*, putative SMR family transporter protein; *arnB*, putative UDP-L-Ara4N-oxoglutarate aminotransferase; *arnC*, putative undecaprenyl-phosphate 4-deoxy-4-formamido-L-arabinose transferase; *arnA1*, putative undecaprenyl-phosphate 4-deoxy-4-formamido-l-arabinose transferase; *arnA2*, putative UDP-glucuronic acid decarboxylase; *arnD*, putative polysaccharide deacetylase.

only *BCAL1929* is associated with the putative *arn* locus (Fig. 26), suggesting the possibility of a single *arnT* in the J2315 genome. $ArnT_{BCAL1929}$ also has low homology to other known ArnT homologs, with the highest being 24% identity to *P. aeruginosa* PA01 ArnT and 24.1% identity to *Francisella tularensis* FlmK (see appendix).

Three putative Ugds were found in the *B. cenocepacia* J2315 genome, one on chromosome 1 ($ugd_{BCAL2946}$) and two on chromosome 2 ($ugd_{BCAM0855}$ and $ugd_{BCAM2034}$). $ugd_{BCAL2946}$, $ugd_{BCAM0855}$, and $ugd_{BCAM2034}$ share 52.5%, 51.8% and 38.4% amino acid sequence identity with *P. aeruginosa* Ugd PA2022, respectively.

The predicted proteins $Ugd_{BCAL2946}$ and $Ugd_{BCAM0855}$ share 73.3% amino acid sequence identity with each other, and $Ugd_{BCAM2034}$ shares 43.1% and 43.0% amino acid sequence identity with $Ugd_{BCAL2946}$ and $Ugd_{BCAM0855}$, respectively (see appendix). The three putative *B. cenocepacia* Ugds share relatively low sequence identity ($ugd_{BCAL2946}$ 21.2%, $ugd_{BCAM0855}$ 20.8% and $ugd_{BCAM2034}$ 23.3%) with the *Streptococcus pyogenes* Ugd, the structure of which was recently determined (Fig. 27; Protein Data Bank, accession codes 1DLI and 1DLJ; (Campbell *et al.*, 2000)). However, a ClustalW alignment with PA01 Ugd PA2022 and PA3559 and *Strep. pyogenes* Ugd (Fig. 28) revealed that $Ugd_{BCAL2946}$, $Ugd_{BCAM0855}$ and $Ugd_{BCAM2034}$ contain a predicted Rossmann fold (GxGxxG) for NAD^+ binding at the N-terminus and all residues involved in the catalytic mechanism (Campbell *et al.*, 2000). Residues such as Cys260 involved in thioester formation and Arg244 involved in UDP-sugar specificity are conserved (equivalent residues Cys274 and Arg258 in $Ugd_{BCAL2946}$, Cys270 and Arg254 in $Ugd_{BCAM0855}$, and Cys266 and Arg250 in $Ugd_{BCAM2034}$).

The chromosomal arrangements of the three putative *ugd* genes are shown in Figures 29-31. $ugd_{BCAL2946}$ is found within a six-gene cluster directly upstream of *hldA* and *hldD*, which encode proteins required for the synthesis of L-*glycero*-D-*manno*-heptose, an important sugar in the LPS inner core oligosaccharide (Fig. 29, (Loutet *et al.*, 2006)). $ugd_{BCAM2034}$ is in a four-gene cluster that contains two open reading

frames similar to *galE* (UDP-galactose 4-epimerase) as well as a predicted glycosyltransferase (Fig. 30). $ugd_{BCAM0855}$, was recently annotated as *bceC* by Moreira and colleagues (Moreira *et al.*, 2003), and is part of the ten-gene *bce* cluster involved in cepacian biosynthesis (Fig. 31).

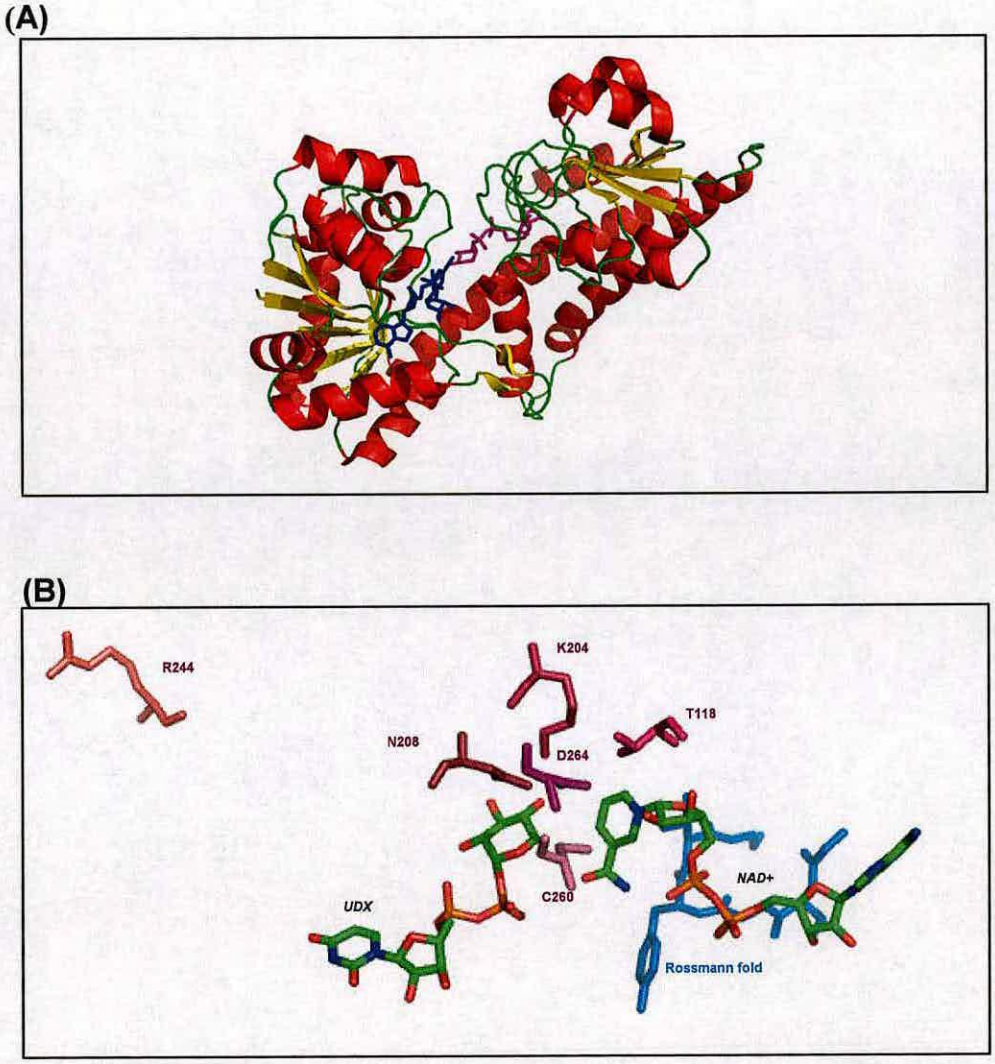

Fig. 27: Structure of Ugd from *Streptococcus pyogenes* (Campbell et al 2000). **(A)** Ugd monomer with UDP-xylopyranose (UDX; pink) and NAD^+ (blue); and **(B)** zoom of the active site highlighting active site residues surrounding the substrates UDX and NAD^+: C260, K204, T118, N208 and D264, as well as R244 and the Rossmann fold.

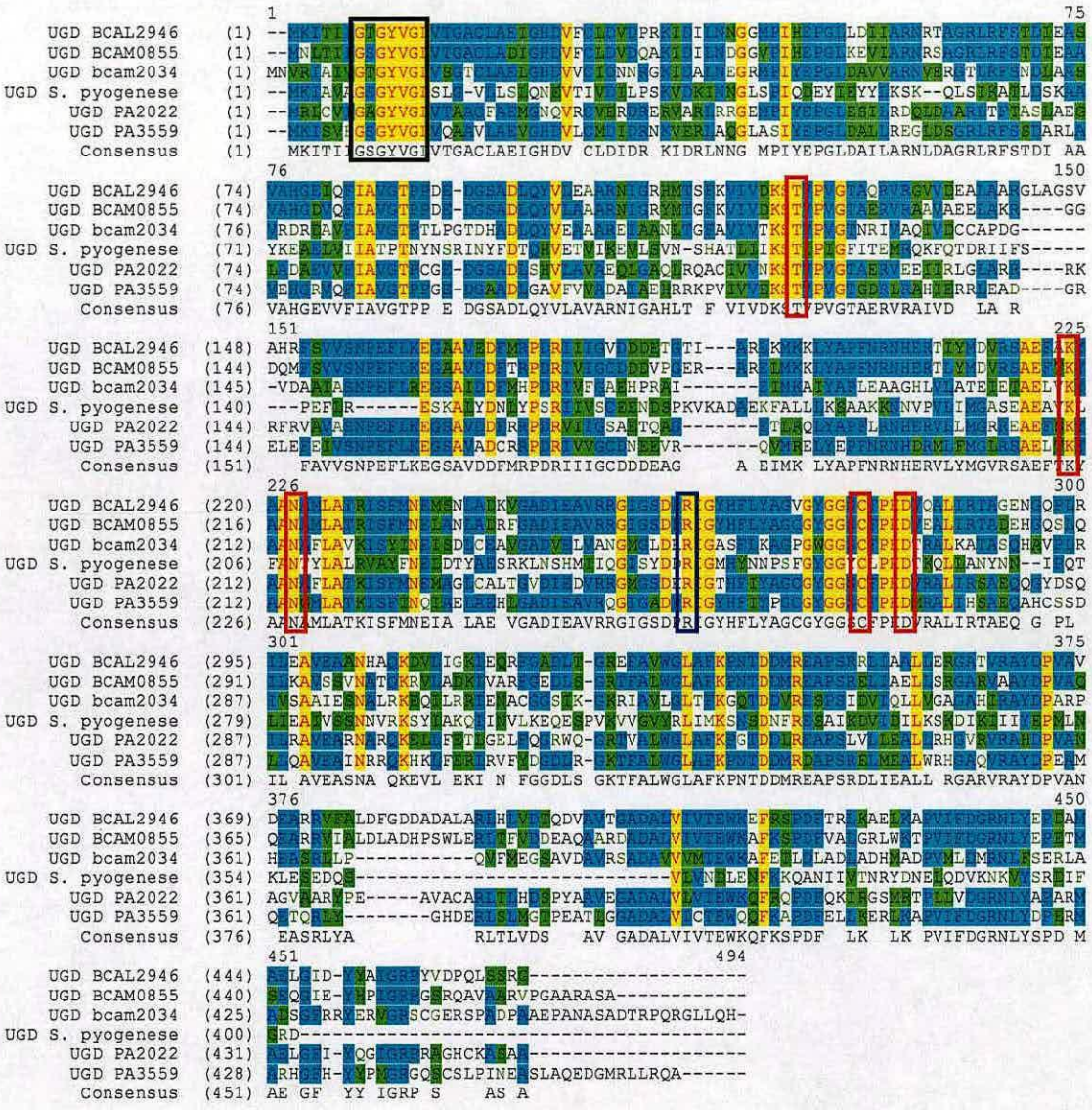

Fig. 28: Sequence alignment of Ugds from *B. cenocepacia, P. aeruginosa* and *Strep. Pyogenes.* Highlighted in red are the active site residues threonine, lysine, asparagine, cysteine, and aspartic acid; highlighted in blue is arginine involved in UDP-glucose specificity and highlighted in black is the Rossmann fold involved in NAD^+ binding.

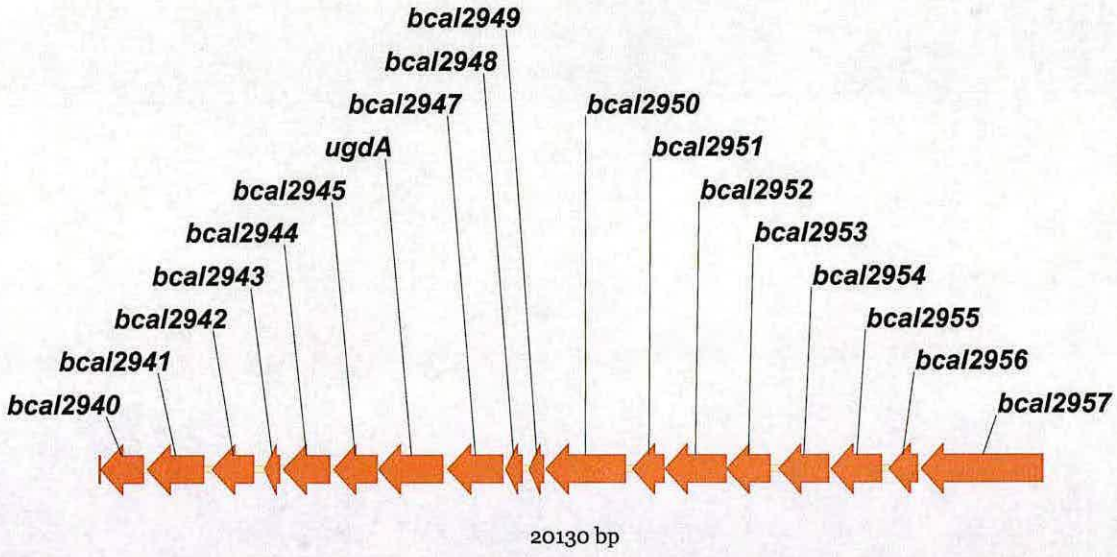

Fig. 29: Physical organization of ugd_A and surrounding genes. *Bcal2940*, putative histone deacetylase-family protein; *bcal2941* putative exported transglycosylase; *bcal2942*, putative cysteine synthase; *bcal2943*, putative helix-hairpin-helix DNA-binding motif-containing protein; *bcal2944*, putative ADP-l-glycero-D-manno-heptose-6-epimerase; *bcal2945*, putative D-beta-D-heptose 7-phosphate kinase; *bcal2946*, putative UDP-glucose dehydrogenase (ugd_A); *bcal2947*, predicted N-acetylglucosaminyl transferase; *bcal2948*, hypothetical protein; *bcal2949*, putative integration host factor beta-subunit; *bcal2950*, putative 30S ribosomal protein S1; *bcal2951*, putative cytidylate kinase; *bcal2952*, putative 3-phosphoshikimate 1-carboxyvinyltransferase; *bcal2953*, putative prephenate dehydrogenase; *bcal2954*, putative chorismate mutase; *bcal2955*, putative phosphoserine aminotransferase; *bcal2956*, hypothetical protein; *bcal2957*, putative DNA gyrase, subunit A

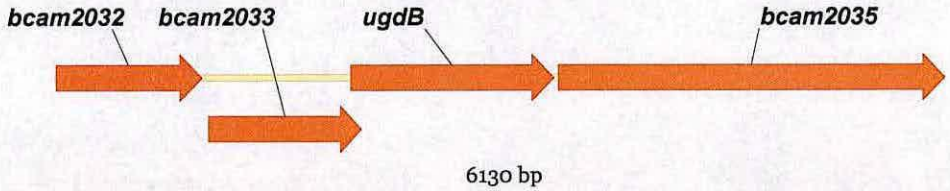

Fig. 30: Physical organization of ugd_B and surrounding genes. *bcam2032*, putative UDP-glucuroninc acid decarboxylase; *bcam2033*, putative UDP-glucose-4-epimerase; *bcal2034*, putative UDP-glucuronic acid decarboxylase or UDP-glucose-4-epimerase (ugd_B); *bcam2035*, putative UDP-glucose-4-epimerase

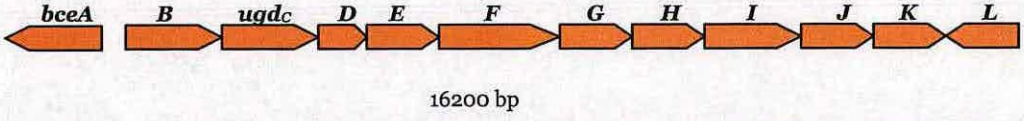

Fig. 31: Physical organization of ugd_C and the *bce* gene cluster. *bceA,* phosphomannose isomerase and GDP-D-mannose pyrophosphorylase; *bceB,* undecaprenyl-phosphate glucosyl-1-phosphate transferase; *bceC,* putative UDP-glucose dehydrogenase *(ugd_C); bceD,* phosphotyrosine phosphatase *bceE,* putative outer-memebrane lipoprotein*; bceF,* tyrosine autokinase *bceG,* putative glycosyltransferase; *bceH,* putative glycosyltransferase; *bceI,* putative polymerase; *bceJ,* putative glycosyltransferase; *bceK,* putative glycosyltransferase; *bceL,* putative repeat unit transporter (Ferreira *et al.*, 2007; Moreira *et al.*, 2003).

4.3.3 Characterisation of three putative *B. cenocepacia* J2315 UDP-glucose dehydrogenases

To characterize the enzymes encoded by $ugd_{BCAL2946}$, $ugd_{BCAM2034}$ and $ugd_{BCAM0855}$, each gene was cloned into a pET28 expression plasmid to add an N-terminal 6 His tag to ease purification. $Ugd_{BCAL2946}$ and $Ugd_{BCAM0855}$ were over-expressed in *E. coli* HSM174 (DE3) and $Ugd_{BCAM2034}$ in BL21 (DE3) cells (Figure 32).

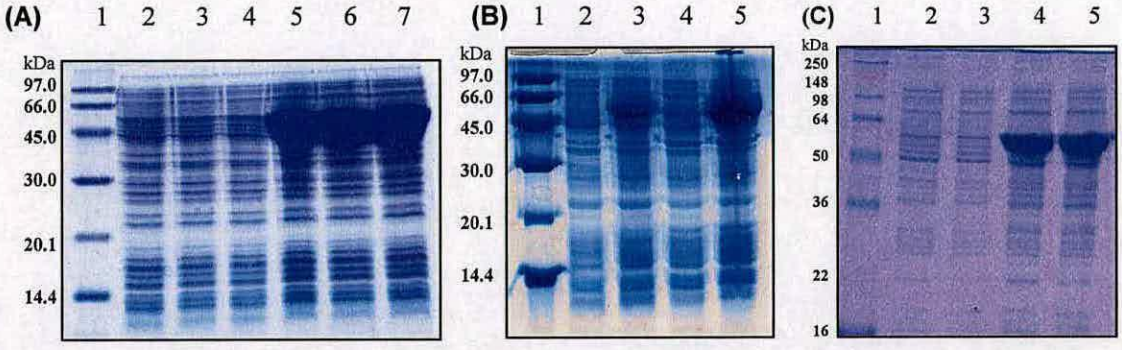

Fig. 32: Expression of Ugd_A, Ugd_B and Ugd_C in *E. coli* (DE3) cells. **(A)** Over-expression of Ugd_A in *E. coli* HSM 174 (DE3): lane 1, LMW marker; lanes 2-4 uninduced controls; lanes 5-7, induced with 1 mM IPTG for 3 hours at 37°C; **(B)** Over-expression of Ugd_B in *E. coli* HSM 174 (DE3) and BL21 (DE3) induced with 0.2 mM IPTG for 4 hours at 25 °C. Lane 1, LMW marker; lane 2 uninduced HSM174 control; lane 3, induced HSM174; lane 4m uninduced BL21 control; lane 5, induced BL2; **(C)** Over-expression of Ugd_C in *E. coli* HSM 174 (DE3). Lane 1, SeeBlue®Plus2 marker; lanes 2 and 3 uninduced controls; lanes 4 and 5, induced with 1 mM IPTG for 3 hours at 37°C.

$Ugd_{BCAL2946}$ and $Ugd_{BCAM0855}$ were soluble and purified using IMAC nickel affinity (Fig. 33) and size exclusion chromatography (Fig. 34). Both Ugd proteins behaved as homodimers (~106 kDa) with similar elution profiles. Molecular weights were confirmed by mass-spectrometry (Fig. 35 (A) and (C)) and native gel electrophoresis (Fig. 34). $Ugd_{BCAM2034}$ was insoluble and was over-expressed at a low temperature and solubilised using DDM and glycerol, followed by purification using nickel NTA agarose beads (Fig. 36) Size-exclusion chromatography and native gel electrophoresis (Fig. 37) indicated a possible mixture of monomer and homodimer conformations of $Ugd_{BCAM2034}$. The molecular weight was confirmed by mass-spectrometry (Fig. 35 (B)).

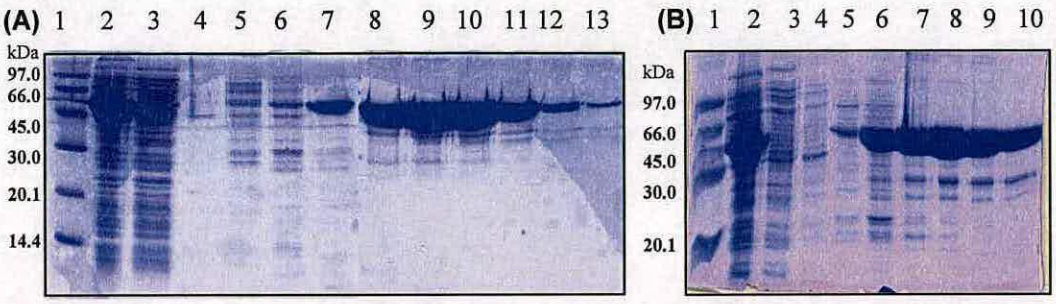

Fig. 33: IMAC nickel affinity chromatography of Ugd_A **(A)** and Ugd_C **(B).** Order on gel **(A):** lane 1, LMW marker; lane 2, cell free extract; lane 3, flow through; lane 4, wash, lanes 5-13, protein eluted on an increasing gradient of imidazole; and gel **(B):** lane 1, LMW marker; lane 2, cell free extract; lane 3, flow through; lane 4, wash, lanes 5-10, protein eluted on an increasing gradient of imidazole.

The enzyme assay was based on the Ugd mechanism proposed by Campbell *et al.* (Campbell *et al.*, 2000) and Ge *et al.* (Ge *et al.*, 2004) (Fig. 38), UDP-glucose is converted to UDP-glucuronic acid in a two-step oxidation via a covalently-bound thioester intermediate. Conversion of this to the final free UDP-glucuronic acid product requires a second mole of NAD^+ so overall the process reduces two moles NAD^+ to two moles NADH. To determine the kinetic parameters, the initial velocity was calculated by measuring the increase in absorbance at 340 nm, due to the production of NADH, divided by two. The molar extinction coefficient of NADH at 340 nm is 6220 M^{-1} cm^{-1}. The data was fitted by non-linear regression with the Hill equation ($V = V_{max}\ [S]^h/([S]^h + K_m{}^h)$). The enzyme turn-over (k_{cat}) and catalytic efficiency (k_{cat}/K_m) were calculated from the V_{max} and K_m values obtained from the graphs (Fig. 39). Both $Ugd_{BCAL2946}$ and $Ugd_{BCAM0855}$ show Ugd activity with very similar kinetic constants, comparable to the two recently characterised *P. aeruginosa* Ugds (Hung *et al.*, 2007) (Table 11). Unfortunately, $Ugd_{BCAM2034}$ showed no *in vitro* activity. To investigate any variation in substrate specificity between the Ugd proteins, the spectrophotometric assay was repeated with UDP-galactose, UDP-acetylglucoseamine and GDP-mannose. None of these were substrates for either enzyme.

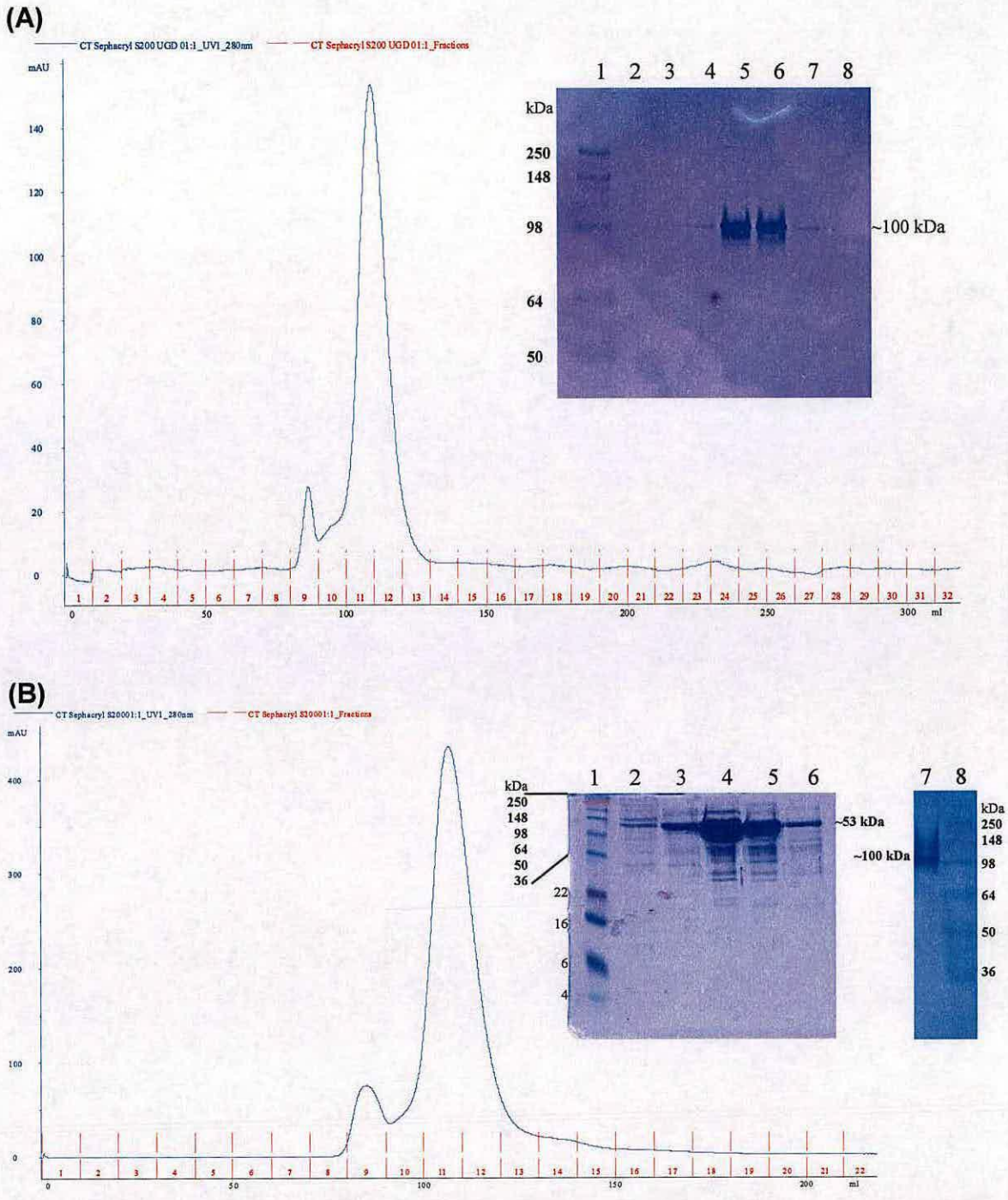

Fig. 34: Size-exclusion chromatography shows that Ugd_A and Ugd_C are dimers. **(A)** Chromatogram of Ugd_A; fractions 8-14 were collected and analysed by non-denaturing gel (inset): lane 1, SeeBlue®Plus2 marker; lanes 2-8, fractions 8-14. **(B)** Chromatogram of Ugd_C; fractions 8-14 were collected and analysed by SDS-PAGE (inset): lane 1, SeeBlue®Plus2 marker; lanes 2-6, fractions 9-13. Fraction 4 was further analysed by non-denaturing gel (inset): lane 7, Ugd_B; lane 8, SeeBlue®Plus2 marker.

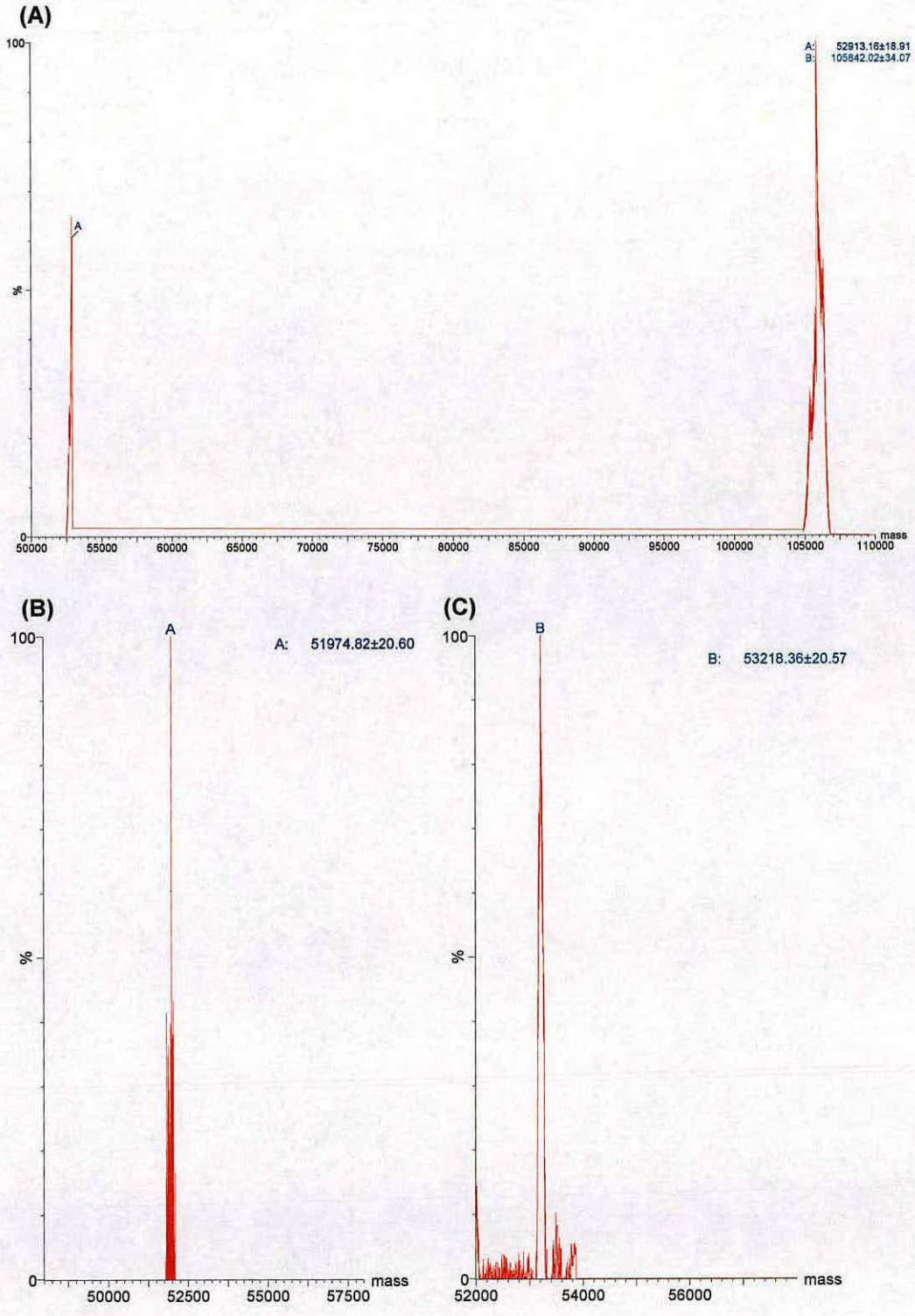

Fig. 35: : LC-ESI-MS data for Ugd_A **(A),** Ugd_B **(B)** and Ugd_C **(C)** . Ugd_A shows the monomer and dimer size of 52913.16 +/-18.91 and 105842.02 +/-34.07 respectively (corresponding to theoretical masses, 53055.64 and 106111.28, minus methionine, 149.21).Ugd_B shows the monomer size of 51974.82 +/-20.6 (corresponding to theoretical mass, 52112.03, minus the methionine, 149.21); and Ugd_C shows the monomer size of 53218.36 +/-20.57 (corresponding to theoretical mass, 53388.85, minus the methionine, 149.21).

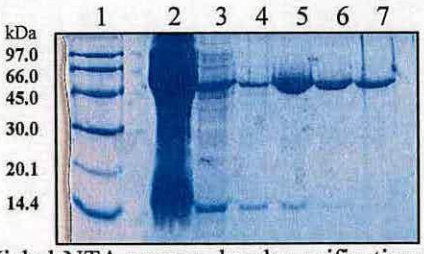

Fig. 36: Nickel NTA agarose beads purification of Ugd_C expressed in *E. coli* BL21 (DE3) induced with 0.2 mM IPTG for 16 hours at 15 °C. Lane 1, LMW marker; lane 2, cell free extract; lane 3, flow through; lane 4, wash, ; lane 4-7, elution in 20, 50, 100 and 200 mM imidazole.

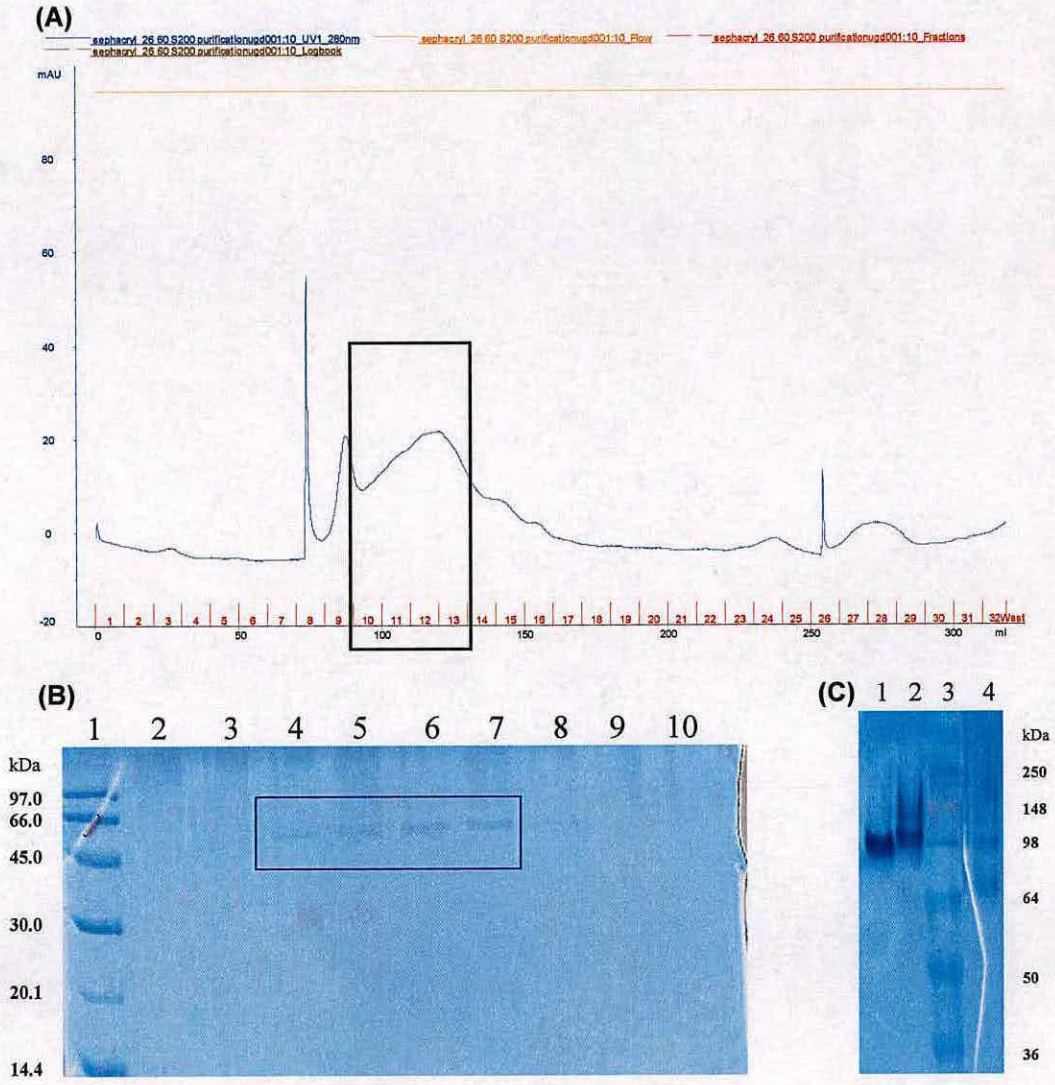

Fig. 37: Size-exclusion chromatography shows Ugd_B is purified as a mixture of monomer and dimer **(A).** Fractions were collected and analysed by SDS-PAGE **(B)**: lane 1, LMW marker; lane 2-10, fractions 8-16. A concentrated sample of Ugd_B was compared to Ugd_A and Ugd_C on a non-denaturing gel **(C)**: lane 1, Ugd_A; lane 2, Ugd_C; lane 3, SeeBlue®Plus2 marker; lane 4, Ugd_B.

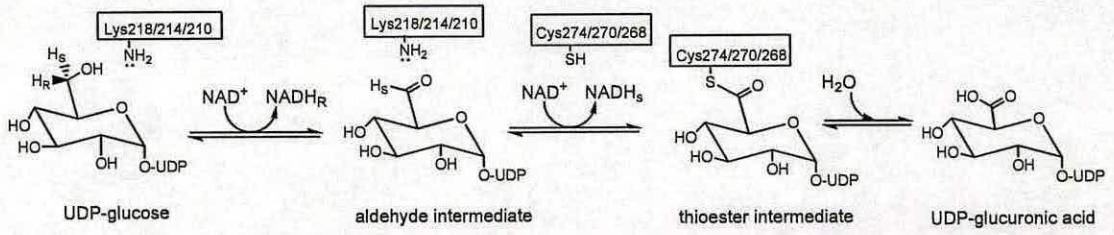

Fig. 38: Proposed Ugd mechanism (Campbell *et al.*, 2000; Ge *et al.*, 2004). UDP-glucose is converted to UDP-glucuronic acid by a 3-step pathway; oxidation form the primary alcohol substrate to an aldehyde intermediate; oxidation to a covalently-bound thioester intermediate; hydrolysis of the thioester to the acid product. Each oxidation reduces a NAD^+ cofactor. The conserved active site lysine residue (218, 214 and 210 in $Ugd_{BCAL2946}$, $Ugd_{BCAM0855}$ and $Ugd_{BCAM2034}$ respectively), is likely to act as the general base for deprotonation of the substrate alcohol and the conserved cysteine (274, 270 and 268 in $Ugd_{BCAL2946}$, $Ugd_{BCAM0855}$ and $Ugd_{BCAM2034}$ respectively) is the residue involved in thioester formation.

From these experiments it appears that $Ugd_{BCAL2946}$ and $Ugd_{BCAM0855}$ have identical enzymatic activities and confirm biochemically the functional assignment of these proteins as UDP-glucose dehydrogenases. Moreover, they appear to have tight substrate specificity for UDP-glucose. $Ugd_{BCAM2034}$ does not have UDP-glucose dehydrogenase activity.

Table 11: Kinetic comparison of Ugds from *B. cenocepacia* J2315 and *P. aeruginosa* PA01 (Hung *et al.*, 2007)

		k_m (mM)	V_{max} (nmol/min)	k_{cat} (min^{-1})	k_{cat}/k_m ($mM^{-1}min^{-1}$)	h
Ugd_A	UDP-Glc	0.02 +/- 0.01	14.38 +/- 0.7	7.99 +/- 0.1	392.36 +/- 0.4	1.25 +/- 0.16
	NAD+	0.17 +/- 0.03	16.61 +/- 1.1	9.23 +/- 0.2	53.95 +/- 0.2	1.50 +/- 0.31
Ugd_C	UDP-Glc	0.02 +/- 0.02	13.73 +/- 0.5	7.63 +/- 0.1	340.35 +/- 0.1	1.41 +/- 0.12
	NAD+	0.21 +/- 0.04	16.88 +/- 1.2	9.38 +/- 0.2	44.50 +/- 0.2	1.49 +/- 0.31
PA 2022	UDP-Glc	0.12 +/- 0.01	11.6 +/- 0.5	14.4 +/- 0.3	117.8 +/- 2.5	1.20 +/- 0.11
	NAD+	0.47 +/- 0.18	18.0 +/- 2.6	22.4 +/- 2.8	47.2 +/- 2.7	1.36 +/- 0.28
PA 3559	UDP-Glc	0.40 +/- 0.03	32.9 +/- 2.6	48.4 +/- 1.5	120.7 +/- 3.7	1.67 +/- 0.19
	NAD+	1.99 +/- 0.67	95.8 +/- 12.0	141.0 +/- 8.9	71.0 +/- 4.5	0.84 +/- 0.09

($V = Vmax\,[S]^h/([S]^h + Km^h)$)

(A)

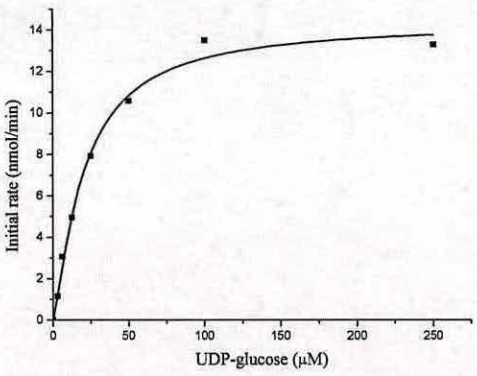

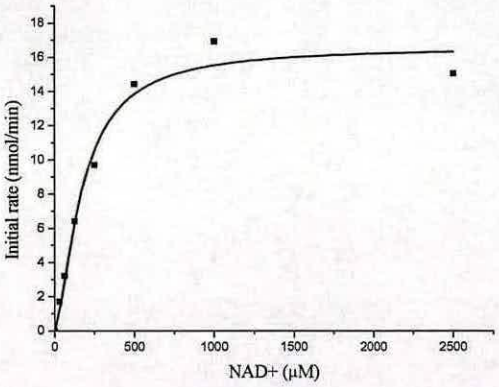

	Value	Error
V_{max}	14.38 nmol.min^{-1}	+/-0.73
K_m	0.02 mM	+/-0.01
h	1.25	+/- 0.16
k_{cat}	7.99 min^{-1}	+/- 0.13
k_{cat}/K_m	392.36 mM^{-1}min^{-1}	+/- 0.37

	Value	Error
V_{max}	16.61 nmol.min^{-1}	+/- 1.11
K_m	0.17 mM	+/- 0.03
h	1.51	+/- 0.31
k_{cat}	9.23 min^{-1}	+/- 0.15
k_{cat}/K_m	53.95 mM^{-1}min^{-1}	+/- 0.19

(B)

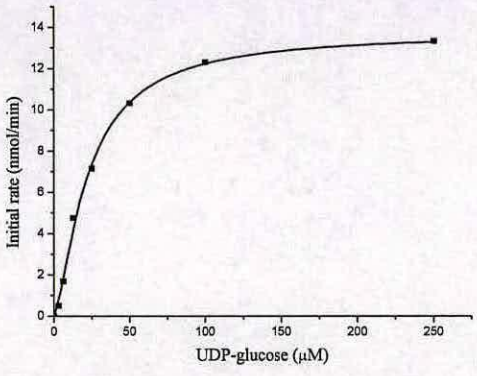

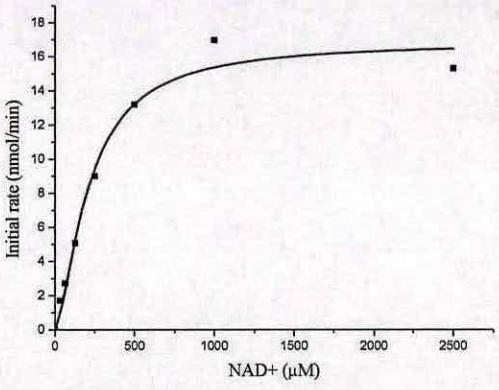

	Value	Error
V_{max}	13.73 nmol.min^{-1}	+/- 0.90
K_m	0.02 mM	+/- 0.01
h	1.41	+/- 0.12
k_{cat}	7.63 min^{-1}	+/- 0.15
k_{cat}/K_m	340.35 mM^{-1}min^{-1}	+/- 0.10

	Value	Error
V_{max}	16.88 nmol.min^{-1}	+/- 1.22
K_m	0.21 mM	+/- 0.04
h	1.50	+/- 0.31
k_{cat}	9.38 min^{-1}	+/- 0.16
k_{cat}/K_m	44.50 mM^{-1}min^{-1}	+/- 0.19

Fig. 39: Kinetic analysis of Ugd_A **(A)** and Ugd_C **(B)** UDP-glucose dehydrogenase activity assays. Parameters were determined by non-linear regression from $V = V_{max}\,[S]^h/([S]^h + K_m^h$ using Origin6.1 software.

4.3.4 Investigating the putative *B. cenocepacia* J2315 aminoarabinose transferase

To date no structural information is available on ArnT from any organism. Previous studies have achieved some degree of characterisation of the isoforms from *E. coli* and *Salmonella* (Bretscher et al., 2006; Trent et al., 2001b). Brescher and co-workers isolated very small amounts of recombinant *S. typhimurium* ArnT expressed in *E. coli* and found that it was a highly alpha-helical 62 kDa protein (Bretscher et al., 2006). A PMB sensitivity assay was used to show that the *Salmonella arnT* could restore resistance in an *E. coli* BL21 (DE3) *ΔarnT* mutant. Trent and colleagues further characterised the ArnTs from *Salmonella* and *E. coli* and showed that they are inner-membrane proteins with 12 possible membrane-spanning domains that transfers L-Ara4N from Upp-L-Ara4N to a lipid A substrate on the periplasmic side of the inner membrane (Trent *et al.*, 2001a; Trent *et al.*, 2001b). In addition, by using ^{32}P-lipid IV_A or Kdo_2-4'^{32}P-lipid IV_A, they showed that ArnT transfers L-Ara4N to the 1-phosphate of lipid A precursor lipid IV_A, but that it requires Kdo in order to add L-Ara4N to the 4'-phosphate (Trent *et al.*, 2001b). To date, no laboratory has managed to isolate sufficient amounts to fully characterise an ArnT enzyme.

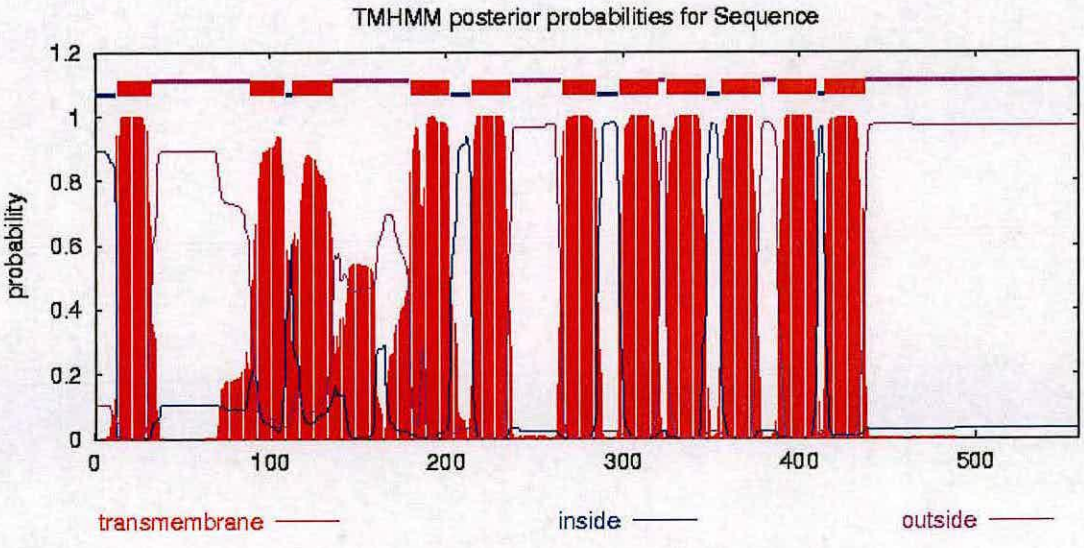

Fig. 40: *B. cenocepacia* J2315 $ArnT_{BCAL1929}$ topology prediction by TMHMM.

Characterisation of the *B. cenocepacia* ArnT has previously not been attempted. Like the *E. coli* and *S. typhimurium* ArnT enzymes, $ArnT_{BCAL1929}$ is a predicted inner membrane protein with 12 possible membrane-spanning domains by TMHMM topology prediction (Fig. 40). The aim of this study was to clone, express and attempt to purify recombinant ArnT from *B. cenocepacia* J2315, and characterise this important Bcc enzyme using biochemical and phenotypic techniques.

First, *B. cenocepacia* J2315 $arnT_{BCAL1929}$ was cloned into pET28a with a C-terminal 6 His tag, and expression was attempted in *E. coli* HSM 174 (DE3), BLR (DE3) and Rosetta (DE3) strain. Expression of $ArnT_{BCAL1929}$ was visualised by Western Blot, however, only very small amounts of protein appeared to be expressed and expression results were difficult to reproduce (Fig. 41). To confirm that $arnT_{C\text{-}term}$ was expressed, an RT-PCR reaction was set up using RNA extracted from IPTG-induced cultures of *E. coli* BLR (DE3) transformed with pET28a/$arnT_{C\text{-}term}$ and *E. coli* Top10 transformed with pTrc99a/$arnT_{C\text{-}term}$. Figure 42 shows clear expression of $arnT_{C\text{-}term}$ from both plasmids in the different *E. coli* strains. pET28a/$arnT_{C\text{-}term}$ is expressed regardless of IPTG induction, but pTrc99a/$arnT_{C\text{-}term}$ is only expressed when uninduced. Since pTrc99a is a low copy number, leaky plasmid which does not require IPTG induction, perhaps over-inducing *arnT* expression is toxic to the *E. coli* cells.

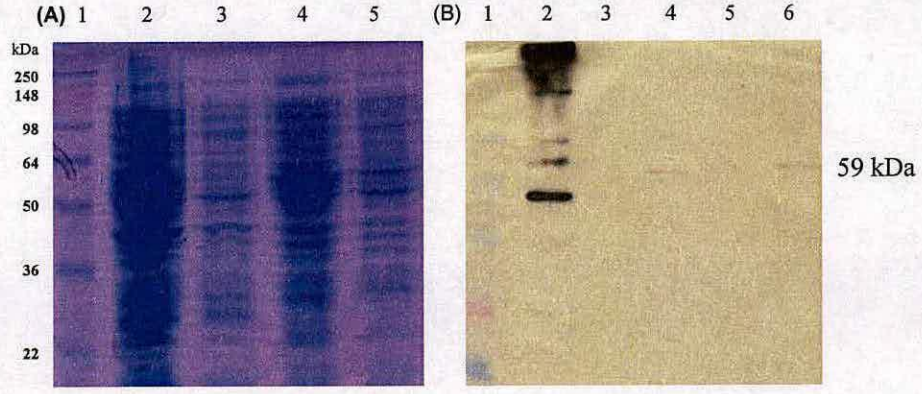

Fig. 41: pET28a/$arnT_{C\text{-}term}$ expression in *E. coli* Rosetta (DE3) (lane 2 and 3) and *E. coli* HMS174 (DE3) (lane 4 an 5) after induction with 1 mM IPTG at 37°C for 3 hours. **(A)** Expression cannot be visualised by SDS-PAGE and **(B)** expression detected by western blot using an anti-C-term His antibody. Lane 1, SeeBlue®Plus2 marker; lane 2, BenchMark™ His-tagged Protein Standard (Invitrogen); lane 3 and 5, uninduced; lane 4 and 6, induced. ArnT appears at 59 kDa.

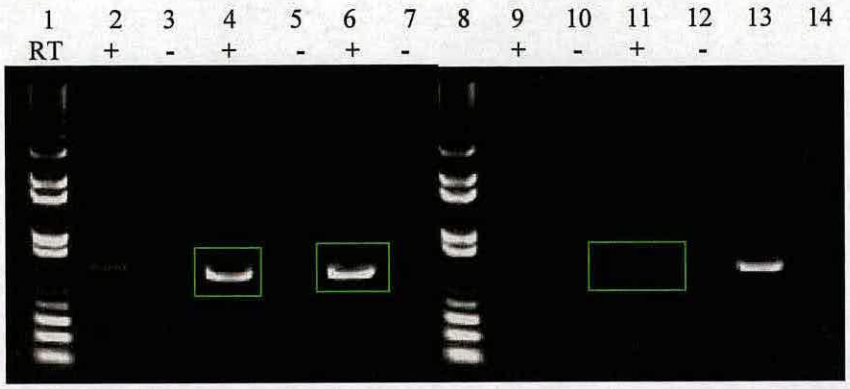

Fig. 42: RT-PCR to confirm C-terminal His tagged *arnT* expression. Lane 1, 1 kb plus DNA ladder; lane 2 and 3, *B. cenocepacia* J2315 RT+ and -; lane 4 and 5, *E. coli* BLR (DE3)/pET28a/$arnT_{C\text{-}term}$ induced RT+ and -; lane 6 and 7, *E. coli* BLR (DE3)/ pET28a/$arnT_{C\text{-}term}$ uninduced RT+ and -; lane 8, 1 kb plus DNA ladder; lane 9 and 10, *E. coli* TOP10/pTrc99a/$arnT_{C\text{-}term}$ induced RT+ and -; lane 11 and 12, *E. coli* TOP10/ pTrc99a/$arnT_{C\text{-}term}$ uninduced RT+ and -; lane 13, *B. cenocepacia* K56-2 +ve DNA control; lane 14, -ve control (no DNA). The green boxes indicate RNA expression of *arnT*, pTrc99a/$arnT_{C\text{-}term}$ uninduced shows weak expression, whilst pET28a/ $arnT_{C\text{-}term}$ shows good expression whether induced or not.

The pTrc99a/$arnT_{C\text{-}term}$ construct was then used to transform the deep-rough *E. coli* strain WBB06 by electroporation. Overnight cultures were used for small-scale LPS extraction, and the LPS samples were incubated with sulfo-NHS-biotin after which any L-Ara4N biotinylation was visualised using streptavidin in a Western blot. In Figure 43, WBB06 containing pTrc99a/$arnT_{C\text{-}term}$ is biotinylated, whereas the Kdo_2-lipidA control is not. This indicated a possible transfer of L-Ara4N to the WBB06 lipid A by $ArnT_{BCAL1929}$.

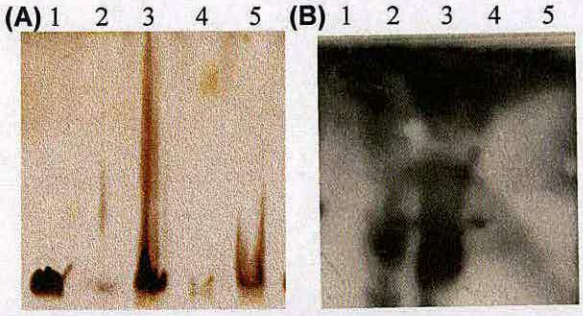

Fig. 43: Biotinylated LPS from *E. coli* WBB06 electroporated with pTrc99a/$arnT_{C\text{-}term}$. **(A)** sodium-m-periodate silver stained gels and **(B)** streptavidin detected western blot: lane 1, Kdo_2-lipidA control; lane 2, WBB06/ pTrc99a/$arnT_{C\text{-}term}$ biotinylated aqueous phase; lane 3, WBB06/pTrc99a/*arnT* biotinylated phenol phase; lane 4, WBB06/ pTrc99a/$arnT_{C\text{-}term}$ aqueous phase control; lane 5, WBB06/pTrc99a/$arnT_{C\text{-}term}$ phenol phase control.

Since expression was difficult observe with a C-terminal 6 His tag, $arnT_{BCAL1929}$ was cloned into pET28a with an N-terminal 6 His tag instead. $ArnT_{N\text{-}term}$ expression was carried out in *E. coli* C41 (DE3) and C43 (DE3) strains and visualised by Western

blot. Figure 44 shows expression in *E. coli* C41 (DE3) using different amounts of IPTG and different induction times. Expression was clearly better, and reproducible, with $arnT_{N\text{-}term}$ compared to $arnT_{C\text{-}term}$. Therefore, *E. coli* C41 (DE3) or C43 (DE3) strains transformed with pET28a/$arnT_{N\text{-}term}$ were used for large scale-induction. Attempts to purify the protein were made by isolating inner-membranes and solubilisation with DDM and glycerol before incubation with TALON resin. Protein was eluted using increasing concentrations of imidazole (Fig. 45). Only very small amounts of protein were purified this way, which unfortunately was not enough to fully characterise the $ArnT_{BCAL1929}$ enzyme.

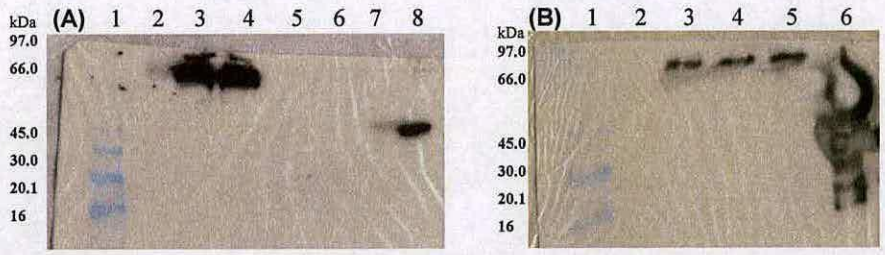

Fig. 44: Western blot showing $ArnT_{N\text{-}term}$ expression in *E. coli* C41 (DE3). **(A)** Effect of induction time induced with 1 mM IPTG: Lane 1, SeeBlue®Plus2 marker; lane 2, pET28a/$arnT_{Nterm}$ control; lane 3, pET28a/$arnT_{Nterm}$ induced 4 hours; lane 4, pET28a/$arnT_{Nterm}$ induced 5 hours; lane 5, pET28a control; lane 6, pET28a induced 4 hours; lane 7, pET28a induced 5 hours; lane 8, Ugd (6His control). **(B)** Effect of different IPTG concentrations at 5 hours induction: Lane 1, SeeBlue®Plus2 marker; lane 2, pET28a/$arnT_{Nterm}$ control; lane 3, pET28a/$arnT_{Nterm}$ induced 0.1 mM IPTG; lane 4, pET28a/$arnT_{Nterm}$ induced 0.5 mM IPTG; lane 5, pET28a/$arnT_{Nterm}$ induced 1 mM IPTG; lane 6, Ugd (6His control).

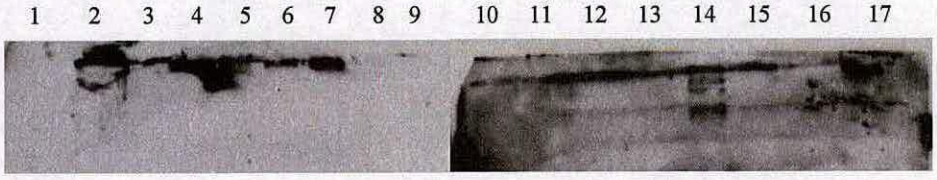

Fig. 45: Inner-membrane prep of $ArnT_{N\text{-}term}$ expressed in *E. coli* C41 (DE3). Lane 1, SeeBlue®Plus2 marker; lane 2, pellet; lane 3, cell free extract after ultracentrifugation; lane 4, inner-membrane pellet; lane 5, pellet after incubation with DDM; lane 6, TALON resin after incubation; lane, 7, TALON resin after flow through; lane, 8, flow through; lane 9, initial wash; lane 10, SeeBlue®Plus2 marker; lane 11, second wash; lane 12, third wash; lane 13, elution with 20 mM imidazole; lane 14, elution with 50 mM imidazole; lane 15, elution with 100 mM imidazole; lane 16, elution with 200 mM imidazole; lane 17, TALON resin after elution.

To test if the *B. cenocepacia* J2315 *arnT* gene was functional in cells, an ArnT assay was set up using the PMB sensitive *E. coli ΔarnT* mutant AY103 (*arnT::kan*) electroporated with either pTrc99a/$arnT_{N\text{-}term}$ or pTrc99a control plasmid (containing *fbpA* from *Neiserria gonorrhoeae*). The strains were plated onto three plates: a kanamycin control plate, an ampicillin plasmid control plate and a PMB assay plate.

All *E. coli* AY103 strains grew on kanamycin, all strains containing the pTrc99a plasmid grew on ampicillin, but only *E. coli* AY103 containing pTrc99a/$arnT_{N\text{-}term}$ grew on PMB (Fig. 46). A PMB MIC assay was set up simultaneously and revealed a PMB sensitive MIC of 0.5 μg/ml for *E. coli* AY103 control and with pTrc99a/fbpA, but a PMB resistant MIC of 4 μg/ml for *E. coli* AY103 containing pTrc99a/$arnT_{N\text{-}term}$ (data not shown). These results suggest that *B. cenocepacia* $ArnT_{BCAL1929}$ can restore PMB resistance of a PMB sensitive *E. coli ΔarnT* mutant. Further work is required to identify if the expressed protein has catalysed attachment of L-Ara4N onto the *E. coli* AY103 LPS.

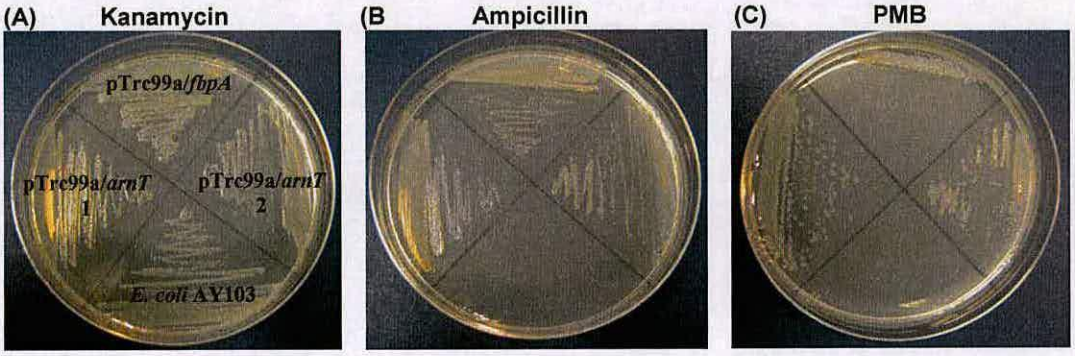

Fig. 46: *B. cenocepacia* J2315 $arnT_{Nterm}$ expressed on a pTrc99a plasmid can restore polymyxin B resistance in sensitive *arnT* mutant *E. coli* AY103. *E. coli* AY103 electroporated with pTrc99a/$arnT_{Nterm}$ or pTrc99a/*fbpA* was streaked on **(A)** kanamycin, **(B)** kanamycin and ampicillin, and **(C)** polymyxin B; top of the plate pTrc99a/*fbpA* control, then clockwise: pTrc99a/$arnT_{Nterm}$ 2, *E. coli* AY103 and pTrc99a/$arnT_{Nterm}$ 1.

In an attempt to show that L-Ara4N was being transferred to the lipid A of *E. coli* AY103 the LPS was isolated and incubated with sulfo-NHS-biotin as described earlier. The Western blot showed slight variations in biotinylation profiles between AY103 with and without ArnT, but were not clear enough to be conclusive (Fig. 48). Knocking out *arnT* in *E. coli* may lead to increased PET modification to compensate for the loss of L-Ara4N modification. Since PET also contains primary amine groups it is likely to also be biotinylated in this assay. To inhibit PET modification the strains were grown in the presence of 1 mM EDTA and the biotinylation was repeated. However, this Western blot was more inconclusive than the first one and did not reveal any potential L-Ara4N bands (Fig. 49). Unfortunately, we were unable to prove that *B. cenocepacia* $ArnT_{BCAL1929}$ transfers L-Ara4N to *E. coli* AY103 lipid A.

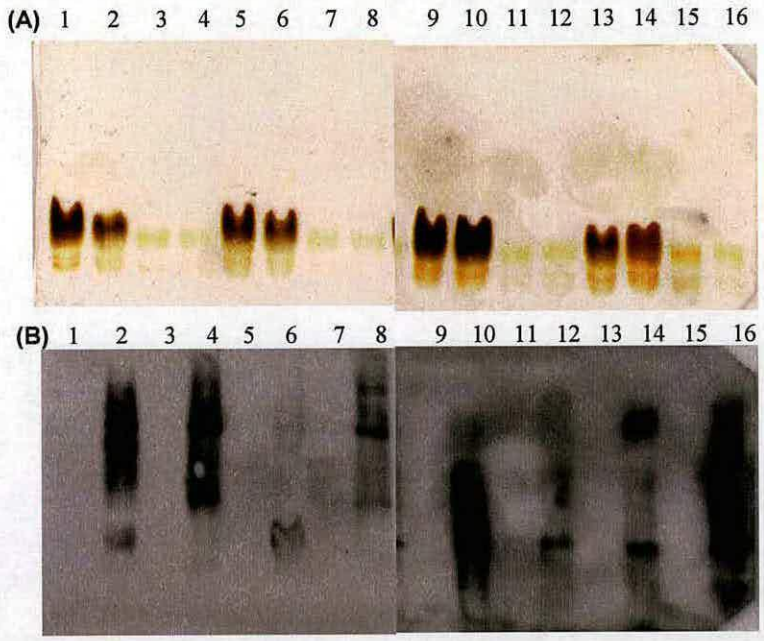

Fig. 48: Biotinylation of *E. coli* AY103 and *E. coli* AY103 containing pTrc99a/*fbpA* or pTrc99a/*arnT*$_{N\text{-}term}$. **(A)** sodium-m-periodate silver stained gels and **(B)** streptavidin detected western blot. On both gels: lane 1 and 2, *E. coli* AY103 water control and biotinylated respectively; lane 3 and 4, *E. coli* AY103 phenol control and biotin; lane 5 and 6, *E. coli* AY103/pTrc99a/*fbpA* water control and biotin; lane 7 and 8, *E. coli* AY103/pTrc99a/*fbpA* phenol control and biotin; lane 9 and 10, *E. coli* AY103/pTrc99a/*arnT*$_{Nterm}$ 1 water control and biotin; lane 11 and 12, *E. coli* AY103/pTrc99a/*arnT*$_{Nterm}$ 1 phenol control and biotin; lane 13 and 14, *E. coli* AY103/pTrc99a/*arnT*$_{Nterm}$ 2 water control and biotin; lane 15 and 16, *E. coli* AY103/pTrc99a/*arnT*$_{Nterm}$ 2 phenol control and biotin.

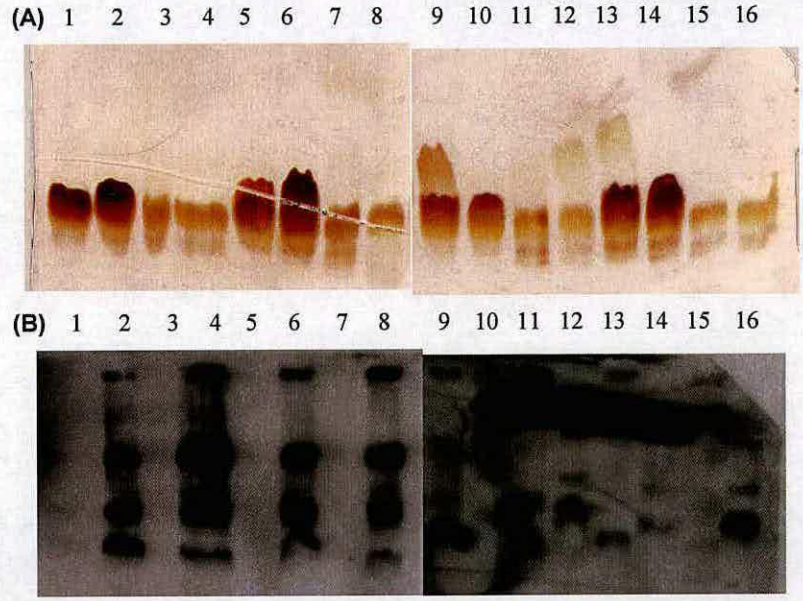

Fig. 49: Biotinylation of *E. coli* AY103 and *E. coli* AY103 containing pTrc99a/*fbpA* or pTrc99a/*arnT*$_{N\text{-}term}$ grown in the presence of 1 mM EDTA. **(A)** sodium-m-periodate silver stained gels and **(B)** streptavidin detected western blot. On both gels: lane 1 and 2, *E. coli* AY103 water control and biotinylated respectively; lane 3 and 4, *E. coli* AY103 phenol control and biotin; lane 5 and 6, *E. coli* AY103/pTrc99a/*fbpA* water control and biotin; lane 7 and 8, *E. coli* AY103/pTrc99a/*fbpA* phenol control and biotin; lane 9 and 10, *E. coli* AY103/pTrc99a/*arnT*$_{Nterm}$ 1 water control and biotin; lane 11 and 12, *E. coli* AY103/pTrc99a/*arnT*$_{Nterm}$ 1 phenol control and biotin; lane 13 and 14, *E. coli* AY103/pTrc99a/*arnT*$_{Nterm}$ 2 water control and biotin; lane 15 and 16, *E. coli* AY103/pTrc99a/*arnT*$_{Nterm}$ 2 phenol control and biotin.

Another *arnT* complementation assay was set up in *B. cenocepacia* conditional *ΔarnT* mutant XOA11 (Ortega *et al.*, 2007). pDA17/$arnT_{N\text{-}term}$ was transferred from *E. coli* DH5α to *B. cenocepacia* XOA11 by triparental mating. *B. cenocepacia* XOA11 control and *B. cenocepacia* XOA11 containing $arnT_{N\text{-}term}$ were grown on plates containing 0.5 % rhamnose or glucose. *B. cenocepacia* XOA11 control grew on rhamnose, but struggled to grow on glucose whereas *B. cenocepacia* XOA11 containing $arnT_{N\text{-}term}$ grew on both plates (Fig. 47). This result indicates that $arnT_{N\text{-}term}$ can restore growth of *B. cenocepacia* conditional *ΔarnT* mutant XOA11 under repressive conditions. However, this experiment needs to be repeated and optimised for future research.

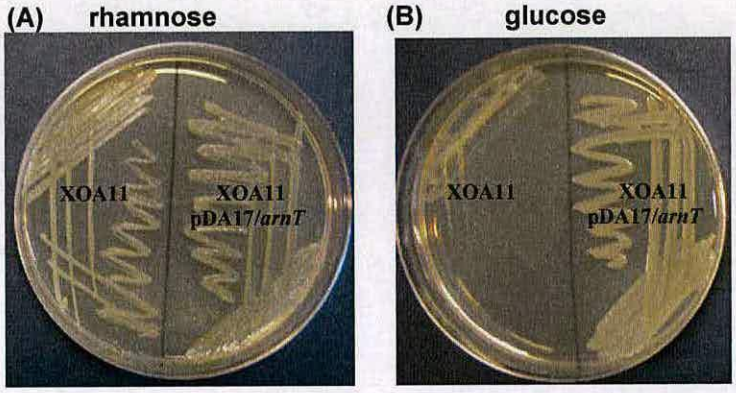

Fig. 47: *B. cenocepacia* J2315 $arnT_{Nterm}$ expressed on a pDA17 plasmid can restore viability in conditional *arnT* mutant *B. cenocepacia* XOA11. *B. cencepacia* XOA11 on the left and *B. cenocepacia* XOA11/pDA17/$arnT_{Nterm}$ on the right growing on **(A)** 0.5% (w/v) rhamnose and **(B)** 0.5% (w/v) glucose.

4.4. Discussion

Bcc LPS is a putative virulence factor which may contribute to a detrimental host immune response in the CF lung, and to the innate resistance of these pathogens to AMPs. Compared to other Gram-negative bacteria, Bcc LPS is both chemically and biologically unusual. Its penta-acylated lipid A core structure with constitutively modified phosphate groups, suggests it would be unlikely to evoke a strong immune response. However, Bcc LPS has been shown to be highly immuno-stimulatory, with IL-6 and TNF-α induction as strong as that induced by *E. coli* LPS (De Soyza *et al.*, 2004; Zughaier *et al.*, 1999). The hexa-acylated lipid A core structure present in *E. coli* LPS is considered to be crucial to its immuno-stimulatory properties (Schromm *et al.*, 2000). Interestingly, Bcc LPS is a poor inducer of IL-1β (Shimomura *et al.*, 2001), a major inflammatory cytokine. However, Shimomura and colleagues reported that when Bcc LPS is incubated with the cationic peptide PMB, IL-1β induction is significantly elevated, whereas *Salmonella* LPS is neutralised (Shimomura *et al.*, 2003). Additionally, in contrast to *Salmonella* LPS, they found that Bcc LPS binds PMB strongly. These interesting and unique properties have not been fully investigated. Studies on the structure and function of Bcc LPS may be informative, not only to understand the complex biology of LPS but to assess the contribution of Bcc LPS to the immunopathology of the CF lung.

Complete structural LPS analysis is challenging and ultimately requires expertise in mass spectrometry and NMR. Initially, analysis may be performed by gel electrophoresis followed by silver staining. This method indicates whether a strain has rough or smooth LPS, and will provide a strain-specific ladder pattern based on the O-antigen. We were interested in whether any lipid A modifications can be visualised by simply staining an LPS gel. In this study, LPS extracted from *B. cenocepacia* clonal ET-12 strains K56-2, J2315 and deep-rough mutant SAL-1 was extracted and compared to an *E. coli* deep-rough standard LPS by gel-electrophoresis and different staining methods.

We found that alcian blue silver staining shows differences in the lipid A and core bands, whereas LPS gels stained by smp silver staining show clear differences between smooth, rough and deep-rough LPS. Interestingly, a difference between the deep-rough *B. cenocepacia* SAL-1 LPS and the deep-rough *E. coli* LPS was observed, which may be due to the added L-Ara4N modifications of SAL-1 or the difference in FA contents. To visualise any L-Ara4N modified LPS we biotinylated the primary amine groups of the sugar. This resulted in clearly observed differences between the modified *B. cenocepacia* J2315 bands and the *E. coli* control. Notably, this method also revealed a slower migrating band for SAL-1, not seen by silver staining. The biotinylated band of SAL-1 LPS correlates with a band only seen in the phenol phase of all three *B. cenocepacia* LPSs. Interestingly, previous LPS studies had only used the water phase, and any phenol specific bands have not been discussed. The chemical differences between the SAL-1 and deep-rough *E. coli* LPSs is likely due to differences in the FA composition rather than L-Ara4N modification. Unfortunately, the SAL-1 LPS structure has not been determined (Miguel Valvano, personal communication).

To be able to use gel electrophoresis as a more detailed analytical tool, standardised analysis of LPS bands is necessary. Steps are also necessary to examine LPS without the denaturing process of silver staining. To investigate the nature of individual bands with minimum denaturation a negative staining method can be applied. This method allows recovery of chemically and biologically intact biomolecules that can be further characterised (Hardy & Castellanos-Serra, 2004). Negative staining and elution is a quick and easy method that can be applied to DNA, proteins and LPS. Unfortunately, this study was not completed in terms of individual band analysis, but will be continued in the laboratory alongside attempts to structurally analyse the LPS of the Bcc. Once a band has been eluted, it can be subjected to structural analyses by mass spectrometry and NMR, as well as by immuno-stimulation and AMP binding assays. This will allow chemical annotation of each of the bands observed in classical LPS ladders, may help determine the inflammatory properties of each LPS species and reveal the molecular details of their interactions with AMPs. This

information could help in designing new antimicrobial compounds to either render the bacteria susceptible to AMPs or help neutralise the inflammatory response.

As well as exploring novel LPS chemical modification tools, the studies in this thesis have focussed on enzymes involved in L-Ara4N biosynthesis which could be potential targets for novel antimicrobial agents. The unique inherent resistance of the Bcc to AMPs has been speculated to be associated with constitutive lipid A modification with L-Ara4N. The enzymes involved in these modifications were recently shown to be essential for *B. cenocepacia* viability (Ortega *et al.*, 2007), providing interesting drug targets of this highly resistant pathogen. This study focused on Ugd and ArnT, the first and the last enzyme in the L-Ara4N biosynthetic pathway.

Out of the three putative *ugd* genes in the *B. cenocepacia* J2315 genome, only $Ugd_{BCAM2946}$ and $Ugd_{BCAM0855}$ encoded proteins with Ugd activity, converting UDP-glucose to UDP- glucuronic acid. The role of the protein encoded by $ugd_{BCAM2034}$ has still to be determined. $Ugd_{BCAM2946}$ and $Ugd_{BCAM0855}$, display high sequence homology, have very similar catalytic profiles and are efficient catalysts with *Km* constants for UDP-glucose and NAD^+ in the low μM range and relatively fast turnover.

A comparison of the roles between the Bcc and *P. aeruginosa* Ugds is worth exploring. *P. aeruginosa* PA01 has two well characterised active enzymes, PA2022 and PA3559, with distinct roles (Hung *et al.*, 2007). PA2022 is suggested to be a constitutively expressed house-keeping gene, whereas PA3559 is induced by low Mg^{2+} concentrations suggesting a role in L-Ara4N modification. This is supported by the fact that a PA3559 knock-out renders *P. aeruginosa* PA01 more susceptible to PMB. In addition, the double knock-out produced less biofilm formation than wild type *P. aeruginosa* PA01. Compared to $Ugd_{BCAM2946}$ and $Ugd_{BCAM0855}$, the pseudomonal Ugds have relatively higher K_m and turnover values. The two *P. aeruginosa* Ugd proteins were also able to utilise UDP-galactose and UDP-N-acetylglucosamine as substrates, but with lower activity compared with UDP-

glucose. In contrast, despite high sequence homology, the two *B. cenocepacia* Ugd proteins displayed narrower substrate specificity. This substrate specificity correlates with the relatively high catalytic efficiency (k_{cat}/K_m) of the enzymes.

To probe the role of the *B. cenocepacia* Ugds in AMP resistance, an in depth study was carried out in collaboration with Slade Loutet and Miguel Valvano (University of Western Ontario, London, Canada). Individual knockouts were created in all three putative *ugd* genes, none of which impaired growth or altered LPS profile compared to wild type *B. cenocepacia* K56-2. However, when grown in 1024 μg/ml PMB only growth of the $\Delta ugd_{BCAL2946}$ mutant was impaired, and the MIC of PMB was reduced from >1024 μg/ml to 128 μg/ml. Growth in PMB could be restored by introducing a wild type $ugd_{BCAL2946}$ or $ugd_{BCAM0855}$, but not $ugd_{BCAM2034}$, on a plasmid. This suggests that out of the three putative *ugd* genes, only $ugd_{BCAL2946}$ is required for the full resistance of *B. cenocepacia* K56-2 to PMB, and also that $Ugd_{BCAM0855}$ can compensate for the loss of function of $Ugd_{BCAL2946}$. This hypothesis is supported by the fact that the encoded enzymes have nearly identical activity. A conditional $ugd_{BCAL2946}$ mutant was then created in a $\Delta ugd_{BCAM0855}$ background. Normal growth was observed under permissive conditions (rhamnose), however, growth was significantly impaired under repressive conditions (glucose), suggesting the combined activity of the proteins encoded by $ugd_{BCAL2946}$ and $ugd_{BCAM0855}$ is required for the viability of *B. cenocepacia.*

Though $Ugd_{BCAM2946}$ and $Ugd_{BCAM0855}$ display very similar kinetic parameters and sequence homology, they are found in gene clusters with different functions; $Ugd_{BCAL2946}$ is found in a LPS related operon (Loutet *et al.*, 2006) and $Ugd_{BCAM0855}$ is found in the *bce* EPS gene cluster discussed earlier. Interestingly, our collaborators found that using real-time PCR, the number of $ugd_{BCAL2946}$ transcripts *in vivo* was significantly higher than the number of $ugd_{BCAM0855}$ transcripts. Since we found that the *bce* gene cluster in *B. cenocepacia* ET-12 isolates contains a disrupted *bceB* gene resulting in lack of EPS biosynthesis, this could account for the lower expression of $ugd_{BCAM0855}$ (*bceC*). The $ugd_{BCAL2946}$ gene is found upstream of *hldA* and *hldD*, encoding heptose modifying enzymes. Notably, the *ΔhldA/ΔhldD* mutant SAL-1 has

deep-rough LPS and is more susceptible to PMB with an MIC of 32μg/ml (Loutet *et al.*, 2006). Interestingly, Burtnick and Woods observed similar reduction in PMB MICs for *B. pseudomallei* when inactivating *ugd* and a heptosyl transferase gene, *waaF* (Burtnick & Woods, 1999). Inactivation of $ugd_{BCAL2946}$ has no polar effect on *hldA* or *hldD* as full resistance can be restored when $ugd_{BCAL2946}$ is expressed *in trans* and the LPS profile remains as wild type. In conclusion, $ugd_{BCAL2946}$ is likely to be involved in the L-Ara4N biosynthetic pathway, and the high cellular expression of $ugd_{BCAL2946}$, together with the loss of viability in the absence of any Ugd activity, further highlights the importance of these enzymes in *B. cenocepacia.*

The last step of the L-Ara4N biosynthetic pathway is catalysed by ArnT, which transfers L-Ara4N from an Upp-L-Ara4N to lipid A. Despite low sequence homology to other ArnTs, there is only one strong candidate *arnT* gene in the *B. cenocepacia* J2315 genome, $arnT_{BCAL1929}$. Ortega and colleagues found this gene to be essential for *B. cenocepacia* viability (Ortega *et al.*, 2007). Analysis of the structure of Bcc LPS revealed the presence of L-Ara4N on the 1- and the 4'-phosphates of the lipid A, as well as the Ko molecule of the inner core (Gronow *et al.*, 2003; Silipo *et al.*, 2007). These multiple sites for L-Ara4N modification suggest that the Bcc could possess more than one *arnT*. However, it has been shown that the *Francisella tularensis arnT* homolog, *flmK*, attaches both galactosamine onto the 1-phosphate and mannose to the 4'-phosphate (Kanistanon *et al.*, 2008). Since the Bcc ArnT protein shares higher sequence homology to FlmK than other characterised amino sugar transferases, it is tempting to speculate that $ArnT_{BCAL1929}$ could also be a multi-functional enzyme.

In our study, we attempted to purify recombinant ArnT from *B. cenocepacia* J2315 expressed in *E. coli*. This proved to be extremely difficult regardless of the different fusion tags and hosts that were tried. The expression of pET-28a/$arnT_{BCAL1929}$ with an N-terminal histidine tag was achieved in *E. coli* C41 (DE3) and C43 (DE3) strains. Furthermore, preliminary data suggest that the $arnT_{BCAL1929}$ construct was active since it was able to restore PMB resistance to a PMB-sensitive *E. coli ΔarnT* mutant. Additionally, $arnT_{BCAL1929}$ expressed on a *Burkholderia* expression plasmid (pDA17)

appears to restore growth of *B. cenocepacia* conditional *ΔarnT* mutant XOA11 under repressive conditions. Unfortunately, attempts to prove L-Ara4N transfer to lipid A in *E. coli ΔarnT* mutant using the biotinylation procedure were unsuccessful. In addition, attempts to purify sufficient quantities of $ArnT_{BCAL1929}$ for biochemical studies were unsuccessful, which is not surprising considering it is an inner membrane protein. Such targets have proven to be particularly challenging (Wagner *et al.*, 2007). Studies of the ArnTs from *E. coli* and *Salmonella* provided some insight into the substrate specificity and cellular location of these isoforms (Bretscher *et al.*, 2006; Trent *et al.*, 2001). However, to date the structures of any ArnT homologs remain to be determined. Future work is required to optimise ArnT purification methods and develop more conclusive L-Ara4N transferase assays.

The main conclusion from these studies is that the enzymes in the L-Ara4N biosynthesis pathway are important for PMB resistance, and for the survival of *B. cenocepacia*, thus providing new antimicrobial targets. The question remains, however, as to why L-Ara4N is essential for *B. cenocepacia* survival? It could be that L-Ara4N LPS modification is essential for membrane stability, and as it is a constitutive modification the bacteria may not have had to develop alternative protective mechanisms. In addition, these experiments were carried out using LB or minimal media culture conditions, and it may be that as yet unknown environmental factors may be able to compensate for the loss of L-Ara4N.

Another explanation could be that there is a transport defect in L-Ara4N deficient mutants. This would be consistent with the accumulation of membranous material observed by transmission electron microscopy of *B. cenocepacia* conditional mutants XOA11 and XOA12 (Ortega *et al.*, 2007). The LPS transport system has not been investigated in the Bcc and could bring surprises. The best available model is that of *E. coli* (Raetz *et al.*, 2007; Tran *et al.*, 2008). In this organism the lipid A is flipped across the inner membrane to the periplasmic side by MsbA after which it is modified with L-Ara4N, from an Upp-L-Ara4N precursor, which itself has been flipped across the inner membrane by ArnEF. The core and O-antigen are then added, and this modified LPS is then transported across the periplasm by the LptA

chaperone, and flipped across the outer membrane by LptDE. Given previous experience of the idiosyncrasies of *Burkholderia*, it might be reasonable to assume that the transport systems differ from that of *E. coli*. For example, the *Burkholderia* lipid A chaperone LptA (or its equivalent) may be absolutely specific for L-Ara4N modified lipid A intermediates. Furthermore, the *Burkholderia* flippases might be extremely intolerant of unmodified lipid A. It could be possible that *Burkholderia* lipid A is modified on the cytoplasmic side of the inner membrane, indicating no requirement for an Upp-Ara4N flippase, but a unique specificity of MsbA for already modified lipid A. To explore these hypotheses, it would be interesting to over-express MsbA or LptA in *B. cenocepacia* XOA11 to determine whether such over-expression could restore the viability of the *ΔarnT* mutant.

To identify more specific antimicrobial targets it will be important to know whether disruption of the L-Ara4N biosynthetic enzymes affects LPS transport or membrane permeability. Nevertheless, an Achilles' heel of the Bcc has certainly been exposed. Cycloserine, a known ArnB inhibitor (Noland *et al.*, 2002), and inhibitors of the other enzymes in L-Ara4N biosynthesis could be used alone, or in combination with other antimicrobial agents to overcome the notorious multi-resistance of these challenging pathogens.

5.1. General Discussion and Future Work

A major aim of this thesis was to investigate putative virulence factors and novel antimicrobial targets of the *Burkholderia cepacia* complex. This group of closely-related pathogens cause life-threatening lung infections in CF patients, largely due to a destructive inflammatory response. In addition, the Bcc are inherently resistant to all classes of antibiotics including AMPs, making Bcc infections very difficult to treat. To my knowledge, there are only three reports of successful antibacterial treatment of cepacia syndrome. These cases required combinations of 4 to 5 antibiotics, both intravenous and nebulised, as well as mucolytic and anti-inflammatory agents (Kazachkov *et al.*, 2001; Weidmann *et al.*, 2008) (Grimwood & Tweed, personal communication). From the armoury of putative Bcc virulence factors, EPS and LPS may play important roles in persistence, immuno-stimulation and resistance in the CF lung. In the case of resistance, the EPS may provide a protective shield around the bacteria which makes it difficult for antimicrobial agents to penetrate the bacterial cell and reach their targets. At the same time, the unique modifications of Bcc LPS make the outer membrane even more impenetrable. Hence, in addition to finding a novel antimicrobial agent that kills Bcc, it may be strategically important to find novel antimicrobial agents that can weaken this protective shield to enable penetration of existing antibiotics.

During the EPS investigation a surprising aspect of Bcc EPS became apparent. Instead of a non-mucoid to mucoid conversion, which is a striking characteristic of *P. aeruginosa* infections in CF patients, the Bcc apparently revert from a mucoid to a non-mucoid phenotype (Zlosnik *et al.*, 2008). This suggests that EPS may be important for initial persistence, and that a loss of mucoidy may contribute to increased virulence. This would explain why, in this study, members of the virulent ET-12 lineage did not produce EPS under any conditions tested. These results raise interesting questions in relation to the role of EPS, both in human infection and in the survival of the Bcc in natural environments. How can the lack of EPS production in *B. cenocepacia* be reconciled with the notorious transmissibility and virulence of this Bcc species? In contrast to the conversion to mucoidy of *P. aeruginosa* in the CF

lung, is loss of EPS a major factor in the transition of this rhizosphere microbe to a human niche? Is EPS production and its role in protection against dehydration in other Bcc species, an important aspect of their survival in natural environments? Finally, if EPS is involved in human infection, how can we explain the fact that *B. cenocepacia* and *B. multivorans* account for 90% of all clinical Bcc isolates (Govan *et al.*, 2007) when these species differ in their ability to produce EPS?

Interestingly, loss of EPS usually correlates with increased motility and increased exposure of LPS. The LPS of the Bcc has been shown to be highly immuno-stimulatory (De Soyza *et al.*, 2004; Shaw *et al.*, 1995), despite having a lipid A structure which would suggest otherwise. It is tempting to speculate, due to the LPS purification methods, that flagella contamination may in fact be responsible for the inflammatory response observed in these studies. Bcc flagella have been shown to directly stimulate IL-8 and NFκB through TLR-5 (Urban *et al.*, 2004). In addition, flagellin-less mutants were shown to survive longer in a rat agar lung infection model by evading an immune response. Interestingly, it has recently been found that TLR5, but neither TLR2 nor TLR4, critically regulate *B. cenocepacia*-induced lung epithelial inflammatory response in a mouse model (deVentura *et al.*, 2008). It would certainly be interesting to investigate the inflammatory role of Bcc flagella versus LPS in future studies.

Whether the LPS is responsible for the detrimental inflammatory response associated with Bcc infection or not, LPS remains a key factor for AMP resistance and membrane stability. In collaboration with Valvano, my colleagues showed that the enzymes involved in L-Ara4N lipid A modification are essential for Bcc viability (Ortega *et al.*, 2007). This important finding provides new antimicrobial targets that may in future improve treatment of Bcc infections. In this thesis, Ugd and ArnT, the first and last enzyme of the L-Ara4N biosynthetic pathway, were investigated. Out of three putative *ugd* genes found in the *B. cenocepacia* J2315 genome, we conclude that $Ugd_{BCAL2946}$ is involved in PMB resistance, whereas $Ugd_{BCAM0855}$ is involved in EPS biosynthesis. Together, these two Ugds are essential for Bcc viability, and $Ugd_{BCAM0855}$ is able to compensate for the loss of $Ugd_{BCAL2946}$ *in vivo*. Only one *arnT*

candidate gene was found in the *B. cenocepacia* J2315 genome, which was associated with the *arn* gene cluster. Some progress was made in the isolation of recombinant ArnT from *B. cenocepacia* J2315 suitable for biochemical studies. However, as intrinsic inner membrane proteins, investigations of amino sugar transferase enzymes remains a considerable challenge.

The essential nature of the L-Ara4N biosynthetic enzymes in viability of the Bcc suggests a potential Achilles' heel. For future research in this area, it will be important to understand why these enzymes are indispensable, and perhaps even more importantly, how these and other LPS modification enzymes are regulated.

The control and regulation of Bcc virulence factors and their role in bacterial pathogenesis remains a mystery. Though these bacteria carry the largest number of TCSs of any bacterial species, very little is known about Bcc virulence regulation. No TCS has yet been discovered that controls Bcc LPS modifications, and the fact that the modifying enzymes are constitutively expressed implies that, in contrast to *E. coli* and *Salmonella,* regulation in the Bcc is independent of environmental stimuli. The putative *B. cenocepacia* response regulators most similar to PhoP and PmrA of *Salmonella* and *P. aeruginosa* are not required for PMB resistance (Flannigan *et al.,* 2007), indicating that they are not regulating LPS modifications. Interestingly, the suggested PhoP-binding site motif, (A/C) GTTA (Groisman, 2001), can be found upstream of *arnT, arnB* and $ugd_{BCAL2946}$ in *B. cenocepacia* J2315, suggesting these genes should be under control of a TCS. In addition, lipid A from a *B. multivorans* strain isolated from a pre-transplant CF lung was heavily modified, whereas after a lung transplant the lipid A from the same strain was less modified and less immuno-stimulatory (Ierano *et al.*, 2008). This implies that something in the CF lung induces LPS modification of these pathogens, perhaps enhancing the detrimental inflammatory response. It would be very interesting to investigate the TCSs of the Bcc and their involvement in the control and regulation of the virulence of these pathogens, in particular to explain the enhanced virulence of *B. cenocepacia* as a species, and of lineages such as ET-12.

Reference List

Allenza, P., Lee, Y. N. & Lessie, T. G. (1982). Enzymes related to fructose utilization in *Pseudomonas cepacia*. *J Bacteriol* **150**, 1348-1356.

Anderson, M. S., Bull, H. G., Galloway, S. M., Kelly, T. M., Mohan, S., Radika, K. & Raetz, C. R. (1993). UDP-N-acetylglucosamine acyltransferase of *Escherichia coli*. The first step of endotoxin biosynthesis is thermodynamically unfavorable. *J Biol Chem* **268**, 19858-19865.

Amann, E., Ochs, B. & Abel, K. J. (1988). Tightly regulated tac promoter vectors useful for the expression of unfused and fused proteins in *Escherichia coli*. *Gene* **69**, 301-315.

Andrews, J. M. (2001). Determination of minimum inhibitory concentrations. *J Antimicrob Chemother* **48 Suppl 1**, 5-16.

Aubert, D. F., Flannagan, R. S. & Valvano, M. A. (2008). A novel sensor kinase-response regulator hybrid controls biofilm formation and type VI secretion system activity in *Burkholderia cenocepacia*. *Infect Immun* 76, 1979-1991.

Babinski, K. J., Kanjilal, S. J. & Raetz, C. R. (2002a). Accumulation of the lipid A precursor UDP-2,3-diacylglucosamine in an *Escherichia coli* mutant lacking the lpxH gene. *J Biol Chem* **277**, 25947-25956.

Babinski, K. J., Ribeiro, A. A. & Raetz, C. R. (2002b). The *Escherichia coli* gene encoding the UDP-2,3-diacylglucosamine pyrophosphatase of lipid A biosynthesis. *J Biol Chem* **277**, 25937-25946.

Bader, M. W., Sanowar, S., Daley, M. E., Schneider, A. R., Cho, U., Xu, W., Klevit, R. E., Le Moual, H. & Miller, S. I. (2005). Recognition of antimicrobial peptides by a bacterial sensor kinase. *Cell* **122**, 461-472.

Barb, A. W., McClerren, A. L., Snehelatha, K., Reynolds, C. M., Zhou, P. & Raetz, C. R. (2007). Inhibition of lipid A biosynthesis as the primary mechanism of CHIR-090 antibiotic activity in *Escherichia coli*. *Biochemistry* **46**, 3793-3802.

Bayer, M. E. (1968). Areas of adhesion between wall and membrane of *Escherichia coli*. *J Gen Microbiol* **53**, 395-404.

Beckman, W. & Lessie, T. G. (1979). Response of *Pseudomonas cepacia* to beta-Lactam antibiotics: utilization of penicillin G as the carbon source. *J Bacteriol* **140**, 1126-1128.

Belunis, C. J. & Raetz, C. R. (1992). Biosynthesis of endotoxins. Purification and catalytic properties of 3-deoxy-D-manno-octulosonic acid transferase from *Escherichia coli*. *J Biol Chem* **267**, 9988-9997.

Belunis, C. J., Clementz, T., Carty, S. M. & Raetz, C. R. (1995). Inhibition of lipopolysaccharide biosynthesis and cell growth following inactivation of the kdtA gene in *Escherichia coli*. *J Biol Chem* **270**, 27646-27652.

Berg, G., Eberl, L. & Hartmann, A. (2005). The rhizosphere as a reservoir for opportunistic human pathogenic bacteria. *Environ Microbiol* **7**, 1673-1685.

Bernier, S. P., Silo-Suh, L., Woods, D. E., Ohman, D. E. & Sokol, P. A. (2003). Comparative analysis of plant and animal models for characterization of *Burkholderia cepacia* virulence. *Infect Immun* **71**, 5306-5313.

Beutler, B. A. (2009). TLRs and innate immunity. *Blood* **113**, 1399-1407.

Bishop, R. E., Gibbons, H. S., Guina, T., Trent, M. S., Miller, S. I. & Raetz, C. R. (2000). Transfer of palmitate from phospholipids to lipid A in outer membranes of gram-negative bacteria. *Embo J* **19**, 5071-5080.

Boman, H. G. (2000). Innate immunity and the normal microflora. *Immunol Rev* **173**, 5-16.

Boon Hinckley, M., Reynolds, C. M., Ribeiro, A. A., McGrath, S. C., Cotter, R. J., Lauw, F. N., Golenbock, D. T. & Raetz, C. R. (2005). A *Leptospira interrogans* enzyme with similarity to yeast Ste14p that methylates the 1-phosphate group of lipid A. *J Biol Chem* **280**, 30214-30224.

Brabetz, W., Muller-Loennies, S., Holst, O. & Brade, H. (1997). Deletion of the heptosyltransferase genes rfaC and rfaF in *Escherichia coli* K-12 results in an Re-type lipopolysaccharide with a high degree of 2-aminoethanol phosphate substitution. *Eur J Biochem* **247**, 716-724.

Breazeale, S. D., Ribeiro, A. A. & Raetz, C. R. (2002). Oxidative decarboxylation of UDP-glucuronic acid in extracts of polymyxin-resistant *Escherichia coli*. Origin of lipid a species modified with 4-amino-4-deoxy-L-arabinose. *J Biol Chem* **277**, 2886-2896.

Breazeale, S. D., Ribeiro, A. A. & Raetz, C. R. (2003). Origin of lipid A species modified with 4-amino-4-deoxy-L-arabinose in polymyxin-resistant mutants of *Escherichia coli*. An aminotransferase (ArnB) that generates UDP-4-deoxyl-L-arabinose. *J Biol Chem* **278**, 24731-24739.

Breazeale, S. D., Ribeiro, A. A., McClerren, A. L. & Raetz, C. R. (2005). A formyltransferase required for polymyxin resistance in *Escherichia coli* and the modification of lipid A with 4-Amino-4-deoxy-L-arabinose. Identification and function oF UDP-4-deoxy-4-formamido-L-arabinose. *J Biol Chem* **280**, 14154-14167.

Bretscher, L. E., Morrell, M. T., Funk, A. L. & Klug, C. S. (2006). Purification and characterization of the L-Ara4N transferase protein ArnT from *Salmonella typhimurium*. *Protein Expr Purif* **46**, 33-39.

Brogden, K. A. (2005). Antimicrobial peptides: pore formers or metabolic inhibitors in bacteria? *Nat Rev Microbiol* **3**, 238-250.

Burkholder, W. (1950). Sour skin, a bacterial rot of onion bulbs. *Phytopath* **40**, 115-117.

Burtnick, M. N. & Woods, D. E. (1999). Isolation of polymyxin B-susceptible mutants of *Burkholderia pseudomallei* and molecular characterization of genetic loci involved in polymyxin B resistance. *Antimicrob Agents Chemother* **43**, 2648-2656.

Bylund, J., Burgess, L. A., Cescutti, P., Ernst, R. K. & Speert, D. P. (2006). Exopolysaccharides from *Burkholderia cenocepacia* inhibit neutrophil chemotaxis and scavenge reactive oxygen species. *J Biol Chem* **281**, 2526-2532.

Campbell, R. E., Mosimann, S. C., van De Rijn, I., Tanner, M. E. & Strynadka, N. C. (2000). The first structure of UDP-glucose dehydrogenase reveals the catalytic residues necessary for the two-fold oxidation. *Biochemistry* **39**, 7012-7023.

Cardona, S. T. & Valvano, M. A. (2005). An expression vector containing a rhamnose-inducible promoter provides tightly regulated gene expression in *Burkholderia cenocepacia*. *Plasmid* **54**, 219-228.

Carty, S. M., Sreekumar, K. R. & Raetz, C. R. (1999). Effect of cold shock on lipid A biosynthesis in *Escherichia coli*. Induction At 12 degrees C of an acyltransferase specific for palmitoleoyl-acyl carrier protein. *J Biol Chem* **274**, 9677-9685.

Castellanos-Serra, L. & Hardy, E. (2006). Negative detection of biomolecules separated in polyacrylamide electrophoresis gels. *Nat Protoc* **1**, 1544-1551.

Cerantola, S., Marty, N. & Montrozier, H. (1996). Structural studies of the acidic exopolysaccharide produced by a mucoid strain of *Burkholderia cepacia*, isolated from cystic fibrosis. *Carbohydr Res* **285**, 59-67.

Cerantola, S., Lemassu-Jacquier, A. & Montrozier, H. (1999). Structural elucidation of a novel exopolysaccharide produced by a mucoid clinical isolate of *Burkholderia cepacia*. Characterization of a trisubstituted glucuronic acid residue in a heptasaccharide repeating unit. *Eur J Biochem* **260**, 373-383.

Cescutti, P., Bosco, M., Picotti, F., Impallomeni, G., Leitao, J. H., Richau, J. A. & Sa-Correia, I. (2000). Structural study of the exopolysaccharide produced by a clinical isolate of *Burkholderia cepacia*. *Biochem Biophys Res Commun* **273**, 1088-1094.

Cescutti, P., Impallomeni, G., Garozzo, D., Sturiale, L., Herasimenka, Y., Lagatolla, C. & Rizzo, R. (2003). Exopolysaccharides produced by a clinical strain of *Burkholderia cepacia* isolated from a cystic fibrosis patient. *Carbohydr Res* **338**, 2687-2695.

Cheung, K. J., Jr., Li, G., Urban, T. A., Goldberg, J. B., Griffith, A., Lu, F. & Burns, J. L. (2007). Pilus-mediated epithelial cell death in response to infection with *Burkholderia cenocepacia*. *Microbes Infect* **9**, 829-837.

Chiarini, L., Cescutti, P., Drigo, L. & other authors (2004). Exopolysaccharides produced by *Burkholderia cenocepacia* recA lineages IIIA and IIIB. *J Cyst Fibros* **3**, 165-172.

Chung, J. W., Altman, E., Beveridge, T. J. & Speert, D. P. (2003). Colonial morphology of *Burkholderia cepacia* complex genomovar III: implications in exopolysaccharide production, pilus expression, and persistence in the mouse. *Infect Immun* **71**, 904-909.

Clementz, T. & Raetz, C. R. (1991). A gene coding for 3-deoxy-D-manno-octulosonic-acid transferase in *Escherichia coli*. Identification, mapping, cloning, and sequencing. *J Biol Chem* **266**, 9687-9696.

Clementz, T., Bednarski, J. J. & Raetz, C. R. (1996). Function of the *htrB* high temperature requirement gene of *Escherchia coli* in the acylation of lipid A: HtrB catalyzed incorporation of laurate. *J Biol Chem* **271**, 12095-12102.

Clementz, T., Zhou, Z. & Raetz, C. R. (1997). Function of the *Escherichia coli msbB* gene, a multicopy suppressor of htrB knockouts, in the acylation of lipid A. Acylation by MsbB follows laurate incorporation by HtrB. *J Biol Chem* **272**, 10353-10360.

Coenye, T., Vandamme, P., LiPuma, J. J., Govan, J. R. & Mahenthiralingam, E. (2003). Updated version of the *Burkholderia cepacia* complex experimental strain panel. *J Clin Microbiol* **41**, 2797-2798.

Conway, B. A., Chu, K. K., Bylund, J., Altman, E. & Speert, D. P. (2004). Production of exopolysaccharide by *Burkholderia cenocepacia* results in altered cell-surface interactions and altered bacterial clearance in mice. *J Infect Dis* **190**, 957-966.

Corzo, J., Perez-Galdona, R., Leon-Barrios, M. & Gutierrez-Navarro, A. M. (1991). Alcian blue fixation allows silver staining of the isolated polysaccharide component of bacterial lipopolysaccharides in polyacrylamide gels. *Electrophoresis* **12**, 439-441.

Cunha, M. V., Sousa, S. A., Leitao, J. H., Moreira, L. M., Videira, P. A. & Sa-Correia, I. (2004). Studies on the involvement of the exopolysaccharide produced by cystic fibrosis-associated isolates of the *Burkholderia cepacia* complex in biofilm formation and in persistence of respiratory infections. *J Clin Microbiol* **42**, 3052-3058.

Davies, J. C., Alton, E. W. & Bush, A. (2007). Cystic fibrosis. *Bmj* **335**, 1255-1259.

Daviskas, E., Anderson, S. D., Gomes, K., Briffa, P., Cochrane, B., Chan, H. K., Young, I. H. & Rubin, B. K. (2005). Inhaled mannitol for the treatment of mucociliary dysfunction in patients with bronchiectasis: effect on lung function, health status and sputum. *Respirology* **10**, 46-56.

De Soyza, A., Ellis, C. D., Khan, C. M., Corris, P. A. & Demarco de Hormaeche, R. (2004). *Burkholderia cenocepacia* lipopolysaccharide, lipid A, and proinflammatory activity. *Am J Respir Crit Care Med* **170**, 70-77.

De Soyza, A., Silipo, A., Lanzetta, R., Govan, J. R. & Molinaro, A. (2008). Chemical and biological features of *Burkholderia cepacia* complex lipopolysaccharides. *Innate Immun* **14**, 127-144.

de Ventura, C. G. M., Le Goffic, R., Balloy, V., Plotkowski, M. C., Chignard, M. & Si-Tahar, M. (2008). TLR 5, but neither TLR2 nor TLR4, is involved in lung epithelial cell response to Burkholderia cenocepacia. *FEMS Immunol Med Microbiol* **54**, 37-44.

de Vries, T. W., Ajubi, N., Slomp, J., Storm, H. (2006). Analyzing DNA from buccal cells is a reliable method for the exclusion of cystic fibrosis. Results of a pilot study. *Genetics in Medicine* **8**, 175-177.

Delgado, M. A., Mouslim, C. & Groisman, E. A. (2006). The PmrA/PmrB and RcsC/YojN/RcsB systems control expression of the *Salmonella* O-antigen chain length determinant. *Mol Microbiol* **60**, 39-50.

DeShazer, D., Waag, D. M., Fritz, D. L. & Woods, D. E. (2001). Identification of a *Burkholderia mallei* polysaccharide gene cluster by subtractive hybridization and demonstration that the encoded capsule is an essential virulence determinant. *Microb Pathog* **30**, 253-269.

Di, A., Brown, M. E., Deriy, L. V. & other authors (2006). CFTR regulates phagosome acidification in macrophages and alters bactericidal activity. *Nat Cell Biol* **8**, 933-944.

Doerrler, W. T., Reedy, M. C. & Raetz, C. R. (2001). An *Escherichia coli* mutant defective in lipid export. *J Biol Chem* **276**, 11461-11464.

Durr, M. & Peschel, A. (2002). Chemokines meet defensins: the merging concepts of chemoattractants and antimicrobial peptides in host defense. *Infect Immun* **70**, 6515-6517.

Ernst, R. K., Adams, K. N., Moskowitz, S. M., Kraig, G. M., Kawasaki, K., Stead, C. M., Trent, M. S. & Miller, S. I. (2006). The *Pseudomonas aeruginosa* lipid A deacylase: selection for expression and loss within the cystic fibrosis airway. *J Bacteriol* **188**, 191-201.

Erridge, C., Bennett-Guerrero, E. & Poxton, I. R. (2002). Structure and function of lipopolysaccharides. *Microbes Infect* **4**, 837-851.

Eshdat, Y. & Mireman, D. (1972). An improved method for the recovery of compounds from paper chromatograms. *J Chromat* **6**, 458-459.

Ferreira, A. S., Leitao, J. H., Sousa, S. A., Cosme, A. M., Sa-Correia, I. & Moreira, L. M. (2007). Functional analysis of *Burkholderia cepacia* genes *bceD* and *bceF*, encoding a phosphotyrosine phosphatase and a tyrosine autokinase, respectively: role in exopolysaccharide biosynthesis and biofilm formation. *Appl Environ Microbiol* **73**, 524-534.

Figurski, D. H. & Helinski, D. R. (1979). Replication of an origin-containing derivative of plasmid RK2 dependent on a plasmid function provided in trans. *Proc Natl Acad Sci USA* **76**, 1648-1652.

Flannagan, R. S., Aubert, D., Kooi, C., Sokol, P. A. & Valvano, M. A. (2007). *Burkholderia cenocepacia* requires a periplasmic HtrA protease for growth under thermal and osmotic stress and for survival in vivo. *Infect Immun* **75**, 1679-1689.

Fry, S. C. (2000). *The growing plant cell wall: Chemical and Metabolic Analysis.* Caldwell, New Jersey: The Blackburn Press

Galanos, C., Luderitz, O., Rietschel, E. T. & other authors (1985). Synthetic and natural *Escherichia coli* free lipid A express identical endotoxic activities. *Eur J Biochem* **148**, 1-5.

Garcia, J. R., Jaumann, F., Schulz, S. & other authors (2001). Identification of a novel, multifunctional beta-defensin (human beta-defensin 3) with specific antimicrobial activity. Its interaction with plasma membranes of Xenopus oocytes and the induction of macrophage chemoattraction. *Cell Tissue Res* **306**, 257-264.

Garrett, T. A., Kadrmas, J. L. & Raetz, C. R. (1997). Identification of the gene encoding the *Escherichia coli* lipid A 4'-kinase. Facile phosphorylation of endotoxin analogs with recombinant LpxK. *J Biol Chem* **272**, 21855-21864.

Ge, X., Penney, L. C., van de Rijn, I. & Tanner, M. E. (2004). Active site residues and mechanism of UDP-glucose dehydrogenase. *Eur J Biochem* **271**, 14-22.

Gibbons, H. S., Kalb, S. R., Cotter, R. J., Raetz, C. H. (2005). Role of Mg2+ and pH in the modification of *Salmonella* lipid A after endocytosis by macrophage tumour cells. *Mol Microbiol* **55**, 425-440.

Gibson, R. L., Burns, J. L. & Ramsey, B. W. (2003). Pathophysiology and management of pulmonary infections in cystic fibrosis. *Am J Respir Crit Care Med* **168**, 918-951.

Govan, J. R., Brown, P. H., Maddison, J., Doherty, C. J., Nelson, J. W., Dodd, M., Greening, A. P. & Webb, A. K. (1993). Evidence for transmission of *Pseudomonas cepacia* by social contact in cystic fibrosis. *Lancet* **342**, 15-19.

Govan, J. R. & Deretic, V. (1996). Microbial pathogenesis in cystic fibrosis: mucoid Pseudomonas aeruginosa and *Burkholderia cepacia. Microbiol Rev* **60**, 539-574.

Govan, J. R., Brown, A. R. & Jones, A. M. (2007). Evolving epidemiology of *Pseudomonas aeruginosa* and the *Burkholderia cepacia* complex in cystic fibrosis lung infection. *Future Microbiol* **2**, 153-164.

Griesenbach, U. & Alton, E. W. (2008). Gene transfer to the lung: Lessons learned from more than 2 decades of CF gene therapy. *Adv Drug Deliv Rev.*

Groisman, E. A., Kayser, J. & Soncini, F. C. (1997). Regulation of polymyxin resistance and adaptation to low-Mg2+ environments. *J Bacteriol* **179**, 7040-7045.

Groisman, E. A. (2001). The pleiotropic two-component regulatory system PhoP-PhoQ. *J Bacteriol* **183**, 1835-1842.

Gronow, S., Noah, C., Blumenthal, A., Lindner, B. & Brade, H. (2003). Construction of a deep-rough mutant of *Burkholderia cepacia* ATCC 25416 and characterization of its chemical and biological properties. *J Biol Chem* **278**, 1647-1655.

Gunn, J. S., Lim, K. B., Krueger, J., Kim, K., Guo, L., Hackett, M. & Miller, S. I. (1998). PmrA-PmrB-regulated genes necessary for 4-aminoarabinose lipid A modification and polymyxin resistance. *Mol Microbiol* **27**, 1171-1182.

Gunn, J. S. (2008). The Salmonella PmrAB regulon: lipopolysaccharide modifications, antimicrobial peptide resistance and more. *Trends Microbiol* **16**, 284-290.

Hamai, H., Keyserman, F., Quittell, L. M. & Worgall, T. S. (2009). Defective CFTR increases synthesis and mass of sphingolipids that affect membrane composition and lipid signaling. *J Lipid Res.*

Harder, J., Bartels, J., Christophers, E. & Schroder, J. M. (2001). Isolation and characterization of human beta -defensin-3, a novel human inducible peptide antibiotic. *J Biol Chem* **276**, 5707-5713.

Hardy, E. & Castellanos-Serra, L. R. (2004). "Reverse-staining" of biomolecules in electrophoresis gels: analytical and micropreparative applications. *Anal Biochem* **328**, 1-13.

Herasimenka, Y., Benincasa, M., Mattiuzzo, M., Cescutti, P., Gennaro, R. & Rizzo, R. (2005). Interaction of antimicrobial peptides with bacterial polysaccharides from lung pathogens. *Peptides* **26**, 1127-1132.

Heyworth, P. G., Cross, A. R. & Curnutte, J. T. (2003). Chronic granulomatous disease. *Curr Opin Immunol* **15**, 578-584.

Hirschfeld, M., Weis, J. J., Toshchakov, V., Salkowski, C. A., Cody, M. J., Ward, D. C., Qureshi, N., Michalek, S. M. & Vogel, S. N. (2001). Signaling by toll-like receptor 2 and 4 agonists results in differential gene expression in murine macrophages. *Infect Immun* **69**, 1477-1482.

Hoiby, N., Frederiksen, B. & Pressler, T. (2005). Eradication of early *Pseudomonas aeruginosa* infection. *J Cyst Fibros* **4 Suppl 2**, 49-54.

Holden, M. T., Seth-Smith, H. M., Crossman, L. C. & other authors (2008). The genome of *Burkholderia cenocepacia* J2315, an epidemic pathogen of cystic fibrosis patients. *J Bacteriol.*

Holmes, A., Govan, J. & Goldstein, R. (1998). Agricultural use of *Burkholderia (Pseudomonas) cepacia*: a threat to human health? *Emerg Infect Dis* **4**, 221-227.

Huber, B., Riedel, K., Hentzer, M., Heydorn, A., Gotschlich, A., Givskov, M., Molin, S. & Eberl, L. (2001). The cep quorum-sensing system of *Burkholderia cepacia* H111 controls biofilm formation and swarming motility. *Microbiology* **147**, 2517-2528.

Hung, R. J., Chien, H. S., Lin, R. Z., Lin, C. T., Vatsyayan, J., Peng, H. L. & Chang, H. Y. (2007). Comparative analysis of two UDP-glucose dehydrogenases in *Pseudomonas aeruginosa* PAO1. *J Biol Chem* **282**, 17738-17748.

Hutchison, M. L., Poxton, I. R. & Govan, J. R. (1998). *Burkholderia cepacia* produces a hemolysin that is capable of inducing apoptosis and degranulation of mammalian phagocytes. *Infect Immun* **66**, 2033-2039.

Ierano, T., Silipo, A., Sturiale, L. & other authors (2008). The structure and proinflammatory activity of the lipopolysaccharide from *Burkholderia multivorans* and the differences between clonal strains colonizing pre and posttransplanted lungs. *Glycobiology* **18**, 871-881.

Isles, A., Maclusky, I., Corey, M., Gold, R., Prober, C., Fleming, P. & Levison, H. (1984). *Pseudomonas cepacia* infection in cystic fibrosis: an emerging problem. *J Pediatr* **104**, 206-210.

Isshiki, Y., Kawahara, K. & Zahringer, U. (1998). Isolation and characterisation of disodium (4-amino-4-deoxy-beta-L- arabinopyranosyl)-(1-->8)-(D-glycero-alpha-D-talo-oct-2-ulopyranosylona te)- (2-->4)-(methyl 3-deoxy-D-manno-oct-2-ulopyranosid)onate from the lipopolysaccharide of *Burkholderia cepacia. Carbohydr Res* **313**, 21-27.

Isshiki, Y., Zahringer, U. & Kawahara, K. (2003). Structure of the core-oligosaccharide with a characteristic D-glycero-alpha-D-talo-oct-2-ulosylonate-(2-->4)-3-deoxy-D-manno-oct-2-ulo sonate [alpha-Ko-(2-->4)-Kdo] disaccharide in the lipopolysaccharide from *Burkholderia cepacia. Carbohydr Res* **338**, 2659-2666.

Kanipes, M. I., Lin, S., Cotter, R. J. & Raetz, C. R. (2001). Ca2+-induced phosphoethanolamine transfer to the outer 3-deoxy-D-manno-octulosonic acid moiety of *Escherichia coli* lipopolysaccharide. A novel membrane enzyme dependent upon phosphatidylethanolamine. *J Biol Chem* **276**, 1156-1163.

Kanistanon, D., Hajjar, A. M., Pelletier, M. R. & other authors (2008). A *Francisella* mutant in lipid A carbohydrate modification elicits protective immunity. *PLoS Pathog* **4**, e24.

Kanjilal-Kolar, S., Basu, S. S., Kanipes, M. I., Guan, Z., Garrett, T. A. & Raetz, C. R. (2006). Expression cloning of three *Rhizobium leguminosarum* lipopolysaccharide core galacturonosyltransferases. *J Biol Chem* **281**, 12865-12878.

Kanjilal-Kolar, S. & Raetz, C. R. (2006). Dodecaprenyl phosphate-galacturonic acid as a donor substrate for lipopolysaccharide core glycosylation in *Rhizobium leguminosarum. J Biol Chem* **281**, 12879-12887.

Karbarz, M. J., Kalb, S. R., Cotter, R. J. & Raetz, C. R. (2003). Expression cloning and biochemical characterization of a *Rhizobium leguminosarum* lipid A 1-phosphatase. *J Biol Chem* **278**, 39269-39279.

Karow, M. & Georgopoulos, C. (1993). The essential *Escherichia coli msbA* gene, a multicopy suppressor of null mutations in the *htrB* gene, is related to the universally conserved family of ATP-dependent translocators. *Mol Microbiol* **7**, 69-79.

Kawasaki, K., Ernst, R. K. & Miller, S. I. (2004). 3-O-deacylation of lipid A by PagL, a PhoP/PhoQ-regulated deacylase of *Salmonella typhimurium*, modulates signaling through Toll-like receptor 4. *J Biol Chem* **279**, 20044-20048.

Kazachkov, M., Lager, J., LiPuma, J. & Barker, P. M. (2001). Survival following *Burkholderia cepacia* sepsis in a patient with cystic fibrosis treated with corticosteroids. *Pediatr Pulmonol* **32**, 338-340.

Keig, P. M., Ingham, E., Vandamme, P. A. & Kerr, K. G. (2002). Differential invasion of respiratory epithelial cells by members of the *Burkholderia cepacia* complex. *Clin Microbiol Infect* **8**, 47-49.

Kelly, T. M., Stachula, S. A., Raetz, C. R. & Anderson, M. S. (1993). The firA gene of *Escherichia coli* encodes UDP-3-O-(R-3-hydroxymyristoyl)-glucosamine N-acyltransferase. The third step of endotoxin biosynthesis. *J Biol Chem* **268**, 19866-19874.

Kenna, D. T., Barcus, V. A., Langley, R. J., Vandamme, P. & Govan, J. R. (2003). Lack of correlation between O-serotype, bacteriophage susceptibility and genomovar status in the *Burkholderia cepacia* complex. *FEMS Immunol Med Microbiol* **35**, 87-92.

Kooi, C., Corbett, C. R. & Sokol, P. A. (2005). Functional analysis of the *Burkholderia cenocepacia* ZmpA metalloprotease. *J Bacteriol* **187**, 4421-4429.

Kropinski, A. M., Berry, D. & Greenberg, E. P. (1986). The basis of silver staining of bacterial lipopolysaccharides in polyacrylamide gels *Current Microbiology* **13**, 29-31.

Kumar, A. S., Mody, K. & Jha, B. (2007). Bacterial exopolysaccharides--a perception. *J Basic Microbiol* **47**, 103-117.

Lamothe, J., Thyssen, S. & Valvano, M. A. (2004). *Burkholderia cepacia* complex isolates survive intracellularly without replication within acidic vacuoles of Acanthamoeba polyphaga. *Cell Microbiol* **6**, 1127-1138.

Lamothe, J., Huynh, K. K., Grinstein, S. & Valvano, M. A. (2007). Intracellular survival of *Burkholderia cenocepacia* in macrophages is associated with a delay in the maturation of bacteria-containing vacuoles. *Cell Microbiol* **9**, 40-53.

Lee, H., Hsu, F. F., Turk, J. & Groisman, E. A. (2004). The PmrA-regulated *pmrC* gene mediates phosphoethanolamine modification of lipid A and polymyxin resistance in *Salmonella enterica. J Bacteriol* **186**, 4124-4133.

Lefebre, M. & Valvano, M. (2001). In vitro resistance of *Burkholderia cepacia* complex isolates to reactive oxygen species in relation to catalase and superoxide dismutase production. *Microbiology* **147**, 97-109.

Leone, S., Molinaro, A., Gerber, I. B., Dubery, I. A., Lanzetta, R. & Parrilli, M. (2006). The O-chain structure from the LPS of the endophytic bacterium *Burkholderia cepacia* strain ASP B 2D. *Carbohydr Res* **341**, 2954-2958.

Lewenza, S., Conway, B., Greenberg, E. P. & Sokol, P. A. (1999). Quorum sensing in *Burkholderia cepacia*: identification of the LuxRI homologs CepRI. *J Bacteriol* **181**, 748-756.

Lewenza, S. & Sokol, P. A. (2001). Regulation of ornibactin biosynthesis and N-acyl-L-homoserine lactone production by CepR in *Burkholderia cepacia*. *J Bacteriol* **183**, 2212-2218.

Loutet, S. A., Flannagan, R. S., Kooi, C., Sokol, P. A. & Valvano, M. A. (2006). A complete lipopolysaccharide inner core oligosaccharide is required for resistance of *Burkholderia cenocepacia* to antimicrobial peptides and bacterial survival in vivo. *J Bacteriol* **188**, 2073-2080.

Loutet, S. A., Bartholdson, S. J., Govan, J. R., Campopiano, D. J. & Valvano, M. A. (2009). Contributions of two UDP-glucose dehydrogenases to viability and polymyxin B resistance of Burkholderia cenocepacia. *Microbiology* **155**, 2029-2039.

Ma, B., Reynolds, C. M. & Raetz, C. R. (2008). Periplasmic orientation of nascent lipid A in the inner membrane of an *Escherichia coli* LptA mutant. *Proc Natl Acad Sci U S A* **105**, 13823-13828.

Mah, T. F. & O'Toole, G. A. (2001). Mechanisms of biofilm resistance to antimicrobial agents. *Trends Microbiol* **9**, 34-39.

Mahenthiralingam, E., Simpson, D. A. & Speert, D. P. (1997). Identification and characterization of a novel DNA marker associated with epidemic *Burkholderia cepacia* strains recovered from patients with cystic fibrosis. *J Clin Microbiol* **35**, 808-816.

Mahenthiralingam, E., Bischof, J., Byrne, S. K., Radomski, C., Davies, J. E., Av-Gay, Y. & Vandamme, P. (2000a). DNA-Based diagnostic approaches for identification of *Burkholderia cepacia* complex, *Burkholderia vietnamiensis, Burkholderia multivorans, Burkholderia stabilis,* and *Burkholderia cepacia* genomovars I and III. *J Clin Microbiol* **38**, 3165-3173.

Mahenthiralingam, E., Coenye, T., Chung, J. W., Speert, D. P., Govan, J. R., Taylor, P. & Vandamme, P. (2000b). Diagnostically and experimentally useful panel of strains from the *Burkholderia cepacia* complex. *J Clin Microbiol* **38**, 910-913.

Mahenthiralingam, E., Urban, T. A. & Goldberg, J. B. (2005). The multifarious, multireplicon *Burkholderia cepacia* complex. *Nat Rev Microbiol* **3**, 144-156.

Mahenthiralingam, E., Baldwin, A. & Dowson, C. G. (2008). *Burkholderia cepacia* complex bacteria: opportunistic pathogens with important natural biology. *J Appl Microbiol* **104**, 1539-1551.

Malott, R. J. & Sokol, P. A. (2007). Expression of the bviIR and cepIR quorum-sensing systems of *Burkholderia vietnamiensis*. *J Bacteriol* **189**, 3006-3016.

Masoud, H., Ho, M., Schollaardt, T. & Perry, M. B. (1997). Characterization of the capsular polysaccharide of *Burkholderia (Pseudomonas) pseudomallei* 304b. *J Bacteriol* **179**, 5663-5669.

McPhee, J. B. & Hancock, R. E. (2005). Function and therapeutic potential of host defence peptides. *J Pept Sci* **11**, 677-687.

Meredith, T. C., Aggarwal, P., Mamat, U., Lindner, B. & Woodard, R. W. (2006). Redefining the requisite lipopolysaccharide structure in *Escherichia coli*. *ACS Chem Biol* **1**, 33-42.

Miroux, B. & Walker, J. E. (1996). Over-production of proteins in *Escherichia coli*: mutant hosts that allow synthesis of some membrane proteins and globular proteins at high levels. *J Mol Biol* **260**, 289-298.

Mohapatra, N. P., Soni, S., Bell, B. L., Warren, R., Ernst, R. K., Muszynski, A., Carlson, R. W. & Gunn, J. S. (2007). Identification of an orphan response regulator required for the virulence of Francisella spp. and transcription of pathogenicity island genes. *Infect Immun* **75**, 3305-3314.

Mohr, C. D., Tomich, M. & Herfst, C. A. (2001). Cellular aspects of *Burkholderia cepacia* infection. *Microbes Infect* **3**, 425-435.

Montminy, S. W., Khan, N., McGrath, S. & other authors (2006). Virulence factors of *Yersinia pestis* are overcome by a strong lipopolysaccharide response. *Nat Immunol* **7**, 1066-1073.

Moreira, L. M., Videira, P. A., Sousa, S. A., Leitao, J. H., Cunha, M. V. & Sa-Correia, I. (2003). Identification and physical organization of the gene cluster involved in the biosynthesis of *Burkholderia cepacia* complex exopolysaccharide. *Biochem Biophys Res Commun* **312**, 323-333.

Moura, J. A., Cristina de Assis, M., Ventura, G. C., Saliba, A. M., Gonzaga, L., Jr., Si-Tahar, M., Marques Ede, A. & Plotkowski, M. C. (2008). Differential interaction of bacterial species from the *Burkholderia cepacia* complex with human airway epithelial cells. *Microbes Infect* **10**, 52-59.

Murray, S., Charbeneau, J., Marshall, B. C. & LiPuma, J. J. (2008). Impact of *Burkholderia* infection on lung transplantation in cystic fibrosis. *Am J Respir Crit Care Med* **178**, 363-371.

Noland, B. W., Newman, J. M., Hendle, J. & other authors (2002). Structural studies of Salmonella typhimurium ArnB (PmrH) aminotransferase: a 4-amino-4-deoxy-L-arabinose lipopolysaccharide-modifying enzyme. *Structure* **10**, 1569-1580.

O'Sullivan, L. A. & Mahenthiralingam, E. (2005). Biotechnological potential within the genus *Burkholderia*. *Lett Appl Microbiol* **41**, 8-11.

Odegaard, T. J., Kaltashov, I. A., Cotter, R. J., Steeghs, L., van der Ley, P., Khan, S., Maskell, D. J. & Raetz, C. R. (1997). Shortened hydroxyacyl chains on lipid A of *Escherichia coli* cells expressing a foreign UDP-N-acetylglucosamine O-acyltransferase. *J Biol Chem* **272**, 19688-19696.

Ortega, X., Hunt, T. A., Loutet, S., Vinion-Dubiel, A. D., Datta, A., Choudhury, B., Goldberg, J. B., Carlson, R. & Valvano, M. A. (2005). Reconstitution of O-specific lipopolysaccharide expression in *Burkholderia cenocepacia* strain J2315, which is associated with transmissible infections in patients with cystic fibrosis. *J Bacteriol* **187**, 1324-1333.

Ortega, X. P., Cardona, S. T., Brown, A. R., Loutet, S. A., Flannagan, R. S., Campopiano, D. J., Govan, J. R. & Valvano, M. A. (2007). A putative gene cluster for aminoarabinose biosynthesis is essential for *Burkholderia cenocepacia* viability. *J Bacteriol* **189**, 3639-3644.

Palmer, K. L., Aye, L. M. & Whiteley, M. (2007). Nutritional cues control *Pseudomonas aeruginosa* multicellular behavior in cystic fibrosis sputum. *J Bacteriol* **189**, 8079-8087.

Parsons, Y. N., Banasko, R., Detsika, M. G., Duangsonk, K., Rainbow, L., Hart, C. A. & Winstanley, C. (2003). Suppression-subtractive hybridisation reveals variations in gene distribution amongst the *Burkholderia cepacia* complex, including the presence in some strains of a genomic island containing putative polysaccharide production genes. *Arch Microbiol* **179**, 214-223.

Partida-Martinez, L. P. & Hertweck, C. (2005). Pathogenic fungus harbours endosymbiotic bacteria for toxin production. *Nature* **437**, 884-888.

Paulus, H., Gray, E. (1964). The biosynthesis of polymyxin B by growing cultures of *Bacillus polymyxa*. *J Biol Chem* **239**, 865-871.

Peeters, E., Nelis, H. J. & Coenye, T. (2008). Evaluation of the efficacy of disinfection procedures against *Burkholderia cenocepacia* biofilms. *J Hosp Infect* **70**, 361-368.

Pfeiffer, R. (1892). Untersuchungen über das Choleragift. *Z Hyg* **11**, 393–411.

Pier, G. B., Grout, M. & Zaidi, T. S. (1997). Cystic fibrosis transmembrane conductance regulator is an epithelial cell receptor for clearance of *Pseudomonas aeruginosa* from the lung. *Proc Natl Acad Sci U S A* **94**, 12088-12093.

Price, N. P., Jeyaretnam, B., Carlson, R. W., Kadrmas, J. L., Raetz, C. R. & Brozek, K. A. (1995). Lipid A biosynthesis in *Rhizobium leguminosarum*: role of a 2-

keto-3-deoxyoctulosonate-activated 4' phosphatase. *Proc Natl Acad Sci U S A* **92**, 7352-7356.

Pugashetti, B. K., Metzger, H. M., Jr., Vadas, L. & Feingold, D. S. (1982). Phenotypic differences among clinically isolated mucoid *Pseudomonas aeruginosa* strains. *J Clin Microbiol* **16**, 686-691.

Que-Gewirth, N. L., Ribeiro, A. A., Kalb, S. R., Cotter, R. J., Bulach, D. M., Adler, B., Girons, I. S., Werts, C. & Raetz, C. R. (2004). A methylated phosphate group and four amide-linked acyl chains in leptospira interrogans lipid A. The membrane anchor of an unusual lipopolysaccharide that activates TLR2. *J Biol Chem* **279**, 25420-25429.

Radika, K. & Raetz, C. R. (1988). Purification and properties of lipid A disaccharide synthase of *Escherichia coli*. *J Biol Chem* **263**, 14859-14867.

Raetz, C. R. & Whitfield, C. (2002). Lipopolysaccharide endotoxins. *Annu Rev Biochem* **71**, 635-700.

Raetz, C. R., Garrett, T. A., Reynolds, C. M. & other authors (2006). Kdo2-Lipid A of *Escherichia coli*, a defined endotoxin that activates macrophages via TLR-4. *J Lipid Res* **47**, 1097-1111.

Raetz, C. R., Reynolds, C. M., Trent, M. S. & Bishop, R. E. (2007). Lipid A modification systems in gram-negative bacteria. *Annu Rev Biochem* **76**, 295-329.

Ratjen, F. & Doring, G. (2003). Cystic fibrosis. *Lancet* **361**, 681-689.

Reckseidler-Zenteno, S. L., DeVinney, R. & Woods, D. E. (2005). The capsular polysaccharide of *Burkholderia pseudomallei* contributes to survival in serum by reducing complement factor C3b deposition. *Infect Immun* **73**, 1106-1115.

Reckseidler, S. L., DeShazer, D., Sokol, P. A. & Woods, D. E. (2001). Detection of bacterial virulence genes by subtractive hybridization: identification of capsular polysaccharide of *Burkholderia pseudomallei* as a major virulence determinant. *Infect Immun* **69**, 34-44.

Reddi, K., Phagoo, S. B., Anderson, K. D. & Warburton, D. (2003). *Burkholderia cepacia*-induced IL-8 gene expression in an alveolar epithelial cell line: signaling through CD14 and mitogen-activated protein kinase. *Pediatr Res* **54**, 297-305.

Reid, D. W. & Bell, S. C. (2009). Sugar sweet and deadly? *Microbiology* **155**, 665-666; discussion 666.

Reik, R., Spilker, T. & Lipuma, J. J. (2005). Distribution of *Burkholderia cepacia* complex species among isolates recovered from persons with or without cystic fibrosis. *J Clin Microbiol* **43**, 2926-2928.

Reynolds, C. M., Kalb, S. R., Cotter, R. J. & Raetz, C. R. (2005). A phosphoethanolamine transferase specific for the outer 3-deoxy-D-manno-octulosonic

acid residue of *Escherichia coli* lipopolysaccharide. Identification of the *eptB* gene and Ca2+ hypersensitivity of an *eptB* deletion mutant. *J Biol Chem* **280**, 21202-21211.

Reynolds, C. M., Ribeiro, A. A., McGrath, S. C., Cotter, R. J., Raetz, C. R. & Trent, M. S. (2006). An outer membrane enzyme encoded by *Salmonella typhimurium lpxR* that removes the 3'-acyloxyacyl moiety of lipid A. *J Biol Chem* **281**, 21974-21987.

Richau, J. A., Leitao, J. H., Correia, M., Lito, L., Salgado, M. J., Barreto, C., Cescutti, P. & Sa-Correia, I. (2000). Molecular typing and exopolysaccharide biosynthesis of *Burkholderia cepacia* isolates from a Portuguese cystic fibrosis center. *J Clin Microbiol* **38**, 1651-1655.

Riedel, K., Hentzer, M., Geisenberger, O. & other authors (2001). N-acylhomoserine-lactone-mediated communication between *Pseudomonas aeruginosa* and Burkholderia cepacia in mixed biofilms. *Microbiology* **147**, 3249-3262.

Riordan, J. R. (2008). CFTR function and prospects for therapy. *Annu Rev Biochem* **77**, 701-726.

Robinson, M., Daviskas, E., Eberl, S., Baker, J., Chan, H. K., Anderson, S. D. & Bye, P. T. (1999). The effect of inhaled mannitol on bronchial mucus clearance in cystic fibrosis patients: a pilot study. *Eur Respir J* **14**, 678-685.

Rosenfeld, Y., Papo, N. & Shai, Y. (2006). Endotoxin (lipopolysaccharide) neutralization by innate immunity host-defense peptides. Peptide properties and plausible modes of action. *J Biol Chem* **281**, 1636-1643.

Sage, A., Linker, A., Evans, L. & Lessie, T. (1990). Hexose phosphate metabolism and exopolysaccharide formation in *Pseudomonas cepacia*. *Curr Microbiol* **20**, 191-198.

Sajjan, U. S., Sun, L., Goldstein, R. & Forstner, J. F. (1995). Cable (cbl) type II pili of cystic fibrosis-associated *Burkholderia (Pseudomonas) cepacia*: nucleotide sequence of the *cblA* major subunit pilin gene and novel morphology of the assembled appendage fibers. *J Bacteriol* **177**, 1030-1038.

Sahly, H., Schubert, S., Harder, J., Rautenberg, P., Ullmann, U., Schroder, J. & Podschun, R. (2003). *Burkholderia* is highly resistant to human Beta-defensin 3. *Antimicrob Agents Chemother* **47**, 1739-1741.

Schromm, A. B., Brandenburg, K., Loppnow, H., Moran, A. P., Koch, M. H., Rietschel, E. T. & Seydel, U. (2000). Biological activities of lipopolysaccharides are determined by the shape of their lipid A portion. *Eur J Biochem* **267**, 2008-2013.

Schwab, U., Leigh, M., Ribeiro, C., Yankaskas, J., Burns, K., Gilligan, P., Sokol, P. & Boucher, R. (2002). Patterns of epithelial cell invasion by different species of the *Burkholderia cepacia* complex in well-differentiated human airway epithelia. *Infect Immun* **70**, 4547-4555.

Shaffer, S. A., Harvey, M. D., Goodlett, D. R. & Ernst, R. K. (2007). Structural heterogeneity and environmentally regulated remodeling of *Francisella tularensis*

subspecies novicida lipid A characterized by tandem mass spectrometry. *J Am Soc Mass Spectrom* **18**, 1080-1092.

Shaw, D., Poxton, I. R. & Govan, J. R. (1995). Biological activity of *Burkholderia (Pseudomonas) cepacia* lipopolysaccharide. *FEMS Immunol Med Microbiol* **11**, 99-106.

Shimomura, H., Matsuura, M., Saito, S., Hirai, Y., Isshiki, Y. & Kawahara, K. (2001). Lipopolysaccharide of *Burkholderia cepacia* and its unique character to stimulate murine macrophages with relative lack of interleukin-1beta-inducing ability. *Infect Immun* **69**, 3663-3669.

Shimomura, H., Matsuura, M., Saito, S., Hirai, Y., Isshiki, Y. & Kawahara, K. (2003). Unusual interaction of a lipopolysaccharide isolated from *Burkholderia cepacia* with polymyxin B. *Infect Immun* **71**, 5225-5230.

Silipo, A., Molinaro, A., Cescutti, P., Bedini, E., Rizzo, R., Parrilli, M. & Lanzetta, R. (2005). Complete structural characterization of the lipid A fraction of a clinical strain of *B. cepacia* genomovar I lipopolysaccharide. *Glycobiology* **15**, 561-570.

Silipo, A., Molinaro, A., Ierano, T. & other authors (2007). The complete structure and pro-inflammatory activity of the lipooligosaccharide of the highly epidemic and virulent gram-negative bacterium *Burkholderia cenocepacia* ET-12 (strain J2315). *Chemistry* **13**, 3501-3511.

Soncini, F. C. a. G., E.A. (1996). Two-component regulatory systems can interact to process multiple environmental signals. *J Bacteriol* **178**, 6796-6801.

Sousa, S. A., Ulrich, M., Bragonzi, A. & other authors (2007). Virulence of *Burkholderia cepacia* complex strains in gp91phox-/- mice. *Cell Microbiol* **9**, 2817-2825.

Sousa, S. A., Moreira, L. M. & Leitao, J. H. (2008). Functional analysis of the *Burkholderia cenocepacia* J2315 BceAJ protein with phosphomannose isomerase and GDP-D-mannose pyrophosphorylase activities. *Appl Microbiol Biotechnol* **80**, 1015-1022.

Sousa, S. A., Moreira L.M., Wopperer J., Eberl L., Sá-Correira I. & Leitão J.H. (2007). The *Burkholderia cepacia bceA* gene encodes a protein with phosphomannose isomerase and GDP-D-mannose pyrophosphorylase activities. *Biochem Biophys Res Commun* **353**, 200-206.

Sperandeo, P., Cescutti, R., Villa, R., Di Benedetto, C., Candia, D., Deho, G. & Polissi, A. (2007). Characterization of *lptA* and *lptB*, two essential genes implicated in lipopolysaccharide transport to the outer membrane of *Escherichia coli*. *J Bacteriol* **189**, 244-253.

Stead, C. M., Beasley, A., Cotter, R. J. & Trent, M. S. (2008). Deciphering the Unusual Acylation Pattern of *Helicobacter pylori* Lipid A. *J Bacteriol* **190**, 7012-7021.

Taccetti, G., Campana, S., Neri, A. S., Boni, V. & Festini, F. (2008). Antibiotic therapy against *Pseudomonas aeruginosa* in cystic fibrosis. *J Chemother* **20**, 166-169.

Tamayo, R., Choudhury, B., Septer, A., Merighi, M., Carlson, R. & Gunn, J. S. (2005). Identification of cptA, a PmrA-regulated locus required for phosphoethanolamine modification of the *Salmonella enterica* serovar typhimurium lipopolysaccharide core. *J Bacteriol* **187**, 3391-3399.

Tanamoto, K., Zahringer, U., McKenzie, G. R., Galanos, C., Rietschel, E. T., Luderitz, O., Kusumoto, S. & Shiba, T. (1984). Biological activities of synthetic lipid A analogs: pyrogenicity, lethal toxicity, anticomplement activity, and induction of gelation of *Limulus amoebocyte* lysate. *Infect Immun* **44**, 421-426.

Teichgraber, V., Ulrich, M., Endlich, N. & other authors (2008). Ceramide accumulation mediates inflammation, cell death and infection susceptibility in cystic fibrosis. *Nat Med* **14**, 382-391.

Tokuda, H. & Matsuyama, S. (2004). Sorting of lipoproteins to the outer membrane in *E. coli. Biochim Biophys Acta* **1694**, IN1-9.

Tomich, M., Herfst, C. A., Golden, J. W. & Mohr, C. D. (2002). Role of flagella in host cell invasion by *Burkholderia cepacia. Infect Immun* **70**, 1799-1806.

Tran, A. X., Karbarz, M. J., Wang, X., Raetz, C. R., McGrath, S. C., Cotter, R. J. & Trent, M. S. (2004). Periplasmic cleavage and modification of the 1-phosphate group of *Helicobacter pylori* lipid A. *J Biol Chem* **279**, 55780-55791.

Tran, A. X., Whittimore, J. D., Wyrick, P. B., McGrath, S. C., Cotter, R. J. & Trent, M. S. (2006). The lipid A 1-phosphatase of *Helicobacter pylori* is required for resistance to the antimicrobial peptide polymyxin. *J Bacteriol* **188**, 4531-4541.

Tran, A. X., Trent, M. S. & Whitfield, C. (2008). The LptA protein of *Escherichia coli* is a periplasmic lipid A-binding protein involved in the lipopolysaccharide export pathway. *J Biol Chem* **283**, 20342-20349.

Trent, M. S., Ribeiro, A. A., Doerrler, W. T., Lin, S., Cotter, R. J. & Raetz, C. R. (2001a). Accumulation of a polyisoprene-linked amino sugar in polymyxin-resistant *Salmonella typhimurium* and *Escherichia coli*: structural characterization and transfer to lipid A in the periplasm. *J Biol Chem* **276**, 43132-43144.

Trent, M. S., Ribeiro, A. A., Lin, S., Cotter, R. J. & Raetz, C. R. (2001b). An inner membrane enzyme in *Salmonella* and *Escherichia coli* that transfers 4-amino-4-deoxy-L-arabinose to lipid A: induction on polymyxin-resistant mutants and role of a novel lipid-linked donor. *J Biol Chem* **276**, 43122-43131.

Trent, M. S., Raetz, C. H. R. (2002). Cloning of EptA, the lipid A phophoethanolamine transferase associated with polymyxin resistance. *J Endotoxin Res* **8**, 158.

Tsai, C. M. & Frasch, C. E. (1982). A sensitive silver stain for detecting lipopolysaccharides in polyacrylamide gels. *Anal Biochem* **119**, 115-119.

Tummler, B. & Kiewitz, C. (1999). Cystic fibrosis: an inherited susceptibility to bacterial respiratory infections. *Mol Med Today* **5**, 351-358.

Tzeng, Y. L., Ambrose, K. D., Zughaier, S., Zhou, X., Miller, Y. K., Shafer, W. M. & Stephens, D. S. (2005). Cationic antimicrobial peptide resistance in *Neisseria meningitidis*. *J Bacteriol* **187**, 5387-5396.

Urban, T. A., Griffith, A., Torok, A. M., Smolkin, M. E., Burns, J. L. & Goldberg, J. B. (2004). Contribution of *Burkholderia cenocepacia* flagella to infectivity and inflammation. *Infect Immun* **72**, 5126-5134.

Valvano, M. A., Keith, K. E. & Cardona, S. T. (2005). Survival and persistence of opportunistic *Burkholderia species* in host cells. *Curr Opin Microbiol* **8**, 99-105.

Vandamme, P., Holmes, B., Vancanneyt, M. & other authors (1997). Occurrence of multiple genomovars of *Burkholderia cepacia* in cystic fibrosis patients and proposal of *Burkholderia multivorans* sp. nov. *Int J Syst Bacteriol* **47**, 1188-1200.

Vanlaere, E., Lipuma, J. J., Baldwin, A., Henry, D., De Brandt, E., Mahenthiralingam, E., Speert, D., Dowson, C. & Vandamme, P. (2008). *Burkholderia latens* sp. nov., *Burkholderia diffusa* sp. nov., *Burkholderia arboris* sp. nov., *Burkholderia seminalis* sp. nov. and *Burkholderia metallica* sp. nov., novel species within the *Burkholderia cepacia* complex. *Int J Syst Evol Microbiol* **58**, 1580-1590.

Venturi, V., Friscina, A., Bertani, I., Devescovi, G. & Aguilar, C. (2004). Quorum sensing in the *Burkholderia cepacia* complex. *Res Microbiol* **155**, 238-244.

Videira, P. A., Garcia, A. P. & Sa-Correia, I. (2005). Functional and topological analysis of the *Burkholderia cenocepacia* priming glucosyltransferase BceB, involved in the biosynthesis of the cepacian exopolysaccharide. *J Bacteriol* **187**, 5013-5018.

Vinogradov, E., Perry, M. B. & Conlan, J. W. (2002). Structural analysis of *Francisella tularensis* lipopolysaccharide. *Eur J Biochem* **269**, 6112-6118.

Vinogradov, E. V., Muller-Loennies, S., Petersen, B. O., Meshkov, S., Thomas-Oates, J. E., Holst, O. & Brade, H. (1997). Structural investigation of the lipopolysaccharide from *Acinetobacter haemolyticus* strain NCTC 10305 (ATCC 17906, DNA group 4). *Eur J Biochem* **247**, 82-90.

Wagner, S., Baars, L., Ytterberg, A. J., Klussmeier, A., Wagner, C. S., Nord, O., Nygren, P. A., van Wijk, K. J. & de Gier, J. W. (2007). Consequences of membrane protein overexpression in Escherichia coli. *Mol Cell Proteomics* **6**, 1527-1550.

Weidmann, A., Webb, A. K., Dodd, M. E. & Jones, A. M. (2008). Successful treatment of cepacia syndrome with combination nebulised and intravenous antibiotic therapy. *J Cyst Fibros* **7**, 409-411.

Werts, C., Tapping, R. I., Mathison, J. C. & other authors (2001). Leptospiral lipopolysaccharide activates cells through a TLR2-dependent mechanism. *Nat Immunol* **2**, 346-352.

Whitchurch, C. B., Alm, R. A. & Mattick, J. S. (1996). The alginate regulator AlgR and an associated sensor FimS are required for twitching motility in *Pseudomonas aeruginosa*. *Proc Natl Acad Sci U S A* **93**, 9839-9843.

White, K. A., Kaltashov, I. A., Cotter, R. J. & Raetz, C. R. (1997). A mono-functional 3-deoxy-D-manno-octulosonic acid (Kdo) transferase and a Kdo kinase in extracts of *Haemophilus influenzae*. *J Biol Chem* **272**, 16555-16563.

Whiteford, M. L., Wilkinson, J. D., McColl, J. H., Conlon, F. M., Michie, J. R., Evans, T. J. & Paton, J. Y. (1995). Outcome of *Burkholderia (Pseudomonas) cepacia* colonisation in children with cystic fibrosis following a hospital outbreak. *Thorax* **50**, 1194-1198.

Wiersinga, W. J., Wieland, C. W., Dessing, M. C. & other authors (2007). Toll-like receptor 2 impairs host defense in gram-negative sepsis caused by *Burkholderia pseudomallei* (Melioidosis). *PLoS Med* **4**, e248.

Wills, P. J. (2007). Inhaled mannitol in cystic fibrosis. *Expert Opin Investig Drugs* **16**, 1121-1126.

Wosten, M. M., Kox, L. F., Chamnongpol, S., Soncini, F. C. & Groisman, E. A. (2000). A signal transduction system that responds to extracellular iron. *Cell* **103**, 113-125.

www.broad.mit.edu

www.cftrust.org.uk.

www.genet.sickkids.on.ca/cftr/.

www.jgi.doe.gov

www.ncbi.nlm.nih.gov/sutils/genom_table.cgi

www.ornl.gov/sci/techresources/Human_Genome/posters/chromosome/cftr.shtlm.

www.pharmaxis.com.au.

www.sanger.ac.uk/

Wyckoff, T. J., Lin, S., Cotter, R. J., Dotson, G. D. & Raetz, C. R. (1998). Hydrocarbon rulers in UDP-N-acetylglucosamine acyltransferases. *J Biol Chem* **273**, 32369-32372.

Yabuuchi, E., Kosako, Y., Oyaizu, H., Yano, I., Hotta, H., Hashimoto, Y., Ezaki, T. & Arakawa, M. (1992). Proposal of *Burkholderia* gen. nov. and transfer of seven

species of the genus *Pseudomonas* homology group II to the new genus, with the type species *Burkholderia cepacia* (Palleroni and Holmes 1981) comb. nov. *Microbiol Immunol* **36**, 1251-1275.

Yan, A., Guan, Z. & Raetz, C. R. (2007). An undecaprenyl phosphate-aminoarabinose flippase required for polymyxin resistance in *Escherichia coli*. *J Biol Chem* **282**, 36077-36089.

Yethon, J. A., Heinrichs, D. E., Monteiro, M. A., Perry, M. B. & Whitfield, C. (1998). Involvement of waaY, waaQ, and waaP in the modification of *Escherichia coli* lipopolysaccharide and their role in the formation of a stable outer membrane. *J Biol Chem* **273**, 26310-26316.

Young, K., Silver, L. L., Bramhill, D., Cameron, P., Eveland, S. S., Raetz, C. R., Hyland, S. A. & Anderson, M. S. (1995). The envA permeability/cell division gene of *Escherichia coli* encodes the second enzyme of lipid A biosynthesis. UDP-3-O-(R-3-hydroxymyristoyl)-N-acetylglucosamine deacetylase. *J Biol Chem* **270**, 30384-30391.

Zasloff, M. (2002). Antimicrobial peptides of multicellular organisms. *Nature* **415**, 389-395.

Zdorovenko, E. L., Vinogradov, E., Wydra, K., Lindner, B. & Knirel, Y. A. (2008). Structure of the oligosaccharide chain of the SR-type lipopolysaccharide of *Ralstonia solanacearum* Toudk-2. *Biomacromolecules* **9**, 2215-2220.

Zhou, Z., White, K. A., Polissi, A., Georgopoulos, C. & Raetz, C. R. (1998). Function of *Escherichia coli* MsbA, an essential ABC family transporter, in lipid A and phospholipid biosynthesis. *J Biol Chem* **273**, 12466-12475.

Zlosnik, J. E., Hird, T. J., Fraenkel, M. C., Moreira, L. M., Henry, D. A. & Speert, D. P. (2008). Differential mucoid exopolysaccharide production by members of the *Burkholderia cepacia* complex. *J Clin Microbiol* **46**, 1470-1473.

Zughaier, S. M., Ryley, H. C. & Jackson, S. K. (1999). Lipopolysaccharide (LPS) from *Burkholderia cepacia* is more active than LPS from Pseudomonas aeruginosa and Stenotrophomonas maltophilia in stimulating tumor necrosis factor alpha from human monocytes. *Infect Immun* **67**, 1505-1507.

Appendix I: ArnT plasmid maps and sequences

B. cenocepacia J2315 ArnT expressing plasmid maps:

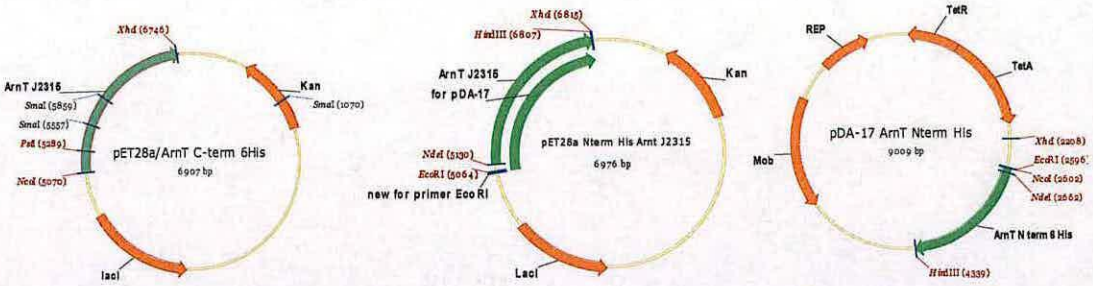

ArnT$_{BCAL1929}$ (N-term) (1692 bp, 1748 bp including 6HIS, 64845.64 Da)

```
   1    MGSSHHHHHH SSGLVPRGSH MNDTPSRLPL NRITLVLLLV ALAIVWFAPL
  51    GLRHLIPSDE GRYAEMAREM FVTGDWITPR YNGYKYFEKP PLQTWLNALT
 101    FAWFGIGEWQ ARLYTAVASF AGVLLVGYTG ARLFNPLSGF LAAVVLASSP
 151    YWNLMGHFNA LDMGLAFWMA LSLCSLLLAQ RPGLRPAAVR GWMWACWAAM
 201    AFAVLSKGLV GLILPGAVLV LYTLVARDWA LWKRLYLVSG LVIFFAIVTP
 251    WFVLVQQRNP EFFNFFFIVQ QFRRYLTPEQ NRPGPLYYFV PVLLVGFLPW
 301    LSVAWQSIRH AVRMPRQPNG FAPMLVLLIW SAFIFLFFSA SHSKLISYVL
 351    PVAPALALII GAYLPLMTAD RFRRHLLGYL VFFVAAAFGI VFLAYQGDAR
 401    TPNALYRAFQ MWLYAGLAVA AALTLVAAWL NRRAGVAAAL ATFGAAWLVF
 451    GTIGGTGHDE FGRYSSGALL APAVRAELAK LPPDTPFYSI EMLDHTFPFY
 501    MGHTTIMVQR QDELAFGISV EPNKWIPTIG EWITRWKQET HALAIMPPGQ
 551    YDALVKEGVP MRVIARDNRR VIVEKPQS
```

ArnT$_{BCAL1929}$ (C-term) (1680 bp, 1698 bp incl. His tag, 63748.48 Da)

```
   1    MDDTPSRLPL NRITLVLLLV ALAIVWFAPL GLRHLIPSDE GRYAEMAREM
  51    FVTGDWITPR YNGYKYFEKP PLQTWLNALT FAWFGIGEWQ ARLYTAVASF
 101    AGVLLVGYTG ARLFNPLSGF LAAVVLASSP YWNLMGHFNA LDMGLAFWMA
 151    LSLCSLLLAQ RPGLRPAAVR GWMWACWAAM AFAVLSKGLV GLILPGAVLV
 201    LYTLVARDWA LWKRLYLVSG LVIFFAIVTP WFVLVQQRNP EFFNFFFIVQ
 251    QFRRYLTPEQ NRPGPLYYFV PVLLVGFLPW LSVAWQSIRH AVRMPRQPNG
 301    FAPMLVLLIW SAFIFLFFSA SHSKLISYVL PVAPALALII GAYLPLMTAD
 351    RFRRHLLGYL VFFVAAAFGI VFLAYQGDAR TPNALYRAFQ MWLYAGLAVA
 401    AALTLVAAWL NRRAGVAAAL ATFGAAWLVF GTIGGTGHDE FGRYSSGALL
 451    APAVRAELAK LPPDTPFYSI EMLDHTFPFY MGHTTIMVQR QDELAFGISV
 501    EPNKWIPTIG EWITRWKQET HALAIMPPGQ YDALVKEGVP MRVIARDNRR
 551    VIVEKPQSLE HHHHHH
```

Amino acid sequence alignment of *B. cenocepacia* BCAL1929 and *P. aeruginosa* PA01 ArnT shows 24% identity

```
                    1                                                  50
ArnT BCAL1929     (1) MNDTPSRLPLNRITLVLLLVALATVWFAPLGLRHLIPSDEGRYAEMAREM
    ArnT PAO1     (1) --------MSRRQTCSLLLIAFGIFYLVPLSNHGLWIPDETRYAQTSQAM
    Consensus     (1)          R T  LLLIA AI W  PL    L   DE RYA IA  M
                    51                                                 100
ArnT BCAL1929    (51) FVTGDWITPRYNGYKYFEKPPLQTWLNALTFAWFGIGEWQARIYTAVASF
    ArnT PAO1    (43) LLGGDWVSPHFLGLRYFEKPVAGYWMIALGQAVFGENLFGVRIASVVAIA
    Consensus    (51)  L GDWISP F G KYFEKP    WL AL  A FG   F  RI S VAS
                   101                                                 150
ArnT BCAL1929   (101) AGVLLVGYTGARLFN-PLSGFLAAVVLASSPYWNLMGHFNALDMGLAFWM
    ArnT PAO1    (93) LSVLLAYLLARRLWRDPRISLACALLYASFGLIAGQSGYANLDPQFTFWV
    Consensus   (101)   VLL    A RLF  P S    ALL AS         F  LD    FWM
                   151                                                 200
ArnT BCAL1929   (150) ALSLCSLLLAQRPGLRPAAVRGWMWACWAAMAFAVLSKGLVCLILPGAVL
    ArnT PAO1    (143) NLSLVALWHALDAGSRRARILGWTLLG-LACGMCFLTKGFLAWLLPVLVA
    Consensus   (151)  LSL AL  A   G R A L GW      A A A LSKG LA ILP  V
                   201                                                 250
ArnT BCAL1929   (200) VLYTLVARDWALWKRLYLVSGLVIFFAIVTPWFVLVQQRNPEFFNFFFIV
    ArnT PAO1    (192) LPYMLWQRRWRELLG-YGALAVLAALLVCLPWALAVHAREADYWRFFFWH
    Consensus   (201) L Y L  R W      Y   ALL    I  PW L V  R  DFF FFF
                   251                                                 300
ArnT BCAL1929   (250) QQFRRYLTPEQNRPGPLYYFVPVLLVGFLPWLSVAWQSIRHAVRMPRQPN
    ArnT PAO1    (241) EHIRRFAGELAQHSRPWWEYIPTLAVACLPWSGLLPSAIRQAWHERRQ--
    Consensus   (251)    RRF   D N   P WFFLPLL VA LPW  L   AIR A    RQ
                   301                                                 350
ArnT BCAL1929   (300) GFAPMLVLLIWSAFIFLFFSASHSKLISYVLPVAPALALIIGAYLPLMTA
    ArnT PAO1    (289) --APVVFLAIWLLLPLAFFSLSRGKLPTYIMPCLLPLALLMGHALVQRLR
    Consensus   (301)   APML L IW       FFS S  KL SYILP    LALIIG  L
                   351                                                 400
ArnT BCAL1929   (350) DRFRRHLLGYLVFFVAAAFGIVFLAYQGDARTPNALYRAFQMWLYAGLAV
    ArnT PAO1    (337) LGNSVALRGNGLLNLGLALLALAALAYLQLRKPVYQEEPFELTLVLLVIG
    Consensus   (351)       L G  L  LA A   L        R P       F LFL   L
                   401                                                 450
ArnT BCAL1929   (400) AAALTLVAAWLNRRAGVAAALATFGAAWLVFGTIGGTGHDEFGRYSSGAL
    ArnT PAO1    (387) AWAAAGLAQWR---YPTRAWAAPLLASWVLIALIPAAMPNHVVQNKTPDL
    Consensus   (401) A A   LA W      L A  A   AAWLL A I A          S  L
                   451                                                 500
ArnT BCAL1929   (450) LAPAVRAELAKLPPDTPFYSTEMLDHTFPFYMGHTTIMVQRQDELAFGIS
    ArnT PAO1    (434) FVAEHLDELTGAR-HLLSNDIGAASALAWRLRRSDVTLYDTRGELKYGIS
    Consensus   (451)       EL           I                 L     EL FGIS
                   501                                                 550
ArnT BCAL1929   (500) VEPNK----WIPTIGEWTTRWKQETHALAIMPP----GQYDALVKEGVPM
    ArnT PAO1    (483) YPEHSQRSVPLADIRQWLWRARQDGSIAVLIRINSASDRYQLALLPGDGE
    Consensus   (501)           I  I  WI R KQD     IL        Y   L  G
                   551          567
ArnT BCAL1929   (542) RVIARDNRRVIVEKPQS
    ArnT PAO1    (533) RYRNGNLVLAILPQVRP
    Consensus   (551) R         IL
```

Amino acid sequence alignment of *B. cenocepacia* BCAL1929 and *E. coli* K12 ArnT shows 22.3% identity

```
                          1                                                  50
    Arnt BCAL1929     (1) MNDTPSRLPLNRITLVLLLVALLAIVWFAPLGLRHLIPSDEGRYAEMAREM
ArnT E. coli K12      (1) --------MKSVRYLIGLFAFTACYYLLPTSTRLLWQPDETRYAEISREM
       Consensus      (1)              LI L   IA  W  PI  R L   DE RYAEIAREM
                         51                                                 100
    Arnt BCAL1929     (51) FVTGDWITPRYNGYKYFEKPPLQTWLNALTFAWFGIGEWQARLYTAVASF
ArnT E. coli K12      (43) LASGDWIVPHLLGLRYFEKPIAGYWINSIGQWLFGANNFGVRAGVIFATL
       Consensus      (51)   SGDWI P   G KYFEKP    WINAI    FG   F  R     AS
                        101                                                 150
    Arnt BCAL1929     (101) AGVLLVGMTGARLFN-PLSQFLAAVVLASSPYWNLMGHFNALDMGLAFWM
ArnT E. coli K12      (93) LTAALVTWFTLRLWRDKRLALLATVIYLSLFIVYAIGTYAVLDPFIAFWL
       Consensus      (101)    LV W   RLF     A LA VI  S      IG F  LD  IAFWL
                        151                                                 200
    Arnt BCAL1929     (150) ALSLCSLLLAQRPGLRPAAVRGWMWACWAAMAFAVLSKGLVGLIIPGAVL
ArnT E. coli K12      (143) VAGMCSFWLAMQAQTWKGKS-AGFLLLGITCGMGVMTKGFLALAVPVLSV
       Consensus      (151)   LCS  LA       A   A         A AVLSKG LAL LP   L
                        201                                                 250
    Arnt BCAL1929     (200) VLYTLVAHDWALWKRLYLVSGLVIFFAIVTPWFVLMQQRNPEFINHFFIV
ArnT E. coli K12      (192) LPWVATQRWKDLF-IYGWLAVISCVLTVLPWGIAIAQREPNFWHVFFWV
       Consensus      (201) L W    K W     IY   ALI     V PW L I QR P FF FFF V
                        251                                                 300
    Arnt BCAL1929     (250) QQFRRYLTPHQNRPGPLYYFVPVLLVGFLPWLSVAWQSIRHAVRMPKQPN
ArnT E. coli K12      (241) EHIQRFALDIAQHRAPFWYYVPVTIAGSLPWLGILPGALYTGWKNRK---
       Consensus      (251)     RF   D N  AP WYFVPVII G LPWL L   AI  A K  K
                        301                                                 350
    Arnt BCAL1929     (300) GFAPMFVLLIWSAFIFLFFSASHSKLISYVLPVAPALALIIGAYLPLMTA
ArnT E. coli K12      (288) -HSATVYLLSWTIMPLLFFSVAKGKLPTYILSCFASLAMLMAHYALLAAK
       Consensus      (301)   A  L LL WS    LFFS A  KL SYIL    ALALIIA Y  L
                        351                                                 400
    Arnt BCAL1929     (350) DR---FRRHLLGYLVFFVAAAFGIVFLAYQGDARTPNALYRAFQMMLYAG
ArnT E. coli K12      (337) NNPLALRINGWINIAFGVTGIIATFVVSPWGPMNTP-----VWQTFESYK
       Consensus      (351)       R      I F V A  A   LA  G   TP       FQ F
                        401                                                 450
    Arnt BCAL1929     (397) LAVAAATTLVAAWLNRRAGVAAALATFGAAWLVFGTIGGTGHDEFGRYSS
ArnT E. coli K12      (382) VFCAWSIFSIWAFFGWYTLTNVEKTWPFAALCPLGLALLVGFSIPDRVME
       Consensus      (401) L  A AI  L AF               AA    G     G     R
                        451                                                 500
    Arnt BCAL1929     (447) GALLAPAVRAELAKLPPD--TPFYSIEMLDHTFPFYMGHTTIMVQRQDEL
ArnT E. coli K12      (432) GKHPQFFVEMTQESLQPSRYILTDSVGVAAGLAWSLQRDDIIMYRQTGEL
       Consensus      (451) G      V      L P        SI M             IM     EL
                        501                                                 550
    Arnt BCAL1929     (495) AFGISVEPNKWIPTIGFWITRWKQET-H----ALAIMPPGQYDALVKEGV
ArnT E. coli K12      (482) KWGLNYPDAKGRFVSGDEFANWLNQHRQEGIITLVISVDRDEDINSLAIP
       Consensus      (501)  FGI     K     GD    W N         L I      D
                        551             569
    Arnt BCAL1929     (540) PMRVIARDNRRVIVEKPQS
ArnT E. coli K12      (532) PADAIDRQERLVLLQYRPK
       Consensus      (551) P   I R  R VII
```

Amino acid sequence alignment of *B. cenocepacia* BCAL1929 and *F. tularensis* FlmK shows 24.1% identity

```
                          1                                                  50
     Arnt BCAL1929      (1) MNDLPSRLPLNRITLVLLLVALAIVWFAPLGLRHLIPSDEGRYAEMAREM
F. tularensis flmK      (1) MNKSKN---SYYFDIFILLIIYIVYFFVFLGWRHLSIPDEGRYPEIAREM
         Consensus      (1) MN S          I ILLI   I FF  LG RHL   DEGRY EIAREM
                         51                                                 100
     Arnt BCAL1929     (51) FVLGDWITPRYNGYKYFFKPPLQTWLNALIFAWFGIGEWQARLYTAVASF
F. tularensis flmK     (48) LSSGNWVTPTINGVPFLQKPPLYYWLEATSMHFFGITPWAIRLPQALFGI
         Consensus     (51)   SG WITP  NG  F DKPPL  WL A S  FFGI  W  RL  AL
                        101                                                 150
     Arnt BCAL1929     (101) AGVILVGYTGARLFNPLSGFLAAVVLASSPYWNLMGHFNALDMGLA--FW
F. tularensis flmK     (98) LGCISIYVFGRYFYSRFAGVLASFILAANVLYFFEAHYANMDIIVATLLW
         Consensus     (101)  G I I   G   F   AG LAA ILAA   W   AHF  LDL LA   W
                        151                                                 200
     Arnt BCAL1929     (149) MALSLCSLLLAQRPGLRPAAVRGWMWACMAAMAFAVLSKGLVGLILPGAV
F. tularensis flmK     (148) IAFFLCLTSLKQT---KTKNKRLLMYAAYFVSALAFLIKGLMAIVFPCMT
         Consensus     (151) IA  LC   L Q    K    R  MWA W   A A LSKGLMAII P
                        201                                                 250
     Arnt BCAL1929     (199) LVLYTLVARDWALWKRLYIVSGLVIFFAIVTPWFVLVQQRNPEFFNFFFI
F. tularensis flmK     (195) IFVWMLITNNWYRLKELYIPFGAVLFVVIVTPWLVLAQQQNPDFLYFFFY
         Consensus     (201) I LW LI   W   K LYI SG VIF  IVTPW VL QQ NPDF  FFF
                        251                                                 300
     Arnt BCAL1929     (249) VQQFRRYITPEQNRPGPLYYFVPVLLVGFLPWLSVAWQSIRHYVRMPRQP
F. tularensis flmK     (245) FQQFYRFVGHGFNNAIGPWFYFVIILAVFLPFSILLLNRLFKGAKIIWQN
         Consensus     (251)  QQF RFL    N     WFF  IIL  FLPF  L  N I  A KI  Q
                        301                                                 350
     Arnt BCAL1929     (299) NG-FNPMLVLLIWSAFIFLFFSASHSKLISYVLPVAPALALIIGAYLPLM
F. tularensis flmK     (295) RKQDSTTFLIALWCLLILIFFSIPSSKIVSYILPIFAPLSLLMALSLEKL
         Consensus     (301)     A   LI IW   I IFFS   SKIISYILPI   LALIIA  L  I
                        351                                                 400
     Arnt BCAL1929     (348) TADR------FRRHLLCYLVFFVAAAFGIVFLAYQGDARTPNALYRAFQM
F. tularensis flmK     (345) IKNNDNVVMFKKMHLTSSIIFLVAAVAVIIFSLTQKVLLNTDAPLAYTTL
         Consensus     (351)           K HL A IIF VAA   IIF   Q       A      L
                        401                                                 450
     Arnt BCAL1929     (392) WLYAGLAVAAALTLVAAWLNRRAGVAAALATFGAAWLVFGTIGGTGHDEF
F. tularensis flmK     (395) VAVSALIVAFSVKFSFKDQIRKAITLIIFALMLLNVLGQLIIPYFDLRTS
         Consensus     (401)    AAL VA AL        RKA      A      L    I
                        451                                                 500
     Arnt BCAL1929     (442) GRYSSGALLAPAVRAELAKLPPDTPFYSIEMLLHTFPFYMGHTTIMVQRQ
F. tularensis flmK     (445) EPLVDKVLKDSNSDTIFVYYNRPQPKHFILKELLKQKGYEEDLPILLNNN
         Consensus     (451)       L               P H I   D     Y     ILLN N
                        501                                                 550
     Arnt BCAL1929     (492) DELAFGISVEPNKWIPTIGEWITRNKQETHALAIMPPGQYDALVKEGVPM
F. tularensis flmK     (495) IYTVYNWNT----YKPEIDNWSREFYYGINQYKQAHNGQNPKYIITYPEF
         Consensus     (501)   I F        W P I  W   F              GQW   L
                        551                                             597
     Arnt BCAL1929     (542) RVIARDNERMIVEKPQS----------------------------
F. tularensis flmK     (541) TEILNNNKDIILFTPEKQLEKLKQTYPNINFEIKGRYNKNVVVSVVK
         Consensus     (551)   I   NK III  P
```

Amino acid sequence alignment of *B. cenocepacia* BCAL1929 with *P. aeruginosa* PA01, *S. typhimurium* and *E. coli* ArnT

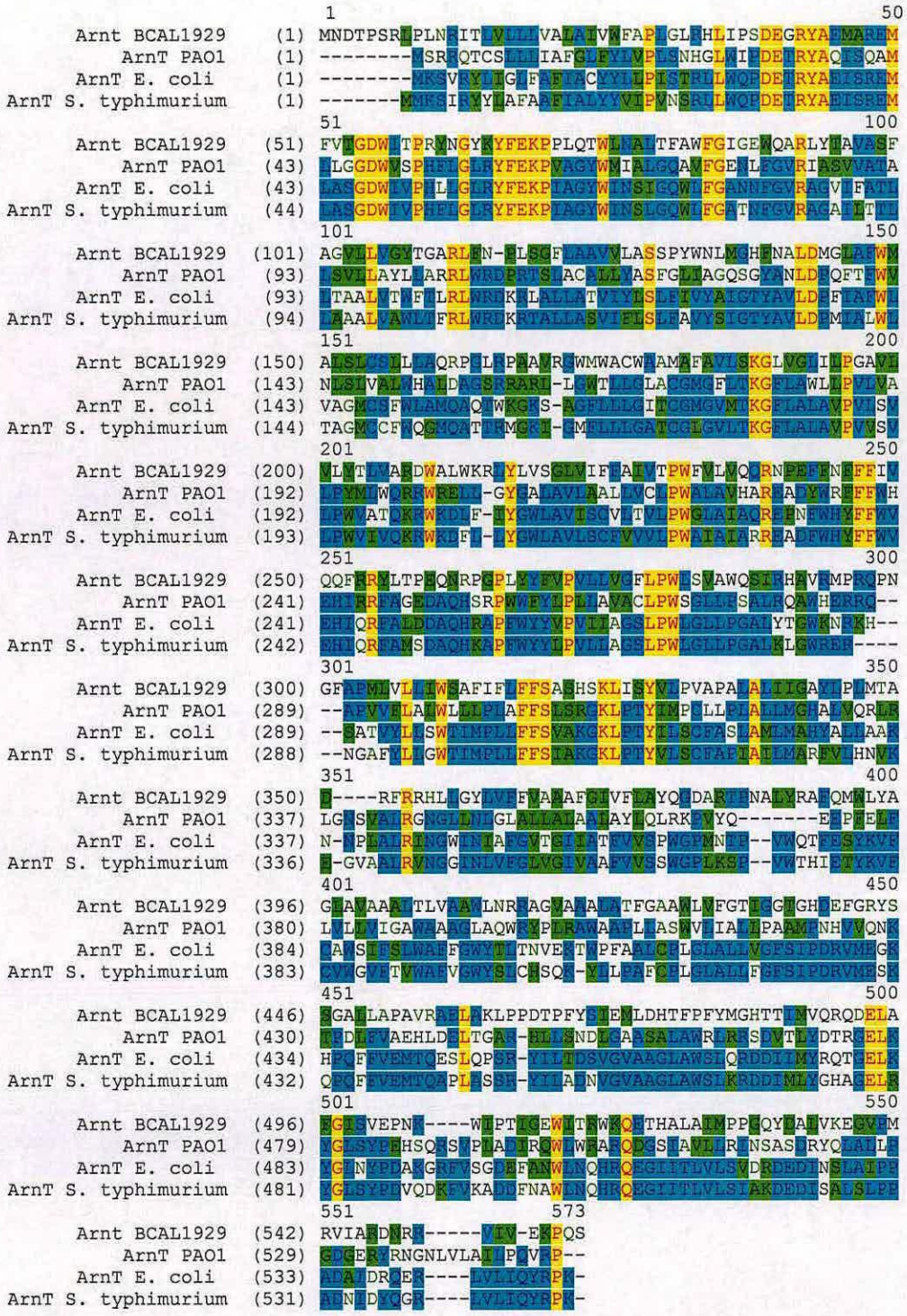

Appendix II: Ugd plasmid maps and sequences

B. cenocepacia J2315 UGD expressing plasmid maps:

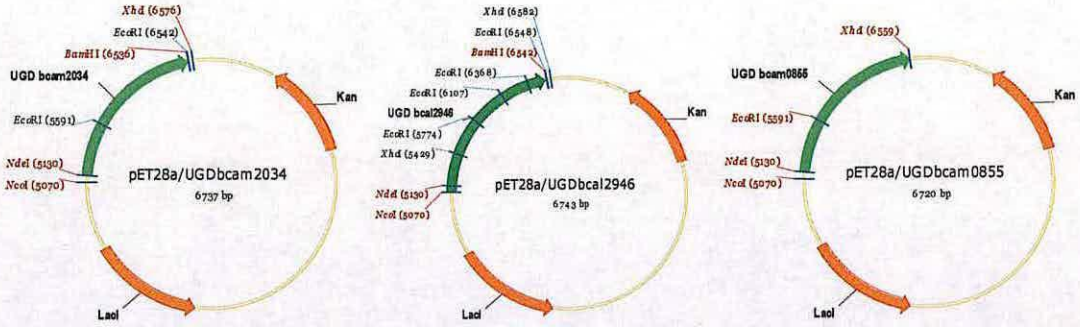

$Ugd_{BCAL2946}$ (1398 bp, 53055.64 Da)

```
   1  MGSSHHHHHH SSGLVPRGSH MKITIIGTGY VGLVTGACLA EIGHDVFCLD
  51  VDPRKIDILN NGGMPIHEPG LLDIIARNRT AGRLRFSTDI EASVAHGEIQ
 101  FIAVGTPPDE DGSADLQYVL EAARNIGRHM TSFKVIVDKS TVPVGTAQRV
 151  RGVVDEALAA RGLAGSVAHR FSVVSNPEFL KEGAAVEDFM RPDRIIIGVD
 201  DDETGTIARE KMKKLYAPFN RNHERTIYMD VRSAEFAKYA ANAMLATRIS
 251  FMNEMSNLAD KVGADIEAVR RGIGSDPRIG YHFLYAGVGY GGSCFPKDVQ
 301  ALIRTAGENG QPLRILEAVE AANHAQKDVL IGKIEQRFGA DLTGREFAVW
 351  GLAFKPNTDD MREAPSRRLI AALLERGATV RAYDPVAVDE ARRVFALDFG
 401  DDADALARLH LVDTQDVAVT GADALVIVTE WKEFRSPDFT RLKAELKAPV
 451  IFDGRNLYEP DAMAELGIDY YAIGRPYVDP QLSSRG
```

$Ugd_{BCAM0855}$ (1436 bp, 53388.85 Da)

```
   1  MGSSHHHHHH SSGLVPRGSH MNLTIIGSGY VGLVTGACLA DIGHDVFCLD
  51  VDQAKIDILN DGGVPIHEPG LKEVIARNRS AGRLRFSTDI EAAVAHGDVQ
 101  FIAVGTPPDE DGSADLQYVL AAARNIGRYM TGFKVIVDKS TVPVGTAERV
 151  RAAVAEELAK RGGDQMFSVV SNPEFLKEGA AVDDFTRPDR IVIGCDDDVP
 201  GERARELMKK LYAPFNRNHE RTLYMDVRSA EFTKYAANAM LATRISFMNE
 251  LANLADRFGA DIEAVRRGIG SDPRIGYHFL YAGCGYGGSC FPKDVEALIR
 301  TADEHGQSLQ ILKAVSSVNA TQKRVLADKI VARFGEDLSG RTFALWGLAF
 351  KPNTDDMREA PSRELIAELL SRGARVAAYD PVAQQEARRV IALDLADHPS
 401  WLERLTFVDD EAQAARDADA LVIVTEWKAF KSPDFVALGR LWKTPVIFDG
 451  RNLYEPETMS EQGIEYHPIG RPGSRQAVAA RVPGAARASA
```

$Ugd_{BCAM2034}$ (1413 bp, 52001.05 Da)

```
   1  MGSSHHHHHH SSGLVPRGSH MNVRIAIVGT GYVGLVSGTC LAELGHDVVC
  51  IDNNRGKIDA LNEGRMPIYE PGLDAVVARN VERGTLRFSN DLAASVRDRD
 101  AVFIAVGTPT LPGTDHADLQ YVEAAAREIA ANLTGFAVIV TKSTVPVGTN
 151  RIVAQIVDCC APDGVDAAIA SNPEFLREGS AIDDFMHPDR IVFGAEHPRA
 201  IEIMKAIYAP LEAAGHLVLA TEIETAELVK YAANAFLAVK ISYINEISDL
 251  CEAVGADVEL VANGMGLDRR IGASFLKAGP GWGGSCFPKD TRALKATASQ
 301  HAVPLRIVSA AIESNALRKE QILRRIENAC GGSIKGKRIA VLGLTFKGQT
 351  DDVRESPSID VIQLLVGAGA HIRAYDPARP HEASRLLPQV FMEGSAVDAV
 401  RSADAVVVMT EWKAFETLDL ADLADHMADP VMLDMRNLFS ERLAADSGFR
 451  RYERVGRSCG ERSPADPAAE PANASADTRP QRGLLQH
```

Amino acid sequence alignment of *B. cenocepacia* BCAL2946 and *P. aeruginosa* PA2022 shows 52.5% identity

```
                      1                                                  50
UGD BCAL2946     (1)  MKTTIIGTGYVGLVTGACLAETGHDVFCLDVDPRKIDILNNGGMPIHEPG
   UGD PA2022    (1)  MRLCVIGAGYVGLVTAACFAEMGNQVRCVERDREKVARLRRGEMPIYEPG
    Consensus    (1)  MKI IIG GYVGLVTAAC AEIG  V CLD D  KI  L  G MPIHEPG
                      51                                                 100
UGD BCAL2946     (51) LLDIIARNRTAGRLRFSTDIEASVAHGETQFIAVGTPPDEDGSADLQMVL
   UGD PA2022    (51) LESIIRDGLDAARLTFTASLAEGLADAEVVFIAVGTPCGEDGSADLSHVL
    Consensus    (51) L  II  N  AARL FS  I   LA AEI FIAVGTP  EDGSADL HVL
                      101                                                150
UGD BCAL2946     (101) EAARNIGRHMTSFKVIVDKSTVPVGTAQRVRGVVDEALAARGLAGSVAHR
   UGD PA2022    (101) AVAEQLGAQIRQACIVVNKSTVPVGTAERVEEIIRLGLARR----RKRFR
    Consensus    (101)   A NIG  L    IIV KSTVPVGTA RV  II  ALA R        R
                      151                                                200
UGD BCAL2946     (151) FSVVSNPEFLKEGAAVEDFMRPDRIIIGVDDDETGTIAREKMRKLYAPFN
   UGD PA2022    (147) VAVASNPEFLKEGSAVDDFRRPDRVIIGSAETQAG----ETLRQLYAPFL
    Consensus    (151)  AV SNPEFLKEGAAVDDF RPDRIIIG  D   G    E LK LYAPF
                      201                                                250
UGD BCAL2946     (201) RNHERTIYMDVRSAEFAKYAANAMLATRISFMNEMSNLADKVGADIEAVR
   UGD PA2022    (193) RNHERVILMGRREAEFSKYAANAFLATKISFMNEMAGLCALTGVDIEDVR
    Consensus    (201) RNHER I M  R AEFAKYAANA LATKISFMNEMA L    G DIE VR
                      251                                                300
UGD BCAL2946     (251) RGIGSDPRIGYHFIYAGVGYGGSCFPKDVQALIRIAGENGQPLRILEAVE
   UGD PA2022    (243) RGMGSDKRIGTHFIYAGCGYGGSCFPKDVRALIRSAEQQGYDSQILRAVE
    Consensus    (251) RGIGSD RIG HFIYAG GYGGSCFPKDV ALIRSA  NG    IL AVE
                      301                                                350
UGD BCAL2946     (301) AANHAQKDVLIGKIEQRFGADLTGREFAVWGLAFKPNTDDMREAPSRRLI
   UGD PA2022    (293) ARNARQKETLFETIGELFQQRWQGRTVALWGLAFKPGTDDLREAPSLVLL
    Consensus    (301) A N  QKDLL   I   F A   GR  ALWGLAFKP TDDLREAPS  LI
                      351                                                400
UGD BCAL2946     (351) AALLERGATVRAMDPVAVDEARRVFALDFGDDADALARLHLVDIQDVAVT
   UGD PA2022    (343) EALLRHGVRVRAHDPVAN--AGVAARYP---EAVACARLTLHDGPYAAVE
    Consensus    (351)  ALL  G  VRAHDPVA   A          DA A ARL L DS   AV
                      401                                                450
UGD BCAL2946     (401) GADALVIVTEWKEFRSPDFTRLKAELKAPVIFDGRNLYEPDAMAELGIDY
   UGD PA2022    (388) GADALVLVTEWKQFRQPDFQKIRGSMRTPLLVDGRNLYAPARMAELGFIY
    Consensus    (401) GADALVIVTEWK FR PDF KIKA LK PLI DGRNLY P  MAELG  Y
                      451          467
UGD BCAL2946     (451) YAIGRPYVDPQLSSRG-
   UGD PA2022    (438) QGIGRPRAGHCKASAA-
    Consensus    (451)  AIGRP      AS A
```

Amino acid sequence alignment of *B. cenocepacia* BCAM0855 and *P. aeruginosa* PA2022 shows 51.8% identity

```
                    1                                                  50
UGD BCAM0855    (1) MNLTIIGSGYVGLVTGACLADIGHDVFCLDVDQAKIDILNDGGVPIHEPG
  UGD PA2022    (1) MRLCVIGAGYVGLVTAACFAEMGNQVRCVERDRERVARLRRGEMPIYEPG
   Consensus    (1) M L IIGAGYVGLVTAAC ADIG  V CLD D  KI  L  G MPIHEPG
                   51                                                 100
UGD BCAM0855   (51) LKEVIARNRSAGRLRFSTDIEAAVAHCDVQFIAVGTPPDEDGSADLQYVL
  UGD PA2022   (51) LESILRDQLDAARLTFTASLAEGLADAEVVFIAVGTPCGEDGSADLSHVL
   Consensus   (51) L  II  N  AARL FS  I  ALA ADV FIAVGTP  EDGSADL HVL
                  101                                                 150
UGD BCAM0855  (101) AAARNIGRYMTGFKVIVDKSTVPVGTAERVRAAVAEELAKRGGDQMFSVV
  UGD PA2022  (101) AVAEQLGAQLRQACIVVNKSTVPVGTAERVEEIIRLGLARRRKRFRVAVA
   Consensus  (101) A A NIG  L    IIV KSTVPVGTAERV   I   LAKR       AV
                  151                                                 200
UGD BCAM0855  (151) SNPEFLKEGAAVDDFTRPDRIVIGCDLDVPGERARELMKKLYAPFNRNHE
  UGD PA2022  (151) SNPEFLKEGSAVDDFRRPDRVIIGSAETQAG----ETLRQLYAPFLRNHE
   Consensus  (151) SNPEFLKEGAAVDDF RPDRIIIG  D   G    E LK LYAPF RNHE
                  201                                                 250
UGD BCAM0855  (201) RTLYMDVRSAEFIKYAANAMLATKISFMNELANLADRFGADIEAVRRGIG
  UGD PA2022  (197) RVLLMGRREAEFSKYAANAFLATKISFMNEMAGLCALTGVDIEDVRRGMG
   Consensus  (201) R L M  R AEFSKYAANA LATKISFMNELA L    G DIE VRRGIG
                  251                                                 300
UGD BCAM0855  (251) SDPRIGYHFLYAGCGYGGSCFPKDVEALIRTADEHGQSLQILKAVSSVNA
  UGD PA2022  (247) SDKRIGTHFIYAGCGYGGSCFPKDVRALIRSAEQQGYDSQILRAVEARNA
   Consensus  (251) SD RIG HFIYAGCGYGGSCFPKDV ALIRSAD  G   QILKAV A NA
                  301                                                 350
UGD BCAM0855  (301) TQKRVLAEKIVARFGEDLSGRTFALWGLAFKPNTDDMREAPSRELIAELL
  UGD PA2022  (297) RQKELLFFTLGELFQGRWQGRTVALWGLAFKPGTDDIREAPSLVLIEALL
   Consensus  (301)  QK LL D I   F     GRT ALWGLAFKP TDDLREAPS  LI  LL
                  351                                                 400
UGD BCAM0855  (351) SRGARVAAMDPVAQQEARRVIALDIADHPSWLERLTFVDDEAQAARDADA
  UGD PA2022  (347) RHGVRVRAHDPVANAGVAARYPEAVA-----CARLTLHDSPYAAVEGADA
   Consensus  (351)   G RV AHDPVAN          LA       RLT  D    A   ADA
                  401                                                 450
UGD BCAM0855  (401) LVTVTEWKAFKSPDFVALGRLWKTPVIFDGRNLYEPETMSEQGIEYHPIG
  UGD PA2022  (392) LVLVTEWKQFRQPDFQKIRGSMRTPLLVDGRNLYAPARMAELGFIYQGIG
   Consensus  (401) LVIVTEWK FK PDF  I    KTPLI DGRNLY P  MAE G  Y  IG
                  451                 471
UGD BCAM0855  (451) RPGSRQAVAARVPGAARASA-
  UGD PA2022  (442) RP--R-------AGHCKASAA
   Consensus  (451) RP  R        G  KASA
```

Amino acid sequence alignment of *B. cenocepacia* BCAM2034 and *P. aeruginosa* PA2022 shows 38.4% identity

```
                    1                                                  50
UGD bcam2034      (1) MNVRIAIVGTGYVGLVSGTCLAELGHDVVCIDNNRGKIDALNEGRMPIYE
  UGD PA2022      (1) --MRICVIGAGYVGLVTATACFAEMGNQVRCVERDRERVARLRRGEMPIYE
   Consensus      (1)   MRI IIG GYVGLVSA C AELG  V CID  R KI  L  G MPIYE
                    51                                                 100
UGD bcam2034     (51) PGLDAVVARNVERGTLRFSNDLAASVRDRGAVFIAVGTPTLPGTDHADLQ
  UGD PA2022     (49) PGLESIIRDQLDAARLTFTASLAEGLADAEVVFIAVGTPCG-EDGSADLS
   Consensus     (51) PGLDAIL  NLD A L FS  LA  L D D VFIAVGTP       ADL
                   101                                                 150
UGD bcam2034    (101) VVEAAARETAANLTGFAVIVTKSTVPVGTNRIVAQIVDCCAPDG---VDA
  UGD PA2022     (98) HVLAVAEQLGAQLRQACIVVNKSTVPVGTAERVEEIIRLGLARRRKRFRV
   Consensus    (101) HV A A  IAANL    IIV KSTVPVGT   V  II
                   151                                                 200
UGD bcam2034    (148) ATASNPEFLKEGSAIDDFMHPDRIVFGAEHPRAIEIMKAIYAPLEAAGHL
  UGD PA2022    (148) AVASNPEFLKEGSAVDDFRRPDRVIIGSAETQAGETLRQLYAPFLRNHER
   Consensus    (151) AIASNPEFLKEGSAIDDF  PDRII GA    A E LK IYAP
                   201                                                 250
UGD bcam2034    (198) VLATEIETAELVKYAANAFLAVKISYINEISDLCEAVGADVELVANGMGL
  UGD PA2022    (198) VLLMGRREAEFSKYAANAFLATKISFMNEMAGLCALTGVDIEDVRRGMGS
   Consensus    (201) VL      AE  KYAANAFLA KISFINEIA LC   G DIE V  GMG
                   251                                                 300
UGD bcam2034    (248) DRRIGASFIKAGPGWGGSCFPKDTRALKATASQHAVPLRIVSAAIESNAL
  UGD PA2022    (248) DKRIGTHFTYAGCGYGGSCFPKDVRALIRSAEQQGYDSQILRAVEARNAR
   Consensus    (251) DKRIG  FI AG GWGGSCFPKD RAL  SA Q A    IL A    NA
                   301                                                 350
UGD bcam2034    (298) RKEQILRRIENACGGSIKGKRIAVLGLTFKGQTDDVRESPSIDVIQLLVG
  UGD PA2022    (298) QKELIFETIGELFQGRWQGHTVAIWGLAFKPGTDDIREAPSIVLIEALIR
   Consensus    (301)  KE I   I     G   GK IAL GL FK  TDDLREAPSI LI  LL
                   351                                                 400
UGD bcam2034    (348) AGAHIRAYDPARPHEASRLLPQVFMEG------SAVDAVRSADAVVVMTE
  UGD PA2022    (348) HGVRVRAHDPVANAGVAARYPEAVACARLTLHDSPYAAVEGADALVLVTE
   Consensus    (351)  G  IRAHDP      A   P     A      S   AV  ADALVLMTE
                   401                                                 450
UGD bcam2034    (392) WKAFETLDLADIADHMADPVMLDMRNLFSERLAAISGFRRYERVGRSCGE
  UGD PA2022    (398) WKQFRQPDFQKIRGSMRTPLLVDGRNLYAPARMAELGF-IYQGIGRPRAG
   Consensus    (401) WK F   D   I   M  PLLLD RNLFA    AD GF  Y  IGR  A
                   451                 477
UGD bcam2034    (442) RSPADPAAEPANASADTRPQRGLLQH-
  UGD PA2022    (447) HCKASAA--------------------
   Consensus    (451)    A  A
```

Amino acid sequence alignment of *B. cenocepacia* BCAL2946 and BCAM0855 shows 73.3% identity

```
                          1                                                  50
UGD BCAL2946        (1)   MKITIIGTGYVGLVTGACLADIGHDVFCLDVDPRKIDILNNGGMPIHEPG
UGD BCAM0855        (1)   MNLTIIGSGYVGLVTGACLADIGHDVFCLDVDQAKIDILNDGGVPIHEPG
    Consensus       (1)   M ITIIGSGYVGLVTGACLADIGHDVFCLDVD  KIDILN GGMPIHEPG
                          51                                                 100
UGD BCAL2946        (51)  LLDIIARNRTAGRLRFSTDIEASVAHGEIQFIAVGTPPDEDGSADLQYVL
UGD BCAM0855        (51)  LKEVIARNRSAGRLRFSTDIEAAVAHGDVQFIAVGTPPDEDGSADLQYVL
    Consensus       (51)  L DIIARNRSAGRLRFSTDIEAAVAHGDIQFIAVGTPPDEDGSADLQYVL
                          101                                                150
UGD BCAL2946        (101) EAARNIGRHMTSFKVIVDKSTVPVGTAQRVRGVVDEALAARGLAGSVAHR
UGD BCAM0855        (101) AAARNIGRYMTGFKVIVDKSTVPVGTAERVRAAVAEELAKR----GGDQM
    Consensus       (101)  AARNIGRHMT FKVIVDKSTVPVGTA RVRA V E LA R
                          151                                                200
UGD BCAL2946        (151) FSVVSNPEFLKEGAAVEDFMRPDRIIIGVDDDETGTIAREKMKKLYAPFN
UGD BCAM0855        (147) FSVVSNPEFLKEGAAVDDFTRPDRIVIGCDDDVPGERARELMKKLYAPFN
    Consensus       (151) FSVVSNPEFLKEGAAVDDF RPDRIIIG DDD  G  ARE MKKLYAPFN
                          201                                                250
UGD BCAL2946        (201) RNHERTIYMDVRSAEFAKYAANAMLATRISFMNEMSNLADKVGADIEAVR
UGD BCAM0855        (197) RNHERTLYMDVRSAEFTKYAANAMLATRISFMNELANLADRFGADIEAVR
    Consensus       (201) RNHERTIYMDVRSAEF KYAANAMLATRISFMNELANLADK GADIEAVR
                          251                                                300
UGD BCAL2946        (251) RGIGSDPRIGYHFLYAGVGYGGSCFPKDVQALIRTAGENGQPLRILEAVE
UGD BCAM0855        (247) RGIGSDPRIGYHFLYAGCGYGGSCFPKDVEALIRTADEHGQSLQILKAVS
    Consensus       (251) RGIGSDPRIGYHFLYAG GYGGSCFPKDV ALIRTA E GQ L IL AV
                          301                                                350
UGD BCAL2946        (301) AANHAQKDVLIGKIEQRFGADLIGREFAVWGLAFKPNTDDMREAPSRRLI
UGD BCAM0855        (297) SVNATQKRVLADKIVARFGEDLSGRTFALWGLAFKPNTDDMREAPSRELI
    Consensus       (301) A N  QK VL  KI  RFG DLSGR FALWGLAFKPNTDDMREAPSR LI
                          351                                                400
UGD BCAL2946        (351) AALLERGATVRAYDPVAVDEARRVFALDFGDDADALARLHLVDTQDVAVT
UGD BCAM0855        (347) AELLSRGARVAAYDPVAQQEARRVIALDLADHPSWLERLTFVDDEAQAAR
    Consensus       (351) A LL RGA V AYDPVA  EARRV ALD AD    L RL  VD    A
                          401                                                450
UGD BCAL2946        (401) GADALVIVTEWKEFKSPDFTRLKAELKAPVIFDGRNLYEPLAMAELGIDY
UGD BCAM0855        (397) DADALVIVTEWKAFKSPDFVALGRLWKTPVIFDGRNLYEPHTMSEQGIEY
    Consensus       (401)  ADALVIVTEWK FKSPDF  L    K PVIFDGRNLYEPD MAE GIDY
                          451                475
UGD BCAL2946        (451) YAIGRPYVDPQLSSRG---------
UGD BCAM0855        (447) HPIGRPGSRQAVAARVPGAARASA-
    Consensus       (451) H IGRP     LAAR
```

Amino acid sequence alignment of *B. cenocepacia* BCAL2946 and BCAM2034 shows 43.1% identity

```
                      1                                                  50
UGD BCAL2946      (1) --MKITIIGTGYVGLVTGACLAEIGHDVFCLDVDPRKIDILNNGGMPIHE
 UGD bcam2034     (1) MNVRIAIVGTGYVGLVSGTCLAEIGHDVVCIDNNRGKIDALNEGRMPIYE
    Consensus     (1)   MKI IIGTGYVGLVSG CLAEIGHDV CID    KID LN G MPIHE
                      51                                                 100
UGD BCAL2946     (49) PGLLDIIARNRTAGRLRFSTDIEASVAHGEIQFIAVGTP-PDEDGSADLQ
 UGD bcam2034    (51) PGLDAVVARNVERGTLRFSNDLAASVRDRDAVFIAVGTPTLPGTDHADLQ
    Consensus    (51) PGL  IIARN   G LRFS DI ASV   D  FIAVGTP       ADLQ
                     101                                                 150
UGD BCAL2946     (98) YVLEAARNIGRHMTSFKVIVDKSTVPVGTAQRVRGVVDEALAARGLAGSV
 UGD bcam2034   (101) YVEAAAREIKANITGFAVIVTKSTVPVGTNRIVAQIVDCCAPDG-----V
    Consensus   (101) YV  AAR IA  LT F VIV KSTVPVGT   V  IVD           V
                     151                                                 200
UGD BCAL2946    (148) AHRFSVVSNPEFLKEGAAVEDFMRPDRIIIGVDDDETGTIAREKMKKIYA
 UGD bcam2034   (146) DA--AIASNPEFLREGSAIDDFMHPDRIVFGAEHPR----AIEIMKATYA
    Consensus   (151)     AI SNPEFLKEGAAIDDFM PDRII G D       A E MK IYA
                     201                                                 250
UGD BCAL2946    (198) PFNRNHERTIYMDVRSAEFAKYAANAMLATRISFMNEMSNLADKVGADIE
 UGD bcam2034   (190) PLEAAGHLVIATDIETAELVKYAANAFLAVKISYTNEISDLCEAVGADVE
    Consensus   (201) P        I  DI SAE  KYAANA LA KISFINEIS L D VGADIE
                     251                                                 300
UGD BCAL2946    (248) AVRRGIGSDPRIGYHFLYAGVGMGGSCFPKDVQALIRTAGENGQPLRIIE
 UGD bcam2034   (240) LVANGMGLDRRIGASFLKAGPGWGGSCFPKDTRALKATASQHAVPLRIVS
    Consensus   (251)  V  GIG D RIG  FL AG GWGGSCFPKD  AL  TA   A PLRIL
                     301                                                 350
UGD BCAL2946    (298) AVEAANHAQKIVLIGKIEQRFGADITGREFAVWGLAFKPNTDDMREAPSR
 UGD bcam2034   (290) AAIESNALRKIQIIRNIENACGKSIKGKRIAVLGLTFKGQTDDVRESPSI
    Consensus   (301) A   AN   KD II KIEN  GA I GK  AV GL FK NTDDMREAPS
                     351                                                 400
UGD BCAL2946    (348) RLIAALLERGATVRAYDPVAVDEARRVFALDFGDDKDALARLHLVDTQDV
 UGD bcam2034   (340) DVIQLLVGAGAHIRAYDPARPHEASRILPQVFMEGE----------AVD
    Consensus   (351)  LI  LL  GA IRAYDP    EA RL    F D A
                     401                                                 450
UGD BCAL2946    (398) AVTGADALVIVTEWKEFRSPDFTRLKAELKAPVIFDGRNLMEPDAMAHLG
 UGD bcam2034   (379) AVRSADAVVVVTEWKAFETLDLADLADHMADPVVLDMRNLFSERLAADSG
    Consensus   (401) AV  ADALVIMTEWK F S D   L   L  PVI D RNLF     AD G
                     451                                490
UGD BCAL2946    (448) IDYYAIG------RPYVDPQLSSRG---------------
 UGD bcam2034   (429) FRRYERVGRSCGERSPADPAAEPANASADTRPQRGLLQH-
    Consensus   (451)    Y         R   DP
```

Amino acid sequence alignment of *B. cenocepacia* BCAM0855 and BCAM2034 shows 43.0% identity

```
                      1                                                  50
UGD BCAM0855      (1) --MNLTIIGSGYVGLVTGACLADIGHDVFCLDVDQAKIDILNDGGVPIHE
 UGD bcam2034     (1) MNVRIAIVGIGYVGLVSGTCLAEIGHDVVCIDNNRGKIDALNEGRMPIYE
    Consensus     (1)   M I IIGSGYVGLVSG CLADIGHDV CID   AKID LNDG MPIHE
                      51                                                 100
UGD BCAM0855     (49) PGLKEVIARNRSAGRLRFSTDIEAAVAHGDVQFIAVGTP-PDEDGSADLQ
 UGD bcam2034    (51) PGLDAVVARNVERGTLRFSNDIAASVRDRDAVFIAVGTPTLPGTDHADLQ
    Consensus    (51) PGL  VIARN   G LRFS DI AAV   D  FIAVGTP       ADLQ
                     101                                                 150
UGD BCAM0855     (98) YVLAAARNIGRYMTGFKVIVDKSTVPVGTAERVRAAVAEELAKRGGDQMF
 UGD bcam2034   (101) YVEAAAREIAANITGFAVIVTKSTVPVG-TNRITVAQIVECCAPDG--VDA
    Consensus   (101) YV AAAR IA  LTGF VIV KSTVPVG   RI A I D  A  G
                     151                                                 200
UGD BCAM0855    (148) SVVSNPEFLKEGAAVDDFTRPDRIVIGCDDDVPGERAREIMKKIYAPFNR
 UGD bcam2034   (148) AIASNPEFLREGSAIDDFMHPDRIVFGAEHPR----AIEIMKAIYAPLEA
    Consensus   (151) AI SNPEFLKEGAAIDDF  PDRIV G D       A EIMK IYAP
                     201                                                 250
UGD BCAM0855    (198) NHERTLYMDVRSAEFTKYAANAMLATRISFMNELANLADRFGADIEAVRR
 UGD bcam2034   (194) AGHLVLATEIETAELVKYAANAFLAVKISYINEISDLCIAVGADVELVAN
    Consensus   (201)      L  DI SAE  KYAANA LA KISFINEIA L D  GADIE V
                     251                                                 300
UGD BCAM0855    (248) GIGSDPRIGYHFLYAGCGYGGSCFPKDVEALIRTADEHGQSLQILKAVSS
 UGD bcam2034   (244) GMGLDRRIGASFLKAGPGWGGSCFPKDTRALKATASQHAVPLRIVSAAIE
    Consensus   (251) GIG D RIG  FL AG GWGGSCFPKD  AL  TA  HA  L IL A
                     301                                                 350
UGD BCAM0855    (298) VNATQKRVIADKIVARFGEDLSGKTFALWGLAFKPNTDDMREAPSRELIA
 UGD bcam2034   (294) SNALRKEQILRKIENACGGSIKGKRIAVLGLTFKGQTDDVRESPSIDVIQ
    Consensus   (301)  NA  K  I  KI    G  I GK  AL GL FK NTDDMREAPS DLI
                     351                                                 400
UGD BCAM0855    (348) ELLSRGARVAAYDPVAQQEARRVIALDLADHPSWLERLTFVDDEAQAARD
 UGD bcam2034   (344) LLVGAGAHIRAYDPARPHEASRLIPQVFMEG----------SAVDAVRS
    Consensus   (351)  LL  GA I AYDP    EA RLI     D              A R
                     401                                                 450
UGD BCAM0855    (398) ADALVIVTEWKAFKSPDFVALGRLWKTPVIFDGRNLYEPETMSEQG-IEY
 UGD bcam2034   (383) ADAVVVMTEWKAFETLDLADLKDHMADPVMLDMRNLFSERLAADSGFRRY
    Consensus   (401) ADALVIMTEWKAF S D   LA      PVI D RNLF     AD G   Y
                     451                                 486
UGD BCAM0855    (447) HPIGRPGSRQHVAARVPGAARASA------------
 UGD bcam2034   (433) ERVGRSCGERSPADPAAEPANASADTRPQRGLLQH-
    Consensus   (451)   IGR     A A      A ASA
```

Appendix III: BceB plasmid maps and sequences

B. cenocepacia J2315 *BceB* expressing plasmid maps:

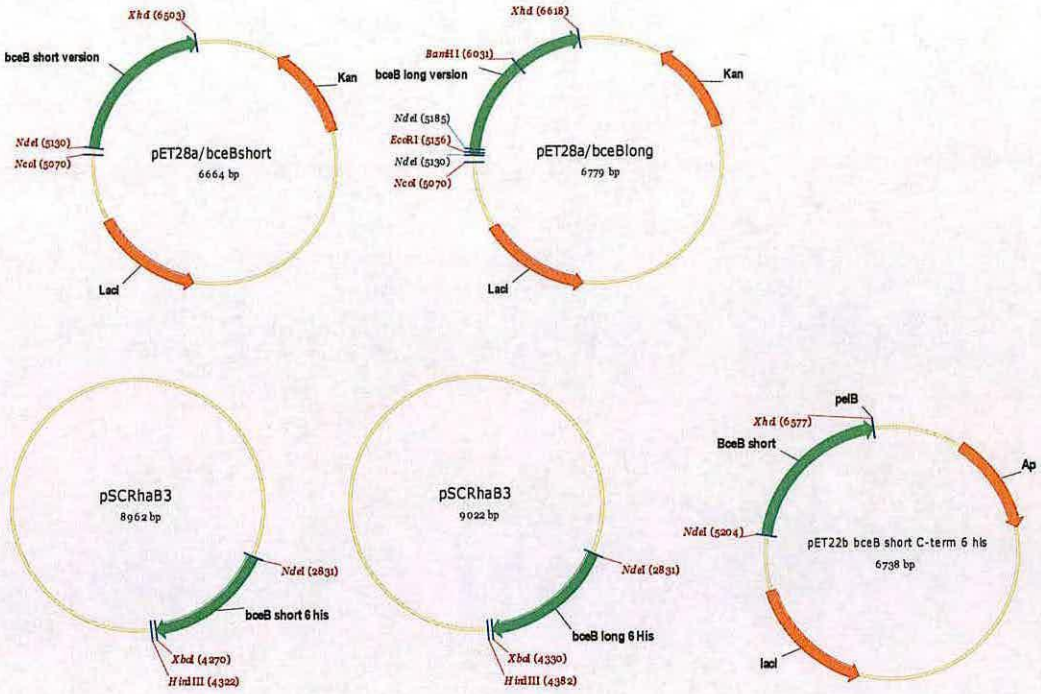

BceB PC184 long (1506 bp with His tag, 1440 without, 55041.55 Da)

```
   1   MRHGLHKELF GKRLFKEEAN MLSVLARVID IAMVVAGALI AAALHRGNVW
  51   FSDLQRTMVL FDCLLVVVCF PAFGIYQSWR GKRLVGLMGR VAFAWLVVEL
 101   AGILMSFSFH QSGELSRLWL GYWAIATVTL LAGSKACVHA VLRRLRRGGF
 151   NLKAVAIVGG TPAARRLIAQ MRARPEAGFN PVCVYDEDAA PGDVALDDVR
 201   IERQFESLVW LVRSRAIREL WLTLPISEER RIHQIVTVFR HDFVNIRFIP
 251   DVRSLSFFNQ EVVEVLGVPA INLAASPITD VRILPKFVFD RMFALAALVM
 301   LAPLMLVIAC LIKATSPGPV FFRQKRKGID GHEFEIYKFR SMKVHQEAAG
 351   TVTQATKNDS RVTPVGRFLR RTSLDELPQF INVLKGEVSV VGPRPHALAH
 401   DDIYKDLVKG YMFRYRIKPG ITGWAQINGY RGETDQIEKM MGRVKLDLYY
 451   MQNWSFWLDI KIVALTLWKG FTGSNAYLEH HHHHH
```

BceB PC184 short (1446 bp with 6 His, 1380 bp without, 52486.44 Da)

```
   1   MLSVLARVID IAMVVTGALI AAALHGGSIG LSDLQRTTVL FDCLLVVVFF
  51   PAFGIYQSWR GKRLVGLMGR VVFAWLAVEL AGILMSFSFH QSGDLSRLWL
 101   GYWALATTVL LAGSKACVHV VLRQLRRGGY NLKAVAIVGG TPAARRLIAQ
 151   MRARPEAGFN PVCVYDESEA PGEVALDDVR IERQFESLVW LVRSRAISEL
 201   WLTLPITEER RIHQIVTVFR HDFVNIRFIP DVRTLSFFNQ EVVEVLGVPA
 251   INLAASPITD VRILPKFVFD RLFALAALTA LAPVMVLIAA LIKLTSRGPV
 301   FFRQKRKGID GHEFEIYKFR SMKVHQEVAG QVTQATKNDS RVTPVGRFLR
 351   RTSLDELPQF INVLKGEMSV VGPRPHALAH DDIYKDLVKG YMFRYRIKPG
 401   ITGWAQINGY RGETDQIEKM MGRVKLDLYY MQNWSFWLDI KIVVLTLWKG
 451   FTGSNAYLEH HHHHH
```

Nucleotide sequence alignment of *B. cenocepacia* J2315 and *B. cenocepacia* PC184 BceB long and short shows 85.9% identity.

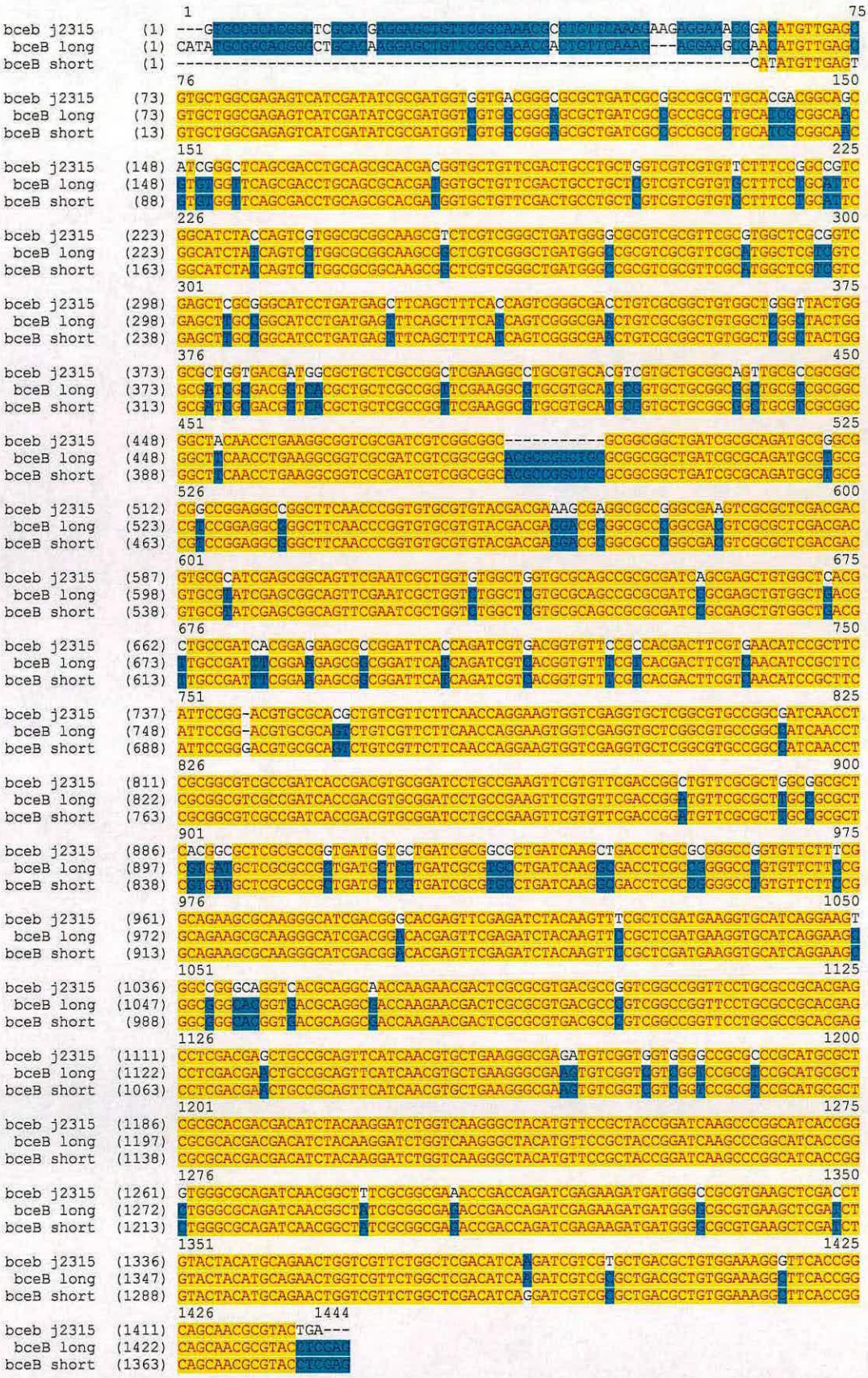

Appendix IV: Sephacryl S-200 calibration

Data from Marine Raman, School of Chemistry, University of Edinburgh

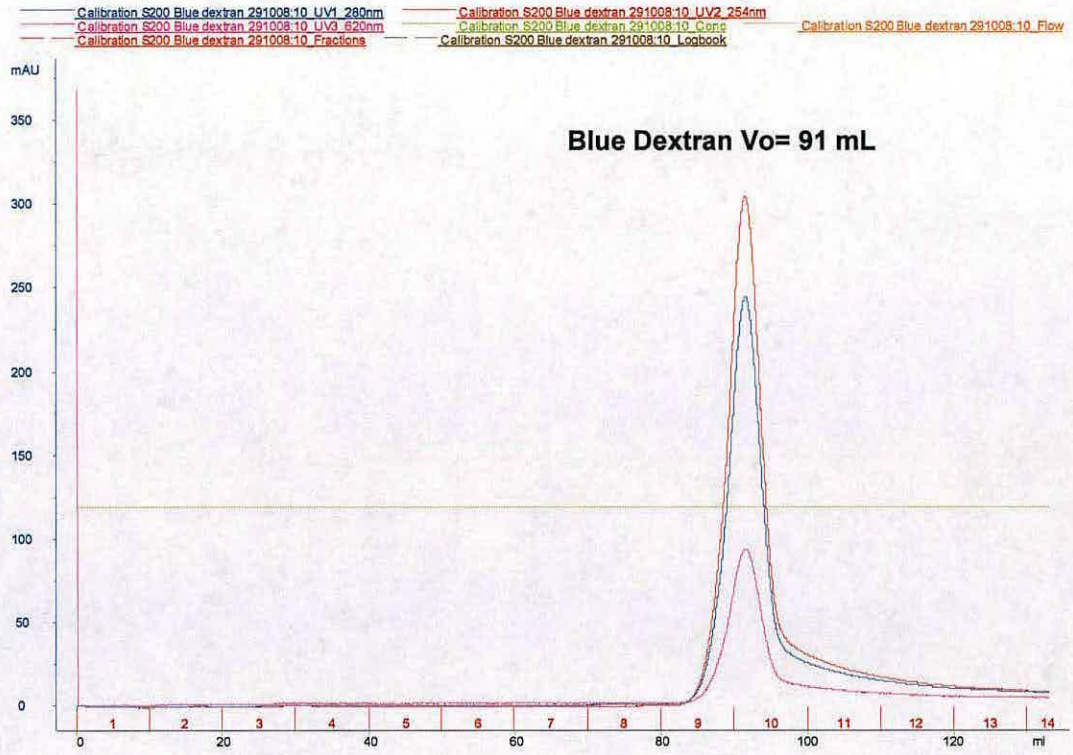

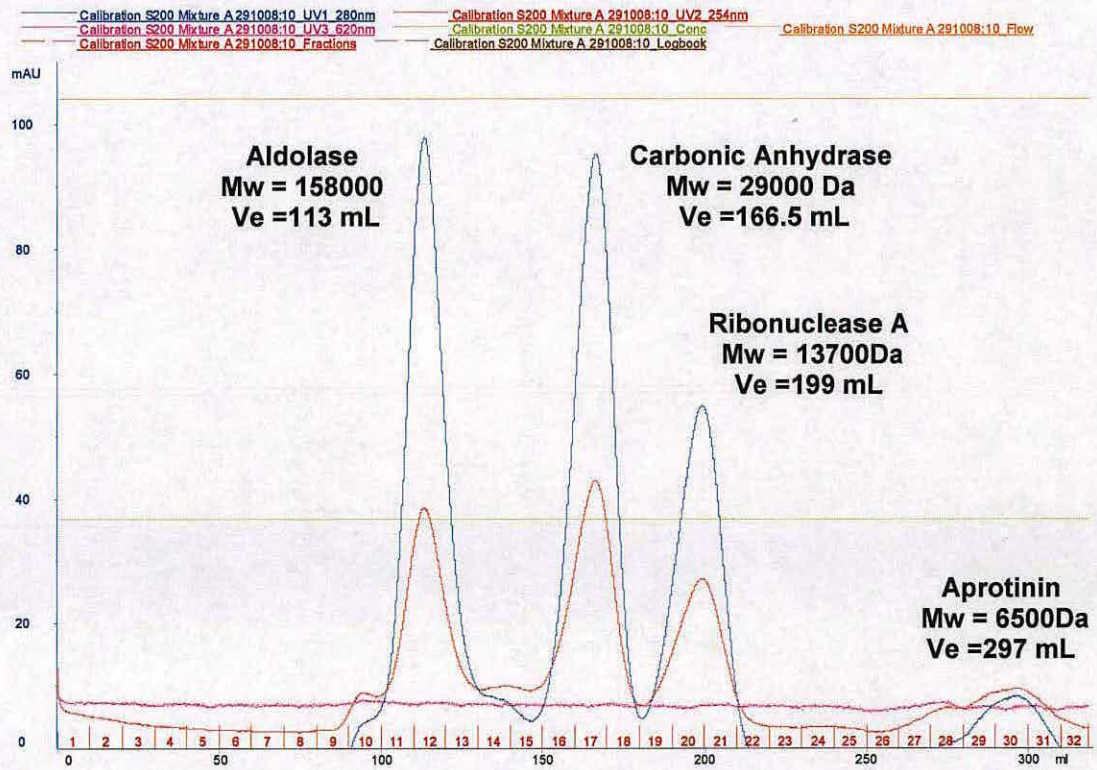

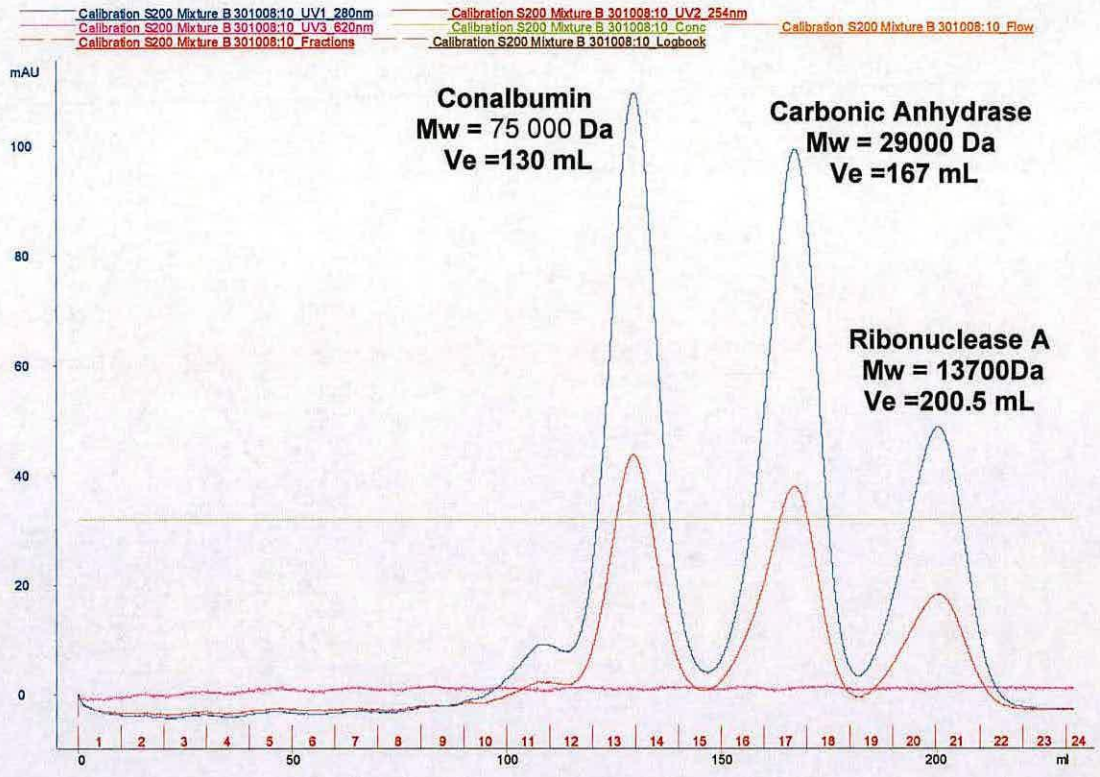

$$K_{av} = V_e - V_0/320-V_0$$

Calibration curve Sephacryl S-200 HiLoad 26/20 HR

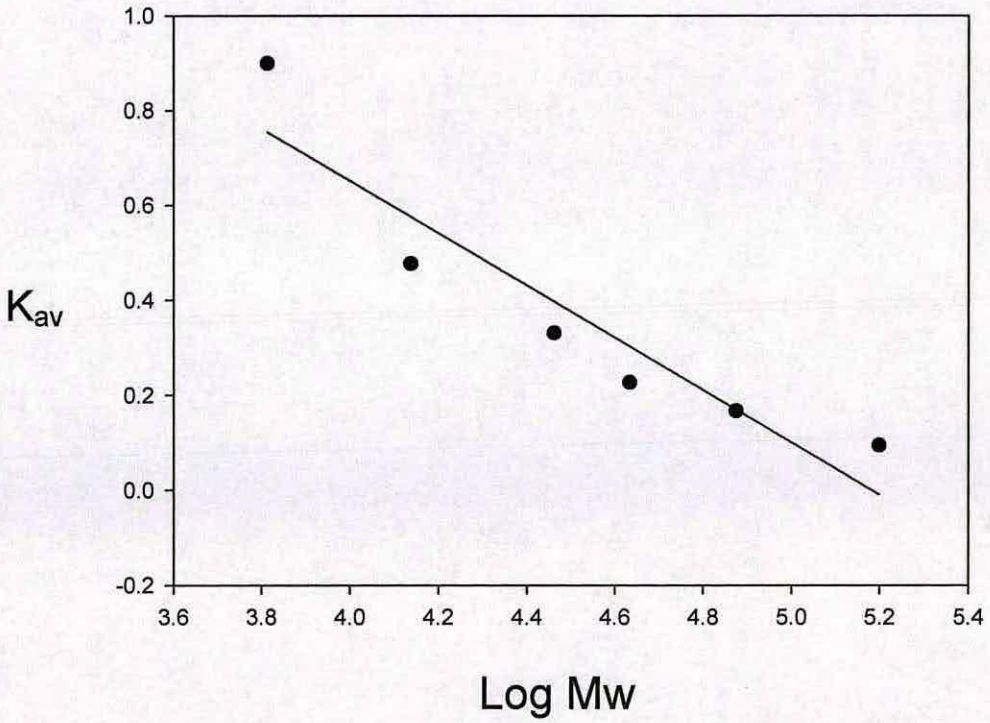

Kav = -0.5511 Log MW + 2.857

Microbiology (2008), **154**, 2513–2521 DOI 10.1099/mic.0.2008/019216-0

Plant host and sugar alcohol induced exopolysaccharide biosynthesis in the *Burkholderia cepacia* complex

S. Josefin Bartholdson,[1,2] Alan R. Brown,[2] Ben R. Mewburn,[3] David J. Clarke,[1] Stephen C. Fry,[3] Dominic J. Campopiano[1] and John R. W. Govan[2]

Correspondence
John R. W. Govan
john.r.w.govan@ed.ac.uk

[1]School of Chemistry, University of Edinburgh, Edinburgh EH9 3JJ, UK
[2]Centre for Infectious Diseases, University of Edinburgh, Edinburgh EH16 4SB, UK
[3]Institute of Molecular Plant Sciences, University of Edinburgh, Edinburgh EH9 3JH, UK

Received 6 August 2007
Revised 2 May 2008
Accepted 5 May 2008

The species that presently constitute the *Burkholderia cepacia* complex (Bcc) have multiple roles; they include soil and water saprophytes, bioremediators, and plant, animal and human pathogens. Since the first description of pathogenicity in the Bcc was based on sour skin rot of onion bulbs, this study returned to this plant host to investigate the onion-associated phenotype of the Bcc. Many Bcc isolates, which were previously considered to be non-mucoid, produced copious amounts of exopolysaccharide (EPS) when onion tissue was provided as the sole nutrient. EPS production was not species-specific, was observed in isolates from both clinical and environmental sources, and did not correlate with the ability to cause maceration of onion tissue. Chemical analysis suggested that the onion components responsible for EPS induction were primarily the carbohydrates sucrose, fructose and fructans. Additional sugars were investigated, and all alcohol sugars tested were able to induce EPS production, in particular mannitol and glucitol. To investigate the molecular basis for EPS biosynthesis, we focused on the highly conserved *bce* gene cluster thought to be involved in cepacian biosynthesis. We demonstrated induction of the *bce* gene cluster by mannitol, and found a clear correlation between the inability of representatives of the *Burkholderia cenocepacia* ET12 lineage to produce EPS and the presence of an 11 bp deletion within the *bceB* gene, which encodes a glycosyltransferase. Insertional inactivation of *bceB* in *Burkholderia ambifaria* AMMD results in loss of EPS production on sugar alcohol media. These novel and surprising insights into EPS biosynthesis highlight the metabolic potential of the Bcc and show that a potential virulence factor may not be detected by routine laboratory culture. Our results also highlight a potential hazard in the use of inhaled mannitol as an osmolyte to improve mucociliary clearance in individuals with cystic fibrosis.

INTRODUCTION

The genus *Burkholderia* includes three closely related microbial species that highlight diverse evolutionary adaptation to different niches and hosts. *Burkholderia mallei* is a soliped-specific pathogen that only occasionally infects humans. *Burkholderia pseudomallei* is a free-living soil microbe and the causative agent of the subtropical human disease melioidosis. The species that presently constitute the *Burkholderia cepacia* complex (Bcc) have multiple roles; they include soil and water saprophytes, rhizosphere parasites, bioremediators, plant growth promoters and plant, animal and human pathogens. Members of the Bcc are particularly associated with life-threatening respiratory infections in patients with chronic granulomatous disease (CGD), and are the most potentially virulent, transmissible and inherently resistant microbes to have emerged as cystic fibrosis (CF) pathogens in recent decades (Govan, 2006; Mahenthiralingam *et al.*, 2005).

Although most species within the Bcc produce a variety of putative virulence factors, the role of these factors in the pathogenesis of human infection is unclear (Mahenthiralingam *et al.*, 2005). Evidence from various model systems (mouse, rat, plant and nematode) suggests

Abbreviations: Bcc, *Burkholderia cepacia* complex; CF, cystic fibrosis; CGD, chronic granulomatous disease; EPS, exopolysaccharide; HPAE-PAD, high-performance anion-exchange chromatography with pulsed amperometric detection; TFA, trifluoroacetic acid.

Three supplementary tables and a supplementary figure are available with the online version of this paper.

that the importance of individual virulence factors, or combinations of factors, depends on the infection model used (Bernier *et al.*, 2003). In addition, studies of Bcc infections in CF patients also suggest a key role of host–pathogen interactions, since clinical outcome in individual patients cannot be predicted even during epidemic outbreaks when multiple patients are infected by the same strain (Govan *et al.*, 1993). The first description of pathogenicity in the Bcc was based on sour skin rot of onion bulbs (Burkholder, 1950). In this study, we returned to this plant host to investigate the onion-associated phenotype of the Bcc, and reveal a link between growth conditions and exopolysaccharide (EPS) production.

EPS is a putative Bcc virulence factor that is involved in persistence of the bacteria in CF lungs (Conway *et al.*, 2004), interactions with antimicrobial peptides (Herasimenka *et al.*, 2005) and the formation of biofilms (Cunha *et al.*, 2004). The EPSs of *Burkholderia* species have recently been comprehensively reviewed (Goldberg, 2007). Recent studies (Zlosnik *et al.*, 2008) have also challenged the previous belief that mucoid, EPS-producing colonial morphotypes of Bcc are rare in both environmental and clinical isolates (Govan & Deretic, 1996). Other studies have shown that mucoid Bcc isolates mostly synthesize one type of EPS, with a highly branched heptasaccharide repeating unit, which was named cepacian (Moreira *et al.*, 2003; Sist *et al.*, 2003). EPS production has been shown to increase when the Bcc are grown in mannitol-rich yeast extract medium (MYEM) (Sage *et al.*, 1990; Zlosnik *et al.*, 2008).

Here we report the novel observation that many Bcc isolates, found to be non-mucoid on typical culture media, produce copious amounts of EPS when onion tissue is provided as the sole nutrient. Chemical and molecular analyses suggest that EPS biosynthesis is strain-specific and that the plant compounds responsible are primarily sugars and sugar alcohols. We show that the EPS phenotype on onion media is associated with the previously described *bce* cluster (Moreira *et al.*, 2003), thought to be involved in cepacian biosynthesis.

METHODS

Bacterial strains and culture conditions. Bcc isolates used in this study are described in Table 1 and include 16 isolates from the two published Bcc strain panels (Coenye *et al.*, 2003; Mahenthiralingam *et al.*, 2000). Additional Bcc strains investigated included *Burkholderia pyrrocinia* BTS7, *Burkholderia cenocepacia* BTS2, as well as 19 *Burkholderia multivorans*, 14 *Burkholderia cenocepacia* IIIA and 11 *Burkholderia cenocepacia* IIIB isolates from our collection. Isolates were recovered from storage at −80 °C by subculture on nutrient agar (NA; Columbia base agar, Oxoid) and subsequently grown on media composed of 1.5 % (w/v) bacteriological agar (Oxoid) containing 2 % (w/v) sugars and fractions from various isolation methods below.

Sugars and other related chemicals were purchased from Sigma-Aldrich, BDH AnalaR, MP Biochemicals, Fluka BioChemika or Acros Organics.

Onion maceration. White onion slices were placed in Petri dishes and inoculated with stationary-phase Bcc cultures (10^6 c.f.u.) that had been cultured overnight in 2.5 % (w/v) nutrient broth No 2 (Oxoid) with 0.5 % (w/v) yeast extract. The onions were left at 30 °C for 5 days. The results were assessed by eye, and onion maceration recorded as positive or negative.

Onion extract agar. Peeled white onions (1 kg) were chopped, homogenized in a blender at room temperature, and filtered through muslin. The filtrate was filter-sterilized through a 0.22 μm filter and lyophilized to give a yellow sticky powder (typical yield 62 g). Twenty grams of lyophilized onion extract and 15 g bacteriological agar were made up to 1 l with distilled H_2O, then autoclaved at 121 °C for 15 min. Strains were subcultured onto onion agar and incubated for 72 h at 30 °C. Mucoidy was recorded on a scale ranging from non-mucoid (−) to very mucoid (+ + +).

Sugar agar. Sugar agar contained 20 g of the sugar of interest, 2 g yeast extract, and 15 g bacteriological agar dissolved in 1 l distilled H_2O (Sage *et al.*, 1990). The sugars used were as follows: D-fructose, D-galactose, D-mannitol, D-glucose, glycerol, lactose, L-rhamnose, D-mannose, maltose, sucrose, *myo*-inositol, ribitol (adonitol) and D-glucitol (sorbitol). The fructan polysaccharide inulin was also tested.

As a control, isolates were grown on bacteriological agar containing 0.2 % (w/v) yeast extract alone.

Reverse-phase chromatography. Twenty millilitres of onion extract, 2 % (w/v) in distilled H_2O, was loaded onto a pre-packed C8 column (10 g/60.0 ml, Varian, Anachem) and bound material was eluted stepwise using three concentrations of methanol (20 %, 50 % and 80 %, v/v; Fisher Scientific). Each fraction was lyophilized, dissolved in distilled H_2O and incorporated into 1.5 % (w/v) bacteriological agar.

Ethyl acetate partitioning. To separate any lipids, non-polar, non-acidic and polar compounds, the resolubilized onion extract was brought to pH 7.0 using NaOH and partitioned against ethyl acetate (Fisher Scientific) at 1 : 1 (v/v). The phases were separated, and the aqueous phase was brought to pH 2.0 using HCl and the extraction was repeated. Following both extractions, the organic and aqueous layers were evaporated or lyophilized respectively, and then redissolved in distilled H_2O, pH adjusted to 7.0, and incorporated into 1.5 % (w/v) bacteriological agar.

Acid hydrolysis. The aqueous phase residue of the ethyl acetate partitioned onion extract was redissolved in distilled H_2O (50 mg ml^{-1}) and was hydrolysed in 2 M TFA (trifluoroacetic acid; Sigma) at 60 °C or 120 °C for 1 h.

Paper electrophoresis. To fractionate the extract based on the presence or absence of functional groups, the freeze-dried aqueous phase of the onion extract was weighed and resuspended in distilled H_2O to a final concentration of 50 mg ml^{-1}. One millilitre was loaded at a central origin on a Whatman no.1 paper (57 × 42 cm). The following standards were added in the margins of the paper: glucose 6-phosphate, glucose, glucosamine, methyl green (Sigma) and orange G (BDH). Electrophoresis was conducted at 1 kV for 20 min, in volatile buffers at pH 2.0 or 6.5 with white spirit or toluene as coolant (Fry, 2000).

Paper chromatography. One millilitre aliquots of each of the redissolved aqueous phase of the onion extract and the TFA-hydrolysed samples (50 mg ml^{-1}) were chromatographed on Whatman no. 1 paper alongside markers (ferulic acid, rhamnose, glucose, lactose, mannose, galactose, fructose, mannitol and glycerol) in butan-1-ol/acetic acid/water (12 : 3 : 5, by vol.) for up to 60 h.

Table 1. EPS biosynthesis of *B. cepacia* complex species when grown on agar supplemented with various substrates

All strains tested are from the two published Bcc panels (Coenye *et al.*, 2003; Mahenthiralingam *et al.*, 2000), except for BTS2 and BTS7, which were donated by Paola Cescutti. EPS production was scored on a scale from – (no EPS) to +++ (very mucoid). Mucoid growth described as +++ is shown in Fig. 1(b). YE, yeast extract agar.

Species	Strain	Source	YE	Onion	Glucose	Sucrose	Fructose	Inulin	Glycerol	Mannitol	Glucitol	Ribitol	Inositol	Mannose
B. cepacia	ATCC 25416	Onion	–	++	–	++	+++	–	+++	+++	+++	+++	+++	+
B. cepacia	CEP509	CF	–	–	–	+	++	+	++	++	+	+	+	–
B. multivorans	C1576	CF	–	++	–	+	+++	+	++	+++	+++	+++	+++	–
B. multivorans	ATCC 17616	Soil	–	++	–	+	+++	+	++	+++	+++	+++	+++	–
B. cenocepacia	J2315*	CF	–	–	–	–	–	–	–	–	–	–	–	–
B. cenocepacia	K56-2*	CF	–	–	–	–	–	–	–	–	–	–	–	–
B. cenocepacia	BC7*	CF	–	–	–	–	–	–	–	–	–	–	–	–
B. cenocepacia	PC184	CF	–	++	–	+	++	+	+	++	+	+	+	–
B. cenocepacia	BTS2	CF	–	++	–	+	++	+	+	++	++	+	++	–
B. stabilis	LMG14294	CF	–	–	–	–	+	–	–	+	–	–	–	–
B. vietnamiensis	LMG10929	Rice	–	+++	–	++	+++	+	+++	+++	+	–	+++	++
B. vietnamiensis	PC259	CF	–	++	–	+	+++	+	++	+++	+	–	–	–
B. dolosa	E12	CF	–	++	–	–	+++	–	++	++	–	+	+++	–
B. ambifaria	AMMD	Soil	–	+++	–	+	+++	+	+++	+++	+++	+++	+++	–
B. anthina	W92^T	Soil	–	+++	–	–	+++	+	+++	+++	+++	+++	+++	++
B. anthina	C1765	CF	–	+	–	–	+++	–	+++	+++	–	+++	+	+
B. pyrrocinia	BTS7	CF	–	+++	–	+	+++	+++	+++	+++	+++	+++	+++	+
B. pyrrocinia	C1469	CF	–	++	–	++	++	+	++	+++	+++	+++	++	–

*ET12 isolates.

Staining and elution methods. Electrophoretograms and chromatograms were stained with silver nitrate (Fry, 2000) to reveal monosaccharides, oligosaccharides, alditols, saccharinic acids and phenols, and with aniline hydrogen phthalate to reveal monosaccharides and reducing disaccharides. The paper strips of interest from both methods were eluted by a syringe method with distilled H_2O (Eshdat & Mirelman, 1972). The eluted material was incorporated into 1.5 % (w/v) bacteriological agar with 0.2 % (w/v) yeast extract.

High-performance anion-exchange chromatography with pulsed amperometric detection (HPAE-PAD). Twenty microlitres each of the aqueous phases of the onion extract and the TFA-hydrolysed samples (0.1 mg ml^{-1}) were analysed by HPAE–PAD (Dionex). The system consisted of an AS3500 autosampler, GP40 gradient pump, ED40 electrochemical detector, and PC10 pneumatic controller. The amperometry detector cell contained a gold electrode and a pH-Ag/AgCl combination reference electrode. CarboPac MA-1, PA-1 and PA-100 columns and guard columns were used for the separation of alditols, monosaccharides and oligosaccharides, respectively. Eluents, degassed by bubbling with helium, were as follows: MA-1, 600 mM NaOH at 0.4 ml min^{-1} (isocratic); PA-1, 20 mM NaOH for 3 min, then H_2O for 32 min, then a 0–200 mM NaOH gradient over 10 min (all at 1.0 ml min^{-1} with post-column addition of base); PA-100, 100 mM NaOH throughout, supplemented with a 0–200 mM NaOAc gradient over 30 min, then 200–800 mM NaOAc over 10 min (all at 1.0 ml min^{-1}). Analytes were identified by comparison of retention times to those of standards and quantified by integration of peak area with Chromeleon software (Dionex).

Investigation of conserved EPS gene clusters in Bcc species. Genome sequences representing five Bcc species were examined to determine if two previously published EPS gene clusters within *B. cenocepacia* J2315, the *bce* gene cluster (Moreira *et al.*, 2003) and the *wcb* gene cluster (Parsons *et al.*, 2003), are conserved across the Bcc. The amino acid sequences for every ORF within each of the two gene clusters within *B. cenocepacia* J2315 (genome sequence available at the Wellcome Trust Sanger Institute; http://www.sanger.ac.uk/) were used to search by TBLASTN the following Bcc genome sequences: *Burkholderia ambifaria* AMMD, *Burkholderia vietnamiensis* G4, *B. multivorans* ATCC 17616, *Burkholderia* sp. 383 (all sequences are available at the US Department of Energy Joint Genome Institute; http://www.jgi.doe.gov/) and *Burkholderia dolosa* AU0158 (available at the Broad Institute; http://www.broad.mit.edu/). TBLASTN searches were performed using default parameters (BLOSUM 62, Word size 3).

RT-PCR analysis of EPS biosynthetic gene clusters. The EPS-producing strain, *B. ambifaria* AMMD, was cultured in 0.2 % (w/v) yeast extract with or without supplementation with 2 % (w/v) mannitol. RNA was extracted from mid-exponential phase cultures (RNeasy Protect Bacteria Mini kit; Qiagen) and DNase I-treated (RNase-free DNase set; Qiagen), prior to reverse transcription with 1.5 μg RNA template, random primers and SuperScript III Reverse Transcriptase (Invitrogen). cDNAs and corresponding non-RT controls were used as template in PCR reactions specific for two distinct *wza* homologues (Bamb_5549 and Bamb_3621) located within two separate putative EPS biosynthetic gene clusters. Primer sequences are available upon request.

PCR analysis of *bceB* gene. Using the *bceB* gene sequence of *B. cenocepacia* J2315, *bceB* homologues were identified within the publicly available genome sequences of *B. ambifaria* AMMD, *B. cepacia* sp. 383, *B. cenocepacia* AU1054, *B. cenocepacia* HI2424, *B. cenocepacia* PC184, *B. vietnamiensis* G4 and *B. dolosa* AU0158. The eight gene sequences were aligned, and PCR primers flanking the location of the previously described 11 bp deletion in *B. cenocepacia* J2315 (Moreira *et al.*, 2003) were designed based on conserved regions across the eight aligned sequences (For 5′-TGAAGGCGGT[G/C]GCGATCGTC-3′; Rev 5′-TCGAT[G/C]CGCACGTCGTCGAG-3′). For preparation of genomic DNA, one or two bacterial colonies were resuspended in 20 μl lysis solution [0.25 % (w/v) SDS, 0.05 M NaOH] and incubated at 95 °C for 15 min. After brief centrifugation, 180 μl sterile water was added and centrifugation performed at 13 000 *g* for 5 min. Two microlitres of supernatant containing genomic DNA was used as template in PCR assays. PCRs were performed in a 50 μl volume containing 300 nM forward and reverse primer, 1.5 mM $MgCl_2$, 260 μM of each dNTP, 4 % (v/v) DMSO, 1 U *Taq* polymerase (Invitrogen) and appropriate manufacturer's reaction buffer. Thermal cycling was performed on a GeneAmp PCR System 9700 (Applied Biosystems) with the following parameters: 94 °C 3 min; 40 cycles of 94 °C (30 s), 60 °C (30 s) and 72 °C (30 s); 72 °C 10 min. PCR products were electrophoresed on a 4 % E-Gel (Invitrogen) and visualized by UV illumination. The *B. cenocepacia* J2315 *bceB* gene sequence harbouring the 11 bp deletion yields a PCR product of 140 bp, compared to 151 bp from the wild-type sequence found in *B. cenocepacia* IST 432 (Videira *et al.*, 2005).

PCR analysis of BCESM and *cblA*. Genomic DNA was prepared as described above. PCRs were performed as described previously (Mahenthiralingam *et al.*, 1997; Sajjan *et al.*, 1995).

Insertional inactivation of *bceB* in *B. ambifaria* AMMD. Insertional inactivation of *bceB* was performed using the pGPΩTp suicide vector, essentially as described previously (Flannagan *et al.*, 2007). In brief, a 300 bp fragment internal to the *bceB* ORF of *B. ambifaria* AMMD and flanked by *Xba*I and *Eco*RI sites was PCR-amplified and ligated into the corresponding sites in pGPΩTp following appropriate restriction. Resulting plasmids were transformed into *Escherichia coli* GT115 competent cells (InvivoGen) and subsequently introduced into *B. ambifaria* AMMD by triparental mating. Resulting exconjugants were selected using gentamicin (50 mg l^{-1}) and trimethoprim (100 mg l^{-1}), and mutants identified by PCR using a chromosomal-specific primer in conjunction with the vector-specific primer RSF1300 (Flannagan *et al.*, 2007).

RESULTS

EPS production on onion agar

When a lyophilized onion extract was incorporated into agar at 2 % (w/v) as the sole nutrient, members of the Bcc were not only able to grow, but a majority of isolates also produced copious amounts of EPS, as typified by *B. ambifaria* AMMD (Fig. 1a, b). This phenotype is not observed when the Bcc are cultured on *B. cepacia* media (Mast Diagnostics), nutrient agar and other common laboratory media. Induction of EPS biosynthesis on onion agar was observed in all Bcc species investigated, but was not observed in all strains within a species (Table 1 and Supplementary Tables S1, S2 and S3, available with the online version of this paper). The exception was the single strain of *Burkholderia stabilis* available for testing. Of particular interest was the failure of the well-characterized *B. cenocepacia* ET12 representatives J2315, K56-2 and BC7 to produce EPS on onion agar. In addition, there was no correlation between induction of Bcc EPS on onion agar and the ability of individual Bcc strains to cause maceration of onion bulbs (data not shown).

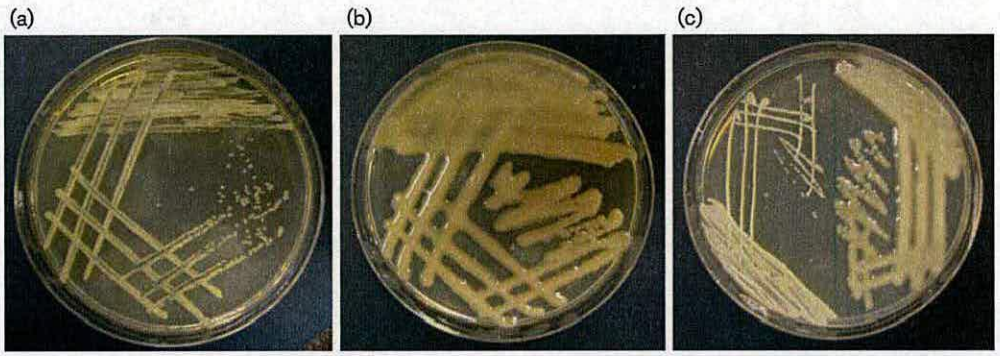

Fig. 1. Growth of *B. ambifaria* AMMD on (a) nutrient agar (non-mucoid); (b) onion agar (mucoid), and (c) comparison of AMMD *bceB* mutant (left) and AMMD wild-type (right) on mannitol agar.

The onion factor

Attempts were made to identify the 'onion factor' responsible for inducing EPS biosynthesis by use of standard biochemical methods for extracting and fractionating phytochemicals. The causative factor was retained on drying *in vacuo*, and remained in the aqueous phase after partition with ethyl acetate at pH 7.0 and pH 2.0. When further physicochemical analyses discounted the role of proteins and lipids, attention was turned to the carbohydrate content of onion extract. After preparative paper electrophoresis in buffers at pH 2.0 and 6.5, the only biological activity recovered from paper strips co-migrated with the standard glucose, indicating the absence of ionizable functional groups such as phosphate, acid or amine (data not shown). Analytical paper chromatography and HPAE-PAD identified the major carbohydrate components as sucrose, glucose, fructose and fructans (Fig. 2). The HPAE-PAD chromatograms in Fig. 2 show characteristic peaks of glucose, fructose and sucrose. Sucrose breaks down to fructose and glucose upon mild hydrolysis, as do the fructans to fructose. Fructose breaks down under complete hydrolysis as expected for a ketose sugar, whilst the aldose sugar glucose remains stable. The ability of these and related compounds to stimulate EPS biosynthesis in Bcc was then investigated (Table 1). Glycerol and mannitol were included as these sugar alcohols have previously been noted to enhance EPS biosynthesis in *Pseudomonas aeruginosa* (Whitchurch *et al.*, 1996) and the Bcc (Sage *et al.*, 1990; Zlosnik *et al.*, 2008). Glucitol was included because of its close degradative relationship with fructose and mannitol (Allenza *et al.*, 1982). These experiments showed that within a particular Bcc species, EPS biosynthesis was strain-specific and that the most potent inducers of EPS were fructose and all alditols tested, most significantly mannitol and glucitol, as well as the cyclitol *myo*-inositol. Importantly, the profile of EPS biosynthesis production with these sugars was similar to that observed with onion extract (Table 1). EPS biosynthesis was not observed on agar containing yeast extract alone, nor in the presence of glucose (Table 1), galactose, lactose or maltose (data not shown) with any Bcc strains tested.

Investigation of the molecular basis for EPS biosynthesis

With the exception of the single *B. stabilis* strain tested, all Bcc species were shown to be capable of producing EPS when grown on onion agar (Table 1 and Supplementary Tables S1–S3), suggesting the presence of a conserved EPS biosynthetic gene cluster. Therefore genome sequences representing five Bcc species (*B. ambifaria*, *B. multivorans*, *B. vietnamiensis*, *B. dolosa* and *Burkholderia* sp. 383) were examined to determine if two putative EPS gene clusters within *B. cenocepacia* J2315, the *bce* gene cluster (Moreira *et al.*, 2003) and the *wcb* gene cluster (Parsons *et al.*, 2003), are conserved across the Bcc. The *wcb* gene cluster was found to be poorly conserved, with between one-third and one-half of J2315 ORFs having no direct homologues within the species examined (data not shown). Notably, within the EPS-producing *B. ambifaria* AMMD strain, over half of the J2315 *wcb*-associated ORFs have no homologues, and the remaining homologous ORFs are not organized within a gene cluster. In contrast, the *bce* gene cluster was conserved across all species examined, in terms of both sequence homology and organization of ORFs (Supplementary Fig. S1). In the course of these genome comparisons, a third putative polysaccharide biosynthetic gene cluster was observed on chromosome 2 of *B. cenocepacia* J2315. This cluster encodes two putative EPS transporter proteins (BCAM1330 and BCAM1331), an acyltransferase (BCAM1333), several glycosyltransferases (BCAM1335, BCAM1337, BCAM1338), a polysaccharide biosynthesis protein (BCAM1336) and a mannose-6-phosphate isomerase (BCAM1340). This cluster is conserved amongst several Bcc species, albeit to a lesser extent than the *bce* gene cluster (data not shown). In the EPS-producing *B. ambifaria* AMMD, this gene cluster maps to ORFs Bamb_3621 through to Bamb_3629.

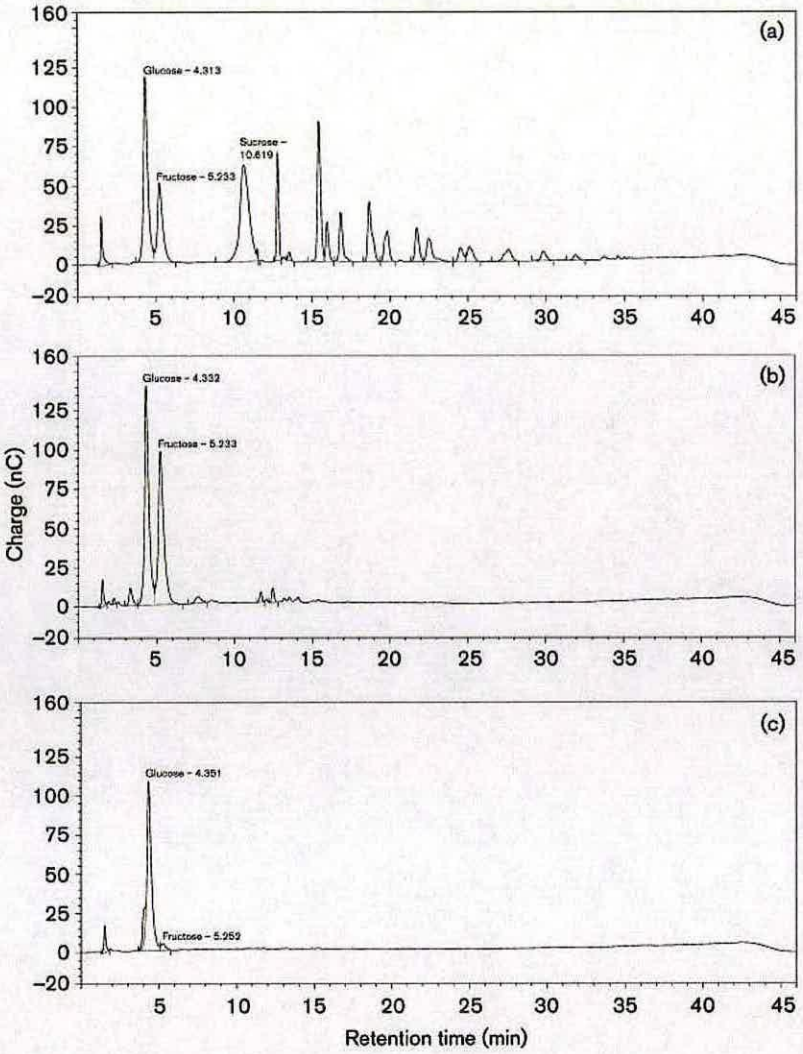

Fig. 2. HPAE-PAD chromatograms: Carbopac PA-100 column separation of sugars in onion extract. (a) Crude onion extract; (b) onion extract hydrolysed by 2 M TFA 60 °C 1 h; (c) onion extract hydrolysed by 2 M TFA 120 °C 1 h. Glucose, fructose and sucrose peaks were clearly identified based on standards (not shown), and hydrolysis pattern. Peaks with retention times between 12 and 36 min appear to be oligosaccharides of fructose based on their degradation to fructose under mild hydrolysis.

To investigate which polysaccharide gene cluster is induced by growth on mannitol, the expression of representative genes from two distinct EPS gene clusters was assessed in *B. ambifaria* AMMD grown in the presence and absence of mannitol. The genes studied each encode homologues of the Wza EPS export protein: Bamb_5549 of the *bce* gene cluster (equivalent to *bceE*, BCAM0858 of *B. cenocepacia* J2315), and Bamb_3621 of the novel putative polysaccharide gene cluster described above (BCAM1330 of *B. cenocepacia* J2315). As shown in Fig. 3, expression of Bamb_3621 was not observed under either growth condition. In contrast, expression of the *bceE* homologue (Bamb_5549) was clearly induced by the presence of mannitol. We therefore focused on the *bce* gene cluster to investigate why some Bcc isolates, most notably those of the *B. cenocepacia* ET12 lineage, failed to produce EPS under any growth conditions.

A PCR assay was designed to screen isolates for an 11 bp deletion in the *bceB* gene that has been suggested to be responsible for loss of EPS production in the CF isolate *B. cenocepacia* J2315 (Moreira *et al.*, 2003). Of the panel of strains shown in Table 1, only the *B. cenocepacia* ET12 isolates J2315, K56-2 and BC7 harbour the 11 bp deletion (data not shown). This result prompted us to test a panel of *B. cenocepacia* IIIA strains containing both ET12 and non-ET12 isolates. There was a clear correlation between the 11 bp deletion and the presence of both *cblA* (cable pilus) and BCESM (*B. cepacia* epidemic strain marker), indicating that this deletion is a conserved feature within the ET12 lineage (Fig. 4). In our study, with the exception of strain E3051, the presence of the deletion correlated with the lack of EPS production in all *B. cenocepacia* IIIA isolates examined (Fig. 4; Supplementary Table S1). Furthermore, the 11 bp deletion in the *bceB* gene was not observed in any *B. cenocepacia* IIIB or *B. multivorans* isolates studied (see Supplementary Tables S2 and S3).

Using proven methods for the complementation of gene function in *B. cenocepacia* (Ortega *et al.*, 2005), attempts were made to complement BceB function within *B. cenocepacia* K56-2 by introducing a wild-type *bceB* ORF

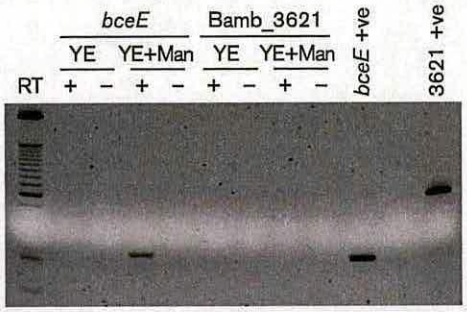

Fig. 3. Induction of the *bce* gene cluster by mannitol. RT-PCR analysis was performed to assess the expression of two distinct *wza* homologues (*bceE* and Bamb_3621) of *B. ambifaria* AMMD in the absence and presence of mannitol. The *bceE* gene (Bamb_5549) is located within the *bce* gene cluster, whilst Bamb_3621 is located within a distinct putative EPS biosynthetic gene cluster. Expression was assessed in yeast extract (YE) and yeast extract supplemented with 2% (w/v) mannitol (YE+Man). Expression of Bamb_3621 was not detected in YE or YE+Man. In contrast, *bceE* expression was strongly induced by growth in YE+Man. For each sample, RT and non-RT reactions (+/−) are shown alongside each other. Genomic DNA positive controls are shown for each gene (*bceE* +ve, 3621 +ve).

Fig. 4. *bceB* PCR analysis of representative *B. cenocepacia* IIIA isolates. For each isolate, EPS production is indicated as mucoid (M) or non-mucoid (NM) alongside PCR analysis of *bceB*, and the epidemic strain markers *cblA* and BCESM. All PCR products are pictured alongside the 1 kb Plus DNA Ladder (Invitrogen). NTC, no template control. The *bceB* PCR assay yields a 151 bp product from wild-type sequence and a 140 bp product from sequence harbouring an 11 bp deletion (as previously reported within J2315). With one exception (E3051), lack of EPS production within *B. cenocepacia* IIIA isolates correlated with the 11 bp deletion within *bceB*. This deletion was only observed within strains that were positive for both *cblA* and BCESM, indicating it to be a conserved feature of the ET12 lineage. The *bceB* deletion was not observed in a strain harbouring just one of the two epidemic strain markers (E1001).

amplified from *B. cenocepacia* PC184. Whilst expression of 6His-tagged BceB was detected in *E. coli* C41(DE3) cells, previously shown to support expression of membrane-bound proteins (Miroux & Walker, 1996), we were unable to detect expression within *B. cenocepacia* K56-2 (data not shown). Consequently, we chose to disrupt the *bceB* ORF of an EPS-producer. Insertional inactivation of the *bceB* gene resulted in loss of EPS production in *B. ambifaria* AMMD when grown on mannitol agar (Fig. 1c) and on onion agar (data not shown).

DISCUSSION

In this study, we returned to the original Bcc host and report that Bcc isolates previously considered non-mucoid produce copious amounts of EPS when onion tissue is provided as the sole nutrient, highlighting the metabolic potential of this group of organisms. This novel and surprising observation is not species-specific, and is exhibited by isolates of both clinical and environmental origin. The onion components responsible for EPS induction are primarily the carbohydrates sucrose, fructose and fructans. Additionally, all alcohol sugars tested are able to induce EPS production, in particular mannitol and glucitol.

The reasons why EPS biosynthesis is readily induced by onion extracts and, in particular, by fructose and the hexitol sugars mannitol and glucitol require further investigation. An ability to respond to inulin was confined to certain strains, all of which responded well to fructose. This suggests that the fructan polysaccharide was only active in bacteria that can hydrolyse it to fructose. The ability of one strain (BTS7) to respond particularly strongly to inulin could possibly be due to its enhanced ability to hydrolyse inulin to fructose. Interestingly, the similar profile of EPS induction shown by fructose and alcohol sugars agrees well with a previous study which showed that the initial steps of utilization of these sugars in the Bcc differ from those in most other pseudomonads. Growth of Bcc on fructose involves active transport followed by fructokinase conversion to fructose 6-phosphate then degradation via the Entner–Doudoroff pathway (Allenza *et al.*, 1982). Growth on mannitol and glucitol also requires this pathway following active uptake and intracellular oxidation to fructose.

The role of Bcc EPS as a putative virulence factor is unclear. The influence of mannitol and other alcohol sugars on EPS production suggests that the prevalence of EPS in the Bcc may have been underestimated. In addition, given the variety of human, animal, plant and other models studied, the role of EPS may be influenced by the host involved and the route of administration. EPS has been associated with altered Bcc clearance in a mouse model of infection (Conway *et al.*, 2004), and EPS-deficient Bcc mutants displayed reduced mortality within a CGD mouse model (Sousa *et al.*, 2007a). Similarly, a role for EPS in persistence

in human airways is suggested by its capacity to scavenge reactive oxygen species and inhibit neutrophil chemotaxis (Bylund *et al.*, 2006). In our study, EPS biosynthesis did not correlate with the ability to cause onion rot, which is perhaps to be expected since pectinases rather than EPS are likely to play the major role in the maceration of plant tissue. Cunha *et al.* (2004) did not observe a clear correlation between EPS biosynthesis *in vitro* and the ability of Bcc strains to establish chronic infections within the CF lung. Recent evidence, however, suggests a subtle and unexpected role for Bcc EPS in CF lung infection. Consistent with our findings, Zlosnik *et al.* (2008) reported that isolates of *B. cenocepacia*, the most virulent Bcc species, are most frequently non-mucoid. They also observed a mucoid to non-mucoid conversion in sequential isolates of Bcc from chronically infected CF patients. This apparent loss of mucoidy *in vivo*, and its absence in the virulent *B. cenocepacia* ET12 lineage, provides an intriguing contrast with the characteristic non-mucoid to mucoid conversion observed with alginate-producing *P. aeruginosa*. Zlosnik and colleagues suggest that Bcc EPS could be responsible for the persistence of Bcc in CF airways whilst loss of EPS leads to increased disease severity.

In our investigation of EPS biosynthesis determinants, we focused on the highly conserved *bce* gene cluster. Previously described by Moreira *et al.* (2003), the *bce* gene cluster has had several of its encoded proteins characterized (Ferreira *et al.*, 2007; Sousa *et al.*, 2007b; Videira *et al.*, 2005) and is thought to be involved in cepacian biosynthesis. In the present study, we demonstrated induction of the *bce* gene cluster by mannitol, and found a clear correlation between the inability of representatives of the *B. cenocepacia* ET12 lineage to produce EPS and the presence of an 11 bp deletion within the *bceB* gene, originally described within the genome sequence of *B. cenocepacia* J2315 (Moreira *et al.*, 2003). Consistent with this correlation, insertional inactivation of *bceB*, which encodes a glycosyltransferase, resulted in the loss of EPS production by *B. ambifaria* AMMD when grown on onion media. Combined, these observations highlight the pivotal role of the *bce* gene cluster in onion-induced EPS biosynthesis, and suggest that the observed EPS is cepacian. However, mutations elsewhere within the *bce* gene cluster, or in other EPS-related gene clusters, must be responsible for the lack of EPS biosynthesis in *B. cenocepacia* strain E3051 (Supplementary Table S1), and in other EPS-negative Bcc strains in our study which lack the 11 bp deletion in *bceB* (Supplementary Tables S2 and S3).

The ability of hexoses and hexitols, in particular mannitol, to enhance EPS biosynthesis in the *B. cepacia* complex has disturbing implications for therapeutic intervention in CF. Recent attempts to improve airway clearance with hypertonic saline 5% (w/v) have been handicapped by the problem of salty taste and the salt-sensitive nature of many antimicrobial peptides. Thus, attention has turned to the use of non-ionic osmolytes, including inhaled mannitol (Daviskas *et al.*, 2008; Robinson *et al.*, 1999; Wills, 2007), which is marketed as Bronchitol (Pharmaxis). Robinson and colleagues acknowledged that the majority of *P. aeruginosa* and Bcc isolates are able to utilize mannitol as a carbon and energy source. However, they felt that the nutritional influence of mannitol as a therapeutic osmolyte would be minimal given the abundance of other nutrients already present in CF respiratory secretions. On a cautionary note, they state that this potential problem would need to be confirmed by quantitative microbiology. The potential induction of virulence determinants during osmolyte therapy has to our knowledge not been considered. Our results also provide justification for the continued exclusion of CF individuals known to be infected with Bcc from ongoing trials of inhaled mannitol (http://clinicaltrials.gov; identifier NCT00117208 and NCT00251056).

ACKNOWLEDGEMENTS

We thank Catherine Doherty (University of Edinburgh, UK) for the strain panels, Rosanna Hennessy (University of Edinburgh, UK) for the RT-PCR data, Paola Cescutti (Università di Trieste, Italy) for *Burkholderia pyrrocinia* BTS7 and *B. cenocepacia* BTS2, and Miguel Valvano (University of Western Ontario, Canada) for the suicide vector pGPΩTp and complementation vector pSCRhaB3. S. J. B., A. R. B., J. R. W. G. and D. J. C. thank the CF Trust and the Big Lottery Fund, D. J. C. and D. J. C. also thank the Royal Society of Edinburgh, and S. C. F. and B. R. M. thank the Biotechnology and Biological Sciences Research Council for financial support.

REFERENCES

Allenza, P., Lee, Y. N. & Lessie, T. G. (1982). Enzymes related to fructose utilization in *Pseudomonas cepacia*. *J Bacteriol* **150**, 1348–1356.

Bernier, S. P., Silo-Suh, L., Woods, D. E., Ohman, D. E. & Sokol, P. A. (2003). Comparative analysis of plant and animal models for characterization of *Burkholderia cepacia* virulence. *Infect Immun* **71**, 5306–5313.

Burkholder, W. (1950). Sour skin, a bacterial rot of onion bulbs. *Phytopathology* **40**, 115–117.

Bylund, J., Burgess, L. A., Cescutti, P., Ernst, R. K. & Speert, D. P. (2006). Exopolysaccharides from *Burkholderia cenocepacia* inhibit neutrophil chemotaxis and scavenge reactive oxygen species. *J Biol Chem* **281**, 2526–2532.

Coenye, T., Vandamme, P., LiPuma, J. J., Govan, J. R. & Mahenthiralingam, E. (2003). Updated version of the *Burkholderia cepacia* complex experimental strain panel. *J Clin Microbiol* **41**, 2797–2798.

Conway, B. A., Chu, K. K., Bylund, J., Altman, E. & Speert, D. P. (2004). Production of exopolysaccharide by *Burkholderia cenocepacia* results in altered cell-surface interactions and altered bacterial clearance in mice. *J Infect Dis* **190**, 957–966.

Cunha, M. V., Sousa, S. A., Leitao, J. H., Moreira, L. M., Videira, P. A. & Sa-Correia, I. (2004). Studies on the involvement of the exopolysaccharide produced by cystic fibrosis-associated isolates of the *Burkholderia cepacia* complex in biofilm formation and in persistence of respiratory infections. *J Clin Microbiol* **42**, 3052–3058.

Daviskas, E., Anderson, S. D., Eberl, S. & Young, I. H. (2008). Effect of increasing doses of mannitol on mucus clearance in patients with bronchiectasis. *Eur Respir J* **31**, 765–772.

Eshdat, Y. & Mirelman, D. (1972). An improved method for the recovery of compounds from paper chromatograms. *J Chromatogr* **65**, 458–459.

Ferreira, A. S., Leitao, J. H., Sousa, S. A., Cosme, A. M., Sa-Correia, I. & Moreira, L. M. (2007). Functional analysis of *Burkholderia cepacia* genes *bceD* and *bceF*, encoding a phosphotyrosine phosphatase and a tyrosine autokinase, respectively: role in exopolysaccharide biosynthesis and biofilm formation. *Appl Environ Microbiol* **73**, 524–534.

Flannagan, R. S., Aubert, D., Kooi, C., Sokol, P. A. & Valvano, M. A. (2007). *Burkholderia cenocepacia* requires a periplasmic HtrA protease for growth under thermal and osmotic stress and for survival in vivo. *Infect Immun* **75**, 1679–1689.

Fry, S. C. (2000). *The Growing Plant Cell Wall: Chemical and Metabolic Analysis.* Caldwell, NJ: The Blackburn Press.

Goldberg, J. B. (2007). Polysaccharides of *Burkholderia* spp. In *Burkholderia: Molecular Microbiology and Genomics*, pp. 93–110. Edited by T. Coenye & P. Vandamme. Norwich, UK: Horizon Bioscience.

Govan, J. R. W. (2006). *Burkholderia cepacia* complex and *Stenotrophomonas maltophilia*. In *Cystic Fibrosis in the 21st Century: Progress in Respiratory Research*, pp. 145–152. Edited by A. Bush, E. W. F. W. Alton, J. C. Davies, U. Griesenbach & A. Jaffe. Basel: Karger.

Govan, J. R. & Deretic, V. (1996). Microbial pathogenesis in cystic fibrosis: mucoid *Pseudomonas aeruginosa* and *Burkholderia cepacia*. *Microbiol Rev* **60**, 539–574.

Govan, J. R., Brown, P. H., Maddison, J., Doherty, C. J., Nelson, J. W., Dodd, M., Greening, A. P. & Webb, A. K. (1993). Evidence for transmission of *Pseudomonas cepacia* by social contact in cystic fibrosis. *Lancet* **342**, 15–19.

Herasimenka, Y., Benincasa, M., Mattiuzzo, M., Cescutti, P., Gennaro, R. & Rizzo, R. (2005). Interaction of antimicrobial peptides with bacterial polysaccharides from lung pathogens. *Peptides* **26**, 1127–1132.

Mahenthiralingam, E., Simpson, D. A. & Speert, D. P. (1997). Identification and characterization of a novel DNA marker associated with epidemic *Burkholderia cepacia* strains recovered from patients with cystic fibrosis. *J Clin Microbiol* **35**, 808–816.

Mahenthiralingam, E., Coenye, T., Chung, J. W., Speert, D. P., Govan, J. R., Taylor, P. & Vandamme, P. (2000). Diagnostically and experimentally useful panel of strains from the *Burkholderia cepacia* complex. *J Clin Microbiol* **38**, 910–913.

Mahenthiralingam, E., Urban, T. A. & Goldberg, J. B. (2005). The multifarious, multireplicon *Burkholderia cepacia* complex. *Nat Rev Microbiol* **3**, 144–156.

Miroux, B. & Walker, J. E. (1996). Over-production of proteins in *Escherichia coli*: mutant hosts that allow synthesis of some membrane proteins and globular proteins at high levels. *J Mol Biol* **260**, 289–298.

Moreira, L. M., Videira, P. A., Sousa, S. A., Leitao, J. H., Cunha, M. V. & Sa-Correia, I. (2003). Identification and physical organization of the gene cluster involved in the biosynthesis of *Burkholderia cepacia* complex exopolysaccharide. *Biochem Biophys Res Commun* **312**, 323–333.

Ortega, X., Hunt, T. A., Loutet, S., Vinion-Dubiel, A. D., Datta, A., Choudhury, B., Goldberg, J. B., Carlson, R. & Valvano, M. A. (2005). Reconstitution of O-specific lipopolysaccharide expression in *Burkholderia cenocepacia* strain J2315, which is associated with transmissible infections in patients with cystic fibrosis. *J Bacteriol* **187**, 1324–1333.

Parsons, Y. N., Banasko, R., Detsika, M. G., Duangsonk, K., Rainbow, L., Hart, C. A. & Winstanley, C. (2003). Suppression-subtractive hybridisation reveals variations in gene distribution amongst the *Burkholderia cepacia* complex, including the presence in some strains of a genomic island containing putative polysaccharide production genes. *Arch Microbiol* **179**, 214–223.

Robinson, M., Daviskas, E., Eberl, S., Baker, J., Chan, H. K., Anderson, S. D. & Bye, P. T. (1999). The effect of inhaled mannitol on bronchial mucus clearance in cystic fibrosis patients: a pilot study. *Eur Respir J* **14**, 678–685.

Sage, A., Linker, A., Evans, L. R. & Lessie, T. G. (1990). Hexose phosphate metabolism and exopolysaccharide formation in *Pseudomonas cepacia*. *Curr Microbiol* **20**, 191–198.

Sajjan, U. S., Sun, L., Goldstein, R. & Forstner, J. F. (1995). Cable (*cbl*) type II pili of cystic fibrosis-associated *Burkholderia* (*Pseudomonas*) *cepacia*: nucleotide sequence of the *cblA* major subunit pilin gene and novel morphology of the assembled appendage fibers. *J Bacteriol* **177**, 1030–1038.

Sist, P., Cescutti, P., Skerlavaj, S., Urbani, R., Leitao, J. H., Sa-Correia, I. & Rizzo, R. (2003). Macromolecular and solution properties of cepacian: the exopolysaccharide produced by a strain of *Burkholderia cepacia* isolated from a cystic fibrosis patient. *Carbohydr Res* **338**, 1861–1867.

Sousa, S. A., Ulrich, M., Bragonzi, A., Burke, M., Worlitzsch, D., Leitão, J. H., Meisner, C., Eberl, L., Sá-Correia, I. & Döring, G. (2007a). Virulence of *Burkholderia cepacia* complex strains in gp91phox$^{-/-}$ mice. *Cell Microbiol* **9**, 2817–2825.

Sousa, S. A., Moreira, L. M., Wopperer, J., Eberl, L., Sá-Correira, I. & Leitão, J. H. (2007b). The *Burkholderia cepacia bceA* gene encodes a protein with phosphomannose isomerase and GDP-D-mannose pyrophosphorylase activities. *Biochem Biophys Res Commun* **353**, 200–206.

Videira, P. A., Garcia, A. P. & Sa-Correia, I. (2005). Functional and topological analysis of the *Burkholderia cenocepacia* priming glucosyltransferase BceB, involved in the biosynthesis of the cepacian exopolysaccharide. *J Bacteriol* **187**, 5013–5018.

Whitchurch, C. B., Alm, R. A. & Mattick, J. S. (1996). The alginate regulator AlgR and an associated sensor FimS are required for twitching motility in *Pseudomonas aeruginosa*. *Proc Natl Acad Sci U S A* **93**, 9839–9843.

Wills, P. J. (2007). Inhaled mannitol in cystic fibrosis. *Expert Opin Investig Drugs* **16**, 1121–1126.

Zlosnik, J. E., Hird, T. J., Fraenkel, M. C., Moreira, L. M., Henry, D. A. & Speert, D. P. (2008). Differential mucoid exopolysaccharide production by members of the *Burkholderia cepacia* complex. *J Clin Microbiol* **46**, 1470–1473.

Edited by: P. Cornelis

Microbiology (2009), 155, 2029–2039 DOI 10.1099/mic.0.027607-0

Contributions of two UDP-glucose dehydrogenases to viability and polymyxin B resistance of *Burkholderia cenocepacia*

Slade A. Loutet,[1] S. Josefin Bartholdson,[2,3] John R. W. Govan,[2] Dominic J. Campopiano[3] and Miguel A. Valvano[1,4]

Correspondence
Miguel A. Valvano
mvalvano@uwo.ca

[1]Department of Microbiology and Immunology, Infectious Diseases Research Group, Siebens-Drake Research Institute, University of Western Ontario, London, Ontario N6A 5C1, Canada

[2]Centre for Infectious Diseases, University of Edinburgh Medical School, Edinburgh EH16 4SB, UK

[3]School of Chemistry, University of Edinburgh, Edinburgh EH9 3JJ, UK

[4]Department of Medicine, Infectious Diseases Research Group, Siebens-Drake Research Institute, University of Western Ontario, London, Ontario N6A 5C1, Canada

Received 16 January 2009
Revised 7 March 2009
Accepted 16 March 2009

Burkholderia cenocepacia is highly resistant to antimicrobial peptides and we hypothesized that the conversion of UDP-glucose to UDP-glucuronic acid, a reaction catalysed by the enzyme UDP-glucose dehydrogenase (Ugd) would be important for this resistance. The genome of *B. cenocepacia* contains three predicted *ugd* genes: $ugd_{BCAL2946}$, $ugd_{BCAM0855}$ and $ugd_{BCAM2034}$, all of which were individually inactivated. Only inactivation of $ugd_{BCAL2946}$ resulted in increased sensitivity to polymyxin B and this sensitivity could be overcome when either $ugd_{BCAL2946}$ or $ugd_{BCAM0855}$ but not $ugd_{BCAM2034}$ was expressed from plasmids. The growth of a conditional $ugd_{BCAL2946}$ mutant, created in the $\Delta ugd_{BCAM0855}$ background, was significantly impaired under non-permissive conditions. Growth could be rescued by either $ugd_{BCAL2946}$ or $ugd_{BCAM0855}$ expressed *in trans*, but not by $ugd_{BCAM2034}$. Biochemical analysis of the purified, recombinant forms of $Ugd_{BCAL2946}$ and $Ugd_{BCAM0855}$ revealed that they are soluble homodimers with similar *in vitro* Ugd activity and comparable kinetic constants for their substrates UDP-glucose and NAD^+. Purified $Ugd_{BCAM2034}$ showed no *in vitro* Ugd activity. Real-time PCR analysis showed that the expression of $ugd_{BCAL2946}$ was 5.4- and 135-fold greater than that of $ugd_{BCAM0855}$ and $ugd_{BCAM2034}$, respectively. Together, these data indicate that the combined activity of $Ugd_{BCAL2946}$ and $Ugd_{BCAM0855}$ is essential for the survival of *B. cenocepacia* but only the most highly expressed *ugd* gene, $ugd_{BCAL2946}$, is required for polymyxin B resistance.

INTRODUCTION

Burkholderia cenocepacia belongs to the *Burkholderia cepacia* complex (Bcc), a group of ten phenotypically similar environmental Gram-negative bacteria (Balandreau *et al.*, 2001), which are also opportunistic human pathogens causing chronic, sometimes fatal, pulmonary infections in cystic fibrosis (CF) patients (Isles *et al.*, 1984; Mahenthiralingam *et al.*, 2005). Treatment of these infections is difficult as Bcc bacteria are inherently resistant to most clinically relevant antimicrobial agents (Aaron *et al.*, 2000; Burns *et al.*, 1996; Gold *et al.*, 1983), including antimicrobial peptides (APs) (Loutet *et al.*, 2006; Turner *et al.*, 1998).

APs are short, amphipathic, positively charged peptides produced by organisms from bacteria to mammals (Brogden, 2005). They are part of the innate immune response (Ganz, 2003; Zanetti, 2004) and have been shown to kill bacteria through the disruption of the inner membrane (Brogden, 2005) and also through inhibition of intracellular processes (Patrzykat *et al.*, 2002). APs have been proposed as agents for treatment of infections by other CF lung pathogens, such as *Pseudomonas aeruginosa* (Zhang *et al.*, 2005). Unfortunately, due to the extraordinary resistance of *B. cenocepacia* to the killing effects of APs, they are unlikely to be useful agents for treatment of lung infections by *B. cenocepacia*. Understanding the determinants of AP resistance in *B. cenocepacia* is important because they could provide targets for the

Abbreviations: APs, antimicrobial peptides; Ara4N, 4-amino-4-*deoxy*-L-arabinose; CF, cystic fibrosis; DDM, dodecylmaltoside; pmB, polymyxin B; Ugd, UDP-glucose dehydrogenase.

Supplementary methods and tables of strains and primers are available with the online version of this paper.

development of novel antimicrobial agents that could be co-administered with APs. For example, in *B. cenocepacia* L-*glycero*-D-*manno*-heptose sugars of the lipopolysaccharide (LPS) core oligosaccharide are required for AP resistance and *in vivo* survival (Loutet *et al.*, 2006) and small molecule inhibitors of the synthesis of these sugars have been identified (De Leon *et al.*, 2006).

A widely recognized mechanism of AP resistance in Gram-negative bacteria is the decoration of lipid A phosphate residues with the positively charged sugar 4-amino-4-*deoxy*-L-arabinose (Ara4N), which requires the synthesis of a UDP-Ara4N precursor (Ernst *et al.*, 1999; Helander *et al.*, 1994; Nummila *et al.*, 1995; Vaara *et al.*, 1981). Ara4N substitution reduces the net negative charge of the lipid A molecule and hampers the ability of APs to bind to the outer membrane (Vaara *et al.*, 1981). In *P. aeruginosa* and *Salmonella enterica*, these substitutions are induced upon treatment with APs (Bader *et al.*, 2005; McPhee *et al.*, 2003) and are dispensable for growth under normal laboratory conditions. In *B. cepacia*, a species closely related to *B. cenocepacia*, Ara4N is constitutively incorporated into both lipid A and the LPS core oligosaccharide (Silipo *et al.*, 2005). Preliminary evidence suggests that this is also true in *B. cenocepacia* (X. P. Ortega & M. A. Valvano, unpublished data) and UDP-Ara4N synthesis was recently shown to be essential for *B. cenocepacia* viability (Ortega *et al.*, 2007). These results highlight the importance of Ara4N in this organism and its abundance in LPS likely contributes significantly to the organism's unusually high AP resistance.

The initial step in the synthesis of UDP-Ara4N is the conversion of UDP-glucose to UDP-glucuronic acid, which is catalysed by the enzyme UDP-glucose dehydrogenase (Ugd) (Breazeale *et al.*, 2002; Raetz & Whitfield, 2002; Strominger *et al.*, 1957). A recent study by Hung *et al.* (2007) described two Ugd-encoding genes in *P. aeruginosa*. Both Ugd enzymes were purified as homodimers, and biochemical analysis confirmed Ugd activity, but revealed distinct expression and enzymic properties, indicating different roles for the two Ugd proteins *in vivo*.

The *B. cenocepacia* genome (Holden *et al.*, 2009) contains three predicted *ugd* genes, designated $ugd_{BCAL2946}$, $ugd_{BCAM0855}$ and $ugd_{BCAM2034}$ (gene designations correspond to the Sanger Centre annotation of the strain J2315 genome, http://www.sanger.ac.uk/Projects/B_cenocepacia/, where BCAL denotes genes in the large chromosome and BCAM genes in the mid-size chromosome). In this study, we examined in detail the function of these genes and show that only $ugd_{BCAL2946}$ is required for resistance to polymyxin B (pmB), while the combination of $ugd_{BCAL2946}$ and $ugd_{BCAM0855}$ is required for bacterial survival. We purified $Ugd_{BCAL2946}$, $Ugd_{BCAM0855}$ and $Ugd_{BCAM2034}$ but only the recombinant forms of $Ugd_{BCAL2946}$ and $Ugd_{BCAM0855}$ possess Ugd activity with similar substrate reaction kinetics. Finally, we show that in cells the number of RNA transcripts of $ugd_{BCAL2946}$ is substantially higher than either $ugd_{BCAM0855}$ or $ugd_{BCAM2034}$.

METHODS

Reagents. Unless otherwise noted all chemicals and antibiotics, restriction endonucleases and DNA polymerases were purchased from Sigma-Aldrich, Roche Diagnostics and Qiagen, respectively.

Bacterial strains and culture conditions. Strains and plasmids used in this study are described in Supplementary Table S1, available with the online version of this paper. *B. cenocepacia* and *Escherichia coli* strains were routinely cultured at 37 °C either in Luria Broth (LB) supplemented with 1.6 % (w/v) Bacto Agar (Becton Dickinson) or in liquid LB. When required, trimethoprim or tetracycline was added at a final concentration of 100 μg ml^{-1} for selection of *B. cenocepacia* strains, and at 50 μg ml^{-1} and 20 μg ml^{-1}, respectively, for selection of *E. coli* strains. Kanamycin and gentamicin were used at 40 μg ml^{-1} and 50 μg ml^{-1}, respectively.

Mutagenesis and cloning. A complete description of the mutagenesis and cloning experiments can be found in Supplementary Methods and the primers used are listed in Supplementary Table S2. To inactivate the putative *ugd* genes, suicide plasmids containing internal fragments of each *ugd* gene were created. The fragments were PCR amplified, restriction enzyme digested, ligated into the plasmid pGPlox (Table S1), used to transform *E. coli* SY327 (Miller & Mekalanos, 1988), and confirmed by colony PCR and restriction digest. The resulting plasmids – pSL23 ($ugd_{BCAL2946}$), pSL29 ($ugd_{BCAM2034}$) and pSL31 ($ugd_{BCAM0855}$) – were transferred into *B. cenocepacia* strain K56-2 (Mahenthiralingam *et al.*, 2000) by triparental mating with the pRK2013 helper plasmid (Figurski & Helinski, 1979). Exconjugants were screened for plasmid insertion into the correct location by PCR and Southern blot hybridization. The resulting mutants were named SAL8 ($ugd_{BCAL2946}$::pSL23), SAL12 ($ugd_{BCAM2034}$::pSL29) and SAL15 ($ugd_{BCAL0855}$::pSL31).

To construct an unmarked $ugd_{BCAM0855}$ deletion mutant, two fragments of this gene were PCR amplified, restriction enzyme digested, ligated as a triple ligation into pGPI-SceI (Flannagan *et al.*, 2008), screened as described above, and the resulting plasmid, pSL43, was transferred to K56-2. Putative mutants (SAL22) were screened by PCR for recombination of the plasmid into the chromosome. To delete the backbone of pSL43 from the chromosome, pDAI-SceI (Flannagan *et al.*, 2008) was introduced into SAL22, and this resulted in the isolation of strain SAL23, which carries a 986 bp deletion removing most of $ugd_{BCAM0855}$. pDAI-SceI was cured from SAL23 by serial passage in the absence of tetracycline for 1 week. The final mutant construct was confirmed by Southern blot hybridization.

Plasmids for the conditional mutagenesis of *hldA* and $ugd_{BCAL2946}$ were constructed as described above with fragments corresponding to the 5′ ends of the two genes cloned into the plasmid pSC201 (Ortega *et al.*, 2007), resulting in plasmids pSL26 (*hldA*) and pSL27 ($ugd_{BCAL2946}$). These plasmids were transferred into SAL23, resulting in strains SAL25 (conditional *hldA*) and SAL26 (conditional $ugd_{BCAL2946}$). A conditional $ugd_{BCAL2946}$ mutant in the K56-2 background (SAL10), also constructed with pSL27, was previously described (Ortega *et al.*, 2007).

For complementation experiments each of the putative *ugd* genes was cloned into pDA17 (Aubert *et al.*, 2008). Plasmids were confirmed as described above, inserts were verified by sequencing (Robarts Research Institute DNA Sequencing Facility, London, ON, Canada), and the resulting plasmids were named pSL37 ($ugd_{BCAL2946}$), pSL38 ($ugd_{BCAM2034}$) and pSL39 ($ugd_{BCAM0855}$).

For expression and purification of the Ugd proteins, the *B. cenocepacia* J2315 $ugd_{BCAL2946}$, $ugd_{BCAM0855}$ and $ugd_{BCAM2034}$ genes were PCR amplified, cloned using the pGEM-T Easy vector system (Promega), and sequenced. Genes were liberated by restriction enzyme digest, ligated into pET28a (Novagen), and used to transform

E. coli Top10 cells. The resulting plasmids were confirmed by restriction digests and named pJB1 (pET28a/$ugd_{BCAL2946}$), pJB2 (pET28a/$ugd_{BCAM0855}$) and pJB3 (pET28a/$ugd_{BCAM2034}$), with each *ugd* expressed with an N-terminal His_6 fusion tag.

Growth curves. Cells were cultured overnight to stationary phase and then diluted to an OD_{600} of 0.05 in LB. Cultures were aliquoted to 100-well honeycomb plates in 300 µl volumes. Plates were incubated in a Bioscreen C automated growth curve reader at 37 °C with constant, low shaking for 24 h with OD_{600} readings taken every hour. For growth curves with pmB, cells were diluted to approximately 2×10^5 c.f.u. ml^{-1} in LB. Then 10 × stock solutions of pmB dissolved in 0.2 % (w/v) BSA + 0.02 % (v/v) acetic acid were added to cells to give final concentrations of pmB ranging from 16 to 1024 µg ml^{-1} in twofold increments. Cells were also treated with the pmB diluent indicated above as a vehicle control. Triplicate 300 µl aliquots of the cells with either vehicle control or the various concentrations of pmB were incubated in the Bioscreen C automated growth curve reader, as described above, for 18 h. MIC_{50} values reported are the mode of three independent experiments. An assay for growth of conditional mutants was performed as previously described (Ortega *et al.*, 2007). Expression of putative essential genes was repressed with 1.0 % (w/v) glucose and induced with 1.0 % (w/v) rhamnose.

LPS extraction and analysis. LPS samples were prepared and analysed as previously described (Hitchcock & Brown, 1983; Loutet *et al.*, 2006).

Western blotting. Cells were grown overnight in liquid LB with appropriate antibiotics. A volume of culture equivalent to 1 ml at an OD_{600} of 0.2 was centrifuged for 1 min at 8000 *g*; cells were resuspended in 20 µl H_2O and 10 µl of 3 × loading dye, and boiled for 10 min. Aliquots (15 µl) of boiled samples were separated by gel electrophoresis using 14 % (w/v) SDS-polyacrylamide gels and transferred to a nitrocellulose membrane. The membrane was washed briefly with H_2O and stained with a solution of 0.1 % (w/v) Ponceau S in 5 % (v/v) acetic acid to confirm the transfer of equal amounts of protein to the membrane in each lane. The membrane was rinsed with Tris-buffered saline, pH 7.5 (TBS) to remove Ponceau S stain and then blocked for 2 h with 10 % (v/v) Western blocking reagent (Roche) in TBS at room temperature and incubated with murine anti-FLAG M2 monoclonal antibody diluted 1 : 10 000 overnight at 4 °C. The membrane was incubated at room temperature for 2 h with goat anti-mouse IgG antibody conjugated to Alexa Fluor 680 (Molecular Probes) diluted 1 : 20 000. Proteins were visualized using a Licor Infrared Imaging System with Odyssey software version 2.1.

Purification of recombinant Ugd proteins. To prepare recombinant $Ugd_{BCAL2946}$ and $Ugd_{BCAM0855}$ proteins for biochemical analysis, a large-scale culture (4 l LB with kanamycin) was performed with *E. coli* HMS 174 (DE3) transformed with pJB1 or pJB2. Each batch was grown to an OD_{600} of 0.6, and induced with 0.5 mM IPTG for 3 h at 37 °C with shaking. Both $Ugd_{BCAL2946}$ and $Ugd_{BCAM0855}$ were highly overexpressed in soluble forms and cell-free extracts were prepared by sonic disruption of the *E. coli* cell paste. The enzymes were isolated from ultrafiltered cell-free extracts by FPLC (ÄKTA Basic instrument) using a 5 ml HisTrap column (GE Healthcare). The binding buffer consisted of 20 mM Tris, 500 mM NaCl, 5 mM imidazole, pH 7.5, and the elution buffer was identical except that it contained 500 mM imidazole. The eluted His-tagged Ugd proteins were judged >90 % pure after this step. The enzymes were dialysed against 150 mM NaCl and 20 mM Tris, pH 7.5, and further purified by size exclusion chromatography using a HiPrep 26/60 Sephacryl S-200 column (GE Healthcare). The calibrated column was equilibrated with 150 mM NaCl and 20 mM Tris, pH 7.5. The molecular masses of the Ugd proteins, estimated from their column elution volumes and by non-denaturing gel electrophoresis, were consistent with dimers (data not shown). The subunit molecular masses were confirmed by electrospray-mass spectrometry (ESI-MS) and were within 0.1 % of the theoretical values (data not shown). The protein concentration was determined by a BCA assay (Pierce) and a typical yield was ~3 mg Ugd per litre of *E. coli* culture.

To prepare recombinant $Ugd_{BCAM2034}$, a large-scale culture (4 l LB with kanamycin) was performed with *E. coli* BL21 (DE3) transformed with pJB3. Each batch was grown to an OD_{600} of 0.6, and induced by addition of 0.2 mM IPTG for 16 h at 15 °C with shaking. To solubilize $Ugd_{BCAM2034}$ for purification, the pellet was resuspended and homogenized in 5 ml binding buffer containing 25 % (w/v) sucrose, 1 mM EDTA and a protease inhibitor tablet per gram of cell pellet. Thirty mg lysozyme, 5 µl DNase and 5 mM $MgCl_2$ were added and the cell paste was left to stir for 1 h at 4 °C. A cell-free extract was prepared by sonic disruption of the *E. coli* cell paste, which was incubated with 1 % (w/v) dodecylmaltoside (DDM) and 20 % (v/v) glycerol for 1 h at 4 °C with stirring before centrifugation at 25 000 *g* for 45 min. The supernatant was incubated with equilibrated nickel NTA agar beads (Qiagen) for 3 h. The beads were then washed in elution buffer [20 mM Tris, pH 7.5, 500 mM NaCl, 0.1 % (w/v) DDM and 10 % glycerol] with 10 mM imidazole. Protein was eluted in elution buffer containing 20, 50, 100 or 200 mM imidazole. The molecular mass of $Ugd_{BCAM2034}$ was estimated from size-exclusion chromatography (as above), ESI-MS and non-denaturing gel electrophoresis (data not shown).

***In vitro* Ugd activity assay.** Ugd oxidizes UDP-glucose to UDP-glucuronic acid, and in the process also reduces 2 mol NAD^+ to 2 mol NADH. The absorption coefficient of NADH is 6.220 mM^{-1} cm^{-1} at 340 nm. A standard Ugd activity assay was set up using 200 µl H_2O, 100 µl purified Ugd (1 mg ml^{-1}), 200 µl buffer (100 mM Tris, pH 7.5), 250 µl NAD^+ (10 mM; Roche) at 25 °C. The reaction was initiated by the addition of 250 µl UDP-glucose (1 mM; Calbiochem) and the production of NADH was monitored at 340 nm on a Cary 50 UV visible spectrophotometer (Varian). Initial velocities were determined for UDP-glucose using concentrations ranging from 0 to 0.25 mM, and for NAD^+ using concentrations ranging from 0 to 2.5 mM. To determine kinetic constants, one substrate was held constant at the maximum concentration, while the other was varied. The kinetic parameters (k_{cat}, K_m, V_{max}) were determined by non-linear regression from $V = V_{max}[S]^h/([S]^h + K_m{}^h)$ using Origin 6.1 software. Substrate specificity was investigated by replacing the substrate UDP-glucose with either UDP-galactose, UDP-acetylglucosamine or GDP-mannose (Calbiochem), and performing the standard assay.

Real-time PCR analysis. *B. cenocepacia* strain K56-2 was grown overnight in liquid LB, diluted to an OD_{600} of 0.1 and grown to a final OD_{600} between 0.5 and 0.7. RNA was prepared from approximately 5×10^8 c.f.u. with the Ribo-Pure Bacteria kit (Ambion) according to the manufacturer's instructions. RNA was treated with DNase I (Ambion) and the concentration of RNA was determined with an ND-1000 spectrophotometer (NanoDrop Technologies). One microgram of RNA was converted to cDNA using Transcriptor Reverse Transcriptase (Roche) in a reaction volume of 30 µl with reverse primers 3136 (*hisD*), 3246 ($ugd_{BCAM0855}$), 3247 ($ugd_{BCAL2946}$) and 3364 ($ugd_{BCAM2034}$) according to the manufacturer's instructions and supplemented with Protector RNase Inhibitor (Roche), 0.5 × Q solution (Qiagen) and 10 % (v/v) DMSO. A second reaction containing nuclease-free water (Qiagen) instead of Transcriptor Reverse Transcriptase was included as a negative control.

The real-time PCRs were conducted using the Rotor-Gene 6000 (Corbett Life Science) in final reaction volumes of 20 µl. Reactions of 18 µl, containing FastStart SYBR Green (Roche), primer pairs 3247/3255 ($ugd_{BCAL2946}$), 3361/3364 ($ugd_{BCAM2034}$), 3246/3248

($ugd_{BCAM0855}$) or 3136/3143 (*hisD*), and nuclease-free water were prepared and to these 2 µl of the reverse transcription reactions was added in triplicate. Negative controls were 2 µl of the reverse transcription reaction done without Transcriptor Reverse Transcriptase and 2 µl of nuclease-free water. The segment of each gene analysed was also amplified from chromosomal DNA and used in standard curve reactions containing 10^6, 10^5, 10^4, 10^3 and 10^2 copies of the PCR products per reaction. The thermal cycling conditions were 95 °C for 10 min, 35 cycles at 95 °C for 10 s, 60 °C for 15 s, and 72 °C for 30 s. Data were acquired on the green channel at the end of each cycle. After the PCR a melt curve was obtained by increasing the temperature from 72 °C to 95 °C in 1 °C increments, with data acquired on the green channel at each degree. Data were analysed using the Rotor-Gene 6000 software provided by the manufacturer. For each analysed gene, the number of copies per reaction was quantified by comparison to the standard curve and adjusted based on the PCR efficiency calculated from the standard curve. A mean value from three replicates was calculated for the internal control *hisD*. Each replicate value of each *ugd* gene was divided by the mean of the *hisD* results in order to obtain a ratio of each value to *hisD*.

Statistical analyses. Statistical analyses were done with GraphPad Prism 4.

RESULTS

Identification of three putative *ugd* genes in *B. cenocepacia*

A TBLASTN analysis of the genome of *B. cenocepacia* strain J2315 (Holden *et al.*, 2009) using the *P. aeruginosa* strain PAO1 Ugd (PA2022; accession no. NP_250712) gave three high scoring hits: $ugd_{BCAL2946}$, $ugd_{BCAM0855}$ and $ugd_{BCAM2034}$. The presence of these genes was also confirmed in strain K56-2, which is clonally related to J2315 (Mahenthiralingam *et al.*, 2000), but much more amenable to genetic manipulation. The chromosomal arrangements of these genes are shown in Fig. 1(a). $ugd_{BCAL2946}$ is directly upstream of *hldA* and *hldD* within a six-gene cluster. *hldA* and *hldD* encode proteins required for the synthesis of L-*glycero*-D-*manno*-heptose, a critical residue of the LPS inner-core oligosaccharide (Loutet *et al.*, 2006). $ugd_{BCAM0855}$, annotated as *bceC* by Moreira *et al.* (2003), is in a ten-gene cluster (the final five genes of which are not depicted in Fig. 1a) that plays a role in exopolysaccharide synthesis in *B. cepacia* (Moreira *et al.*, 2003). This exopolysaccharide is not produced in *B. cenocepacia* strains J2315 or K56-2 due to the presence of transposable insertion elements within other genes of this cluster (M. S. Saldías & M. A. Valvano, unpublished data). $ugd_{BCAM2034}$ is in a four-gene cluster that contains two open reading frames similar to *galE* (UDP-galactose 4-epimerase) as well as a predicted glycosyltransferase. The sequences of the three predicted *ugd* genes in strain K56-2 are identical to those in the sequenced J2315 strain.

The three loci $ugd_{BCAL2946}$, $ugd_{BCAM0855}$ and $ugd_{BCAM2034}$ are predicted to encode proteins sharing, respectively, 53 %, 52 % and 39 % amino acid sequence identity with *P. aeruginosa* PA2022. The predicted proteins $Ugd_{BCAL2946}$ and $Ugd_{BCAM0855}$ share 74 % amino acid sequence identity. The predicted $Ugd_{BCAM2034}$ shares 44 % and 45 % amino acid sequence identity with $Ugd_{BCAL2946}$ and $Ugd_{BCAM0855}$, respectively. Fig. 1(b) shows a CLUSTAL W alignment of the three predicted Ugd proteins of *B. cenocepacia*, *P. aeruginosa* Ugd PA2022 and *Streptococcus pyogenes* Ugd (accession no. AAA26899). Despite low pair-wise sequence identity (~21 %) with the *S. pyogenes* Ugd, for which high-resolution crystal structures are available (Protein Data Bank, accession nos 1DLI and 1DLJ) (Campbell *et al.*, 2000), each of the three predicted Ugd proteins contains a predicted Rossmann fold for NAD^+ binding (Rossman, 1981) at the N terminus, and residues involved in the catalytic mechanism (Campbell *et al.*, 2000), such as Cys260 involved in thioester formation and Arg244 involved in UDP-sugar specificity, are conserved (equivalent residues Cys274 and Arg258 in $Ugd_{BCAL2946}$, Cys270 and Arg254 in $Ugd_{BCAM0855}$, and Cys266 and Arg250 in $Ugd_{BCAM2034}$).

A mutation in $ugd_{BCAL2946}$ confers sensitivity to polymyxin B

To assess the function of the candidate *ugd* genes, three mutant strains were constructed, each with a different putative *ugd* gene inactivated by insertional mutagenesis: SAL8 ($ugd_{BCAL2946}$::pSL23), SAL12 ($ugd_{BCAM2034}$::pSL29) and SAL15 ($ugd_{BCAM0855}$::pSL31). SAL12 and SAL15 grew similarly to the parental strain, K56-2 (Fig. 2). In contrast, SAL8 exhibited a slightly slower growth rate in exponential phase, but eventually reached the same cell density as K56-2, SAL12 and SAL15 (Fig. 2). There were no detectable differences in the LPS profiles of mutant strains compared to that of the parental K56-2 when LPS was prepared from cells, separated by gel electrophoresis, and stained with silver (data not shown); however, detection of subtle changes to LPS structure may require a more sensitive method of analysis. The *ugd* mutants were tested for their ability to grow in LB medium containing pmB at a concentration of 1024 µg ml^{-1}. Fig. 3(a) shows that the growth of SAL8 was significantly impaired at this concentration of pmB, in comparison to K56-2 and the other two mutants. In vehicle control incubations, K56-2, SAL12 and SAL15 all grew equivalently and the growth of SAL8 was slightly slower in the exponential phase of growth (Fig. 3a inset), similar to the results shown above with LB alone. The MIC_{50} values for pmB were also calculated for all the strains. For K56-2, SAL12 and SAL15 the MIC_{50} values for pmB were all greater than 1024 µg ml^{-1} (the highest concentration tested). For SAL8, the MIC_{50} value for pmB was 128 µg ml^{-1}.

Next, SAL8 was transformed with a series of plasmids, each containing a different putative *ugd* gene fused to the FLAG epitope at the 3′ end of the gene. Growth of SAL8(pDA17) containing a vector control or SAL8(pSL38) encoding $ugd_{BCAM2034}$ was poor in 128 µg ml^{-1} pmB (Fig. 3b). In fact, the plasmids actually appeared to exacerbate the

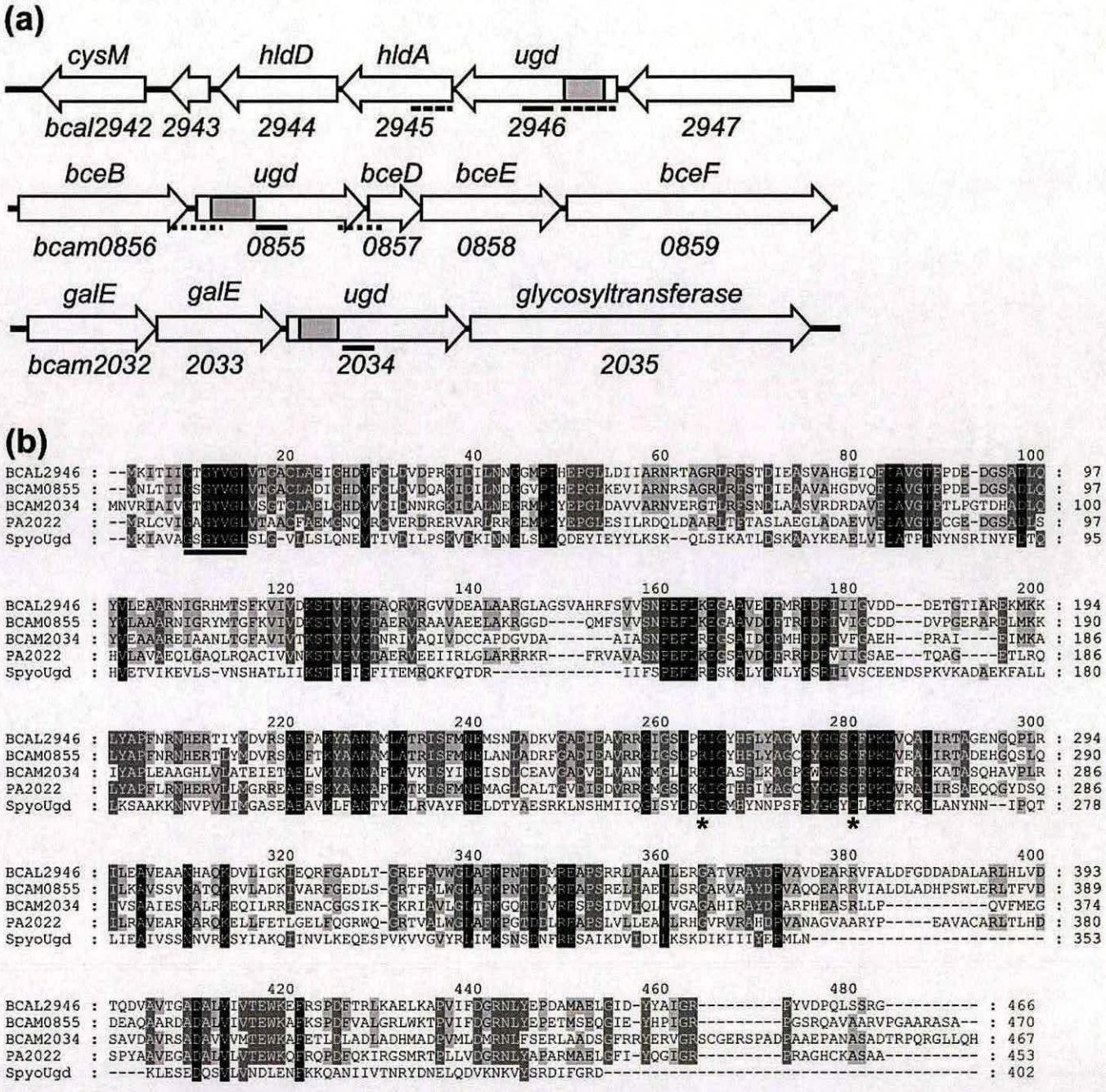

Fig. 1. Identification and chromosomal arrangement of putative *ugd* genes. (a) Each *ugd* gene is schematically depicted with neighbouring genes. The nomenclature below each gene is that used in the annotation of the sequenced genome of *B. cenocepacia* strain J2315. Designations above the genes are based on either TBLASTX analysis or previous publications (Iwanicka-Nowicka *et al.*, 2007; Loutet *et al.*, 2006; Moreira *et al.*, 2003). The grey bars within the *ugd* genes represent the internal fragments that were cloned into the *ugd* mutagenesis plasmids (pSL23, pSL29 and pSL31 for $ugd_{BCAL2946}$, $ugd_{BCAM2034}$ and $ugd_{BCAM0855}$, respectively). The dashed lines below *hldA* and $ugd_{BCAL2946}$ represent the PCR fragments used to generate plasmids for conditional mutagenesis (pSL26 and pSL27 for *hldA* and $ugd_{BCAL2946}$, respectively). The dotted lines below $ugd_{BCAM0855}$ and its neighbouring genes represent the two fragments that were cloned into the plasmid (pSL43) used for unmarked mutagenesis of $ugd_{BCAM0855}$. The solid lines below each *ugd* gene represent the regions analysed by real-time PCR. (b) CLUSTAL W alignment of the three putative Ugd proteins of *B. cenocepacia*, *P. aeruginosa* PA2022 and Ugd from *S. pyogenes*. Residues conserved in all five proteins, four of the five, or three of the five are highlighted in black, dark grey and light grey, respectively. The line below the alignment indicates the conserved GXGXXG motif of the Rossmann fold required for NAD binding. Asterisks denote residues Arg-244 and Cys-260 of *S. pyogenes* Ugd shown to be important for catalysis.

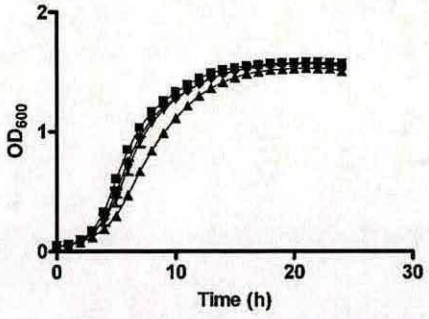

Fig. 2. *B. cenocepacia* K56-2 and the panel of *ugd* mutants grow similarly. Growth of K56-2 (■), SAL8 (▲), SAL12 (▼) and SAL15 (◆) was monitored in a Bioscreen C automated growth curve reader for 24 h. Shown are the means of data from three independent experiments done in triplicate; error bars denote the standard error of the mean.

sensitivity to pmB in SAL8 since growth was impaired by >95 % at this concentration of pmB. The growth of SAL8 transformed with pSL37 ($ugd_{BCAL2946}$) after 18 h was not statistically different in the presence or absence of 128 μg pmB ml^{-1}, similar to the growth of K56-2 under these conditions. SAL8 transformed with pSL39 ($ugd_{BCAM0855}$) regained in part the ability to grow in the presence of 128 μg pmB ml^{-1}. Western blot analysis showed that all three putative Ugd proteins were expressed in SAL8 (Fig. 4), although not to the same levels. The predicted masses for Ugd-$FLAG_{BCAL2946}$, Ugd-$FLAG_{BCAM2034}$, and Ugd-$FLAG_{BCAM0855}$ are 51.7 kDa, 50.9 kDa and 52.1 kDa, respectively. Bands indicated with arrows correspond approximately to the predicted sizes. In addition, we observed numerous faster-migrating bands for the Ugd-FLAG constructs that were consistent between experiments. These bands were interpreted as degradation products due to proteolytic cleavage either in the cell or during the sample preparation. Ponceau S staining of the membrane before Western blotting indicated that equal amounts of protein were transferred to the membrane in each lane (data not shown). Similar complementation results were obtained with a series of vectors expressing Ugd proteins not fused to the FLAG epitope (data not shown). Together, these experiments indicate that of the three putative *ugd* genes, only $ugd_{BCAL2946}$ is required for the full resistance of *B. cenocepacia* strain K56-2 to pmB and also that the protein encoded by $ugd_{BCAM0855}$ can compensate for the function of the protein encoded by $ugd_{BCAL2946}$.

The combined activity of $Ugd_{BCAL2946}$ and $Ugd_{BCAM0855}$ is essential for viability

Due to the role of Ugd in the synthesis of UDP-Ara4N, we hypothesized that the combined Ugd activity of *B. cenocepacia* is essential for viability of the organism. Based on the results described above, we predicted that the combination of $ugd_{BCAL2946}$ and $ugd_{BCAM0855}$ would be

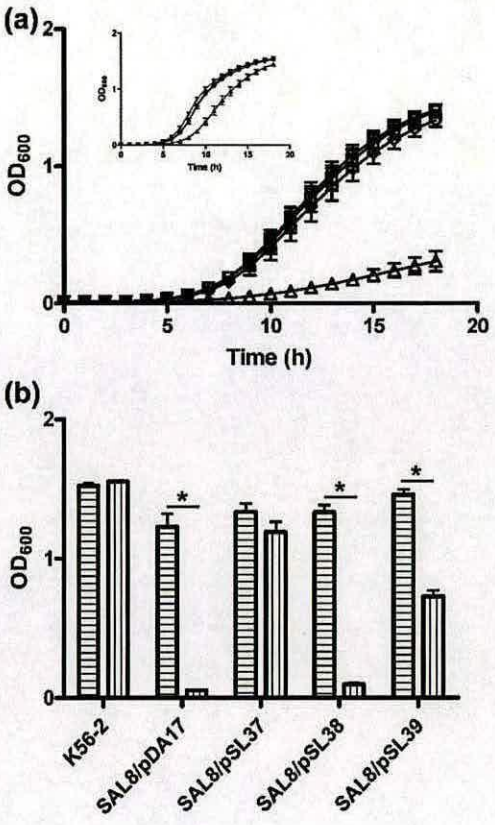

Fig. 3. SAL8 is the only *ugd* mutant that is sensitive to pmB. (a) Growth of K56-2 (■,□), SAL8 (▲, △), SAL12 (▼, ▽) and SAL15 (◆, ◇) in either a vehicle control (filled symbols, shown in inset) or 1024 μg pmB ml^{-1} (empty symbols) was monitored for 18 h. (b) End point OD_{600} of K56-2 and SAL8 with either pDA17 (plasmid control), pSL37 ($ugd_{BCAL2946}$), pSL38 ($ugd_{BCAM2034}$) or pSL39 ($ugd_{BCAM0855}$) grown for 18 h in either a vehicle control (horizontally striped bars) or 128 μg pmB ml^{-1} (vertically striped bars). Shown are the mean and standard error of the mean for data from three independent experiments done in triplicate. *, Statistically significant difference ($P<0.05$) between vehicle control and pmB treatments by unpaired *t*-test.

essential. To test this, a strain containing an unmarked $ugd_{BCAM0855}$ deletion was created (SAL23). Like SAL15, SAL23 did not show impaired resistance to pmB (data not shown). SAL23 was then used for the creation of conditional mutants in $ugd_{BCAL2946}$ (SAL26) and the downstream gene, *hldA* (SAL25).

These strains were tested for their ability to grow under inducing (rhamnose) and repressing (glucose) conditions. The wild-type strain K56-2 transformed with pSCrhaB2 (to allow for growth in medium supplemented with trimethoprim) grew equally well on plates with either glucose or rhamnose (Fig. 5, first lane). XOA11, a positive control for a conditional mutant of an essential gene required for Ara4N transfer to lipid A, grew well in the presence of rhamnose but growth was substantially impaired in the

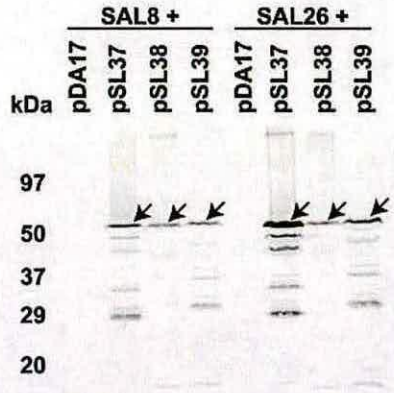

Fig. 4. All three Ugd-FLAG constructs are expressed in SAL8 and SAL26. Western blot analysis using anti-FLAG antibodies was done for both SAL8 and SAL26 containing either pDA17 (plasmid control), pSL37 ($ugd_{BCAL2946}$), pSL38 ($ugd_{BCAM2034}$) or pSL39 ($ugd_{BCAM0855}$). Arrows indicate bands that correspond to the full-length Ugd-FLAG constructs. This is a representative image of three independent experiments.

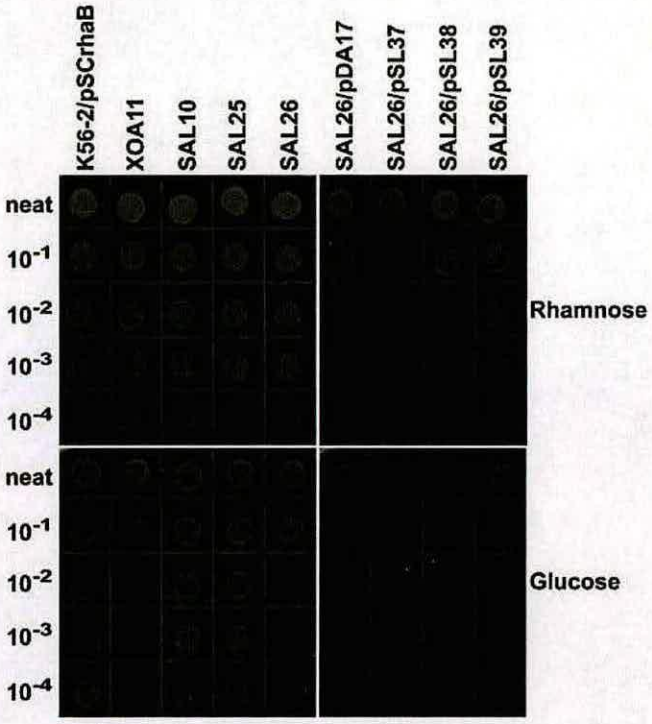

Fig. 5. The combined activity of $Ugd_{BCAL2946}$ and $Ugd_{BCAM0855}$ is essential for viability of *B. cenocepacia* strain K56-2. Left panels: K56-2 with pSCrhaB (for growth of wild-type on agar plates with trimethoprim), XOA11 (positive control for a strain with a conditional mutant in an essential gene), SAL10 (negative control, $ugd_{BCAL2946}$ conditional mutant in the presence of a functional copy of $ugd_{BCAM0855}$), SAL25 (negative control, $\Delta ugd_{BCAM0855}$ strain with a conditional mutation in *hldA*, the gene downstream of $ugd_{BCAL2946}$) and SAL26 ($\Delta ugd_{BCAM0855}$ strain with a conditional mutation in $ugd_{BCAL2946}$) were grown overnight, serially diluted, and 10 µl drops were plated on media containing either rhamnose (inducing conditions, top panel) or glucose (repressing conditions, bottom panel). Mutants with a conditional lethal phenotype grow well on agar plates with rhamnose but grow much more poorly on glucose. Right panels: growth of SAL26 in the presence of either pDA17 (plasmid control), pSL37 ($ugd_{BCAL2946}$), pSL38 ($ugd_{BCAM2034}$) or pSL39 ($ugd_{BCAM0855}$) under inducing or repressing conditions of chromosomally encoded $ugd_{BCAL2946}$. Shown is a representative image of three independent experiments.

presence of glucose (Fig. 5, second lane), as previously demonstrated (Ortega *et al.*, 2007). Two negative control strains, SAL10 (a $ugd_{BCAL2946}$ conditional mutant with an intact $ugd_{BCAM0855}$ gene) and SAL25 (the conditional *hldA* mutant lacking $ugd_{BCAM0855}$ but with $ugd_{BCAL2946}$ intact) both grew equally well in the presence of either glucose or rhamnose (Fig. 5, third and fourth lanes, respectively). Finally, SAL26, the conditional $ugd_{BCAL2946}$ mutant lacking an intact $ugd_{BCAM0855}$ gene, grew well in the presence of rhamnose but like XOA11 its growth was very poor in the presence of glucose (Fig. 5, fifth lane).

Next, experiments were carried out to determine which of the three putative *ugd* genes could complement the conditional growth defect of SAL26. In the presence of rhamnose, the growth of SAL26 transformed with any of the plasmids was similar to that of untransformed SAL26 cells (Fig. 5, top right panel). However, growth of SAL26 in the presence of glucose improved significantly in cells transformed with either pSL37 or pSL39 but not with pSL38 or the plasmid control, pDA17 (Fig. 5, bottom right panel). Western blot analysis showed that all three Ugd-FLAG constructs were expressed in SAL26, with protein profiles similar to those in SAL8 (Fig. 4); Ponceau S staining of the membrane showed that there was equal transfer of proteins in each of the lanes (data not shown). Together, these experiments indicate that the combined activity of the proteins encoded by $ugd_{BCAL2946}$ and $ugd_{BCAM0855}$ is required for the viability of *B. cenocepacia*.

$Ugd_{BCAL2946}$ and $Ugd_{BCAM0855}$ have similar reaction kinetics

To further characterize the proteins encoded by $ugd_{BCAL2946}$, $ugd_{BCAM0855}$ and $ugd_{BCAM2034}$, the genes were cloned into a pET28 vector to add an N-terminal His_6 tag. $Ugd_{BCAL2946}$ and $Ugd_{BCAM0855}$ were overexpressed in *E. coli* and purified using nickel affinity and size exclusion chromatography. The $Ugd_{BCAL2946}$ and $Ugd_{BCAM0855}$ proteins were soluble and behaved as homodimers (~106 kDa) with similar elution profiles (data not shown). $Ugd_{BCAM2034}$ was insoluble and required low-temperature induction and an additional solubilization step prior to purification as a mixture of monomer (~52 kDa) and homodimer (~104 kDa) (data not shown). The enzyme assay was based on the Ugd mechanism proposed by

Campbell *et al.* (2000) and Ge *et al.* (2004): UDP-glucose is converted to UDP-glucuronic acid in a two-step oxidation via a covalently bound thioester intermediate. Conversion of this to the final free UDP-glucuronic acid product requires a second mole of NAD^+ so overall the process reduces two NAD^+ to two NADH. To determine the kinetic parameters, the initial velocity was calculated by measuring the increase in absorbance at 340 nm, due to the production of NADH, divided by two. The data were fitted by non-linear regression with the Hill equation ($V = V_{max}\,[S]^h/([S]^h + K_m{}^h$). The enzyme turnover (k_{cat}) and catalytic efficiency (k_{cat}/K_m) were calculated from the V_{max} and K_m values obtained. Both $Ugd_{BCAL2946}$ and $Ugd_{BCAM0855}$ showed Ugd activity with very similar kinetic constants (Table 1), while $Ugd_{BCAM2034}$ showed no *in vitro* activity with UDP-glucose as a substrate To investigate any substrate specificity variation between the Ugd proteins, the spectrophotometric assay was repeated with three additional UDP-sugars (UDP-galactose, UDP-acetylglucosamine and GDP-mannose) that replaced UDP-glucose. None of these molecules were substrates for any of the enzymes (data not shown). From these experiments we conclude that $Ugd_{BCAL2946}$ and $Ugd_{BCAM0855}$ have very similar enzymic activities and confirm biochemically the functional assignment of these proteins as UDP-glucose dehydrogenases.

Expression of *ugd*$_{BCAL2946}$ is higher than that of *ugd*$_{BCAM0855}$ or *ugd*$_{BCAM2034}$

Since both $Ugd_{BCAL2946}$ and $Ugd_{BCAM0855}$ demonstrated very similar kinetic parameters, we investigated whether these proteins are differentially expressed *in vivo*. RNA was prepared from *B. cenocepacia* cells in exponential growth and the number of RNA transcripts of each *ugd* gene was quantified and compared to the number of transcripts of the constitutively active gene *hisD*. The number of $ugd_{BCAL2946}$ transcripts was on average 5.4 times and 135 times higher than the number of $ugd_{BCAM0855}$ or $ugd_{BCAM2034}$ transcripts, respectively (Fig. 6). Melting curves for each portion of each gene analysed by real-time PCR were similar to the positive controls and there were no detectable differences in band sizes by agarose gel electrophoresis (data not shown), indicating that the products amplified after the reverse transcription reaction were the same as those amplified in the positive controls. These results indicate that $ugd_{BCAL2946}$ is highly expressed relative to the expression of $ugd_{BCAM0855}$, while the expression of $ugd_{BCAM2034}$ under the condition tested (exponential growth) is negligible. These results help to explain why only the mutant defective in $ugd_{BCAL2946}$ has a phenotype in terms of pmB sensitivity, and also why the double mutant ($\Delta ugd_{BCAM0855}$, $ugd_{BCAL2946}$ conditional) fails to grow under non-permissive conditions.

DISCUSSION

We demonstrate here that the proteins encoded by two *B. cenocepacia* genes, $ugd_{BCAL2946}$ and $ugd_{BCAM0855}$, possess the predicted dehydrogenase activity, which results in the conversion of UDP-glucose into UDP-glucuronic acid. $Ugd_{BCAL2946}$ and $Ugd_{BCAM0855}$ are efficient catalysts with low micromolar K_m values for UDP-glucose and NAD^+ and relatively fast turnover. The similar catalytic profile for these enzymes is not surprising since they show 74 % amino acid sequence identity. The two *P. aeruginosa* Ugd proteins described by Hung *et al.* (2007) utilized UDP-galactose and UDP-*N*-acetylglucosamine as substrates, but with much lower activity compared with UDP-glucose. However, apart from UDP-glucose, the two *B. cenocepacia* Ugd proteins did not exhibit any activity when any of the other three UDP-sugar substrates were used. This substrate specificity correlates with the high catalytic efficiency (k_{cat}/K_m) of the enzymes, and the similar biochemical profiles of $Ugd_{BCAL2946}$ and $Ugd_{BCAM0855}$ explain why they can compensate each other's function *in vivo* during complementation assays.

B. cenocepacia is highly resistant to APs and understanding the molecular basis of this resistance is a longstanding goal of our groups. Here, we show that only $ugd_{BCAL2946}$ is necessary for resistance to the AP pmB, as the insertional inactivation of this gene led to an eightfold increase in sensitivity to pmB. This phenotype does not appear to be due to a polar effect on *hldA* and *hldD*, the two genes downstream of $ugd_{BCAL2946}$, based on two experimental

Table 1. Kinetic parameters of $Ugd_{BCAL2946}$ and $Ugd_{BCAM0855}$

Parameters were determined by non-linear regression from $V = V_{max}\,[S]^h/([S]^h + K_m{}^h$ using Origin6.1 software.

Protein	V_{max} (nmol min^{-1})	K_m (mM)	h	k_{cat} (min^{-1})	k_{cat}/K_m (mM^{-1} min^{-1})
			UDP-glucose		
$Ugd_{BCAL2946}$	14.38 ± 0.73	0.02 ± 0.01	1.25 ± 0.16	7.99 ± 0.13	392.36 ± 0.37
$Ugd_{BCAM0855}$	13.73 ± 0.90	0.02 ± 0.01	1.41 ± 0.12	7.63 ± 0.15	340.35 ± 0.10
			NAD^+		
$Ugd_{BCAL2946}$	16.61 ± 1.11	0.17 ± 0.03	1.51 ± 0.31	9.23 ± 0.15	53.95 ± 0.19
$Ugd_{BCAM0855}$	16.88 ± 1.22	0.21 ± 0.04	1.50 ± 0.31	9.38 ± 0.16	44.50 ± 0.19

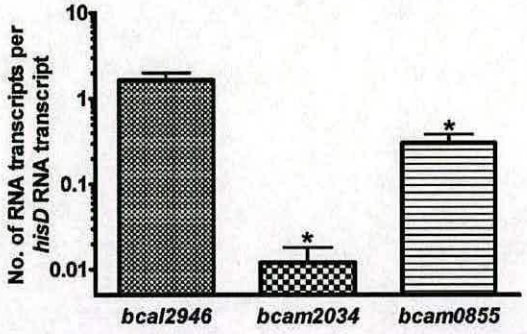

Fig. 6. $ugd_{BCAL2946}$ is more highly expressed than either $ugd_{BCAM2034}$ or $ugd_{BCAM0855}$. Shown are real-time PCR results from three experiments completed in triplicate; error bars represent the standard error of the mean. For each *ugd* gene the data are standardized to values obtained for the internal control gene, *hisD*. *, Statistically significant difference ($P<0.01$) compared to results for $ugd_{BCAL2946}$ by unpaired *t*-test.

observations: (i) the sensitivity can be restored *in trans* when $ugd_{BCAL2946}$ is expressed from a plasmid, and (ii) disruption of *hldA* and *hldD* has a profound effect on the structure of the LPS molecule (Loutet *et al.*, 2006), which we did not observe in the $ugd_{BCAL2946}$ mutant. In fact, no differences were found in the LPS profiles of any of the *ugd* mutants compared to the LPS profile of the parental strain, although we cannot rule out subtle modifications in the LPS molecule that would require a more detailed analysis, currently under way in our laboratories. The pmB-sensitive phenotype of the $ugd_{BCAL2946}$ mutant was also complemented by a plasmid-encoded $ugd_{BCAM0855}$ but not by $ugd_{BCAM2034}$. The lack of complementation by $ugd_{BCAM2034}$ was not due to lack of protein expression since all three *ugd* genes revealed a polypeptide of the expected molecular mass when cloned in a plasmid and expressed as protein-FLAG fusions. Also, lack of complementation was not due to the presence of the C-terminal FLAG epitope, since the same results were obtained in experiments using untagged proteins. These data suggest that $Ugd_{BCAL2946}$ accounts for the cellular Ugd activity required for the resistance of *B. cenocepacia* to pmB.

We have previously demonstrated that the synthesis of UDP-Ara4N is essential for the viability of *B. cenocepacia* (Ortega *et al.*, 2007). Since the conversion of UDP-glucose into UDP-glucuronic acid is an obligatory step for the synthesis of UDP-Ara4N, we reasoned that a mutant lacking both $ugd_{BCAL2946}$ and $ugd_{BCAM0855}$ would not be viable. Indeed, a double mutant in which $ugd_{BCAM0855}$ is deleted and $ugd_{BCAL2946}$ is conditionally expressed was non-viable under non-permissive conditions. This result suggests that $Ugd_{BCAL2946}$ and $Ugd_{BCAM0855}$ account for the majority of the cellular Ugd activity required for UDP-Ara4N synthesis.

Studies in other Gram-negative bacterial species have shown that the expression of *ugd* genes can be complex. In *Salmonella*, a variety of regulatory systems control the expression of the *ugd* gene. In the presence of high Fe^{3+}, *ugd* expression is upregulated by PmrA, the response regulator of the two-component regulatory system PmrA-PmrB (Wösten *et al.*, 2000). Under low Mg^{2+} conditions, activation of the two-component regulatory system PhoP-PhoQ occurs, activated PhoP upregulates expression of another protein, PmrD, which in turn activates the PmrA-PmrB system, and *ugd* expression is upregulated by PmrA (Kox *et al.*, 2000). Finally, the RcsC-YojN-RcsB phospho-relay system can also control the expression of the *ugd* gene in *Salmonella* from a second promoter that is independent of PmrA (Mouslim & Groisman, 2003). A recent study in *P. aeruginosa* demonstrated that this common CF lung pathogen also possesses two *ugd* genes and that the two genes are differentially expressed (Hung *et al.*, 2007). Hung *et al.* (2007) showed that in *P. aeruginosa* strain PAO1 the expression of *PA3559* was induced under low Mg^{2+} conditions and that this gene was required for pmB resistance, while *PA2022* was more constitutively expressed and was not required for pmB resistance. Similar results were obtained for *PA3559* by McPhee *et al.* (2006), who also showed that the promoter of *PA3559* has two binding sites each for the PhoP and PmrA proteins of *P. aeruginosa*. With three genes predicted to encode UDP-glucose dehydrogenase, the regulation of Ugd activity may be even more complicated in *B. cenocepacia*. We have shown that in cells in the exponential growth phase $ugd_{BCAL2946}$ is more highly expressed than either $ugd_{BCAM0855}$ or $ugd_{BCAM2034}$. Little else is known about the regulatory control of expression of $ugd_{BCAL2946}$, $ugd_{BCAM0855}$ and $ugd_{BCAM2034}$ and it is something we are currently investigating. None of these *ugd* genes is directly linked to the *arn* locus in *B. cenocepacia*, which itself has an unusual gene order (Ortega *et al.*, 2007), and this also suggests that there are differences in operon regulation between *Burkholderia* and other Gram-negative organisms. It is interesting to note that the response regulators of *B. cenocepacia* most similar to the PhoP and PmrA proteins of *P. aeruginosa* and *Salmonella* are not required for pmB resistance (Flannagan *et al.*, 2007), which suggests that they are probably not required for expression of at least $ugd_{BCAL2946}$. *B. cenocepacia* does, however, contain numerous other two-component regulatory systems that could participate in the response to pmB. The finding that $ugd_{BCAL2946}$ is more highly expressed than the other two *ugd* genes suggests to us that this difference may account for the fact that sensitivity to pmB is only seen in the $ugd_{BCAL2946}$ mutant strain.

We have shown that the protein encoded by $ugd_{BCAM2034}$ does not appear to be a player in the total cellular Ugd activity: mutation of the gene neither affects pmB resistance nor is required for the essential synthesis of UDP-Ara4N, the gene cannot rescue the pmB sensitivity of SAL8 or the inability of SAL26 to grow under non-permissive conditions, the gene is poorly expressed in rapidly dividing cells, and the purified form of the protein

does not have *in vitro* Ugd activity under the conditions we tested. Further analysis of the protein encoded by *BCAM2034* is required before an enzymic function can be assigned to it.

In summary, we have demonstrated that the most highly expressed *ugd* gene of *B. cenocepacia* is required for resistance to pmB and that the two most highly expressed genes are required for viability. However, we cannot conclusively state why disruption of $ugd_{BCAL2946}$ results in increased sensitivity to pmB. We hypothesize that it is due to small decreases in UDP-Ara4N in the LPS molecule of SAL8 at some point in growth; however, it is also possible that UDP-glucuronic acid is required for some other pathway required for pmB resistance in *B. cenocepacia*. Studies are ongoing in our laboratories to determine why UDP-Ara4N is essential for the survival of *B. cenocepacia*, where Ara4N is located in the LPS molecule and whether there are changes in the Ara4N content of the LPS molecules of our conditional mutants as well as the LPS molecules of the individual *ugd* mutants described in this study.

ACKNOWLEDGEMENTS

We thank Dr J. Parkhill for access to the annotation of the genome sequence of *Burkholderia cenocepacia* strain J2315 and Dr David J. Clarke for his help with protein analysis. This work was funded by a grant from the Canadian Cystic Fibrosis Foundation (to M. A. V.). A doctoral research award from the Canadian Institutes of Health Research supported S. A. L. M. A. V. holds a Canada Research Chair in Infectious Disease and Microbial Pathogenesis. D. J. C. and J. R. W. G. thank the Cystic Fibrosis Trust (UK) and the Big Lottery Fund for the award of a studentship to S. J. B. via the UK CF Microbiology Consortium.

REFERENCES

Aaron, S. D., Ferris, W., Henry, D. A., Speert, D. P. & Macdonald, N. E. (2000). Multiple combination bactericidal antibiotic testing for patients with cystic fibrosis infected with *Burkholderia cepacia*. *Am J Respir Crit Care Med* **161**, 1206–1212.

Aubert, D. F., Flannagan, R. S. & Valvano, M. A. (2008). A novel sensor kinase-response regulator hybrid controls biofilm formation and type VI secretion system activity in *Burkholderia cenocepacia*. *Infect Immun* **76**, 1979–1991.

Bader, M. W., Sanowar, S., Daley, M. E., Schneider, A. R., Cho, U., Xu, W., Klevit, R. E., Le Moual, H. & Miller, S. I. (2005). Recognition of antimicrobial peptides by a bacterial sensor kinase. *Cell* **122**, 461–472.

Balandreau, J., Viallard, V., Cournoyer, B., Coenye, T., Laevens, S. & Vandamme, P. (2001). *Burkholderia cepacia* genomovar III is a common plant-associated bacterium. *Appl Environ Microbiol* **67**, 982–985.

Breazeale, S. D., Ribeiro, A. A. & Raetz, C. R. (2002). Oxidative decarboxylation of UDP-glucuronic acid in extracts of polymyxin-resistant *Escherichia coli*. Origin of lipid A species modified with 4-amino-4-deoxy-L-arabinose. *J Biol Chem* **277**, 2886–2896.

Brogden, K. A. (2005). Antimicrobial peptides: pore formers or metabolic inhibitors in bacteria? *Nat Rev Microbiol* **3**, 238–250.

Burns, J. L., Wadsworth, C. D., Barry, J. J. & Goodall, C. P. (1996). Nucleotide sequence analysis of a gene from *Burkholderia* (*Pseudomonas*) *cepacia* encoding an outer membrane lipoprotein involved in multiple antibiotic resistance. *Antimicrob Agents Chemother* **40**, 307–313.

Campbell, R. E., Mosimann, S. C., van De Rijn, I., Tanner, M. E. & Strynadka, N. C. (2000). The first structure of UDP-glucose dehydrogenase reveals the catalytic residues necessary for the two-fold oxidation. *Biochemistry* **39**, 7012–7023.

De Leon, G. P., Elowe, N. H., Koteva, K. P., Valvano, M. A. & Wright, G. D. (2006). An in vitro screen of bacterial lipopolysaccharide biosynthetic enzymes identifies an inhibitor of ADP-heptose biosynthesis. *Chem Biol* **13**, 437–441.

Ernst, R. K., Yi, E. C., Guo, L., Lim, K. B., Burns, J. L., Hackett, M. & Miller, S. I. (1999). Specific lipopolysaccharide found in cystic fibrosis airway *Pseudomonas aeruginosa*. *Science* **286**, 1561–1565.

Figurski, D. H. & Helinski, D. R. (1979). Replication of an origin-containing derivative of plasmid RK2 dependent on a plasmid function provided *in trans*. *Proc Natl Acad Sci U S A* **76**, 1648–1652.

Flannagan, R. S., Aubert, D., Kooi, C., Sokol, P. A. & Valvano, M. A. (2007). *Burkholderia cenocepacia* requires a periplasmic HtrA protease for growth under thermal and osmotic stress and for survival in vivo. *Infect Immun* **75**, 1679–1689.

Flannagan, R. S., Linn, T. & Valvano, M. A. (2008). A system for the construction of targeted unmarked gene deletions in the genus *Burkholderia*. *Environ Microbiol* **10**, 1652–1660.

Ganz, T. (2003). Defensins: antimicrobial peptides of innate immunity. *Nat Rev Immunol* **3**, 710–720.

Ge, X., Penney, L. C., van de Rijn, I. & Tanner, M. E. (2004). Active site residues and mechanism of UDP-glucose dehydrogenase. *Eur J Biochem* **271**, 14–22.

Gold, R., Jin, E., Levison, H., Isles, A. & Fleming, P. C. (1983). Ceftazidime alone and in combination in patients with cystic fibrosis: lack of efficacy in treatment of severe respiratory infections caused by *Pseudomonas cepacia*. *J Antimicrob Chemother* **12** (*Suppl A*), 331–336.

Helander, I. M., Kilpelainen, I. & Vaara, M. (1994). Increased substitution of phosphate groups in lipopolysaccharides and lipid A of the polymyxin-resistant *pmrA* mutants of *Salmonella typhimurium*: a ^{31}P-NMR study. *Mol Microbiol* **11**, 481–487.

Hitchcock, P. J. & Brown, T. M. (1983). Morphological heterogeneity among *Salmonella* lipopolysaccharide chemotypes in silver-stained polyacrylamide gels. *J Bacteriol* **154**, 269–277.

Holden, M. T., Seth-Smith, H. M., Crossman, L. C., Sebaihia, M., Bentley, S. D., Cerdeño-Tárraga, A. M., Thomson, N. R., Bason, N., Quail, M. A. & other authors (2009). The genome of *Burkholderia cenocepacia* J2315, an epidemic pathogen of cystic fibrosis patients. *J Bacteriol* **191**, 261–277.

Hung, R. J., Chien, H. S., Lin, R. Z., Lin, C. T., Vatsyayan, J., Peng, H. L. & Chang, H. Y. (2007). Comparative analysis of two UDP-glucose dehydrogenases in *Pseudomonas aeruginosa* PAO1. *J Biol Chem* **282**, 17738–17748.

Isles, A., Maclusky, I., Corey, M., Gold, R., Prober, C., Fleming, P. & Levison, H. (1984). *Pseudomonas cepacia* infection in cystic fibrosis: an emerging problem. *J Pediatr* **104**, 206–210.

Iwanicka-Nowicka, R., Zielak, A., Cook, A. M., Thomas, M. S. & Hryniewicz, M. M. (2007). Regulation of sulfur assimilation pathways in *Burkholderia cenocepacia*: identification of transcription factors CysB and SsuR and their role in control of target genes. *J Bacteriol* **189**, 1675–1688.

Kox, L. F., Wösten, M. M. & Groisman, E. A. (2000). A small protein that mediates the activation of a two-component system by another two-component system. *EMBO J* **19**, 1861–1872.

Loutet, S. A., Flannagan, R. S., Kooi, C., Sokol, P. A. & Valvano, M. A. (2006). A complete lipopolysaccharide inner core oligosaccharide is required for resistance of *Burkholderia cenocepacia* to antimicrobial peptides and bacterial survival in vivo. *J Bacteriol* **188**, 2073–2080.

Mahenthiralingam, E., Coenye, T., Chung, J. W., Speert, D. P., Govan, J. R., Taylor, P. & Vandamme, P. (2000). Diagnostically and experimentally useful panel of strains from the *Burkholderia cepacia* complex. *J Clin Microbiol* **38**, 910–913.

Mahenthiralingam, E., Urban, T. A. & Goldberg, J. B. (2005). The multifarious, multireplicon *Burkholderia cepacia* complex. *Nat Rev Microbiol* **3**, 144–156.

McPhee, J. B., Lewenza, S. & Hancock, R. E. (2003). Cationic antimicrobial peptides activate a two-component regulatory system, PmrA-PmrB, that regulates resistance to polymyxin B and cationic antimicrobial peptides in *Pseudomonas aeruginosa*. *Mol Microbiol* **50**, 205–217.

McPhee, J. B., Bains, M., Winsor, G., Lewenza, S., Kwasnicka, A., Brazas, M. D., Brinkman, F. S. L. & Hancock, R. E. W. (2006). Contribution of the PhoP-PhoQ and PmrA-PmrB two-component regulatory systems to Mg^{2+}-induced gene regulation in *Pseudomonas aeruginosa*. *J Bacteriol* **188**, 3995–4006.

Miller, V. L. & Mekalanos, J. J. (1988). A novel suicide vector and its use in construction of insertion mutations: osmoregulation of outer membrane proteins and virulence determinants in *Vibrio cholerae* requires *toxR*. *J Bacteriol* **170**, 2575–2583.

Moreira, L. M., Videira, P. A., Sousa, S. A., Leitão, J. H., Cunha, M. V. & Sá-Correia, I. (2003). Identification and physical organization of the gene cluster involved in the biosynthesis of *Burkholderia cepacia* complex exopolysaccharide. *Biochem Biophys Res Commun* **312**, 323–333.

Mouslim, C. & Groisman, E. A. (2003). Control of the *Salmonella ugd* gene by three two-component regulatory systems. *Mol Microbiol* **47**, 335–344.

Nummila, K., Kilpelainen, I., Zähringer, U., Vaara, M. & Helander, I. M. (1995). Lipopolysaccharides of polymyxin B-resistant mutants of *Escherichia coli* are extensively substituted by 2-aminoethyl pyrophosphate and contain aminoarabinose in lipid A. *Mol Microbiol* **16**, 271–278.

Ortega, X. P., Cardona, S. T., Brown, A. R., Loutet, S. A., Flannagan, R. S., Campopiano, D. J., Govan, J. R. & Valvano, M. A. (2007). A putative gene cluster for aminoarabinose biosynthesis is essential for *Burkholderia cenocepacia* viability. *J Bacteriol* **189**, 3639–3644.

Patrzykat, A., Friedrich, C. L., Zhang, L., Mendoza, V. & Hancock, R. E. (2002). Sublethal concentrations of pleurocidin-derived antimicrobial peptides inhibit macromolecular synthesis in *Escherichia coli*. *Antimicrob Agents Chemother* **46**, 605–614.

Raetz, C. R. & Whitfield, C. (2002). Lipopolysaccharide endotoxins. *Annu Rev Biochem* **71**, 635–700.

Rossman, M. G. (1981). Evolution of glycolytic enzymes. *Philos Trans R Soc Lond B Biol Sci* **293**, 191–203.

Silipo, A., Molinaro, A., Cescutti, P., Bedini, E., Rizzo, R., Parrilli, M. & Lanzetta, R. (2005). Complete structural characterization of the lipid A fraction of a clinical strain of *B. cepacia* genomovar I lipopolysaccharide. *Glycobiology* **15**, 561–570.

Strominger, J. L., Maxwell, E. S., Axelrod, J. & Kalckar, H. M. (1957). Enzymatic formation of uridine diphosphoglucuronic acid. *J Biol Chem* **224**, 79–90.

Turner, J., Cho, Y., Dinh, N. N., Waring, A. J. & Lehrer, R. I. (1998). Activities of LL-37, a cathelin-associated antimicrobial peptide of human neutrophils. *Antimicrob Agents Chemother* **42**, 2206–2214.

Vaara, M., Vaara, T., Jensen, M., Helander, I., Nurminen, M., Rietschel, E. T. & Mäkelä, P. H. (1981). Characterization of the lipopolysaccharide from the polymyxin-resistant *pmrA* mutants of *Salmonella typhimurium*. *FEBS Lett* **129**, 145–149.

Wösten, M. M. S. M., Kox, L. F. F., Chamnongpol, S., Soncini, F. C. & Groisman, E. A. (2000). A signal transduction system that responds to extracellular iron. *Cell* **103**, 113–125.

Zanetti, M. (2004). Cathelicidins, multifunctional peptides of the innate immunity. *J Leukoc Biol* **75**, 39–48.

Zhang, L., Parente, J., Harris, S. M., Woods, D. E., Hancock, R. E. & Falla, T. J. (2005). Antimicrobial peptide therapeutics for cystic fibrosis. *Antimicrob Agents Chemother* **49**, 2921–2927.

Edited by: J. H. Cove